European Journal of Taxonomy 1010: 1–145
https://doi.org/10.5852/ejt.2025.1010.3021
europeanjournaloftaxonomy.eu
ISSN 2118-9773
2025 · Labarque F.M. *et al.*

Received: 9 February 2024 • *Accepted: 5 June 2025* • *Published: 22 August 2025*

Topic editor: Magalie Castelin • *Section editor: Arnaud Henrard* • *Desk editor: Kristiaan Hoedemakers*

Monograph

urn:lsid:zoobank.org:pub:90524F49-7BA2-4B8A-9BE3-450CB77A31A0

Ray spider rush: Fast-tracking integrative taxonomy in Panama's cloud forests

Facundo M. LABARQUE [1,*], Luis N. PIACENTINI [2], Joan PONS [3], Gustavo HORMIGA [4], Miquel A. ARNEDO [5] & Martín J. RAMÍREZ [6]

[1] Departamento de Ecologia e Biologia Evolutiva (DEBE), Universidade Federal de São Carlos (UFSCar), campus São Carlos, Rodovia Washington Luís, km 235, CEP 13565-905, São Carlos, SP, Brazil.
[1,2,6] División Aracnología, Museo Argentino de Ciencias Naturales, Av. Angel Gallardo 470, C1405DJR Buenos Aires, Argentina.
[3] Department of Biodiversity and Conservation, Mediterranean Institute for Advanced Studies, IMEDEA, Balearic Islands, Spain.
[4] Department of Biological Sciences, The George Washington University, Washington, DC 20052, USA.
[5] Departament de Biologia Evolutiva, Ecologia i Ciències Ambientals & Institut de Recerca de la Biodiversitat (IRBio), Universitat de Barcelona, Barcelona, Spain.

[1] Corresponding author: facundo.labarque@ufscar.br
[2] Email: piacentini@macn.gov.ar
[3] Email: jpons@imedea.uib-csic.es
[4] Email: hormiga@gwu.edu
[5] Email: marnedo@ub.edu
[6] Email: ramirez@macn.gov.ar

Abstract. Taxonomy, a pivotal scientific discipline, plays a crucial role in biodiversity assessments and conservation by defining and cataloging species and higher taxa. However, tropical regions, housing a significant portion of global biodiversity, offer challenges to traditional taxonomy, leaving a substantial part of this diversity unexplored due to limited resources. This study employs a combined approach of gross morphological sorting and DNA-based species delimitation to accelerate species identification and discovery in the orb weaving spider family Theridiosomatidae (ray spiders) within Panamanian cloud forests. Using this methodology, we navigate the taxonomic challenges posed by this species-rich family, with relatively uniform sexual organs in closely related species. Employing a semi-quantitative sampling protocol, we estimate species accumulation curves and non-parametric richness, and assess various biodiversity metrics of over 3333 specimens, resulting in an integrative taxonomic revision revealing 27 new species and a new genus. Three new species of *Chthonos* Coddington, 1986 are described: *Chthonos dobo* sp. nov. (♂♀), *Chthonos kaibe* sp. nov. (♂♀), *Chthonos kwati* sp. nov. (♂♀). Seven new species of *Epeirotypus* O. Pickard-Cambridge, 1894 are described: *Epeirotypus bule* sp. nov. (♀), *Epeirotypus drune* sp. nov. (♀), *Epeirotypus jane* sp. nov. (♀), *Epeirotypus kote* sp. nov. (♂♀), *Epeirotypus kra*

sp. nov. (♂♀), *Epeirotypus kwakwa* sp. nov. (♂♀), *Epeirotypus tain* sp. nov. (♀). One new species of *Naatlo* Coddington, 1986 is described: *Naatlo chi* sp. nov. (♂♀). Two new species of *Ogulnius* O. Pickard-Cambridge, 1882 are described: *Ogulnius zbodro* sp. nov. (♂♀) and *Ogulnius debonaja* sp. nov. (♂♀). We describe *Tantra* gen. nov. based on male and female characters. Eight new species are described: *Tantra bribri* gen. et sp. nov. (♂♀), *Tantra bugle* gen. et sp. nov. (♂♀), *Tantra embera* gen. et sp. nov. (♂♀), *Tantra kuna* gen. et sp. nov. (♂♀), *Tantra naso* gen. et sp. nov. (♂♀), *Tantra ngabe* gen. et sp. nov. (♂♀), *Tantra sichid* gen. et sp. nov. (♀), and *Tantra wounaan* gen. et sp. nov. (♂♀). *Tantra kullki* (Dupérré & Tapia, 2017) comb. nov. is transferred from *Theridiosoma* O. Pickard-Cambridge, 1879. Six new species of *Baalzebub* Coddington, 1986 are described: *Baalzebub absoguedi* sp. nov. (♀), *Baalzebub antomia* sp. nov. (♂), *Baalzebub innatuledi* sp. nov. (♂♀), *Baalzebub jaibana* sp. nov. (♂♀), *Baalzebub nele* sp. nov. (♀), *Baalzebub sukia* sp. nov. (♂♀). The male of *Baalzebub albonotatus* (Petrunkevitch, 1930) and *Theridiosoma goodnightorum* Archer, 1953 are described for the first time. Redescriptions and illustrations of *Epilineutes globosus* (O. Pickard-Cambridge, 1896), *Naatlo fauna* (Simon, 1897), and *Wendilgarda clara* Keyserling, 1886 are provided. Notably, we find that gross morphology remains a reliable tool for rapid species sorting, while crude or genetic identification methods offer consistent estimates for alpha diversity. The prevalence of endemic species at mid and high elevations further underscores the importance of our findings.

Keywords. Symphytognathoids, Neotropical Region, integrative taxonomy, DNA barcoding, *Tantra* gen. nov.

Labarque F.M., Piacentini L.N., Pons J., Hormiga G., Arnedo M.A. & Ramirez M.J. 2025. Ray spider rush: Fast-tracking integrative taxonomy in Panama's cloud forests. *European Journal of Taxonomy* 1010: 1–145. https://doi.org/10.5852/ejt.2025.1010.3021

Introduction

Taxonomy plays a crucial role in biodiversity research, yet species discovery in hyperdiverse regions vastly outpaces formal taxonomic revision, leading to a significant time lag in species documentation (Wheeler 2004, 2008; Fontaine *et al*. 2012; Agnarsson *et al*. 2013). This taxonomic impediment has fueled ongoing debates on how to balance rigor with efficiency in species descriptions, particularly in the face of a global biodiversity crisis (Taylor 1983; Myers *et al*. 2000; Godfray 2002, 2007; Rivera-Quiroz & Álvarez-Padilla 2023). Traditional taxonomy, though fundamental, is often slow and resource-intensive, relying on highly specialized morphological analyses (Fontaine *et al*. 2012). Meanwhile, molecular tools have revolutionized species delimitation (Hebert *et al*. 2003a; Pons *et al*. 2006; Coddington *et al*. 2016) but remain underutilized in spider taxonomy – only 6% of studies include genetic data, and fewer than 14% use an integrative approach (Bond *et al*. 2022). Recent efforts emphasize the need for pragmatic taxonomic workflows that integrate morphology and molecular data to accelerate species documentation while maintaining taxonomic reliability (Wheeler 2004, 2023; Dayrat 2005; Will *et al.* 2005; Padial *et al*. 2009; Cao *et al*. 2016). Our study aligns with this shift, employing an integrative approach that leverages DNA barcoding and morphological sorting to efficiently delimit and describe species.

We focus on ray spiders (family Theridiosomatidae Simon, 1881), a group of minute ecribellate orb-weavers that remain taxonomically underexplored despite their widespread tropical distribution (Coddington 1986; World Spider Catalog 2025). The family currently includes 22 genera and 150 species, but species delimitation is challenging due to the uniformity of genital morphology, the primary diagnostic feature in spider taxonomy (Labarque & Griswold 2014; Bond *et al*. 2022). While some species exhibit distinct opisthosomal coloration, these traits are often insufficient for distinguishing closely related species (Coddington 1986; Miller *et al*. 2009; Wienskoski 2010; Dupérré & Tapia 2017; Zhao & Li 2012; Suzuki *et al*. 2022; Zhang *et al*. 2023). Given these challenges, Theridiosomatidae

provides an ideal model to test how integrative taxonomy improves species delimitation, particularly for taxa with cryptic diversity and subtle morphological differences (Castalanelli *et al*. 2014; Lopardo & Uhl 2014; Oh *et al*. 2022).

Tropical spider diversity exhibits high species turnover across altitudinal gradients, with minimal overlap between local assemblages (Nogueira *et al*. 2006; Ricetti & Bonaldo 2008; Agnarsson *et al*. 2013). By conducting an extensive inventory across cloud forests in Panama, we assess species richness, endemism, and diversity patterns while testing the efficiency of an integrative taxonomic framework (Olson 1994; Coddington *et al*. 2009).

To overcome the limitations of purely morphological taxonomy, we employ an integrative framework that combines morphological sorting, DNA barcoding, and photographic documentation. Unlike barcode-based approaches that omit morphological descriptions (e.g., Sharkey *et al*. 2021), our study balances molecular data with detailed morphological validation, ensuring that species hypotheses remain testable and reproducible (Bond *et al*. 2022).

To facilitate accessibility and future taxonomic work, we provide high-resolution images of entire specimens and key morphological traits instead of traditional scientific illustrations. While light photography has become increasingly accepted in taxonomy (Bond *et al*. 2022), we acknowledge that image resolution may limit fine-scale morphological interpretation. However, the combination of DNA barcoding, morphological descriptions, and interpretative analysis ensures species are thoroughly diagnosed rather than relying solely on a single data source (Álvarez-Padilla *et al*. 2020; Rivera-Quiroz & Álvarez-Padilla 2023). In addition to species descriptions, we apply semi-quantitative sampling protocols to estimate species accumulation curves, diversity metrics, and endemism, evaluating how well our approach captures Theridiosomatidae diversity across Panamanian cloud forests (Coddington *et al*. 2009).

In summary, this study applies an integrative taxonomic framework to the Theridiosomatidae of Panamanian cloud forests, combining morphological sorting, DNA barcoding, and photographic documentation to enhance species delimitation. By bridging the gap between traditional taxonomy and modern biodiversity informatics, we aim to accelerate species discovery while maintaining scientific rigor. Our findings contribute to the ongoing discourse on pragmatic taxonomy, demonstrating how a balanced methodology can streamline species documentation without compromising reliability (Godfray *et al*. 2008). Beyond taxonomy, our study provides insights into species richness, endemism, and diversity patterns, reinforcing the importance of rapid yet robust taxonomic workflows in addressing biodiversity loss.

Material and methods

Study area

Sampling was conducted between June and July of 2007 and 2008 at four one-hectare plots along the mountain rainforests of the Cordillera Central in western Panama, spanning from the Costa Rican border to the Isthmus of Panama. The collecting sites, including coordinates and elevation (meters above sea level), are as follows: (1) PILA: La Amistad International Park (8.890500° N, 82.618778° W, 2299 m a.s.l.), (2) RFF: Fortuna Forest Reserve (8.750083° N, 82.239083° W, 1135 m a.s.l.), (3) COPE: G.D. Omar Torrijos Herrera National Park (8.668083° N, 80.592583° W, 760 m a.s.l.), and (4) PNAC: Altos de Campana National Park (8.683444° N, 79.929833° W, 895 m a.s.l.). These sites form a longitudinal transect of ~300 km, with the greatest distance between localities being 180 km (RFF to COPE) and the shortest 45 km (PILA to RFF) (Fig. 1).

Semi-quantitative sampling

Spiders were collected using standardized semi-quantitative protocols (Coddington *et al.* 1991; Sørensen *et al.* 2002; Scharff *et al.* 2003) designed to maximize species representation while ensuring efficiency. Four collection methods were used: 'Looking Up', direct collection above knee level to arm reach; 'Looking Down', direct collection below knee level to the ground; 'Beating', spiders collected from a sheet after striking vegetation with a stick; and 'Cryptic', active searches under stones, leaf-litter, dead logs, and decaying plant debris. Pitfalls were excluded due to shallow soil layers and high groundwater levels. At each site, 125 one-hour samples were collected within a one-hectare plot by five collectors over five consecutive days, each collecting five samples per day during both daylight and nighttime hours. Each specimen received a unique alphanumeric code encoding the sampling metadata, including locality, method, time, date, and collector (Table 1). While the same day number may occur in different years (e.g., "12" for 12 June 2007 and 2008), the full code is unambiguous because it integrates all contextual information. COPE and PILA were sampled in 2008, while RFF and PNAC were sampled in 2007, ensuring chronological distinction among samples. Specimens were preserved in 100% ethanol and stored at -20°C for DNA barcoding. Additionally, non-quantitative samples (NQ) were collected outside plot boundaries to supplement the semi-quantitative protocol.

Specimen identification

Species identification represents a major challenge in biodiversity studies, particularly in hyperdiverse tropical environments where taxonomic knowledge is limited (see Coddington *et al*. 1991). To address this, we developed a three-step approach that integrates DNA barcoding with morphological examination to accelerate species identification and discovery.

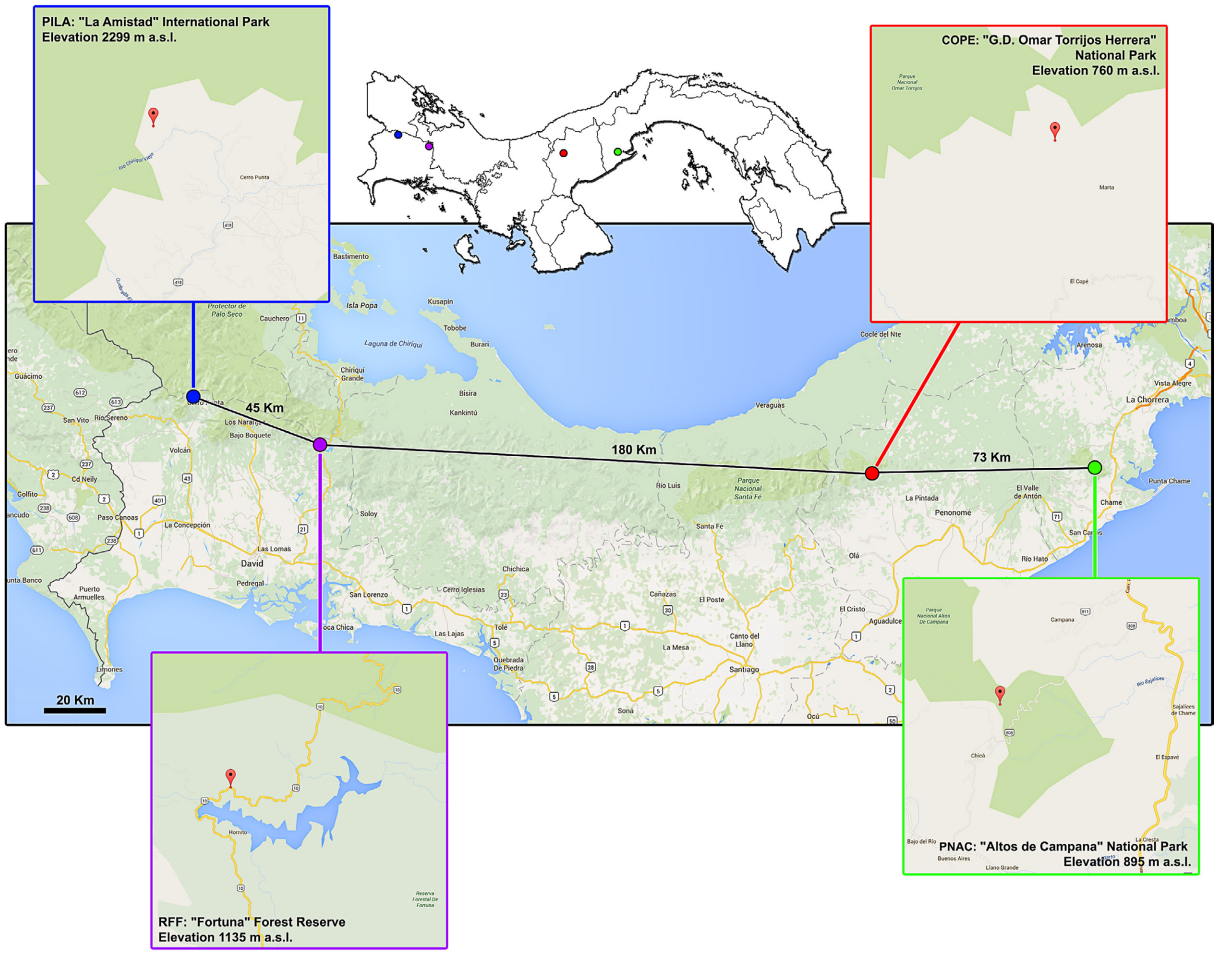

Fig. 1. Sampling locations and elevations (meters above sea level) in Panamanian protected areas.

Table 1. Codes used for specimens, indicating the sampling protocols for the semiquatitative analyses, locality, method, sample number, time, day, collector and specimen number. Every specimen received a unique identifier; for example, SFU1NAA029 indicates: NP Fortuna, looking up, first sample at night, 10 June 2007, collected by M. Arnedo, specimen 029 in the sample.

Project		**Locality** (125 samples each)		**Method**		**Sample number** (one hour each)		**Time**		**Day**		**Collector**		**Specimen number**	
Pancoding Spiders	**S**	Fortuna	**F**	Beating	**B**	first	**1**	Day	**D**	7 Jun. 2007	**7**	Miquel Arnedo	**A**	3 digits	###
		Campana	**C**	Cryptic	**C**	second	**2**	Night	**N**	8 Jun. 2007	**8**	Dimitar Dimitrov	**D**		
		Omar Torrijos Herrera	**T**	Looking down	**D**					9 Jun. 2007	**9**	Gustavo Hormiga	**H**		
		La Amistad	**A**	Looking up	**U**					10 Jun. 2007	**A**	Facundo Labarque	**L**		
										11 Jun. 2007	**B**	Martín Ramírez	**R**		
										12 Jun. 2007	**C**	Ligia Benavides	**B**		
										14 Jun. 2007	**D**	Luis Piacentini	**P**		
										15 Jun. 2007	**E**				
										16 Jun. 2007	**F**				
										17 Jun. 2007	**G**				
										18 Jun. 2007	**H**				
										19 Jun. 2007	**I**				
										4 Jun. 2008	**4**				
										5 Jun. 2008	**5**				
										6 Jun. 2008	**6**				
										7 Jun. 2008	**7**				
										8 Jun. 2008	**8**				
										9 Jun. 2008	**9**				
										12 Jun. 2008	**C**				
										13 Jun. 2008	**D**				
										14 Jun. 2008	**E**				
										15 Jun. 2008	**F**				
										16 Jun. 2008	**G**				
										17 Jun. 2008	**H**				

Fast morphospecies identification

Initially, specimens were sorted into species or morphospecies (Oliver & Beatti 1996) based on gross external morphology (e.g., body length, coloration, and shape) along with a preliminary examination of external sexual organs (male palp and female epigyne), without dissection to minimize time and effort. This process was guided primarily by the global taxonomic revision of Theridiosomatidae (Coddington 1986). Morphospecies were assigned a provisional identification code consisting of the genus name, followed by a species number (e.g., sp.1, sp.2, sp.3) and the morphotype author's initials (e.g., *Epeirotypus* sp.1 FML, where FML stand for Facundo M. Labarque).

GMYC cluster identification

Next, DNA barcoding was performed for up to ten individuals per morphospecies and per plot (five males and five females when possible; see Molecular data). We applied the General Mixed Yule-Coalescent (GMYC) model (Pons *et al.* 2006) to delimit species, as it has been shown to outperform distance-based approaches (Powell *et al.* 2011). The GMYC method identifies clusters of coalescent sequences – interpreted as candidate species – by detecting the transition from interspecific to intraspecific branching in an ultrametric tree (Planas *et al.* 2013). Although GMYC is widely used and generally robust (Fujisawa & Barraclough 2013; Talavera *et al.* 2013), it has been reported to over-split the data, which we accounted for in subsequent validation steps.

Integrative identification

Finally, we combine the candidate species identified through both the fast morphospecies sorting and the GMYC clustering. In cases where discrepancies arose between these two approaches, we conducted a detailed dissection and examination of genitalic characters to resolve inconsistencies and validate species delimitation.

Morphological data

The examined material is deposited in the following institutions (abbreviation and curators in parentheses): Museo Argentino de Ciencias Naturales "Bernardino Rivadavia", Buenos Aires, Argentina (MACN-Ar, M. Ramírez), Museo de Invertebrados GB Fairchild, Universidad de Panamá (MIUP, D. Quintero); Museum of Comparative Zoology, Harvard, USA (MCZ, M. Srivastava), and the Centre de Recursos de Biodiversitat Animal, Universitat de Barcelona, Spain (CRBA, A. Serra).

Morphological examinations were conducted using Leica M205 A, Leica M165 C, and Nikon SMZ1500 stereo microscopes with incident light, and a compound Olympus BH-2 microscope with transmitted light. Digital images were captured with Leica DFC295, Leica DFC290, and Nikon DXM1200 digital cameras, respectively. Extended focal range images were processed with Leica Application Suite ver. 3.6.0., or Helicon Focus ver. 3.10.3, 4.01 Pro and 4.62 Pro (Khmelik *et al.* 2006). Preparations were carefully cleaned using fine brushes, a thin jet of alcohol from a pipette, or an ultrasonic cleaner (Bransonic 1510R MT). Specimens were preserved in 100% ethanol (or 75% ethanol in some cases), stored at -20°C, and sequenced within two years of collection. Coloration descriptions are based on ethanol-preserved specimens (see Taxonomy). For scanning electron microscope (SEM) imaging, preparations were critical-point dried, mounted on adhesive copper tape (Electron Microscopy Sciences, EMS 77802), and secured with colloidal graphite paint (EMS 12660). Prior to SEM examination under high vacuum with a FEI XL30 TMP or a LEO 1450VP, the preparations were sputter-coated with Au-Pd. Female genitalia were digested with KOH and examined in clove oil or lactic acid after dissection. All measurements are reported in millimeters (mm).

Names of new taxa derived from Panamanian native people languages and other sources (see Taxonomy) were translated into English using Glosbe Dictionary (https://glosbe.com/).

The genus descriptions in Taxonomy only present novel information, as full descriptions are available in Coddington (1986) and Labarque & Griswold (2014). Given the high quality of these references, we opted not to replicate their descriptions.

Abbreviations

The following abbreviations are used throughout the text and figures (see Taxonomy):

Prosoma

AME = anterior median eye
PME = posterior median eye

Legs

PsM = prolateral strong macrosetae
RmP = retrolateral membranous patch on tibia I
TH = laterally higher thoracic area

Opisthosoma

AT = anterior tubercle
LT = lateral tubercle
PT = posterior tubercle

Male palp

C = conductor
CA = conductor apophysis
Ce = conductor posterior extension
E = embolus
EA = embolic apophysis
ED = embolic division
MA = median apophysis
mEA = embolic apophysis mesal branch
P = paracymbium
pEA = embolic apophysis prolateral branch
PP = paracymbial process
rEA = embolic apophysis retrolateral branch
SR = setae row
ST = subtegulum
T = tegulum
TP = tegular pocket
TPa = tegular pocket anterior side
TS = tegular striae
Tsp = tegular spur

Epigyne and vulva

BS = bifid septum
CD = copulatory duct
CDe = copulatory duct ending
CP = central pit
DP = epigynal dorsal plate
EF = epigynal flap
ELS = epigynal lateral spur
EP = epigynal plate
FD = fertilization ducts
GD = patch of gland ducts
LP = lateral pit
S = spermatheca
SC = dorsal scape
TG = transverse groove
UE = uterus externus

Molecular data

The dataset comprises 249 sequences, of which 246 were newly sequenced in this study, while three were obtained from GenBank (HM030436, HM030431, GU456915). We excluded a sequence (EU003286, *Epeirotypus brevipes*) due to its high proportion of missing data (14%). Theridiosomatidae has been proposed as the sister group to all other symphytognathoid families, the Anterior Tracheal System clade (ANTS; see Lopardo *et al.* 2010; Kulkarni *et al.* 2020, 2023). To provide a robust phylogenetic framework, we included three outgroup taxa: *Mysmena* sp.1 FML (Mysmenidae Petrunkevitch, 1928), *Anapis monteverde* (Anapidae Simon, 1895), and *Patu digua* (Symphytognathidae Hickman, 1931) (Table 2). Due to technical limitations, we were unable to obtain molecular data from *Baalzebub absoguedi* sp. nov., *Baalzebub antomia* sp. nov., and *Tantra sichid* gen. et sp. nov. (see Table 3). Voucher identifiers, GenBank accession numbers, and BOLD Systems sequence identifiers (Ratnasingham & Hebert 2007) are provided in Table 2.

Total genomic DNA was extracted from freshly collected specimens preserved in 100% ethanol, using four legs of medium-sized adults or whole individuals for very small-sized immatures. DNA extraction were conducted at three institutions, employing distinct protocols: Centre de Recursos de Biodiversitat Animal, Universitat de Barcelona (CRBA, Spain), used Qiagen DNeasy Tissue Kits for manual extractions, Institut Mediterrani d'Estudis Avançats (IMEDEA, Spain), used an ABI PRISM® 6700 Automated Nucleic Acid Workstation (Applied Biosystems) with Wizard® SV 96 Genomic DNA Purification System (PROMEGA), and the Biodiversity Institute of Ontario (BIO, Canada) followed the Glass-fiber DNA extraction protocol (Ivanova *et al.* 2006). Each tissue sample was placed in sterilized cryotubes (CRBA) or 96-well plates containing 100% ethanol (IMEDEA, BIO), with one well per plate left empty as a negative control. DNA was extracted following an overnight incubation at 50°C in a lysis buffer (5 mL) with Proteinase K (500 µL, 20 mg/L), followed by centrifugation. Samples were processed using a robotic liquid-handling system that automates binding, vacuum filtration, and washing steps, ensuring high-throughput sample processing (Ivanova *et al.* 2006) (IMEDEA, BIO). DNA concentration and purity were assessed via spectrophotometry, and quality was confirmed through electrophoresis in 1.8% agarose/TBE gel (CRBA).

A ~675 bp fragment of the mitochondrial cytochrome c oxidase subunit I (*cox* 1) gene, a widely used marker in DNA barcoding studies (Hebert *et al.* 2003a, 2003b; Astrin *et al.* 2006), was amplified using primers listed in Table 4. The polymerase chain reaction (PCR) cocktail contained primers (0.1 µM each), dNTPs (0.2 mM each) and AmpliTaq DNA polymerase (0.1 U/µl for a 25 µl reaction), and $MgCl_2$ (2 mM) for CRBA and IMEDEA, while BIO followed standard protocols from the Canadian Centre for DNA barcoding (Ivanova & Grainger 2007). PCR products were visualized on 1.8% agarose/TBE gel and purified using Millipore MultiScreen® 96-well filtration plates (Multiscreen HTS 96 FB MSFBN6B50) following the manufacturer's specifications (CRBA). DNA was sequenced on the forward chain (IMEDEA) or bi-directionally (CRBA, BIO) through the cycle sequencing method using dye terminators (Sanger *et al.* 1977) and the ABI PRISM BigDye Terminator Cycle Sequencing Ready Reaction with AmpliTaq DNA Polymerase FS kit. Sequenced products were cleaned using Princeton Separations CentriSep columns and run out on an ABI PRISM 3100 automated sequencer (CRBA, IMEDEA) or an ABI3730XL Genetic Analyzer (Applied Biosystems) (BIO).

Sequence errors and ambiguities were edited using the STADEN PACKAGE ver. 1.4.0 (http://staden.sourceforge.net/). Each sequence was BLASTed (Altschul *et al.* 1997; http://ncbi.nlm.nih.gov/) against the GenBank nucleotide database. We excluded samples of low-quality with ambiguous readings from the matrix. Sequences were managed in BIOEDIT ver. 7.0.5.2 (Hall 1999) and stop codons were checked in DNASP ver. 5.10.1 (Librado & Rozas 2009) (CRBA, IMEDEA). Sequences were also handled in CODONCODE ALIGNER ver. 3.0.2 (CodonCode Corporation) (BIO).

Table 2 (continued on next ten pages). List of the specimens used for the molecular phylogenetic analysis in the study, vouchers codes, DNA protocol, identification type (quantity), sex and localities. BIO=Biodiversity Intitute of Ontario; COPE=G.D. Omar Torrijos Herrera National Park; IMEDEA=Institut Mediterrani d'Estudis Avançats; PILA=La Amistad International Park; PNAC=Altos de Campana National Park; RFF=Forest Reserve Fortuna; CRBA=Centre de Recursos de Biodiversitat Animal. Numbers in parentheses=taxa quantity; Bold numbers=GMYC haplotypes (as in Fig. 2); Bold taxa=GenBank-only data.

Voucher Codes	BOLD Sequence ID / GenBank ID	Protocol	Family / Subfamily	Fast Identification (27)	GMYC Cluster Number	Integrative Identification (29)	Sex	Locality
SCD1NDR015	SPIPO354-10	BIO	Mysmenidae (MYS, 1)			*Mysmena* sp.1 FML	F	COPE
SFC1DBR021	SPIPO006-10	BIO	Anapidae (ANA, 1)	*Anapis monteverde*		*Anapis monteverde* Platnick & Shadab, 1978	F	RFF
SFC1DAH006	SPIPO778-10	BIO	Symphytognathidae (SYM, 1)			*Patu digua* Forster & Platnick, 1977	F	RFF
	– / GU456915	–	Theridiosomatidae (THS, 246)		**15**	***Coddingtonia euryopoides* Miller, Griswold & Yin, 2009**		–
	– / HM030431	–	THS / Epeirotypinae (73)		**4**	***Epeirotypus chavarria* Coddington, 1986**		–
SFC1N8H018	SPIPA404-10	BIO		*Epeirotypus* sp.1 FML	5	*Epeirotypus kwakwa* sp. nov.	F	RFF
SFC1NAR016	epes1168 / PX096944	CRBA		*Epeirotypus* sp.1 FML	5	*Epeirotypus kwakwa* sp. nov.	F	RFF
SFC1NCD018	SPIPA400-10	BIO		*Epeirotypus* sp.1 FML	5	*Epeirotypus kwakwa* sp. nov.	F	RFF
SFD1D8R010	epes1120 / PX096942	CRBA		*Epeirotypus* sp.1 FML	**5**	*Epeirotypus kwakwa* sp. nov.	M	RFF
SFD1DAR018	epes1166 / PX096941	CRBA		*Epeirotypus* sp.1 FML	5	*Epeirotypus kwakwa* sp. nov.	F	RFF
SFD1NBL015	epes1058 / PX096940	CRBA		*Epeirotypus* sp.1 FML	**5**	*Epeirotypus kwakwa* sp. nov.	F	RFF
SFD1NCD016	SPIPA402-10	BIO		*Epeirotypus* sp.1 FML	5	*Epeirotypus kwakwa* sp. nov.	F	RFF
SFU1N7H029	SPIPA401-10	BIO		*Epeirotypus* sp.1 FML	**5**	*Epeirotypus kwakwa* sp. nov.	F	RFF
SFU1NCD030	epes1167 / PX096943	CRBA		*Epeirotypus* sp.1 FML	5	*Epeirotypus kwakwa* sp. nov.	F	RFF
SFU2NCH029	SPIPA403-10	BIO		*Epeirotypus* sp.1 FML	**5**	*Epeirotypus kwakwa* sp. nov.	M	RFF
SAD1NFP007	epes2176 / PX096956	CRBA		*Epeirotypus* sp.2 FML	**6**	*Epeirotypus kote* sp. nov.	F	PILA
SAU1NGA024	epes2205 / PX096958	CRBA		*Epeirotypus* sp.2 FML	6	*Epeirotypus kote* sp. nov.	M	PILA
SAU1NGH021	epes2204 / PX096957	CRBA		*Epeirotypus* sp.2 FML	6	*Epeirotypus kote* sp. nov.	M	PILA
SAU1NHA026	epes2206 / PX096959	CRBA		*Epeirotypus* sp.2 FML	**6**	*Epeirotypus kote* sp. nov.	F	PILA
SFB1DAH019	epes2183 / PX096947	CRBA		*Epeirotypus* sp.2 FML	7	*Epeirotypus kra* sp. nov.	M	RFF
SFD1DAA016	epes2184 / PX096948	CRBA		*Epeirotypus* sp.2 FML	7	*Epeirotypus kra* sp. nov.	F	RFF

Table 2 (continued). List of the specimens used for the molecular phylogenetic analysis in the study, vouchers codes, DNA protocol, identification type (quantity), sex and localities. BIO=Biodiversity Intitute of Ontario; COPE=G.D. Omar Torrijos Herrera National Park; IMEDEA= Institut Mediterrani d'Estudis Avançats; PILA=La Amistad International Park; PNAC=Altos de Campana National Park; RFF=Forest Reserve Fortuna; CRBA=Centre de Recursos de Biodiversitat Animal. Numbers in parentheses=taxa quantity; Bold numbers=GMYC haplotypes (as in Figure 2); Bold taxa=GenBank-only data.

Voucher Codes	BOLD Sequence ID / GenBank ID	Protocol	Family / Subfamily	Fast Identification (27)	GMYC Cluster Number	Integrative Identification (29)	Sex	Locality
SFU1N8A024	epes2203 / PX096949	CRBA		*Epeirotypus* sp.2 FML	7	*Epeirotypus kra* sp. nov.	F	RFF
SFU1NAA009	epes2053 / PX096945	CRBA		*Epeirotypus* sp.2 FML	**7**	*Epeirotypus kra* sp. nov.	M	RFF
SFU2NBD029	epes2063 / PX096946	CRBA		*Epeirotypus* sp.2 FML	7	*Epeirotypus kra* sp. nov.	F	RFF
SFU1N7H026	SPIPA391-10	BIO		*Epeirotypus* sp.3 FML	7	*Epeirotypus kra* sp. nov.	F	RFF
SFU1N8L020	epes3111 / PX096951	CRBA		*Epeirotypus* sp.3 FML	7	*Epeirotypus kra* sp. nov.	M	RFF
SFU1NBH019	SPIPA390-10	BIO		*Epeirotypus* sp.3 FML	7	*Epeirotypus kra* sp. nov.	F	RFF
SFU1NCA029	epes3208 / PX096953	CRBA		*Epeirotypus* sp.3 FML	7	*Epeirotypus kra* sp. nov.	F	RFF
SFU2NBA026	epes3209 / PX096954	CRBA		*Epeirotypus* sp.3 FML	7	*Epeirotypus kra* sp. nov.	F	RFF
SFU2NCH031	epes3207 / PX096952	CRBA		*Epeirotypus* sp.3 FML	7	*Epeirotypus kra* sp. nov.	F	RFF
SFU2NBH025	epes4070 / PX096965	CRBA		*Epeirotypus* sp.4 FML	**9**	*Epeirotypus tain* sp. nov.	F	RFF
SFD1DAL018	epes5062 / PX096955	CRBA		*Epeirotypus* sp.5 FML	7	*Epeirotypus kra* sp. nov.	F	RFF
STC1D5H013	SPIPA395-10	BIO		*Epeirotypus* sp.6 FML	**3**	*Epeirotypus jane* sp. nov.	F	COPE
SAC1DHH007	SPIPA389-10	BIO		*Epeirotypus* sp.7 FML	8	*Epeirotypus bule* sp. nov.	F	PILA
SAU1NCL062	SPIPA385-10	BIO		*Theridiosoma* sp.7 FML	10	*Epeirotypus drune* sp. nov.	F	PILA
SAC1DHH012	epes7100 / PX096960	CRBA		*Epeirotypus* sp.7 FML	**10**	*Epeirotypus drune* sp. nov.	F	PILA
SAU1NCL035	epes7240 / PX096962	CRBA		*Epeirotypus* sp.7 FML	8	*Epeirotypus bule* sp. nov.	F	PILA
SAU1NCR002	SPIPA387-10	BIO		*Epeirotypus* sp.7 FML	**8**	*Epeirotypus bule* sp. nov.	F	PILA
SAU1NCR048	epes7237 / PX096961	CRBA		*Epeirotypus* sp.7 FML	10	*Epeirotypus drune* sp. nov.	F	PILA
SAU2NCL028	epes7239 / PX096964	CRBA		*Epeirotypus* sp.7 FML	8	*Epeirotypus bule* sp. nov.	F	PILA
SAU2NCL033	epes7238 / PX096963	CRBA		*Epeirotypus* sp.7 FML	**8**	*Epeirotypus bule* sp. nov.	F	PILA
SFB1D9R032	naafa191 / PX096968	CRBA		*Naatlo fauna*	11	*Naatlo fauna* (Simon, 1897)	F	RFF
SFB1DAR028	naafa056 / PX096967	CRBA		*Naatlo fauna*	**11**	*Naatlo fauna*	M	RFF
SFB2D9R026	SPIPA373-10	BIO		*Naatlo fauna*	11	*Naatlo fauna*	M	RFF
SFC1DBR019	naafa118 / PX096966	CRBA		*Naatlo fauna*	**11**	*Naatlo fauna*	F	RFF

Table 2 (continued). List of the specimens used for the molecular phylogenetic analysis in the study, vouchers codes, DNA protocol, identification type (quantity), sex and localities. BIO=Biodiversity Intitute of Ontario; COPE=G.D. Omar Torrijos Herrera National Park; IMEDEA= Institut Mediterrani d'Estudis Avançats; PILA=La Amistad International Park; PNAC=Altos de Campana National Park; RFF=Forest Reserve Fortuna; CRBA=Centre de Recursos de Biodiversitat Animal. Numbers in parentheses=taxa quantity; Bold numbers=GMYC haplotypes (as in Figure 2); Bold taxa=GenBank-only data.

Voucher Codes	BOLD Sequence ID / GenBank ID	Protocol	Family / Subfamily	Fast Identification (27)	GMYC Cluster Number	Integrative Identification (29)	Sex	Locality
SFD1NBR033	SPIPA374-10	BIO		*Naatlo fauna*	11	*Naatlo fauna*	F	RFF
SFU1N8A036	SPIPA376-10	BIO		*Naatlo fauna*	11	*Naatlo fauna*	F	RFF
SFU1N8R028	SPIPA375-10	BIO		*Naatlo fauna*	11	*Naatlo fauna*	F	RFF
SFU1NBR037	naafa189 / PX096969	CRBA		*Naatlo fauna*	**11**	*Naatlo fauna*	M	RFF
SFU1NCD031	SPIPA377-10	BIO		*Naatlo fauna*	11	*Naatlo fauna*	M	RFF
SFU1NCL016	naafa190 / PX096970	CRBA		*Naatlo fauna*	**11**	*Naatlo fauna*	F	RFF
SCB1DFR042	naas1187 / PX096980	CRBA		*Naatlo* sp.1 FML	12	*Naatlo chi* sp. nov.	M	PNAC
SCB1DGD011	naas1192 / PX096977	CRBA		*Naatlo* sp.1 FML	12	*Naatlo chi* sp. nov.	F	PNAC
SCB1DIA010	SPIPA371-10	BIO		*Naatlo* sp.1 FML	12	*Naatlo chi* sp. nov.	F	PNAC
SCC1NER014	SPIPA370-10	BIO		*Naatlo* sp.1 FML	12	*Naatlo chi* sp. nov.	F	PNAC
SCC1NHD013	SPIPA372-10	BIO		*Naatlo* sp.1 FML	12	*Naatlo chi* sp. nov.	F	PNAC
SCC2NFH008	SPIPA369-10	BIO		*Naatlo* sp.1 FML	12	*Naatlo chi* sp. nov.	F	PNAC
SCU1NDH021	naas1115 / PX096976	CRBA		*Naatlo* sp.1 FML	**12**	*Naatlo chi* sp. nov.	M	PNAC
SCU1NGH027	naas1272 / PX096978	CRBA		*Naatlo* sp.1 FML	12	*Naatlo chi* sp. nov.	M	PNAC
SFB1D8L018	SPIPA364-10	BIO		*Naatlo* sp.1 FML	**14**	*Naatlo chi* sp. nov.	F	RFF
SFB1D9H035	naas1112 / PX096971	CRBA		*Naatlo* sp.1 FML	**13**	*Naatlo chi* sp. nov.	F	RFF
SFC1DAH012	naas1271 / PX096972	CRBA		*Naatlo* sp.1 FML	13	*Naatlo chi* sp. nov.	F	RFF
SFU1N7R038	naas1273 / PX096974	CRBA		*Naatlo* sp.1 FML	**14**	*Naatlo chi* sp. nov.	F	RFF
SFU1N8H023	SPIPA366-10	BIO		*Naatlo* sp.1 FML	14	*Naatlo chi* sp. nov.	F	RFF
SFU1NBR036	SPIPA363-10	BIO		*Naatlo* sp.1 FML	13	*Naatlo chi* sp. nov.	F	RFF
SFU1NCR036	naas1269 / PX096975	CRBA		*Naatlo* sp.1 FML	**14**	*Naatlo chi* sp. nov.	F	RFF
SFU1NCR045	SPIPA367-10	BIO		*Naatlo* sp.1 FML	13	*Naatlo chi* sp. nov.	F	RFF
SFU2NBH044	naas1268 / PX096973	CRBA		*Naatlo* sp.1 FML	**14**	*Naatlo chi* sp. nov.	F	RFF
SFU2NCH028	SPIPA365-10	BIO		*Naatlo* sp.1 FML	**13**	*Naatlo chi* sp. nov.	F	RFF

Table 2 (continued). List of the specimens used for the molecular phylogenetic analysis in the study, vouchers codes, DNA protocol, identification type (quantity), sex and localities. BIO=Biodiversity Intitute of Ontario; COPE=G.D. Omar Torrijos Herrera National Park; IMEDEA= Institut Mediterrani d'Estudis Avançats; PILA=La Amistad International Park; PNAC=Altos de Campana National Park; RFF=Forest Reserve Fortuna; CRBA=Centre de Recursos de Biodiversitat Animal. Numbers in parentheses=taxa quantity; Bold numbers=GMYC haplotypes (as in Figure 2); Bold taxa=GenBank-only data.

Voucher Codes	BOLD Sequence ID / GenBank ID	Protocol	Family / Subfamily	Fast Identification (27)	GMYC Cluster Number	Integrative Identification (29)	Sex	Locality
STB1D9A009	SPIPA368-10	BIO		*Naatlo* sp.1 FML	12	*Naatlo chi* sp. nov.	M	COPE
STB1D9R019	naas1270 / PX096984	CRBA		*Naatlo* sp.1 FML	12	*Naatlo chi* sp. nov.	M	COPE
STC1D5A014	naas1188 / PX096982	CRBA		*Naatlo* sp.1 FML	12	*Naatlo chi* sp. nov.	M	COPE
STD1N7B029	naas1186 / PX096981	CRBA		*Naatlo* sp.1 FML	**12**	*Naatlo chi* sp. nov.	F	COPE
STD1N7H025	naas1266 / PX096983	CRBA		*Naatlo* sp.1 FML	12	*Naatlo chi* sp. nov.	F	COPE
STD1N7R022	naas1267 / PX096985	CRBA		*Naatlo* sp.1 FML	**12**	*Naatlo chi* sp. nov.	F	COPE
SCD1NFD017	naas1185 / PX096979	CRBA		*Naatlo* sp.1 FML	**12**	*Naatlo chi* sp. nov.	F	PNAC
SFU2NBH023	epes3054 / PX096950	CRBA		*Epeirotypus* sp.3 FML	7	*Epeirotypus kra* sp. nov.	F	RFF
SCD1DFR014	SPIPA119-10	BIO	THS / Ogulniinae (22)	*Ogulnius* sp.1 FML	1	*Ogulnius zbodro* sp. nov.	F	PNAC
SCD1DFR031	SPIPA120-10	BIO		*Ogulnius* sp.1 FML	1	*Ogulnius zbodro* sp. nov.	F	PNAC
SCD1DHR010	SPIPA361-10	BIO		*Ogulnius* sp.1 FML	1	*Ogulnius zbodro* sp. nov.	F	PNAC
SCD1NGR012	SPIPA362-10	BIO		*Ogulnius* sp.1 FML	1	*Ogulnius zbodro* sp. nov.	M	PNAC
SAC1DDB013	oguoc103 / PX097010	CRBA		*Ogulnius* cf *obtectus*	**2**	*Ogulnius debonaja* sp. nov.	F	PILA
SAU1NCB026	oguoc196 / PX097012	CRBA		*Ogulnius* cf *obtectus*	2	*Ogulnius debonaja sp. nov.*	F	PILA
SAU2NCL030	oguoc198 / PX097013	CRBA		*Ogulnius* cf *obtectus*	2	*Ogulnius debonaja sp. nov.*	F	PILA
SAU2NCL034	oguoc194 / PX097011	CRBA		*Ogulnius* cf *obtectus*	2	*Ogulnius debonaja sp. nov.*	F	PILA
SCD1DFH007	oguoc195 / PX097019	CRBA		*Ogulnius* cf *obtectus*	1	*Ogulnius zbodro* sp. nov.	F	PNAC
SCC1DER017	ogus1119 / PX097021	CRBA		*Ogulnius* sp.1 FML	1	*Ogulnius zbodro* sp. nov.	M	PNAC
SCD1DFD013	SPIPA360-10	BIO		*Ogulnius* sp.1 FML	1	*Ogulnius zbodro* sp. nov.	F	PNAC
SCD1DFR015	ogus1110 / PX097020	CRBA		*Ogulnius* sp.1 FML	1	*Ogulnius zbodro* sp. nov.	F	PNAC
SCD1NER013	oguoc193 / PX097018	CRBA		*Ogulnius* sp.1 FML	**1**	*Ogulnius zbodro* sp. nov.	F	PNAC
SAB1DDA002	SPIPA356-10	BIO		*Ogulnius* sp.2 FML	**2**	*Ogulnius debonaja sp. nov.*	F	PILA
SAB1DHL021	ogus2197 / PX097015	CRBA		*Ogulnius* sp.2 FML	2	*Ogulnius debonaja sp. nov.*	M	PILA
SAC1DEH003	ogus2199 / PX097009	CRBA		*Ogulnius* sp.2 FML	**2**	*Ogulnius debonaja sp. nov.*	M	PILA
SAD1NGL022	ogus2200 / PX097016	CRBA		*Ogulnius* sp.2 FML	2	*Ogulnius debonaja sp. nov.*	M	PILA

Table 2 (continued). List of the specimens used for the molecular phylogenetic analysis in the study, vouchers codes, DNA protocol, identification type (quantity), sex and localities. BIO=Biodiversity Intitute of Ontario; COPE=G.D. Omar Torrijos Herrera National Park; IMEDEA= Institut Mediterrani d'Estudis Avançats; PILA=La Amistad International Park; PNAC=Altos de Campana National Park; RFF=Forest Reserve Fortuna; CRBA=Centre de Recursos de Biodiversitat Animal. Numbers in parentheses=taxa quantity; Bold numbers=GMYC haplotypes (as in Figure 2); Bold taxa=GenBank-only data.

Voucher Codes	BOLD Sequence ID / GenBank ID	Protocol	Family / Subfamily	Fast Identification (27)	GMYC Cluster Number	Integrative Identification (29)	Sex	Locality
SAD1NHB024	ogus2101 / PX097014	CRBA		*Ogulnius* sp.2 FML	2	*Ogulnius debonaja sp. nov.*	F	PILA
SAU1NCL037	SPIPA359-10	BIO		*Ogulnius* sp.2 FML	2	*Ogulnius debonaja sp. nov.*	M	PILA
SAU1NDB035	ogus2102 / PX097017	CRBA		*Ogulnius* sp.2 FML	**2**	*Ogulnius debonaja sp. nov.*	M	PILA
SAU1NDL029	SPIPA355-10	BIO		*Ogulnius* sp.2 FML	2	*Ogulnius debonaja sp. nov.*	M	PILA
SAU2NCA003	SPIPA358-10	BIO		*Ogulnius* sp.2 FML	**2**	*Ogulnius debonaja sp. nov.*	F	PILA
SAB1DEA003	chts1248 / PX096992	CRBA	THS / Platoninae (22)	*Chthonos* sp.1 FML	**21**	*Chthonos dobo* sp. nov.	F	PILA
SAB1DEL024	SPIPA410-10	BIO		*Chthonos* sp.1 FML	21	*Chthonos dobo* sp. nov.	M	PILA
SAD1NGB019	chts1247 / PX096996	CRBA		*Chthonos* sp.1 FML	**21**	*Chthonos dobo* sp. nov.	M	PILA
SAD1NGL021	SPIPA411-10	BIO		*Chthonos* sp.1 FML	21	*Chthonos dobo* sp. nov.	F	PILA
SAD1NHH012	chts1245 / PX096995	CRBA		*Chthonos* sp.1 FML	**21**	*Chthonos dobo* sp. nov.	F	PILA
SAU1NFB025	chts1243 / PX096993	CRBA		*Chthonos* sp.1 FML	**21**	*Chthonos dobo* sp. nov.	F	PILA
SAU1NGA027	chts1246 / PX096994	CRBA		*Chthonos* sp.1 FML	21	*Chthonos dobo* sp. nov.	M	PILA
SAU1NHB013	SPIPA412-10	BIO		*Chthonos* sp.1 FML	21	*Chthonos dobo* sp. nov.	F	PILA
SAU1NHP003	SPIPA413-10	BIO		*Chthonos* sp.1 FML	**21**	*Chthonos dobo* sp. nov.	M	PILA
SFB1DAL021	chts1123 / PX096990	CRBA		*Chthonos* sp.1 FML	19	*Chthonos dobo* sp. nov.	M	RFF
SFU1N7D015	chts1059 / PX096989	CRBA		*Chthonos* sp.1 FML	**19**	*Chthonos dobo* sp. nov.	F	RFF
SFU1N7L018	SPIPA409-10	BIO		*Chthonos* sp.1 FML	19	*Chthonos dobo* sp. nov.	M	RFF
SFU1NBD019	chts1242 / PX096991	CRBA		*Chthonos* sp.1 FML	**19**	*Chthonos dobo* sp. nov.	M	RFF
SFU2NAA035	chts1241 / PX096997	CRBA		*Chthonos* sp.1 FML	**20**	*Chthonos dobo* sp. nov.	F	RFF
SFU2NAD028	chts1244 / PX096998	CRBA		*Chthonos* sp.1 FML	**20**	*Chthonos dobo* sp. nov.	F	RFF
SCU2NDA009	chts3g12 / PX097003	IMEDEA		*Chthonos* sp.2 FML	16	*Chthonos kaibe* sp. nov.	M	PNAC
SFD1NCR006	SPIPA408-10	BIO		*Chthonos* sp.2 FML	**18**	*Chthonos kwati* sp. nov.	M	RFF
SFU1NAD034	chts2061 / PX096999	CRBA		*Chthonos* sp.2 FML	**18**	*Chthonos kwati* sp. nov.	F	RFF
SCB1DED007	chts3e12 / PX097002	IMEDEA		*Chthonos* sp.3 FML	**16**	*Chthonos kaibe* sp. nov.	M	PNAC
SCU1NFH016	chts3109 / PX097000	CRBA		*Chthonos* sp.3 FML	**16**	*Chthonos kaibe* sp. nov.	F	PNAC

Table 2 (continued). List of the specimens used for the molecular phylogenetic analysis in the study, vouchers codes, DNA protocol, identification type (quantity), sex and localities. BIO=Biodiversity Intitute of Ontario; COPE=G.D. Omar Torrijos Herrera National Park; IMEDEA= Institut Mediterrani d'Estudis Avançats; PILA=La Amistad International Park; PNAC=Altos de Campana National Park; RFF=Forest Reserve Fortuna; CRBA=Centre de Recursos de Biodiversitat Animal. Numbers in parentheses=taxa quantity; Bold numbers=GMYC haplotypes (as in Figure 2); Bold taxa=GenBank-only data.

Voucher Codes	BOLD Sequence ID / GenBank ID	Protocol	Family / Subfamily	Fast Identification (27)	GMYC Cluster Number	Integrative Identification (29)	Sex	Locality
SCU2NDD007	chts3117 / PX097001	CRBA		*Chthonos* sp.3 FML	16	*Chthonos kaibe* sp. nov.	M	PNAC
STU1N7H024	SPIPA406-10	BIO		*Chthonos* sp.3 FML	**17**	*Chthonos kaibe* sp. nov.	M	COPE
	HM030436	–	THS / Theridiosomatinae (128)		**30**	***Theridiosoma gemmosum* (L. Koch, 1877)**		
SCD1DFR022	SPIPA420-10	BIO		*Baalzebub* sp.1 FML	**25**	*Baalzebub jaibana* sp. nov.	F	PNAC
SCD1DHR006	SPIPA416-10	BIO		*Baalzebub* sp.1 FML	25	*Baalzebub jaibana* sp. nov.	F	PNAC
SAC1DER002	SPIPA422-10	BIO		*Baalzebub baubo*	27	*Baalzebub innatuledi* sp. nov.	F	PILA
SAC1DFB011	baaba254 / PX096882	CRBA		*Baalzebub baubo*	**28**	*Baalzebub sukia* sp. nov.	F	PILA
SAC1NDA004	baaba257 / PX096880	CRBA		*Baalzebub baubo*	27	*Baalzebub innatuledi* sp. nov.	F	PILA
SAC2NDB010	SPIPA423-10	BIO		*Baalzebub baubo*	**27**	*Baalzebub innatuledi* sp. nov.	F	PILA
SAD1NGA015	baaba104 / PX096878	CRBA		*Baalzebub baubo*	**27**	*Baalzebub innatuledi* sp. nov.	M	PILA
SAD1NGB023	baaba258 / PX096881	CRBA		*Baalzebub baubo*	27	*Baalzebub innatuledi* sp. nov.	M	PILA
SAD1NHL025	baaba256 / PX096879	CRBA		*Baalzebub baubo*	27	*Baalzebub innatuledi* sp. nov.	M	PILA
SAU1NCH032	SPIPA425-10	BIO		*Baalzebub baubo*	**28**	*Baalzebub sukia* sp. nov.	M	PILA
SAU1NGH020	SPIPA424-10	BIO		*Baalzebub baubo*	**28**	*Baalzebub sukia* sp. nov.	M	PILA
SCD1DEL017	baaba255 / PX096877	CRBA		*Baalzebub baubo*	**24**	*Baalzebub nele* sp. nov.	F	PNAC
SCD2NGL023	SPIPA417-10	BIO		*Baalzebub baubo*	25	*Baalzebub jaibana* sp. nov.	M	PNAC
SFD1D8R013	baaba060 / PX096875	CRBA		*Baalzebub baubo*	**23**	*Baalzebub nele* sp. nov.	F	RFF
SCD1DFR025	SPIPA418-10	BIO		*Baalzebub* sp.1 FML	25	*Baalzebub jaibana* sp. nov.	F	PNAC
SCU1DHL016	SPIPA419-10	BIO		*Baalzebub* sp.1 FML	25	*Baalzebub jaibana* sp. nov.	F	PNAC
SCU1NEH011	baas1108 / PX096987	CRBA		*Baalzebub* sp.1 FML	**25**	*Baalzebub jaibana* sp. nov.	M	PNAC
SCU1NHR026	baas1116 / PX096988	CRBA		*Baalzebub* sp.1 FML	25	*Baalzebub jaibana* sp. nov.	F	PNAC
SFB1D9H034	epigl202 / PX096885	CRBA		*Epilineutes globosus*	41	*Epilineutes globosus* (O. Pickard-Cambridge, 1896)	F	RFF
SFB1DAL022	epigl201 / PX096884	CRBA		*Epilineutes globosus*	**41**	*Epilineutes globosus*	M	RFF

Table 2 (continued). List of the specimens used for the molecular phylogenetic analysis in the study, vouchers codes, DNA protocol, identification type (quantity), sex and localities. BIO=Biodiversity Intitute of Ontario; COPE=G.D. Omar Torrijos Herrera National Park; IMEDEA= Institut Mediterrani d'Estudis Avançats; PILA=La Amistad International Park; PNAC=Altos de Campana National Park; RFF=Forest Reserve Fortuna; CRBA=Centre de Recursos de Biodiversitat Animal. Numbers in parentheses=taxa quantity; Bold numbers=GMYC haplotypes (as in Figure 2); Bold taxa=GenBank-only data.

Voucher Codes	BOLD Sequence ID / GenBank ID	Protocol	Family / Subfamily	Fast Identification (27)	GMYC Cluster Number	Integrative Identification (29)	Sex	Locality
SFD1D8D007	epigl055 / PX096883	CRBA		*Epilineutes globosus*	**41**	*Epilineutes globosus*	F	RFF
SFD1DAL017	epigl165 / PX096887	CRBA		*Epilineutes globosus*	41	*Epilineutes globosus*	F	RFF
SFD1NBA013	SPIPA381-10	BIO		*Epilineutes globosus*	**41**	*Epilineutes globosus*	F	RFF
SFU1N8A034	epigl064 / PX096886	CRBA		*Epilineutes globosus*	**41**	*Epilineutes globosus*	M	RFF
SFU1NAH031	SPIPA379-10	BIO		*Epilineutes globosus*	41	*Epilineutes globosus*	M	RFF
SFU1NAR037	SPIPA378-10	BIO		*Epilineutes globosus*	41	*Epilineutes globosus*	F	RFF
SFU1NBA005	SPIPA380-10	BIO		*Epilineutes globosus*	41	*Epilineutes globosus*	M	RFF
SFU1NBD031	SPIPA382-10	BIO		*Epilineutes globosus*	41	*Epilineutes globosus*	M	RFF
SCD2NFA020	SPIPA335-10	BIO		*Theridiosoma* sp.6 FML	**40**	*Tantra embera* gen. et sp. nov.	F	PNAC
SAC1DDH014	thech175 / PX096933	CRBA		*Theridiosoma chiripa*	33	*Theridiosoma goodnightorum* Archer, 1953	F	PILA
SAC1NGL018	thech180 / PX096934	CRBA		*Theridiosoma chiripa*	33	*Theridiosoma goodnightorum*	F	PILA
SAC1NHL015	SPIPA351-10	BIO		*Theridiosoma chiripa*	33	*Theridiosoma goodnightorum*	F	PILA
SAD1NCA001	SPIPA352-10	BIO		*Theridiosoma chiripa*	33	*Theridiosoma goodnightorum*	M	PILA
SAD1NCA004	SPIPA353-10	BIO		*Theridiosoma chiripa*	33	*Theridiosoma goodnightorum*	F	PILA
SAD1NCR031	thech170 / PX096931	CRBA		*Theridiosoma chiripa*	33	*Theridiosoma goodnightorum*	M	PILA
SAD1NGL024	thech174 / PX096932	CRBA		*Theridiosoma chiripa*	33	*Theridiosoma goodnightorum*	M	PILA
SAD1NHL021	thech169 / PX096930	CRBA		*Theridiosoma chiripa*	**33**	*Theridiosoma goodnightorum*	M	PILA
SFC2NAR015	thech178 / PX096939	CRBA		*Theridiosoma chiripa*	32	*Theridiosoma goodnightorum*	F	RFF
SFD1D9L004	thech121 / PX096929	CRBA		*Theridiosoma chiripa*	**35**	*Theridiosoma goodnightorum*	F	RFF
SFD1DAR028	thech069 / PX096928	CRBA		*Theridiosoma chiripa*	**35**	*Theridiosoma goodnightorum*	M	RFF
SFD1NAH025	SPIPA354-10	BIO		*Theridiosoma chiripa*	**35**	*Theridiosoma goodnightorum*	F	RFF
SFD1NCD023	SPIPA350-10	BIO		*Theridiosoma chiripa*	**35**	*Theridiosoma goodnightorum*	F	RFF
SFD1NCL025	thech182 / PX096935	CRBA		*Theridiosoma chiripa*	**34**	*Theridiosoma goodnightorum*	M	RFF
SFU1N8L031	thech173 / PX096938	CRBA		*Theridiosoma chiripa*	**32**	*Theridiosoma goodnightorum*	F	RFF

Table 2 (continued). List of the specimens used for the molecular phylogenetic analysis in the study, vouchers codes, DNA protocol, identification type (quantity), sex and localities. BIO=Biodiversity Intitute of Ontario; COPE=G.D. Omar Torrijos Herrera National Park; IMEDEA= Institut Mediterrani d'Estudis Avançats; PILA=La Amistad International Park; PNAC=Altos de Campana National Park; RFF=Forest Reserve Fortuna; CRBA=Centre de Recursos de Biodiversitat Animal. Numbers in parentheses=taxa quantity; Bold numbers=GMYC haplotypes (as in Figure 2); Bold taxa=GenBank-only data.

Voucher Codes	BOLD Sequence ID / GenBank ID	Protocol	Family / Subfamily	Fast Identification (27)	GMYC Cluster Number	Integrative Identification (29)	Sex	Locality
STD1N6R021	thech171 / PX096936	CRBA		*Theridiosoma chiripa*	**31**	*Theridiosoma goodnightorum*	F	COPE
STD1N6R027	thech172 / PX096937	CRBA		*Theridiosoma chiripa*	31	*Theridiosoma goodnightorum*	F	COPE
SFB1DBA017	SPIPA347-10	BIO		*Theridiosoma* sp.3 FML	37	*Tantra ngabe* gen. et sp. nov.	M	RFF
SFC1DBD015	SPIPA346-10	BIO		*Theridiosoma* sp.3 FML	37	*Tantra ngabe* gen. et sp. nov.	M	RFF
SFC1DBH007	thes3212 / PX096909	CRBA		*Theridiosoma* sp.3 FML	37	*Tantra ngabe* gen. et sp. nov.	M	RFF
SFC1DCR013	SPIPA348-10	BIO		*Theridiosoma* sp.3 FML	**37**	*Tantra ngabe* gen. et sp. nov.	F	RFF
SFD1DAA017	SPIPA349-10	BIO		*Theridiosoma* sp.3 FML	37	*Tantra ngabe* gen. et sp. nov.	F	RFF
SFD1DAR027	thes3114 / PX096914	CRBA		*Theridiosoma* sp.3 FML	37	*Tantra ngabe* gen. et sp. nov.	M	RFF
SFD1NAD013	thes3249 / PX096917	CRBA		*Theridiosoma* sp.3 FML	37	*Tantra ngabe* gen. et sp. nov.	F	RFF
SFD1NCA011	SPIPA345-10	BIO		*Theridiosoma* sp.3 FML	37	*Tantra ngabe* gen. et sp. nov.	F	RFF
SFU1NCR044	thes3210 / PX096915	CRBA		*Theridiosoma* sp.3 FML	37	*Tantra ngabe* gen. et sp. nov.	F	RFF
SFU2NAD033	thes3067 / PX096913	CRBA		*Theridiosoma* sp.3 FML	**37**	*Tantra ngabe* gen. et sp. nov.	F	RFF
STC1D8H011	thes3251 / PX096912	CRBA		*Theridiosoma* sp.3 FML	36	*Tantra bribri* gen. et sp. nov.	F	COPE
STC2D6R014	SPIPA318-10	BIO		*Theridiosoma* sp.3 FML	36	*Tantra bribri* gen. et sp. nov.	M	COPE
STD1D6H023	SPIPA317-10	BIO		*Theridiosoma* sp.3 FML	36	*Tantra bribri* gen. et sp. nov.	F	COPE
STD1D7B026	thes3250 / PX096911	CRBA		*Theridiosoma* sp.3 FML	36	*Tantra bribri* gen. et sp. nov.	M	COPE
STD1N7B028	thes3214 / PX096916	CRBA		*Theridiosoma* sp.3 FML	36	*Tantra bribri* gen. et sp. nov.	M	COPE
STD1N7R021	thes3213 / PX096910	CRBA		*Theridiosoma* sp.3 FML	36	*Tantra bribri* gen. et sp. nov.	F	COPE
STU1N5L020	SPIPA319-10	BIO		*Theridiosoma* sp.3 FML	36	*Tantra bribri* gen. et sp. nov.	F	COPE
STU1N6H023	thes3211 / PX096908	CRBA		*Theridiosoma* sp.3 FML	**36**	*Tantra bribri* gen. et sp. nov.	F	COPE
STU1N7A019	SPIPA320-10	BIO		*Theridiosoma* sp.3 FML	36	*Tantra bribri* gen. et sp. nov.	F	COPE
STU1N7L028	SPIPA321-10	BIO		*Theridiosoma* sp.3 FML	36	*Tantra bribri* gen. et sp. nov.	F	COPE
SFB1DAR031	thes4181 / PX096921	CRBA		*Theridiosoma* sp.4 FML	42	*Tantra bugle* gen. et sp. nov.	M	RFF
SFD1NAL019	SPIPA343-10	BIO		*Theridiosoma* sp.4 FML	42	*Tantra bugle* gen. et sp. nov.	M	RFF
SFD1NCH021	SPIPA342-10	BIO		*Theridiosoma* sp.4 FML	42	*Tantra bugle* gen. et sp. nov.	M	RFF

Table 2 (continued). List of the specimens used for the molecular phylogenetic analysis in the study, vouchers codes, DNA protocol, identification type (quantity), sex and localities. BIO=Biodiversity Intitute of Ontario; COPE=G.D. Omar Torrijos Herrera National Park; IMEDEA= Institut Mediterrani d'Estudis Avançats; PILA=La Amistad International Park; PNAC=Altos de Campana National Park; RFF=Forest Reserve Fortuna; CRBA=Centre de Recursos de Biodiversitat Animal. Numbers in parentheses=taxa quantity; Bold numbers=GMYC haplotypes (as in Figure 2); Bold taxa=GenBank-only data.

Voucher Codes	BOLD Sequence ID / GenBank ID	Protocol	Family / Subfamily	Fast Identification (27)	GMYC Cluster Number	Integrative Identification (29)	Sex	Locality
SFU1D9A009	SPIPA344-10	BIO		*Theridiosoma* sp.4 FML	42	*Tantra bugle* gen. et sp. nov.	F	RFF
SFU1NBA029	thes4259 / PX096922	CRBA		*Theridiosoma* sp.4 FML	**42**	*Tantra bugle* gen. et sp. nov.	F	RFF
SFU1NCR034	thes4177 / PX096920	CRBA		*Theridiosoma* sp.4 FML	42	*Tantra bugle* gen. et sp. nov.	F	RFF
SFU2NAD032	thes4113 / PX096919	CRBA		*Theridiosoma* sp.4 FML	42	*Tantra bugle* gen. et sp. nov.	M	RFF
SFU2NBH034	thes4065 / PX096918	CRBA		*Theridiosoma* sp.4 FML	**42**	*Tantra bugle* gen. et sp. nov.	F	RFF
SFC1DBD011	thes5066 / PX096903	CRBA		*Theridiosoma* sp.5 FML	**39**	*Tantra kuna* gen. et sp. nov.	F	RFF
SFC2DCD016	thes5122 / PX096904	CRBA		*Theridiosoma* sp.5 FML	39	*Tantra kuna* gen. et sp. nov.	M	RFF
SFD1D8H025	SPIPA337-10	BIO		*Theridiosoma* sp.5 FML	39	*Tantra kuna* gen. et sp. nov.	M	RFF
SFD1DAL020	thes5262 / PX096907	CRBA		*Theridiosoma* sp.5 FML	39	*Tantra kuna* gen. et sp. nov.	F	RFF
SFD1NAH022	SPIPA338-10	BIO		*Theridiosoma* sp.5 FML	39	*Tantra kuna* gen. et sp. nov.	F	RFF
SFD1NAH037	SPIPA121-10	BIO		*Theridiosoma* sp.5 FML	39	*Tantra kuna* gen. et sp. nov.	M	RFF
SFD1NBH019	SPIPA339-10	BIO		*Theridiosoma* sp.5 FML	39	*Tantra kuna* gen. et sp. nov.	F	RFF
SFD1NBH034	SPIPA122-10	BIO		*Theridiosoma* sp.5 FML	39	*Tantra kuna* gen. et sp. nov.	F	RFF
SFU2NAA014	thes5261 / PX096906	CRBA		*Theridiosoma* sp.5 FML	39	*Tantra kuna* gen. et sp. nov.	M	RFF
SFU2NAH042	thes5260 / PX096905	CRBA		*Theridiosoma* sp.5 FML	39	*Tantra kuna* gen. et sp. nov.	F	RFF
SAB1DDL017	thes6228 / PX096890	CRBA		*Theridiosoma* sp.6 FML	38	*Tantra naso* gen. et sp. nov.	F	PILA
SAB1DER005	SPIPA326-10	BIO		*Theridiosoma* sp.6 FML	38	*Tantra naso* gen. et sp. nov.	F	PILA
SAC1DGB022	SPIPA325-10	BIO		*Theridiosoma* sp.6 FML	38	*Tantra naso* gen. et sp. nov.	F	PILA
SAD1DHP002	thes6226 / PX096892	CRBA		*Theridiosoma* sp.6 FML	**38**	*Tantra naso* gen. et sp. nov.	M	PILA
SAD1NCR003	SPIPA324-10	BIO		*Theridiosoma* sp.6 FML	38	*Tantra naso* gen. et sp. nov.	F	PILA
SAD1NGB029	thes6225 / PX096889	CRBA		*Theridiosoma* sp.6 FML	38	*Tantra naso* gen. et sp. nov.	F	PILA
SAD1NGP019	SPIPA322-10	BIO		*Theridiosoma* sp.6 FML	38	*Tantra naso* gen. et sp. nov.	M	PILA
SAU1NDB029	thes6229 / PX096891	CRBA		*Theridiosoma* sp.6 FML	38	*Tantra naso* gen. et sp. nov.	F	PILA
SAU1NDH032	thes6179 / PX096888	CRBA		*Theridiosoma* sp.6 FML	**38**	*Tantra naso* gen. et sp. nov.	M	PILA
SAU2NFA018	SPIPA323-10	BIO		*Theridiosoma* sp.6 FML	38	*Tantra naso* gen. et sp. nov.	F	PILA

Table 2 (continued). List of the specimens used for the molecular phylogenetic analysis in the study, vouchers codes, DNA protocol, identification type (quantity), sex and localities. BIO=Biodiversity Intitute of Ontario; COPE=G.D. Omar Torrijos Herrera National Park; IMEDEA= Institut Mediterrani d'Estudis Avançats; PILA=La Amistad International Park; PNAC=Altos de Campana National Park; RFF=Forest Reserve Fortuna; CRBA=Centre de Recursos de Biodiversitat Animal. Numbers in parentheses=taxa quantity; Bold numbers=GMYC haplotypes (as in Figure 2); Bold taxa=GenBank-only data.

Voucher Codes	BOLD Sequence ID / GenBank ID	Protocol	Family / Subfamily	Fast Identification (27)	GMYC Cluster Number	Integrative Identification (29)	Sex	Locality
SCC1NHA009	thes6231 / PX096895	CRBA		*Theridiosoma* sp.6 FML	40	*Tantra embera* gen. et sp. nov.	F	PNAC
SCC2NGR018	thes6233 / PX096896	CRBA		*Theridiosoma* sp.6 FML	40	*Tantra embera* gen. et sp. nov.	M	PNAC
SCD1DEL018	SPIPA336-10	BIO		*Theridiosoma* sp.6 FML	40	*Tantra embera* gen. et sp. nov.	F	PNAC
SCD1DFL016	thes6230 / PX096894	CRBA		*Theridiosoma* sp.6 FML	40	*Tantra embera* gen. et sp. nov.	F	PNAC
SCD2NGL022	baaba253 / PX096986	CRBA		*Baalzebub baubo*	**25**	*Baalzebub jaibana* sp. nov.	F	PNAC
SCU2NDA017	thes6106 / PX096893	CRBA		*Theridiosoma* sp.6 FML	**40**	*Tantra embera* gen. et sp. nov.	M	PNAC
SCU2NHH021	thes6107 / PX096899	CRBA		*Theridiosoma* sp.6 FML	**40**	*Tantra embera* gen. et sp. nov.	F	PNAC
STB1D5L027	SPIPA333-10	BIO		*Theridiosoma* sp.6 FML	**40**	*Tantra embera* gen. et sp. nov.	M	COPE
STD1D6B017	SPIPA332-10	BIO		*Theridiosoma* sp.6 FML	40	*Tantra embera* gen. et sp. nov.	M	COPE
STD1N4R020	thes6235 / PX096898	CRBA		*Theridiosoma* sp.6 FML	40	*Tantra embera* gen. et sp. nov.	M	COPE
STD1N6R022	thes6234 / PX096897	CRBA		*Theridiosoma* sp.6 FML	40	*Tantra embera* gen. et sp. nov.	F	COPE
STD1N7L011	thes6227 / PX096900	CRBA		*Theridiosoma* sp.6 FML	**40**	*Tantra embera* gen. et sp. nov.	M	COPE
STD1N7R030	thes6232 / PX096902	CRBA		*Theridiosoma* sp.6 FML	**40**	*Tantra embera* gen. et sp. nov.	F	COPE
STU1N4R024	SPIPA334-10	BIO		*Theridiosoma* sp.6 FML	40	*Tantra embera* gen. et sp. nov.	F	COPE
STU2N8R022	thes6236 / PX096901	CRBA		*Theridiosoma* sp.6 FML	40	*Tantra embera* gen. et sp. nov.	F	COPE
SAB1DHP002	SPIPA329-10	BIO		*Theridiosoma* sp.7 FML	43	*Tantra wounaan* gen. et sp. nov.	F	PILA
SAC1DFH010	thes7263 / PX096927	CRBA		*Theridiosoma* sp.7 FML	**43**	*Tantra wounaan* gen. et sp. nov.	F	PILA
SAC1DHA012	SPIPA328-10	BIO		*Theridiosoma* sp.7 FML	43	*Tantra wounaan* gen. et sp. nov.	F	PILA
SAD1DGH013	thes7099 / PX096926	CRBA		*Theridiosoma* sp.7 FML	**43**	*Tantra wounaan* gen. et sp. nov.	M	PILA
SAD1DHL009	thes7264 / PX096924	CRBA		*Theridiosoma* sp.7 FML	**43**	*Tantra wounaan* gen. et sp. nov.	M	PILA
SAD1DHP001	SPIPA327-10	BIO		*Theridiosoma* sp.7 FML	**43**	*Tantra wounaan* gen. et sp. nov.	M	PILA
SAD1NHL020	SPIPA421-10	BIO		*Epeirotypus* sp.7 FML	**28**	*Baalzebub sukia* sp. nov.	M	PILA
SAD1NFP008	thes7105 / PX096923	CRBA		*Theridiosoma* sp.7 FML	**43**	*Tantra wounaan* gen. et sp. nov.	F	PILA
SAU1NFB026	SPIPA330-10	BIO		*Theridiosoma* sp.7 FML	43	*Tantra wounaan* gen. et sp. nov.	M	PILA
SAU1NHH023	thes7265 / PX096925	CRBA		*Theridiosoma* sp.7 FML	**43**	*Tantra wounaan* gen. et sp. nov.	F	PILA

Table 2 (continued). List of the specimens used for the molecular phylogenetic analysis in the study, vouchers codes, DNA protocol, identification type (quantity), sex and localities. BIO=Biodiversity Intitute of Ontario; COPE=G.D. Omar Torrijos Herrera National Park; IMEDEA= Institut Mediterrani d'Estudis Avançats; PILA=La Amistad International Park; PNAC=Altos de Campana National Park; RFF=Forest Reserve Fortuna; CRBA=Centre de Recursos de Biodiversitat Animal. Numbers in parentheses=taxa quantity; Bold numbers=GMYC haplotypes (as in Figure 2); Bold taxa=GenBank-only data.

Voucher Codes	BOLD Sequence ID / GenBank ID	Protocol	Family / Subfamily	Fast Identification (27)	GMYC Cluster Number	Integrative Identification (29)	Sex	Locality
SFNQP8L012	SPIPA222-10	BIO		*Theridiosoma* sp.8 FML	**42**	*Tantra bugle* gen. et sp. nov.	F	RFF
SFNQK8L001	SPIPA232-10	BIO		*Theridiosoma* sp.9 FML	**26**	*Baalzebub albonotatus* (Petrunkevitch, 1930)	M	RFF
SFD1NBL018	wens1068 / PX097005	CRBA		*Wendilgarda clara*	29	*Wendilgarda clara* Keyserling, 1886	F	RFF
SFD1NBL030	wenclf11 / PX097007	IMEDEA		*Wendilgarda clara*	**29**	*Wendilgarda clara*	M	RFF
SFD1NBL036	wenclg11 / PX097008	IMEDEA		*Wendilgarda clara*	29	*Wendilgarda clara*	M	RFF
SFD2NBL020	wens1057 / PX097004	CRBA		*Wendilgarda clara*	**29**	*Wendilgarda clara*	M	RFF
SFU1N7H040	wencle11 / PX097006	IMEDEA		*Wendilgarda clara*	**29**	*Wendilgarda clara*	M	RFF
SCD1DFR013	baaba252 / PX096876	CRBA		*Baalzebub baubo*	**22**	*Baalzebub nele* sp. nov.	F	PNAC

Table 3 (continued on next page). Summary of species and specimens of Theridiosomatidae Simon, 1881 according to locality and sex. COPE = G.D. Omar Torrijos Herrera National Park; PILA = La Amistad International Park; PNAC = Altos de Campana National Park; RFF = Forest Reserve Fortuna. Bold taxa = only morphological identification (not quantitative).

	Integrative Identification (semi-quantitative)								**Identification After Results (not quantitative)**							
Locality	**PILA**		**RFF**		**COPE**		**PNAC**		**PILA**		**RFF**		**COPE**		**PNAC**	
Sex	**M**	**F**	**M**	**F**	**M**	**F**	**M**	**F**	**M**	**F**	**M**	**F**	**M**	**F**	**M**	**F**
Baalzebub albonotatus											1					
***Baalzebub absoguedi* sp. nov.**														1		
***Baalzebub antomia* sp. nov.**													1			
Baalzebub innatuledi sp. nov.	4	4														
Baalzebub jaibana sp. nov.							2	6								
Baalzebub nele sp. nov.				1				2								
Baalzebub sukia sp. nov.	3	5														
Chthonos dobo sp. nov.	16	15	11	8								4				
Chthonos kaibe sp. nov.					1		3	1								
Chthonos kwati sp. nov.			1	1												
Epeirotypus bule sp. nov.		9														
Epeirotypus drune sp. nov.		4														
Epeirotypus jane sp. nov.						2										
Epeirotypus kote sp. nov.	2	2														
Epeirotypus kra sp. nov.			4	13							3	5				
Epeirotypus kwakwa sp. nov.			7	20												
Epeirotypus tain sp. nov.				1												
Epilineutes globosus			27	20							2	1				
Naatlo chi sp. nov.				28	22	152	17	507			2	32	1	5		
Naatlo fauna			19	25								6				

Table 3 (continued). Summary of species and specimens of Theridiosomatidae Simon, 1881 according to locality and sex. COPE=G.D. Omar Torrijos Herrera National Park; PILA=La Amistad International Park; PNAC=Altos de Campana National Park; RFF=Forest Reserve Fortuna. Bold taxa=only morphological identification (not quantitive).

	Integrative Identification (semi-quantitative)								**Identification After Results (not quantitative)**							
Locality	**PILA**		**RFF**		**COPE**		**PNAC**		**PILA**		**RFF**		**COPE**		**PNAC**	
Sex	**M**	**F**	**M**	**F**	**M**	**F**	**M**	**F**	**M**	**F**	**M**	**F**	**M**	**F**	**M**	**F**
Ogulnius debonaja sp. nov.	73	148							4	10		1	3	1		
Ogulnius zbodro sp. nov.							2	7								
Tantra bribri gen. et sp. nov.					5	17										
Tantra bugle gen. et sp. nov.			47	45							2	3				
Tantra embera gen. et sp. nov.					15	22	16	18								
Tantra kuna gen. et sp. nov.			4	6												
Tantra naso gen. et sp. nov.	9	42														
Tantra ngabe gen. et sp. nov.			6	22							1	2				
***Tantra sichid* gen. et sp. nov.**										1						
Tantra wounaan gen. et sp. nov.	109	224							2	5						
Theridiosoma goodnightorum	13	16	16	37		2					1	1				
Wendilgarda clara			4	1							1					
Adults (semi-quantitative) = 1891	229	469	146	228	43	195	40	541								
Adults (not quantitative) = 102									6	16	13	55	5	7	0	0
Total Adults = 1993																

Table 4. Primer sequences, source and annealing temperatures for mitochondrial cytochrome c oxydase subunit I (COI).

Forward	**Sequence**	**Reference**	**Annealing temperature**
C1-J-1490 / LCO-1490	5'-GGTCAACAAATCATAAAGATATTGG-3'	Folmer *et al.* (1994)	42–45°C
C1-N-2191 / Nancy	5'-CCCGGTAAAATTAAAATATAAACTTC-3'	Folmer *et al.* (1994)	42–45°C
LepF1	5'-ATTCAACCAATCATAAAGATATTGG-3'	Hebert *et al.* (2004)	40°C / 51°C
M13F (-21)	5'-TGTAAAACGACGGCCAGT-3'	Messing (1983)	40°C / 51°C
Reverse	**Sequence**	**Reference**	**Annealing temperature**
C1-N-2198 / HCO-2198	5'-TAAACTTCAGGGTGACCAAAAAATCA-3'	Folmer *et al.* (1994)	42–45°C
C1-N-2198 / HCO-2198	5'-TAAACTTCAGGGTGACCAAAAAATCA-3'	Folmer *et al.* (1994)	42–45°C
LepR1	5'-TAAACTTCTGGATGTCCAAAAAATCA-3'	Hebert *et al.* (2004)	40°C / 51°C
M13R (-27)	5'-CAGGAAACAGCTATGAC-3'	Messing (1983)	40°C / 51°C

Molecular analyses

To streamline our dataset, all *cox* 1 sequences were collapsed into unique haplotypes using COLLAPSE ver. 1.2 (Posada 2004) and TCS ver. 1.21 (Clement *et al*. 2000). Sequences with missing data were removed if they were identical to more complete sequences to ensure the accuracy of downstream analyses.

A maximum-likelihood (ML) analysis was performed using RAxML ver. 8 (Stamatakis 2006, 2014; Stamatakis *et al.* 2008), run remotely via the CIPRES Science Gateway (Miller *et al.* 2010; https://www.phylo.org/). For *cox* 1, we employed three partitioning strategies: (1) treating the entire gene as a single partition (*gene*), (2) separating 1st + 2nd codon positions from the 3rd codon position (*3rd codon*), and (3) assigning independent partitions for each codon position (*codon specific*). Each partition was modeled under the GTR+I+Γ (GTRGAMMAI) evolutionary model. The best-scoring ML tree was selected from 100 random search iterations, and we assessed node support using 1000 non-parametric bootstrap replicates.

To prepare the dataset for species delimitation, the ML tree was transformed into an ultrametric using PATHd8 (Britton *et al.* 2007), fixing the root to 1.0 to obtain relative branch lengths. This approach – combining ML inferences with PATHd8 transformation – is among the recommended strategies for implementing the GMYC model (Talavera *et al.* 2013). We pruned outgroup sequences and removed terminal branches with near-zero length (< 0.0001) using the APE package in R (Paradis *et al.* 2004).

For species delimitation, we applied the GMYC model via SPLITS package ver. 1.0 (Ezard *et al.* 2009) in R, testing both single-threshold (Pons *et al.* 2006) and multiple-threshold (Monaghan *et al.* 2009) versions of the method. To assess the fit of these models, we performed a Likelihood Ratio Test (LRT) to determine whether multiple transition points between coalescent and speciation events improved the model's performance.

Finally, we visualized and edited phylogenetic trees using FIGTREE ver. 1.4 (Rambaut 2006–2014). All alignment matrices, partition schemes, and resulting phylogenetic trees are provided as supplementary material.

Measurements of species diversity

To assess alpha diversity, we estimated species richness using both species accumulation curves and non-parametric richness estimators, all implemented in EstimateS ver. 6 (Colwell 2004). Accumulation curves were generated from over 100 randomized runs to homogenize the sampling effort across plots (Colwell & Coddington 1994). Non-parametric richness estimates – particularly sensitive to the number of rare species – were used to account for the many singletons (species represented by a single specimen) and doubletons (species represented by two specimens), which are commonly encountered in tropical biodiversity surveys, even with intensive sampling (Colwell & Coddington 1994).

To ensure a comprehensive evaluation, we employed both abundance-based and incidence-based estimators (Chao *et al.* 2005; Colwell *et al.* 2005). The former included Chao 1 (Chao 1984), Jackknife 1 (Burnham & Overton 1978, 1979), and the Abundance-based Coverage Estimator (ACE) (Chazdon *et al.* 1998), based on the total number of individuals collected. The latter – based on species presence-absence across samples – included Chao 2 (Chao 1987), Jackknife 2 (Burnham & Overton 1978, 1979), and Incidence-based Coverage Estimator (ICE) (Chazdon *et al.* 1998).

Beta diversity, or species turnover between sites, was quantified using modified similarity indices developed by Chao *et al.* (2005), which adapt the classical Sørensen and Jaccard indices to account for unequal sampling and high number of rare species. These metrics produce similarity values ranging from 0 (completely dissimilar communities) to 1 (identical communities).

Finally, we calculated sampling as the ratio of specimens collected to the number of species recovered, following Coddington *et al.* (1996). According to Coddington *et al.* (2009), a sampling intensity exceeding 340 is considered sufficient for obtaining reliable non-parametric richness estimates in tropical arthropod surveys.

Results

Collection and fast identification

Our fieldwork yielded a total of 3333 specimens of Theridiosomatidae, of which 1993 individuals (~60%) were identified as adults. From these, 1891 were collected through the semi-quantitative sampling protocol, while an additional 102 adults came from non-quantitative (NQ) efforts (Table 3). Using the fast morphospecies identification approach, we initially sorted specimens into seven genera (see Taxonomy) and distinguished 27 morphospecies based on gross morphology (Table 2).

Fig. 2. Maximum likelihood analysis of the *cox 1* dataset with a codon-partition model. Black circles at nodes indicate bootstrap proportions > 0.75. Boxes represent GMYC clusters delimited from the single-threshold model. Lateral bars and species names correspond to the integrative identification.

Molecular analyses and GMYC identification

We successfully obtained DNA sequences from 246 adult specimens, including representatives of all 27 fast-identified morphospecies as well as three outgroups: *Mysmena* sp. (SPIPO354), *Anapis monteverde* (SPIPO006), and *Patu digua* (SPIPO778) (Fig. 2, Table 2). The final dataset consisted of 249 terminals, incorporating three additional sequences from GenBank. After collapsing the matrix, we recovered 101 unique haplotypes, of which 95 correspond to Panamanian Theridiosomatidae (see Supp. file 1, Supp. file 2, Supp. file 3, Supp. file 4).

Maximum-likelihood (ML) analyses under alternative partitioning schemes revealed that the codon-specific partition model yielded the best fit (AICw = 1; Table 5), and all subsequent analyses were conducted using this scheme. AICw (Akaike Information Criterion weight) reflects the relative likelihood of a model being the best among the tested alternatives, with values closer to 1 indicating higher support. The resulting ML tree had a log-likelihood score of –lnL = 9704.248 (Fig. 2, Table 5), where –lnL represents the negative log-likelihood of the tree under the selected model—a measure of model fit, with lower values indicating better likelihood.

The GMYC analysis, performed using single- and multiple-threshold models (excluding the outgroup taxa), significantly outperformed the null model across all partitions (Table 5). The single-threshold model showed slightly higher log-likelihood values and was therefore selected for interpretation. This analysis identified 43 groups, including 24 clusters and 19 singletons (Fig. 2). Of these, 40 corresponded to Panamanian groups (Fig. 3A), and three to legacy sequences: *Coddingtonia euryopoides* Miller, Griswold & Yin, 2009, *Epeirotypus chavarria* Coddington, 1986, and *Theridiosoma gemmosum* (L. Koch, 1877).

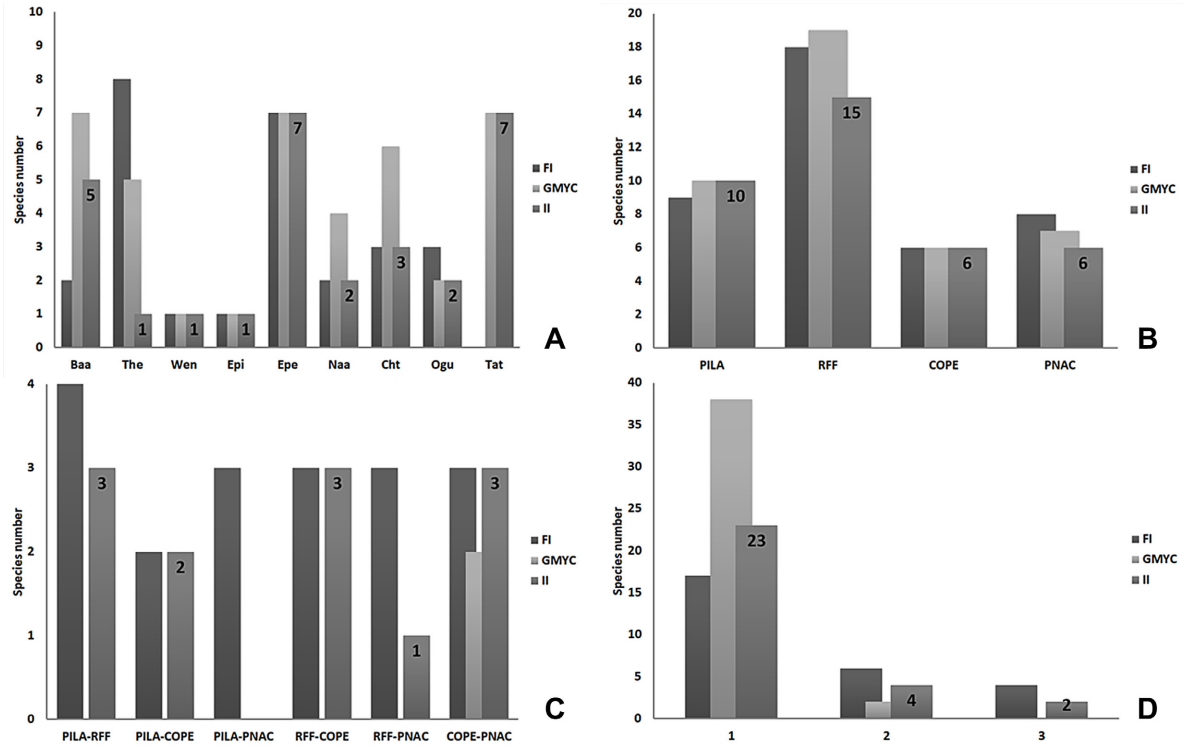

Fig. 3. Summary of quantitative results after cross-validation between both fast identification (FI) and independent coalescence groups (GMYC) to obtain 29 integratively delimited species (II). **A**. Number of species among genera (Baa = *Baalzebub* Coddington, 1986; The = *Theridiosoma* O. Pickard-Cambridge, 1879; Wen = *Wendilgarda* Keyserling, 1886; Epi = *Epilineutes*; Epe = *Epeirotypus* O. Pickard-Cambridge, 1894; Naa = *Naatlo* Coddington, 1986; Cht = *Chthonos* Coddington, 1986; Ogu = *Ogulnius* O. Pickard-Cambridge, 1882; Tat = *Tantra* gen. nov.). **B**. Alpha diversity (COPE = G.D. Omar Torrijos Herrera National Park; PILA = La Amistad International Park; PNAC = Altos de Campana National Park; RFF = Fortuna Forest Reserve). **C**. Beta diversity. **D**. Endemism (x-axis number of localities).

Table 5. Summary of tree statistics and GMYC results for different codon partitions using different models. ML entity counts includes single taxa (e.g., *Baalzebub albonotatus* and GenBank entities), but excludes outgroups. AICc = Akaike information criterion corrected; AICw = Akaike information criterion weight; lk = likelihood; LRT = likelihood ratio test; ML = maximum likelihood. Bold = best-fitting model; –lnL = negative log-likelihood of the tree under the selected model.

Partition	-lnL	AICc	AICw	Method	lk null model	lk GMYC model	lk ratio	LRT	Number ML clusters	Confidence Interval	Number ML entities	Confidence Interval	Threshould time
Gene	10106.128115	20214.3	0	Single	406.5638	473.2875	133.4474	0***	21	21–21	43	43–44	-0.017137
				Multiple	406.5638	473.8893	134.651	0***	21	21–21	45	44–45	-0.017137 -0.006721
3rd Codon	9785.432286	19574.9	0	Single	475.1251	555.5367	160.8232	0***	24	24–24	43	42–44	-0.012465
				Multiple	475.1251	557.0421	163.8339	0***	26	24–26	40	32–44	-0.427075 -0.304391 -0.063662 -0.006629 -0.006186 -0.001988 -0.001766
Codon specific	**9704.248091**	**19414.6**	**1**	Single	480.4394	554.5957	148.3126	0***	24	24–24	43	42–44	-0.012835
				Multiple	480.4394	555.1998	149.5207	0***	24	23–25	46	42–46	-0.012835 -0.002678

Most GMYC clusters were well supported, with bootstrap values (BS) >0.75 (black circles in Fig. 2), except for the pair chts3109-chts3e12 (see *Chthonos kaibe* sp. nov. in Taxonomy). Several genera also received strong support, including *Ogulnius*, *Naatlo* Coddington, 1986, *Chthonos* Coddington, 1986, and *Baalzebub* Coddington, 1986 (Fig. 2). In general, GMYC clusters were composed of haplotypes from a single locality (Fig. 2, Table 2), with the exception of Cluster 12 (*Naatlo chi* sp. nov.) and Cluster 40 (*Tantra embera* gen. et sp. nov.), both of which included haplotypes from two sites (COPE and PNAC).

Integrative identification

The GMYC clusters matched the fast morphospecies identification in 13 cases (48.2%), representing 86 out of 243 specimens (35.4%) (Table 2). In 12 cases (44.4%), a single morphospecies was split into two or more GMYC clusters, involving 155 individuals (63.8%) (Table 2). In two instances (7.4%), two or more morphospecies were merged into a single cluster, accounting for just two specimens (0.8%) (Table 2).

For all cases of incongruence between morphological and molecular delimitations, we conducted a detailed re-examination of the genital morphology. Based on this, 24 out of the 40 Panamanian GMYC groups – comprising 16 clusters and 8 singletons (60%) – could be morphologically diagnosed and were therefore retained as distinct species in our integrative framework. For the remaining 16 GMYC groups (8 clusters and 8 singletons) (40%), we did not identify any diagnostic morphological characters and thus chose to recognize only five nominal species. These species include: *Baalzebub nele* sp. nov., comprising three GMYC singletons (one from RFF and two from PNAC); *Naatlo chi* sp. nov., composed of three GMYC clusters (two from RFF and one spanning PNAC and COPE); *Chthonos dobo* sp. nov., including three GMYC clusters (one from PILA and two from RFF); *Theridiosoma goodnightorum*, represented by one cluster and four singletons from RFF, PILA, and COPE; and *Chthonos kaibe* sp. nov., combined one cluster and one singleton (PNAC and COPE, respectively), despite their non-monophyletic placement.

In these cases, morphological consistency – such as similarities in sexual organs, body form, and coloration – guided our taxonomic decisions even when molecular data revealed splits or non-monophyly. Across the full dataset, our integrative species delimitation was congruent with fast morphospecies identification in 63% of the cases, representing 147 specimens (60.5%) of the total sample (Table 3).

Finally, based on a combination of distinctive morphological characters, we propose a new genus to accommodate a set of species that form a cohesive morphologically defined group. Although the molecular phylogeny does not recover this group as a clade (Figs 2, 3A), its recognition is supported by multiple consistent diagnostic features (see Taxonomy).

Biodiversity patterns

A summary of alpha diversity and beta diversity, as well as patterns of endemism across the four sites, is shown in Fig. 3B–D, based on the three species identification methods: fast identification (FI), GMYC identification (GI), and integrative identification (II). Alpha diversity estimates were largely consistent across methods, with RFF emerging as the most species-rich site, followed by PILA, COPE, and PNAC (Figs 1, 3B). In contrast, beta diversity results varied depending on the identification method used (Fig. 3C). Both FI and II approaches revealed that several species were shared across localities. However, the GMYC-based delimitation detected just two shared clusters – both between COPE and PNAC – highlighting how molecular methods may inflate species counts due to over splitting. Despite these methodological differences, all approaches revealed high levels of endemism: most species were restricted to a single site (Fig. 3D).

We focus further analysis on 29 integratively defined species plus three morphologically defined species (Table 3) to examine abundance patterns, dominant species, and local endemism (Fig. 4A–B). PILA

yielded the highest number of individuals (698), followed by PNAC (581), RFF (374), and COPE (238). In PNAC and COPE, *Naatlo chi* sp. nov. was overwhelmingly dominant, accounting for 90.2% and 72% of all specimens, respectively. In PILA, 79.4% of individuals belonged to just two species: *Tantra wounaan* gen. et sp. nov. (47%) and *Ogulnius debonaja* sp. nov. (32.5%). RFF showed greater evenness: five species accounted for 71.4% of the individuals including *Tantra bugle* gen. et sp. nov. (22.1%), *Naatlo chi* sp. nov. (14.1%), *Theridiosoma goodnightorum* Archer, 1953 (12.5%), *Epilineutes globosus* (O. Pickard-Cambridge, 1896) (11.4%) and *Naatlo fauna* (Simon, 1897) (11.4%). PILA also presented the highest proportion of endemic species (72.7%), followed by RFF (64.7%), COPE (44.4%), and PNAC (33.3%) (Fig. 4B).

To assess inventory completeness, we used the 29 integratively defined species collected through semi-quantitative sampling, excluding the three species found only in non-quantitative samples. Species accumulation curves based on this subset approached asymptotic saturation, indicating sampling completeness (Fig. 4C). Both abundance- and incidence-based estimators suggested that only one or two additional species might have been missed (Fig. 4C). Moreover, rare species were uncommon – only 4% were represented by singletons and 7% by doubletons – further supporting the effectiveness of our sampling protocol (see Fig. 4C). Our overall sampling intensity (specimens per species) was 6.75, well above the threshold typically recommended for tropical arthropod surveys (Colwell & Coddington 1994).

Using the same 28 species, we calculated beta diversity using pairwise Chao-Sørensen (CS) and Chao-Jaccard (CJ) similarity indices (Fig. 4D). COPE and PNAC – the two easternmost sites – were the most

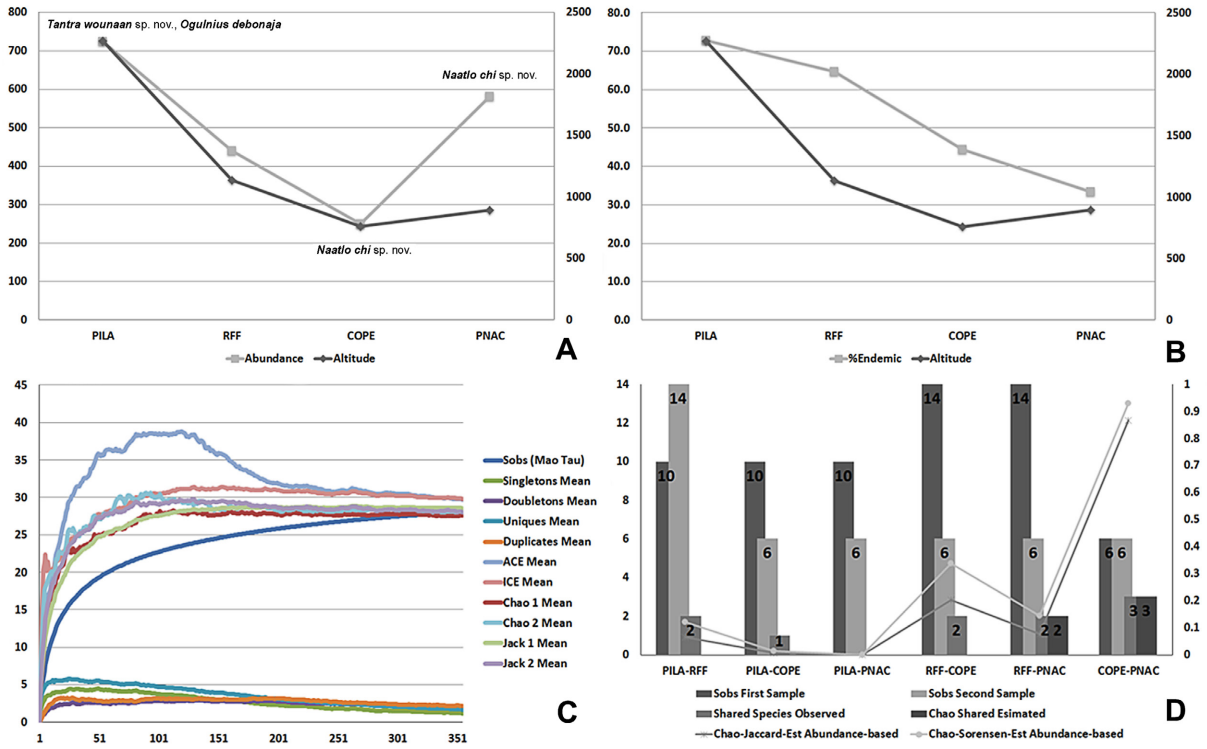

Fig. 4. A. Abundance of endemic species per locality for the 32 species identified (29 integratively defined species plus 3 morphologically defined species). **B**. Same, percentages of endemic species per locality. **C**. Species accumulation curves and non-parametric richness estimates for the 29 integratively defined species collected through semi-quantitative sampling (excluding the three species found only in non-quantitative samples). **D**. Same, pairwise Chao-Sørensen and Chao-Jaccard analyses. Abbreviations: COPE = G.D. Omar Torrijos Herrera National Park; PILA = La Amistad International Park; PNAC = Altos de Campana National Park; RFF = Fortuna Forest Reserve.

similar in species composition (CS: 0.93, CJ: 0.87). By contrast, PILA, located in the west, showed the lowest similarity to the other sites. Surprisingly, RFF, which is geographically close to PILA, shared more species with COPE (CS: 0.34, CJ: 0.20) and PNAC (CS: 0.14, CJ: 0.08) – sites located at 180 km and 253 km to the east – than with its neighboring PILA (CS: 0.12, CJ: 0.06), only 45 km away (Fig. 1). This pattern may reflect elevational rather than geographic influences: while RFF, COPE, and PNAC vary by less than 400 m in elevation, PILA is over 1000 m higher, potentially shaping its more distinct spider community.

Taxonomy

Class Arachnida Lamarck, 1801
Order Araneae Clerck, 1757
Family Theridiosomatidae Simon, 1881

Chthonos Coddington, 1986

Chthonos Coddington, 1986: 33. Type species *Tecmessa pectosa* O. Pickard-Cambridge, 1882.

Diagnosis

Males and females of *Chthonos* can be distinguished from those of other theridiosomatid genera by having prolateral rows of strong macrosetae on the curved (i.e., sinuate) first and second tibiae-metatarsi-tarsi (Figs 8A–C, 9A–C, 10C, 11B, 12A–C, 13B; see also Coddington 1986 and Dupérré & Tapia 2017) (absent in other genera), protruding sternum (Figs 8B, 9B, 10B, 11B, 12B, 13B; see also Coddington 1986) (in contrast with not protuding sternum in the other genera), and opisthosomal setae on sclerotized pits ("flecks" in Coddington 1986) (Figs 8A–C, 9A–C, 10A–C, 11A–C, 12A–C, 13A–C; see also Coddington 1986 and Dupérré & Tapia 2017) (absent in other genera).

Description

Females of *Chthonos* have irregular membranous copulatory ducts (Figs 5A–C, 9D, 11D, 13D) with a dorsal patch of gland ducts near the sides of the spermathecae (Fig. 5A–C). For further genus description details, see Coddington (1986) and Labarque & Griswold (2014).

Chthonos dobo sp. nov.

urn:lsid:zoobank.org:act:6A1057E3-5B3A-4194-B447-78510F828729
Figs 1, 5A–C, 8–9

Diagnosis

Males and females of *Chthonos dobo* sp. nov. resemble those of *Chthonos peruana* (Keyserling, 1886) by the opisthosoma with two pairs of proximally fused lateral tubercles (Figs 8A, 9A; Keyserling 1886: pl. XI figs 144, 144A), but *C. dobo* can be distinguished by the tubercles wider than long, relatively short, that slightly exceed the dorsum of the opisthosoma (Figs 8A–B, 9A–B), whereas in *C. peruana* those tubercles are as wide as long, extending dorsolaterally beyond the opisthosomal border (Keyserling 1886: pl. XI fig. 144).

Etymology

The specific name is derived from 'dobo' which means 'Earth' in the Ngäbere language, currently spoken by the Ngäbe native people of Panama, and refers to the soil, one of the habitats where the species was found.

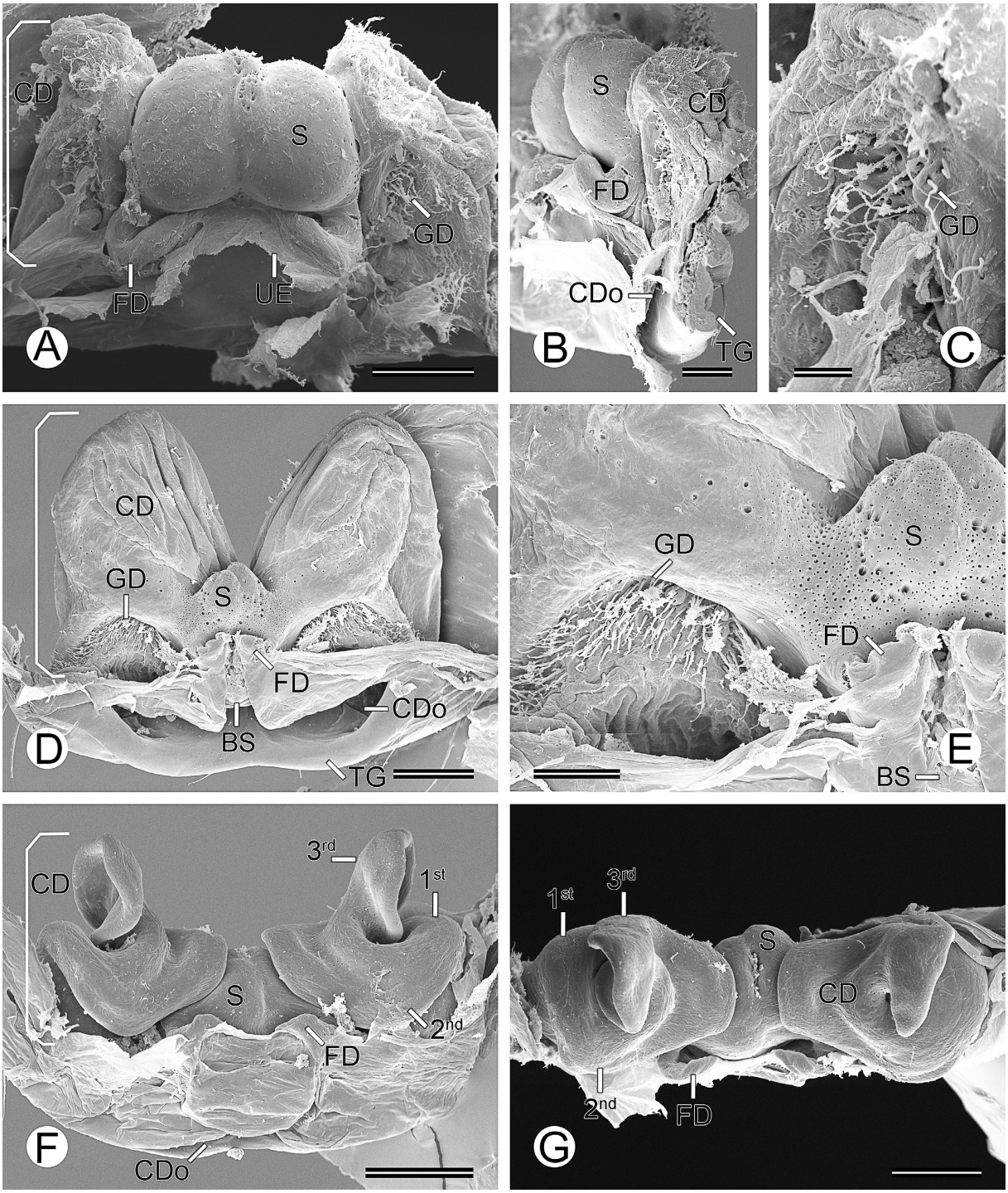

Fig. 5. Female genitalia of Theridiosomatidae Simon, 1881. **A–C**. *Chthonos dobo* sp. nov., ♀, (MACN-Ar 29324). **D–E**. *Epeirotypus kra* sp. nov., ♀ (MACN-Ar 29220). **F–G**. *Ogulnius zbodro* sp. nov., ♀ (MACN-Ar 29309). **A–B, D, F–G**. Vulva, general view (A, D, F = dorsal view; B = lateral view; G = apical view). **C, E**. Patch of gland ducts, detail (C = left; E = right). Abbreviations: BS = bifid septum; CD = copulatory duct; CDo = copulatory duct opening; FD = fertilization duct; GD = patch of gland ducts; S = spermatheca; TG = transverse groove; UE = uterus externus. Scale bars: A, F = 0.05 mm; B = 0.03 mm; C = 0.009 mm; D = 0.01 mm; E, G = 0.04 mm.

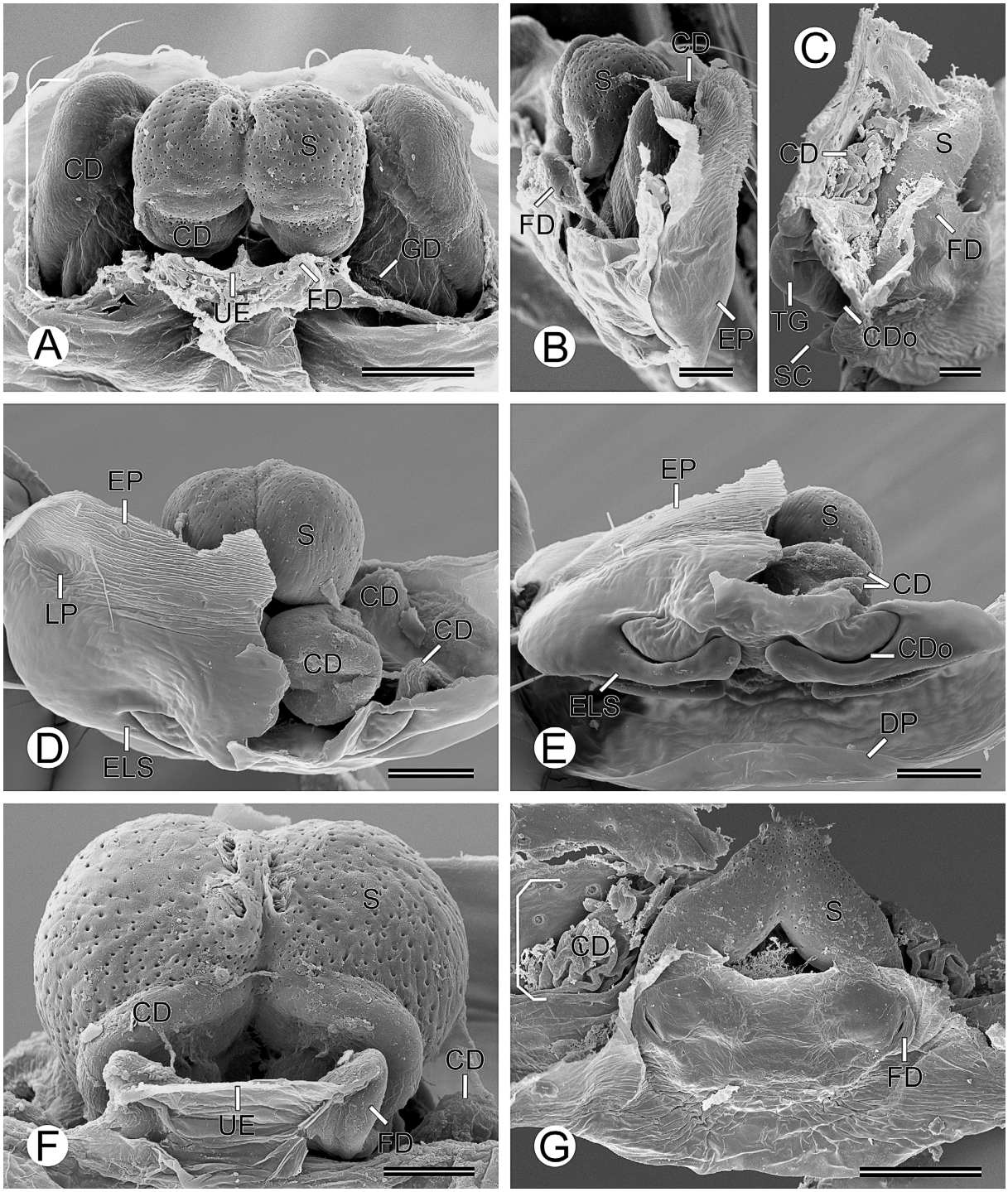

Fig. 6. Female genitalia of Theridiosomatidae Simon, 1881. **A–B**. *Theridiosoma goodnightorum* Archer, 1953, ♀ (CRBA STD1N6R027). **C, G**. *Epilineutes globosus* (O. Pickard-Cambridge, 1896), ♀ (MACN-Ar 29090). **D–F**. *Tantra bugle* gen. et sp. nov., ♀ (CRBA SFU1D9A009). **A–E, G**. Vulva, general view (A, G = dorsal view; B–C = lateral view; D = ventral view; E = posterior view). **F**. Spermathecae, dorsal view, detail. Abbreviations: CD = copulatory duct; CDo = copulatory duct opening; DP = epyginal dorsal plate; ELS = epigynal lateral spur; EP = epigynal plate; FD = fertilization duct; GD = patch of gland ducts; LP = lateral pit; S = spermatheca; SC = dorsal scape; TG = transverse groove; UE = uterus externus. Scale bars: A, D–E, G = 0.05 mm; B = 0.03 mm; C = 0.02 mm; F = 0.025 mm.

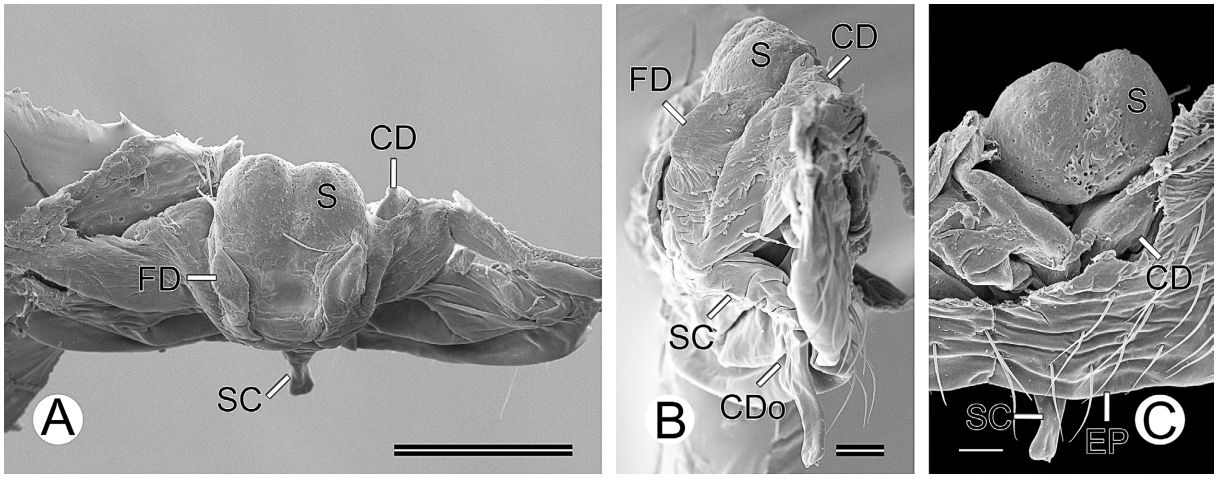

Fig. 7. *Wendilgarda clara* Keyserling, 1886, ♀, vulva (MACN-Ar 29223). **A**. Dorsal view. **B**. Lateral view. **C**. Ventral view. Abbreviations: CD = copulatory duct; CDo = copulatory duct opening; EP = epigynal plate; FD = fertilization duct; S = spermatheca, SC = dorsal scape. Scale bars: A = 0.1 mm; B–C = 0.02 mm.

Type material

Holotype

PANAMA – **Chiriquí Province** • ♂; Reserva Forestal Fortuna, Quebrada Honda, one-hectare PANCODING inventory; 8.750083° N, 82.239083° W; 1135 m a.s.l.; 7–12 Jun. 2007; M. Arnedo, D. Dimitrov, G. Hormiga, F. Labarque and M. Ramírez leg.; voucher code SFU1NAA029; MIUP.

Paratypes

PANAMA – **Chiriquí Province** • 1 ♂; same data as for holotype; voucher code SFB1DAL021; preparation codes FML-00691, LNP-00271; DNA code chts1123; GenBank code PX096990; MACN-Ar 29320 • 1 ♀; same data as for holotype; voucher code SFU1N7D015; preparation codes FML-00755, FML-01146; DNA code chts1241; GenBank code PX096997; MACN-Ar 29324 • 1 ♀; same data as for holotype; voucher code SFU2NAA035; preparation code LNP-00269; DNA code chts1059; GenBank code PX096989; MACN-Ar 29321 • 1 ♂; Parque Internacional La Amistad, Cerro Picacho, one-hectare PANCODING inventory; 8.890500° N, 82.618778° W; 2299 m a.s.l.; 12–17 Jun. 2008; M. Arnedo, L. Benavides, G. Hormiga, F. Labarque, L. Piacentini and M. Ramírez leg.; voucher code SAB1DEL024; DNA barcode SPIPA410-10; MCZ • 1 ♀; same data as for preceding; voucher code SAD1NGL021; DNA barcode SPIPA411-10; MACN-Ar 29319.

Other material

PANAMA – **Chiriquí Province** • 1 ♀; same data as for holotype; voucher code SFU2NAD028; DNA code chts1244; GenBank code PX096998; MCZ • 1 ♂; same data as for holotype; voucher code SFU1NBD019; DNA code chts1242; GenBank code PX096991; MCZ • 1 ♂; same data as for holotype; voucher code SFU1N7L018; DNA barcode SPIPA409-10; MACN-Ar 29322 • 4 ♂♂; same data as for holotype; MCZ • 1 ♂; same data as for holotype; MACN-Ar 29323 • 2 ♂♂, 1 ♀; same data as for holotype; CRBA • 2 ♀♀; same locality as for holotype; 21 Jun. 2008; L. Piacentini and F. Labarque leg.; non-quantitative sample; MACN-Ar • 1 ♀; same data as for preceding; MACN-Ar • 1 ♀; same data as for preceding; 23 Jun. 2008; MACN-Ar • 1 ♂, 4 ♀♀; Parque Internacional La Amistad, Cerro Picacho, one-hectare PANCODING inventory; 8.890500° N, 82.618778° W; 2299 m a.s.l.; 12–17 Jun. 2008; M. Arnedo, L. Benavides, G. Hormiga, F. Labarque, L. Piacentini and M. Ramírez leg.; MCZ • 1 ♀; same

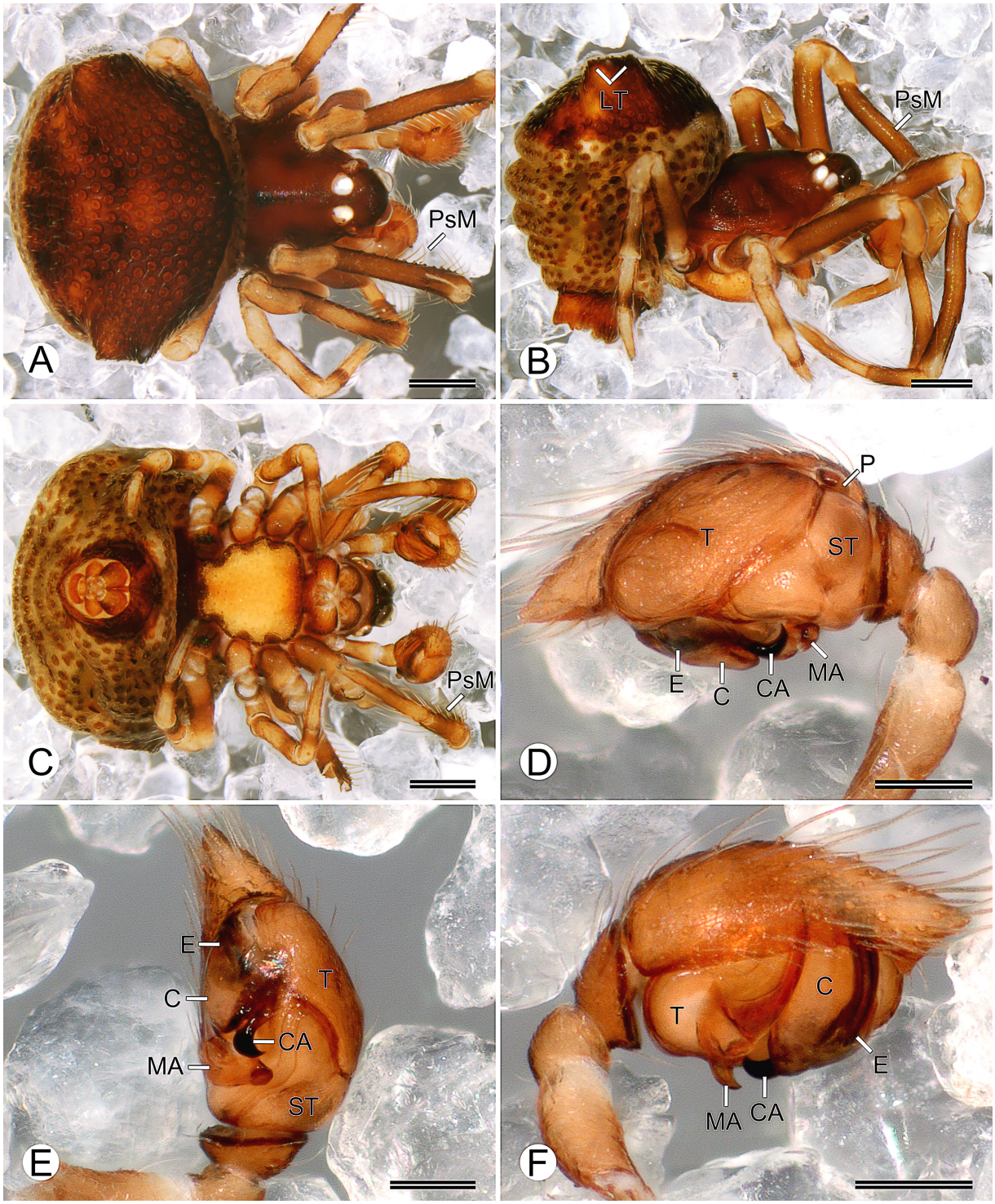

Fig. 8. *Chthonos dobo* sp. nov., paratype, ♂ (MACN-Ar 29320). **A–C**. Habitus (A = dorsal view; B = lateral view; C = ventral view). **D–F**. Left palp (D = retrolateral view; E = ventral view; F = prolateral view). Abbreviations: C = conductor; CA = conductor apophysis; E = embolus; LT = lateral tubercles; MA = median apophysis; P = paracymbium; PsM = prolateral strong macrosetae; ST = subtegulum; T = tegulum. Scale bars: A–C = 0.25 mm; D–F = 0.1 mm.

data as for preceding; voucher code SAD1NHH012; DNA code chts1245; GenBank code PX096995; MCZ • 1 ♀; same data as for preceding; voucher code SAU1NHB013; DNA barcode SPIPA412-10; MCZ • 1 ♂; same data as for preceding; voucher code SAD1NGB019; DNA code chts1247; GenBank code PX096996; MACN-Ar 29316 • 1 ♀; same data as for preceding; voucher code SAU1NFB025; DNA code chts1243; GenBank code PX096993; MACN-Ar 29315 • 1 ♂; same data as for preceding; voucher code SAU1NHP003; DNA barcode SPIPA413-10; MACN-Ar 29317 • 1 ♂; same data as for preceding; voucher code SAU1NGA027; DNA code chts1246; GenBank code PX096994; CRBA • 1 ♀; same data as for preceding; voucher code SAB1DEA003; DNA code chts1248; GenBank code PX096992; CRBA • 3 ♂♂, 3 ♀♀; same data as for preceding; MIUP • 1 ♂; same data as for preceding; MACN-Ar 29314 • 1 ♂; same data as for preceding; MACN-Ar 29311 • 1 ♂; same data as for preceding; MACN-Ar 29313 • 1 ♀; same data as for preceding; MACN-Ar 29312 • 1 ♀; same data as for preceding; MACN-Ar 29318 • 5 ♂♂, 5 ♀♀; same data as for preceding; CRBA.

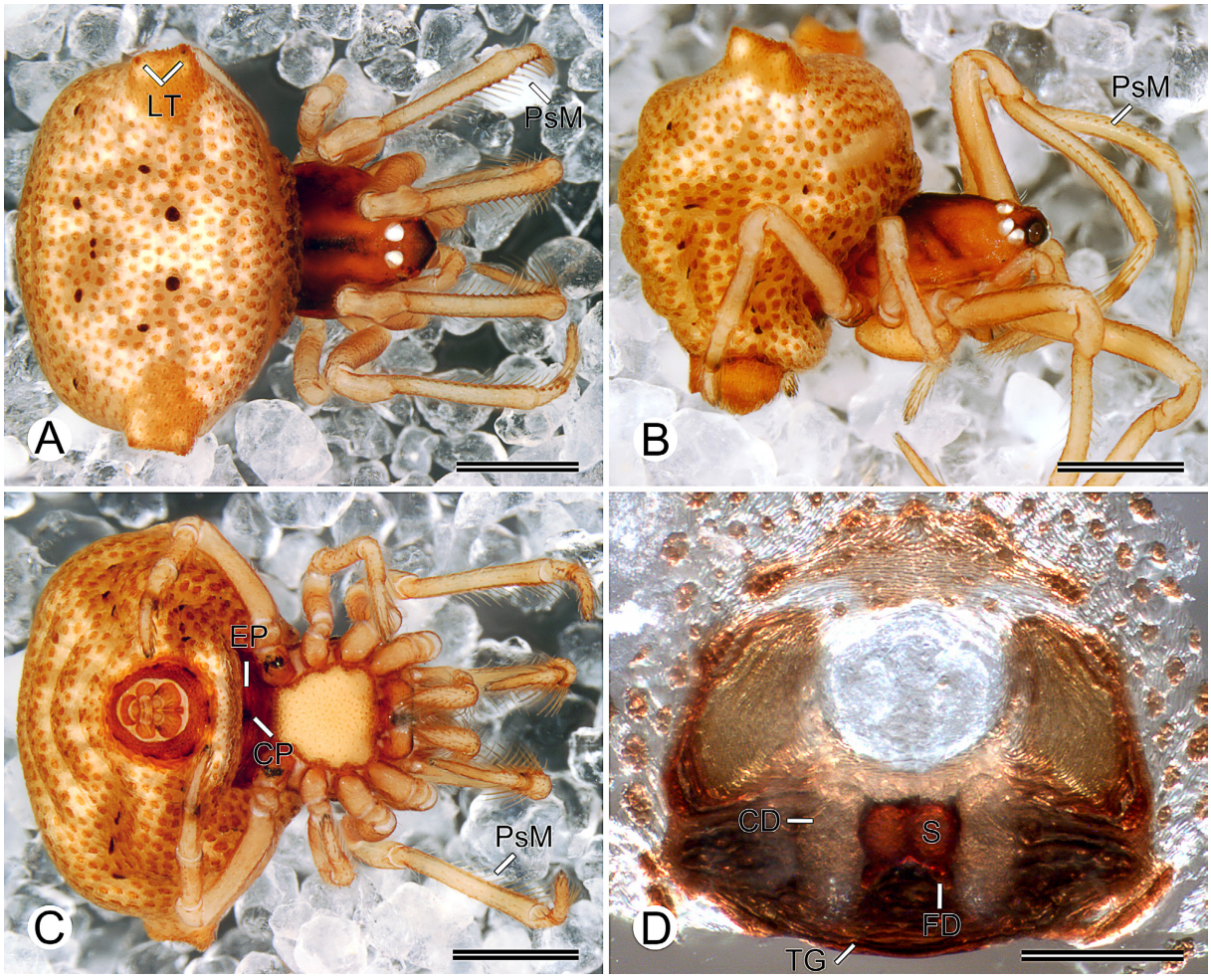

Fig. 9. *Chthonos dobo* sp. nov., paratypes, ♀♀. **A–C**. Habitus (MACN-Ar 29321) (A = dorsal view; B = lateral view; C = ventral view). **D**. Vulva, dorsal view (MACN-Ar 29324). Abbreviations: CD = copulatory duct; CP = central pit; EP = epigynal plate; FD = fertilization duct; LT = lateral tubercles; PsM = prolateral strong macrosetae; S = spermatheca; TG = transverse groove. Scale bars: A–C = 0.5 mm; D = 0.2 mm.

Description

Male (paratype MACN-Ar 29320)
Total length 1.42. Prosoma: length 0.76, width 0.61, height 0.61. Sternum: length 0.40, width 0.42. Eye diameters and interdistances: AME 0.11, PME 0.08, AME–PME 0.10. Opisthosoma: length 1.14, width 1.14, height 0.93. Leg formula: 1243. Dorsal shield of prosoma reddish-brown with darker middle and lateral lines (Fig. 8A). Sternum yellowish-orange (Fig. 8B–C). Opisthosoma color overall yellowish-white with numerous setal sclerotized pits, and dorsal reddish-brown scutum (Fig. 8A–B). Epiandrum, booklung cover, and tracheal spiracle reddish-brown (Fig. 8B–C). Spinneret field orange surrounded by reddish-brown sclerotized ring (Fig. 8B–C). Legs I–II darker than III–IV, femora and tibiae brownish-orange, metatarsi brownish-orange but proximally lighter, patellae and tarsi orange (Fig. 8A–C). Palp: cymbium distally pointed, paracymbium proximally extended ("T-shaped paracymbium" in Coddington 1986), median apophysis retrolateral side with blunt projection extending ventrally, conductor apophysis hooked, embolus entire (i.e., lacking embolic division and apophysis) and covered by conductor (Fig. 8D–F).

Female (paratypes MACN-Ar 29321, MACN-Ar 29324)
Total length 1.73. Prosoma: length 0.82, width 0.65, height 0.66. Sternum: length 0.41, width 0.43. Eye diameters and interdistances: AME 0.10, PME 0.08, AME–PME 0.11. Opisthosoma: length 1.48, width 1.64, height 1.18. Leg formula: 1243. Coloration lighter than male (Fig. 9A–C). Opisthosoma scutum absent (Fig. 9A–B). Epigynal plate reddish-brown (Fig. 9C), with transverse ridges, transverse groove deep, central pit toothed (Figs 5B, 9D). Vulva: copulatory ducts irregular and membranous, with patch of gland ducts dorsally, inserting ventrolaterally posteriorly into spermathecae, spermathecae round, sclerotized, and connate (i.e, fused along the midline), fertilization ducts sclerotized, emerging laterally posteriorly from spermathecae, curving dorsally anteriorly to meet uterus externus (Figs 5A–C, 9D).

Records and biology

Records are limited to collections made at 1135 m a.s.l. in premontane rainforest from Reserva Forestal Fortuna, and at 2299 m a.s.l. in lower montane rainforest from Parque Internacional La Amistad (Fig. 1). Males and females have been collected mostly at night by looking up, though few specimens have been collected during the day by beating and cryptic techniques.

Variation

Some males and females examined have the prosoma and opisthosoma darker than in the described specimens.

Remarks

Males of *C. dobo* sp. nov. differ from those of other Panamanian species of *Chthonos* by the conductor apophysis as wide as long, relatively bulky (Fig. 8E), whereas *C. kaibe* sp. nov. have the apophysis relatively small (Fig. 10E) and *C. kwati* sp. nov. have it longer than wide (Fig. 12E).

Chthonos kaibe sp. nov.
urn:lsid:zoobank.org:act:C03F56CB-F9DD-4EDB-B635-50314EFC5F8E
Figs 1, 10–11

Diagnosis

Males and females of *Chthonos kaibe* sp. nov. resemble the males of *C. kuyllur* Dupérré & Tapia, 2017 by the presence of two pairs of proximally separated lateral tubercles, wider than long, relatively short, that slightly exceed the dorsum of the opisthosoma (Figs 10A–B, 11A–B; Dupérré & Tapia 2017: fig. 1),

but males of *C. kaibe* can be distinguished by having the conductor apophysis retrolaterally hooked, whereas it is hooked prolaterally in *C. kuyllur* (Fig. 10E; Dupérré & Tapia 2017: fig. 2).

Etymology

The specific name is derived from 'kaibe' which means 'alone' in the Ngäbere language, currently spoken by the Ngäbe native people of Panama, and refers to the separated lateral tubercles of the opisthosoma.

Type material

Holotype

PANAMA – **Panama Province** • ♂; Parque Nacional Altos de Campana, one-hectare PANCODING inventory; 8.683444° N, 79.929833° W; 895 m a.s.l.; 14–19 Jun. 2007; M. Arnedo, D. Dimitrov, G. Hormiga, F. Labarque and M. Ramírez leg.; voucher code SCB1DED007; DNA code chts3e12; GenBank code PX097002; MIUP.

Paratypes

PANAMA – **Panama Province** • 1 ♂; same data as for holotype; voucher code SCU2NDD007; preparation codes FML-00693, LNP-00283; DNA code chts3117; GenBank code PX097001; MACN-Ar 29000 • 1 ♀; same data as for holotype; voucher code SCU1NFH016; preparation code LNP-00289; DNA code chts3109; GenBank code PX097000; MACN-Ar 28999 • 1 ♂; same data as for holotype; voucher code SCU2NDA009; DNA code chts3g12; GenBank code PX097003; MCZ. – **Coclé Province** • 1 ♂; Parque Nacional General de División Omar Torrijos Herrera, El Cope, one-hectare PANCODING inventory; 8.668083° N, 80.592583° W; 760 m a.s.l.; 4–9 Jun. 2008; M. Arnedo, L. Benavides, G. Hormiga, F. Labarque and M. Ramírez leg.; voucher code STU1N7H024; DNA barcode SPIPA406-10; MCZ.

Description

Male (paratype MACN-Ar 29000)

Total length 1.50. Prosoma: length 0.80, width 0.62, height 0.61. Sternum: length 0.37, width 0.44. Eye diameters and interdistances: AME 0.10, PME 0.08, AME–PME 0.10. Opisthosoma: length 1.24, width 1.14, height 0.95. Leg formula: 1243. Dorsal shield of prosoma reddish-brown (Fig. 10A). Sternum reddish-brown (Fig. 10B–C). Opisthosoma color overall yellowish-white with numerous setal sclerotized pits, and dorsal reddish-brown scutum with symmetric lighter pattern (Fig. 10A–B). Epiandrum, booklung cover, and tracheal spiracle reddish-brown (Fig. 10B–C). Spinneret field orange surrounded by reddish-brown sclerotized ring (Fig. 10B–C). Legs I–II darker than III–IV, femora and tibiae brownish-orange with lighter middle band, metatarsi brownish-orange but proximally lighter, patellae and tarsi orange (Fig. 10A–C). Palp: cymbium distally pointed, paracymbium proximally extended, median apophysis retrolateral side with blunt projection extending ventrally, conductor apophysis hooked, embolus entire and covered by conductor (Fig. 10D–F).

Female (paratype MACN-Ar 28999)

Total length 1.65. Prosoma: length 0.87, width 0.67, height 0.67. Sternum: length 0.41, width 0.46. Eye diameters and interdistances: AME 0.09, PME 0.08, AME–PME 0.10. Opisthosoma: length 1.26, width 1.42, height 1.04. Leg formula: 1243. Coloration lighter and greenish-browner than male (Fig. 11A–C). Opisthosoma scutum absent (Fig. 11A–B). Epigynal plate reddish-brown (Fig. 10C), with transverse ridges, transverse groove deep, central pit toothed (Fig. 11D). Vulva: copulatory ducts irregular and membranous, with patch of gland ducts dorsally, inserting ventrolaterally posteriorly into spermathecae, spermathecae round, sclerotized, and connate (i.e., fused along the midline), fertilization ducts sclerotized, emerging laterally posteriorly from spermathecae, curving dorsally anteriorly to meet uterus externus (Fig. 11D).

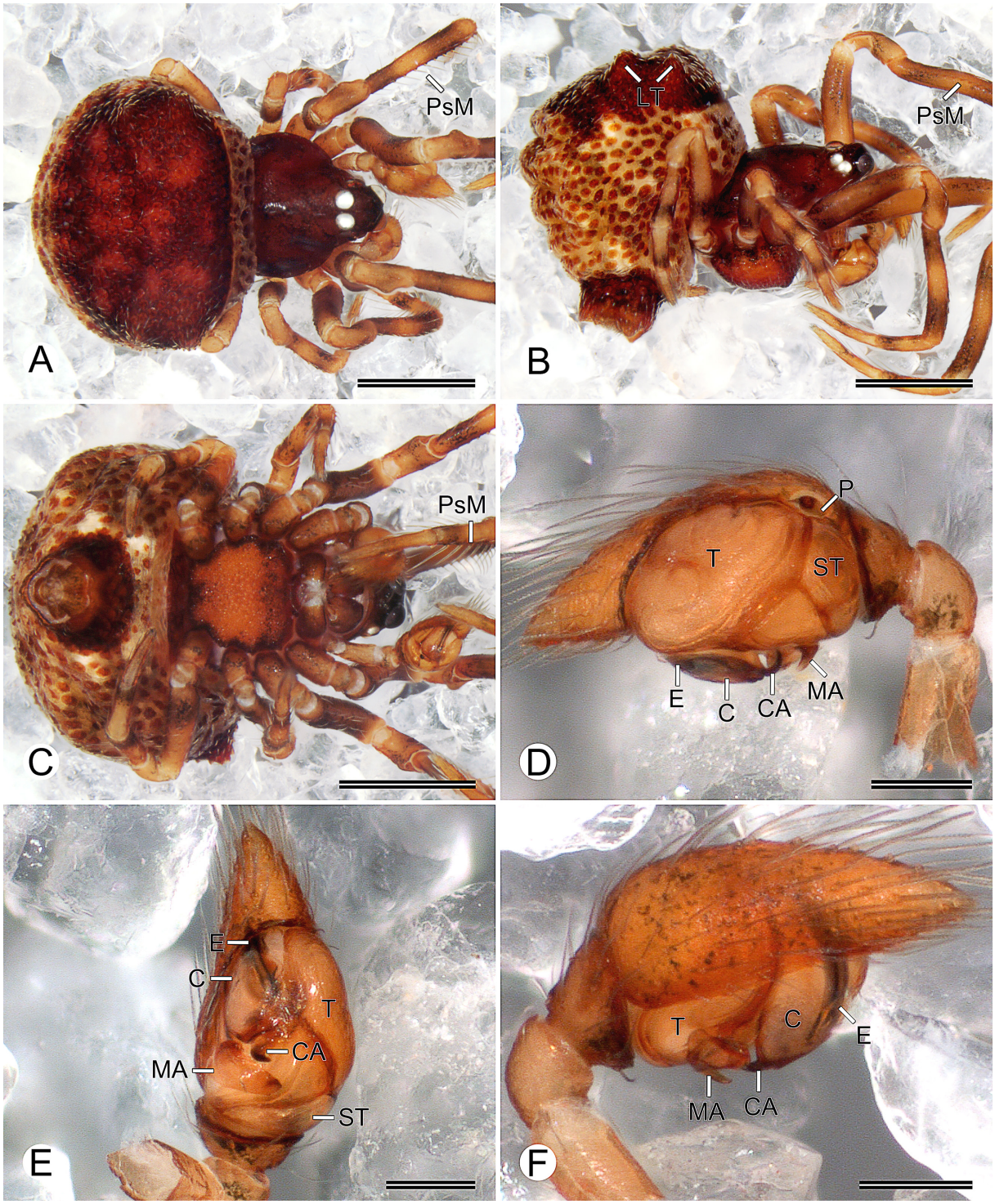

Fig. 10. *Chthonos kaibe* sp. nov., paratype, ♂ (MACN-Ar 29000). **A–C**. Habitus (A = dorsal view; B = lateral view; C = ventral view). **D–F**. Left palp (D = retrolateral view; E = ventral view; F = prolateral view). Abbreviations: C = conductor; CA = conductor apophysis; E = embolus; LT = lateral tubercles; MA = median apophysis; P = paracymbium; PsM = prolateral strong macrosetae; ST = subtegulum; T = tegulum. Scale bars: A–C = 0.5 mm; D–F = 0.1 mm.

Records and biology

Records are limited to collections made at 760 m a.s.l. and 895 m a.s.l. in premontane rainforest from Parque Nacional Altos de Campana and Parque Nacional General de División Omar Torrijos Herrera, respectively (Fig. 1). Males and a single female have been collected mostly at night by looking up; one male specimen was collected during the day by beating.

Variation

Some males examined have the prosoma and opisthosoma darker than the described specimen.

Remarks

Males of *C. kaibe* sp. nov. differ from those of other Panamanian species of *Chthonos* by the conductor apophysis wider than long, less sclerotized, relatively small (Fig. 10E), whereas *C. dobo* sp. nov. have the apophysis heavily sclerotized (i.e., dark; Fig. 8E) and *C. kwati* sp. nov. have it longer than wide (Fig. 12E).

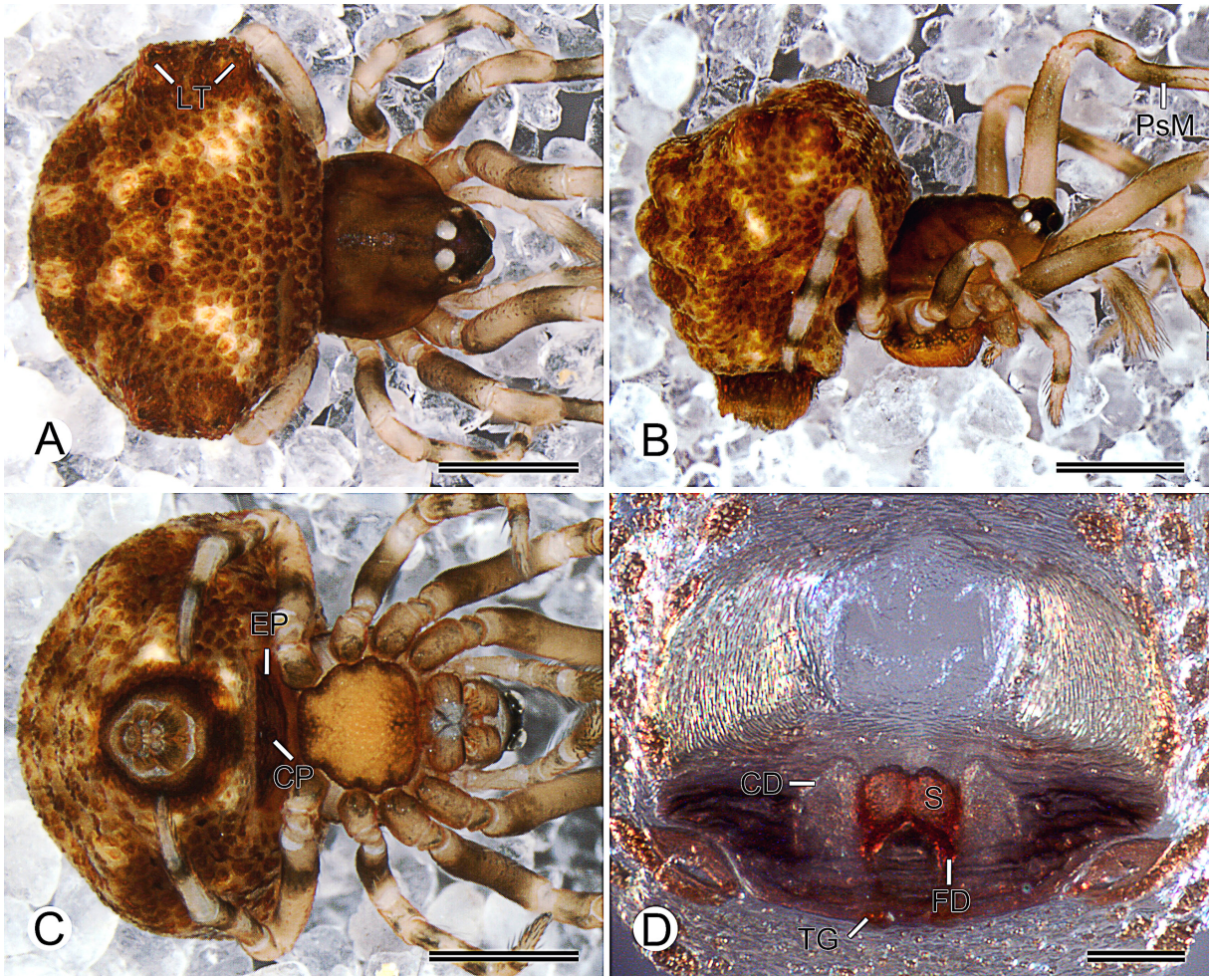

Fig. 11. *Chthonos kaibe* sp. nov., paratype, ♀ (MACN-Ar 28999). **A–C**. Habitus (A = dorsal view; B = lateral view; C = ventral view). **D**. Vulva, dorsal view. Abbreviations: CD = copulatory duct; CP = central pit; EP = epigynal plate; FD = fertilization duct; LT = lateral tubercles; PsM = prolateral strong macrosetae; S = spermatheca; TG = transverse groove. Scale bars: A–C = 0.5 mm; D = 0.1 mm.

Chthonos kwati sp. nov.
urn:lsid:zoobank.org:act:D5C63226-E53A-4A2D-98D3-918F61AD3AB3
Figs 1, 12–13

Diagnosis

Males and females of *Chthonos kwati* sp. nov. resemble the females of *Chthonos tuberosa* (Keyserling, 1886) by the presence of five dorsal opisthosoamal tubercles, including two lateral pairs, each pair separated by their diameter, wider than long and relatively short, and one anterior central tubercle as wide as long (Figs 12A–B, 13A–B; Keyserling 1886: pl. XX figs 303, 303A), but *C. kwati* can be distinguished by the presence of a posterior central tubercle, longer than wide, extending posteriorly.

Etymology

The specific name is derived from 'kwätí' which means 'six' in the Ngäbere language, currently spoken by the Ngäbe native people of Panama, and refers to the six tubercles of the opisthosoma.

Type material

Holotype

PANAMA – **Chiriquí Province** • ♂; Reserva Forestal Fortuna, Quebrada Honda, one-hectare PANCODING inventory, 8.750083° N, 82.239083° W; 1135 m a.s.l.; 7–12 Jun. 2007; M. Arnedo, D. Dimitrov, G. Hormiga, F. Labarque and M. Ramírez leg.; voucher code SFD1NCR006; preparation codes FML-00706, FML-00707; DNA barcode SPIPA408-10; MIUP.

Paratype

PANAMA – **Chiriquí Province** • 1 ♀; same data as for holotype; voucher code SFU1NAD034; preparation code LNP-00279; DNA code chts2061; GenBank code PX096999; MACN-Ar 29067.

Description

Male (holotype MIUP SFD1NCR006)

Total length 1.64. Prosoma: length 0.81, width 0.65, height 0.64. Sternum: length 0.40, width 0.49. Eye diameters and interdistances: AME 0.10, PME 0.09, AME–PME 0.10. Opisthosoma: length 1.4, width 1.14, height 1.06. Leg formula: 1243. Dorsal shield of prosoma reddish-brown (Fig. 12A). Sternum reddish-brown (Fig. 12B–C). Opisthosoma color overall yellowish-white with numerous setal sclerotized pits, and dorsal reddish-brown scutum with symmetric lighter pattern (Fig. 12A–B). Epiandrum, booklung cover, and tracheal spiracle reddish-brown (Fig. 12B–C). Spinneret field orange surrounded by reddish-brown sclerotized ring (Fig. 12B–C). Legs I–II darker than III–IV, femora and tibiae greenish-brown with lighter middle band, metatarsi greenish-brown but proximally lighter, patellae greenish-brown and tarsi orange (Fig. 12A–C). Palp: cymbium distally pointed, paracymbium proximally extended, median apophysis retrolateral side with blunt projection extending ventrally, conductor apophysis hooked, embolus entire and covered by conductor (Fig. 12D–F).

Female (paratype MACN-Ar 29067)

Total length 1.98. Prosoma: length 0.89, width 0.69, height 0.71. Sternum: length 0.41, width 0.48. Eye diameters and interdistances: AME 0.10, PME 0.09, AME–PME 0.11. Opisthosoma: length 1.59, width 1.55, height 1.35. Leg formula: 1243. Coloration lighter than male (Fig. 13A–C). Opisthosoma scutum absent (Fig. 13A–B). Epigynal plate reddish-brown (Fig. 13C), with transverse ridges, transverse groove deep, central pit toothed (Fig. 13D). Vulva: copulatory ducts irregular and membranous, with patch of gland ducts dorsally, inserting ventrolaterally posteriorly into spermathecae, spermathecae round, sclerotized, and connate (i.e, fused along midline), fertilization ducts sclerotized, emerging laterally posteriorly from spermathecae, curving dorsally anteriorly to meet uterus externus (Fig. 13D).

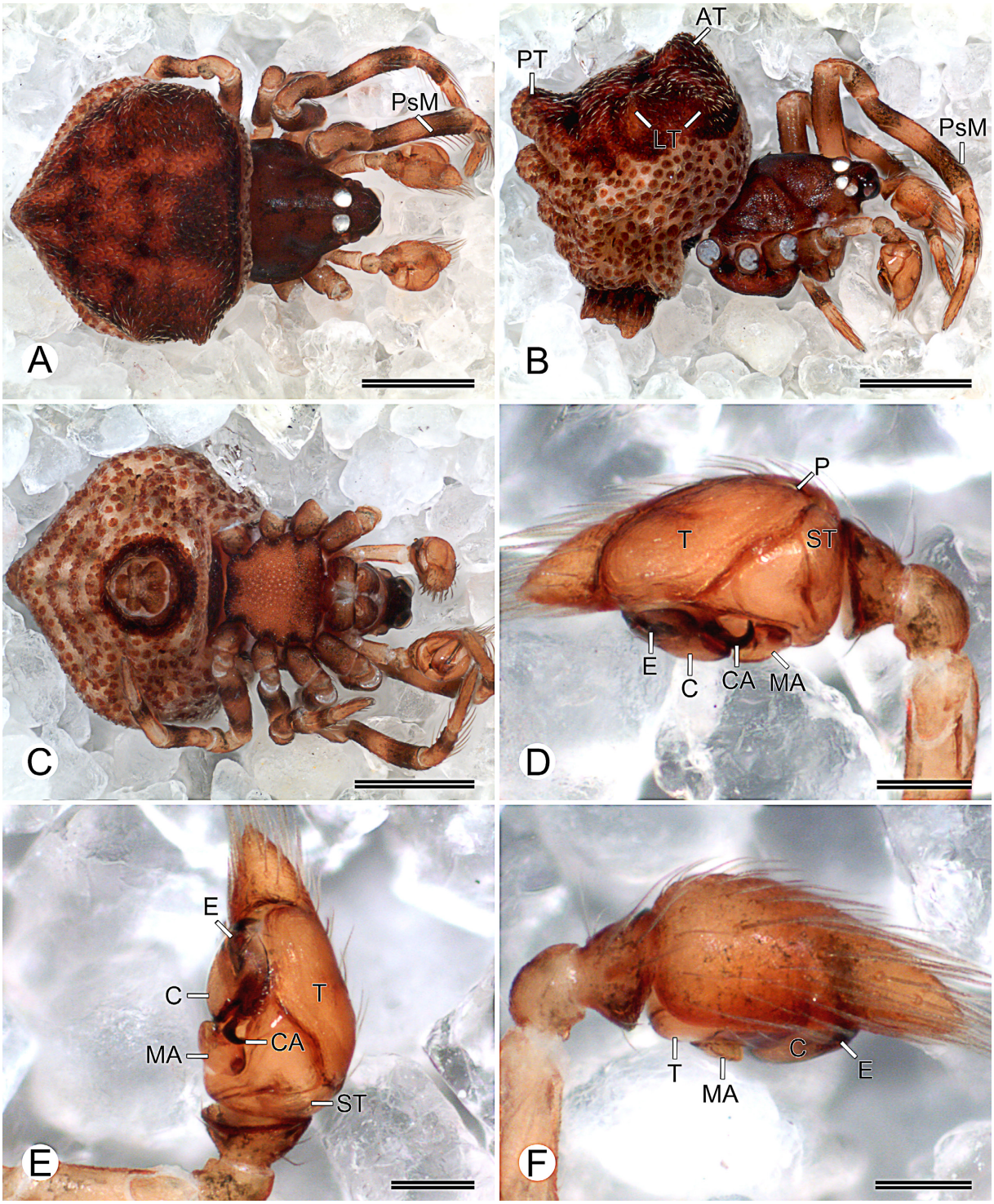

Fig. 12. *Chthonos kwati* sp. nov., holotype, ♂ (MIUP SFD1NCR006). **A–C**. Habitus (A = dorsal view; B = lateral view; C = ventral view). **D–F**. Left palp (D = retrolateral view; E = ventral view; F = prolateral view). Abbreviations: AT = anterior tubercle; C = conductor; CA = conductor apophysis; E = embolus; LT = lateral tubercles; MA = median apophysis; P = paracymbium; PsM = prolateral strong macrosetae; PT = posterior tubercle; ST = subtegulum; T = tegulum. Scale bars: A–C = 0.5 mm; D–F = 0.1 mm.

Records and biology

Records are limited to collections made at 1135 m a.s.l. in premontane rainforest from Reserva Forestal Fortuna (Fig. 1). The male and female have been collected at night by looking down and looking up, respectively.

Remarks

Males of *C. kwati* sp. nov. differ from those of other Panamanian species of *Chthonos* by having the conductor apophysis longer than wide, forming a straight angle hook (Fig. 12E), whereas *C. dobo* sp. nov. and *C. kaibe* sp. nov. have the apophysis wider than long (Figs 8E, 10E).

The type specimen of *Chthonos tuberosa* was examined. *Tecmessa tuberosa* Keyserling, 1886: 252, pl. 20 fig. 303 [♀] [type ♀ from Brazil, Santa Catarina, Blumenau (British Museum of Natural History), examined].

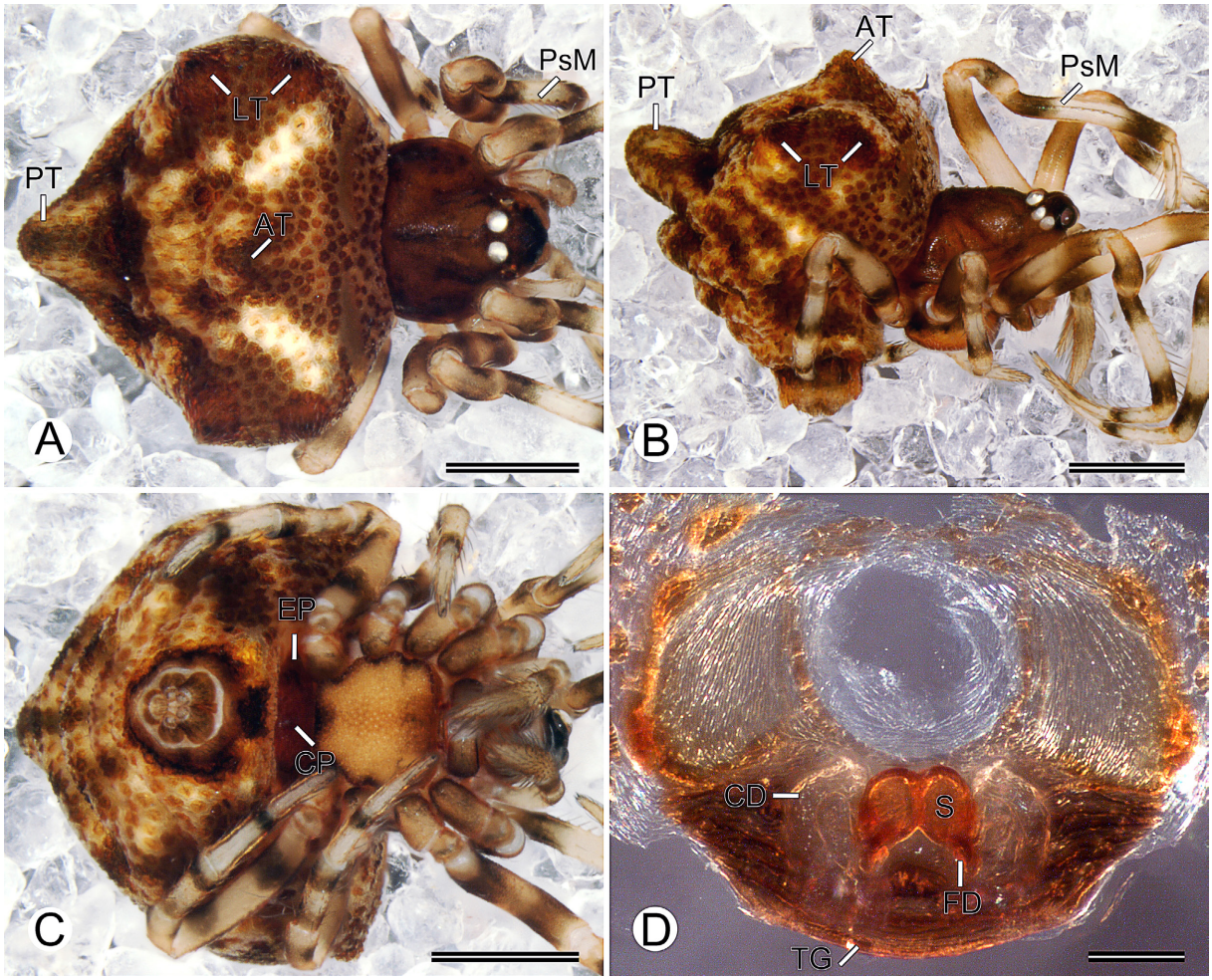

Fig. 13. *Chthonos kwati* sp. nov., paratype, ♀ (MACN-Ar 29067). **A–C**. Habitus (A = dorsal view; B = lateral view; C = ventral view). **D**. Vulva, dorsal view. Abbreviations: AT = anterior tubercle; CD = copulatory duct; CP = central pit; EP = epigynal plate; FD = fertilization duct; LT = lateral tubercles; PsM = prolateral strong macrosetae; PT = posterior tubercle; S = spermatheca; TG = transverse groove. Scale bars: A–C = 0.5 mm; D = 0.1 mm.

Epeirotypus O. Pickard-Cambridge, 1894

Epeirotypus O. Pickard-Cambridge, 1894: 134. Type species *Epeirotypus brevipes* O. Pickard-Cambridge, 1894.

Diagnosis

Males of *Epeirotypus* can be distinguished from those of other theridiosomatid genera by the long, bulky embolus distally acute (Figs 14E, 16E, 18E; see also Coddington 1986) (in contrast with entire, thin laminated, or distally lobed embolus in the other genera). Females of *Epeirotypus* can be distinguished from those of other genera by the domed (i.e., elevated ventrally) epigynal plate (Miller *et al.* 2009: fig. 3b) (absent in other genera except for *Naatlo*), a vulval bifid sclerotized septum (i.e., see BS in figures) formed by posterior projections extending behind the spermathecae and fusing along the midline (absent in other genera), and the distal section of the copulatory ducts heavily sclerotized in connection with the spermathecae (Figs 5D, 15C–D, 17C–D, 19C–D, 20C–D, 21C–D, 22C–D, 23C–D; see also Coddington 1986) (in contrast with irregular and membranous or completely sclerotized copulatory ducts).

Description

Females of *Epeirotypus* have massive proximal copulatory ducts (i.e., more than three times diameter of distal region of copulatory ducts) with dorsal patches of gland ducts, and distal copulatory ducts heavily sclerotized (i.e., dark) inserting dorsolaterally posteriorly into spermathecae (Figs 5D–E, 15D, 17D, 19D, 20D, 21D, 22D, 23D). For further genus description details, see Coddington (1986) and Labarque & Griswold (2014).

Epeirotypus kwakwa sp. nov.

urn:lsid:zoobank.org:act:0258B6F6-96F3-46B5-B866-E1D33917F3D6

Figs 1, 14–15

Diagnosis

Males and females of *Epeirotypus kwakwa* sp. nov. resemble those of *Epeirotypus chavarria* by the ovoid opisthosoma lacking lateral posterior tubercles (Figs 14A–C, 15A–C; Coddington 1986: figs 56–57), common in the other species of the genus, but *E. kwakwa* can be distinguished by an olive-green pattern on the dorsum of the opisthosoma that resembles the number eight (Figs 14A, 15A), whereas *E. chavarria* have the opisthosoma off-white (Coddington 1986: figs 56–57). Females of *E. kwakwa* can also be distinguished by the vulval bifid sclerotized septum forming a squared angle posteriorly (Fig. 15D), whereas *E. chavarria* have the bifid septum forming a rectangle (Coddington 1986: fig. 60).

Etymology

The specific name is derived from ‘kwä, kwä’ which means ‘eight’ in the Ngäbere language, currently spoken by the Ngäbe native people of Panama, and refers to the dorsal coloration pattern of the opisthosoma forming the number eight.

Type material

Holotype

PANAMA – **Chiriquí Province** • ♂; Reserva Forestal Fortuna, Quebrada Honda, one-hectare PANCODING inventory; 8.750083° N, 82.239083° W; 1135 m a.s.l.; 7–12 Jun. 2007; M. Arnedo, D. Dimitrov, G. Hormiga, F. Labarque and M. Ramírez leg.; voucher code SFU2NCH029; DNA barcode SPIPA403-10; MIUP.

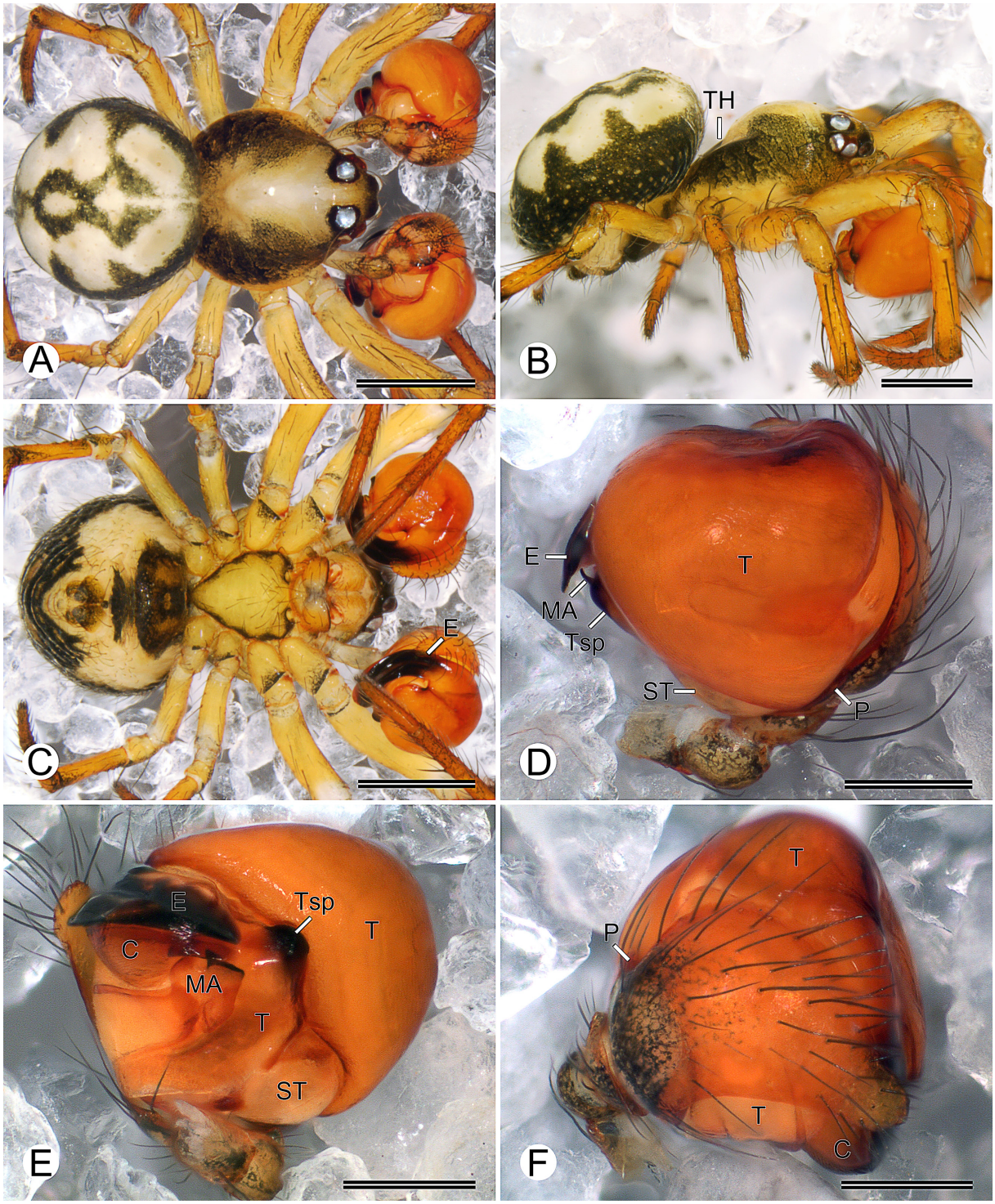

Fig. 14. *Epeirotypus kwakwa* sp. nov., paratype, ♂ (MACN-Ar 28996). **A–C** Habitus (A = dorsal view; B = lateral view; C = ventral view). **D–F**. Left palp (D = retrolateral view; E = ventral view; F = prolateral view). Abbreviations: C = conductor; E = embolus; MA = median apophysis; P = paracymbium; ST = subtegulum; T = tegulum; TH = laterally higher thoracic area; Tsp = tegular spur. Scale bars: A–C = 0.5 mm; D–F = 0.2 mm.

Paratypes

PANAMA – **Chiriquí Province** • 1 ♂; same data as for holotype; voucher code SFD1D8R010; preparation codes FML-00687, LNP-00270; DNA code epes1120; GenBank code PX096942; MACN-Ar 28996 • 1 ♀; same data as for holotype; voucher code SFD1NBL015; preparation codes FML-00697, LNP-00267; DNA code epes1058; GenBank code PX096940; MACN-Ar 28995 • 1 ♀; same data as for holotype; voucher code SFD1DAR018; DNA code epes1166; GenBank code PX096941; MCZ • 1 ♀; same data as for holotype; voucher code SFC1N8H018; DNA barcode SPIPA404-10; MCZ • 1 ♀; same data as for holotype; voucher code SFC1NCD018; DNA barcode SPIPA400-10; MCZ.

Other material

PANAMA – **Chiriquí Province** • 1 ♀; same data as for holotype; voucher code SFD1NCD016; DNA barcode SPIPA402-10; MACN-Ar 28993 • 1 ♀; same data as for holotype; voucher code SFU1N7H029; DNA barcode SPIPA401-10; MACN-Ar 28994 • 1 ♀; same data as for holotype; voucher code SFC1NAR016; DNA code epes1168; GenBank code PX096944; CRBA • 1 ♀; same data as for holotype; voucher code SFU1NCD030; DNA code epes1167; GenBank code PX096943; CRBA • 2 ♂♂, 3 ♀♀;

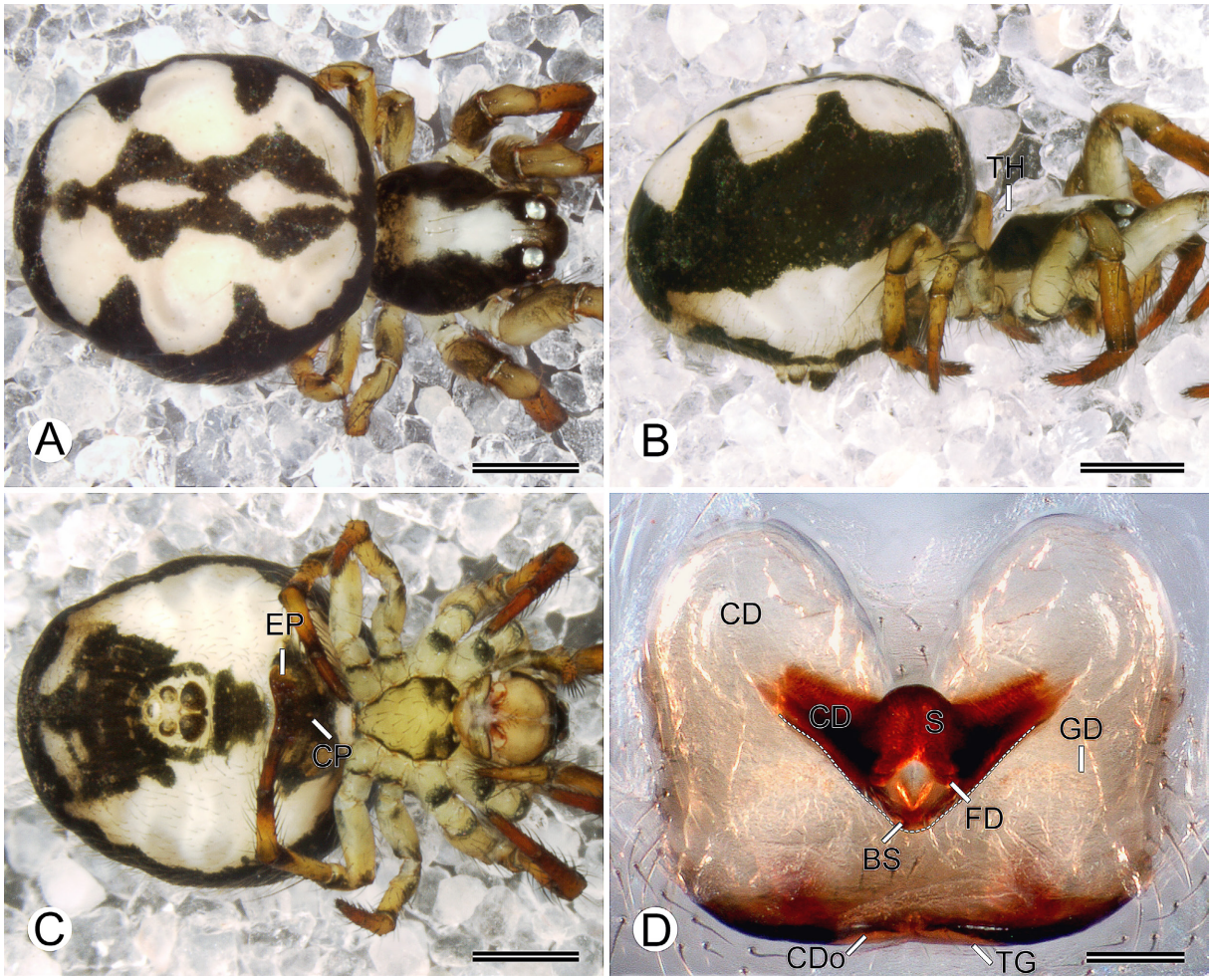

Fig. 15. *Epeirotypus kwakwa* sp. nov., paratype, ♀ (MACN-Ar 28995). **A–C**. Habitus (A = dorsal view; B = lateral view; C = ventral view). **D**. Vulva, dorsal view (note the profile of the bifid septum extending posteriorly). Abbreviations: BS = bifid septum; CD = copulatory duct; CDo = copulatory duct opening; CP = central pit; EP = epigynal plate; FD = fertilization duct; GD = patch of gland ducts; S = spermatheca; TG = transverse groove; TH = laterally higher thoracic area. Scale bars: A–C = 0.5 mm; D = 0.1 mm.

same data as for holotype; MCZ • 1 ♂, 1 ♀; same data as for holotype; MIUP • 1 ♂, 4 ♀♀; same data as for holotype; MACN-Ar 28992 • 1 ♂, 4 ♀♀; same data as for holotype; CRBA.

Description

Male (paratype MACN-Ar 28996)
Total length 1.53. Prosoma: length 1.19, width 0.76, height 0.78. Sternum: length 0.43, width 0.37. Eye diameters and interdistances: AME 0.08, PME 0.09, AME–PME 0.10. Opisthosoma: length 1.25, width 0.85, height 0.94; without tubercles. Leg formula: 1243. Dorsal shield of prosoma dark olive-green laterally, yellowish-white centrally forming irregular band (Fig. 14A–B). Dorsum of ocular area yellowish-white (Fig. 14A). Thoracic area of prosoma laterally higher (Fig. 14B; see "shoulders" in Coddington 1986). Sternum greenish-yellow with olive-green borders (Fig. 14C). Dorsum of opisthosoma olive-green with three pairs of whitish-gray patches laterally, all fused, and two middle whitish-gray patches (Fig. 14A–B). Epiandrium, booklung cover, tracheal spiracle, spinneret field and behind anal tubercle olive-green, surrounded by whitish-gray area (Fig. 14C). Legs I–II darker than III–IV, femora yellowish-white, patella, tibiae, metatarsi and tarsi orange (Fig. 14A–C). Palp: paracymbium wider than long, tegulum retrolaterally massive, tegular spur rounded, median apophysis rounded, distally notched, with projection extending distally, conductor reduced, partially covering embolus, embolus long, bulky and distally acute (Fig. 14D–F).

Female (paratype MACN-Ar 28995)
Total length 2.59. Prosoma: length 1.01, width 0.72, height 0.59. Sternum: length 0.46, width 0.39. Eye diameters and interdistances: AME 0.08, PME 0.10, AME–PME 0.09. Opisthosoma: length 1.74, width 1.55, height 1.37. Leg formula: 1243. Coloration olive-greener than male (Fig. 15A–C). Sternum with two olive-green patches close to sternal pits (Fig. 15C). Spinneret field surrounded by olive-green line (Fig. 15B–C). Epigynal plate olive-green (Fig. 15C), domed, with transverse groove, central pit deep (Fig. 15C). Vulva: copulatory ducts massive, proximally with patch of gland ducts dorsally, heavily sclerotized distally inserting dorsolaterally posteriorly into spermathecae, spermathecae anteriorly sharp, sclerotized, and connate (i.e., fused one above the other), fertilization ducts sclerotized, relative small, emerging dorsally posteriorly from spermathecae, curving anteriorly to meet uterus externus (Fig. 15D).

Records and biology

Records are limited to collections made at 1135 m a.s.l. in premontane rainforest from Reserva Forestal Fortuna (Fig. 1). Males and females have been collected mostly at night by looking down, although some specimens were also collected at night by looking up and cryptic techniques, and others during the day by looking down.

Epeirotypus kra sp. nov.
urn:lsid:zoobank.org:act:2F5F5100-B6C2-43B0-91FF-9260961A0906
Figs 1, 5D–E, 16–17

Diagnosis

Males and females of *Epeirotypus kra* sp. nov. resemble those of *E. kote* sp. nov. by the whitish-yellow body coloration (Figs 16A–C, 17A–C, 18A–C, 19A–C), but males of *E. kra* can be distinguished by the median apophysis distal projection relatively acute (Fig. 16E), whereas *E. kote* have the projection wider (Fig. 18E). Females of *E. kra* can be distinguished by the vulval bifid sclerotized septum forming a rectangle posteriorly (Fig. 17D), whereas in *E. kote* the bifid septum resembles an inverted trapezoid (Fig. 19D).

Etymology

The specific name is derived from 'krä' which means 'thin' in the Ngäbere language, currently spoken by the Ngäbe native people of Panama, and refers to the relatively low prosoma.

Type material

Holotype

PANAMA – **Chiriquí Province** • ♂; Reserva Forestal Fortuna, Quebrada Honda, one-hectare PANCODING inventory; 8.750083° N, 82.239083° W; 1135 m a.s.l.; 7–12 Jun. 2007; M. Arnedo, D. Dimitrov, G. Hormiga, F. Labarque and M. Ramírez leg.; voucher code SFB1DAH019; DNA code epes2183; GenBank code PX096947; MIUP.

Paratypes

PANAMA – **Chiriquí Province** • 1 ♂; same data as for holotype; voucher code SFU1N8L020; preparation codes FML-00688, LNP-00255; DNA code epes3111; GenBank code PX096951; MCZ • 1 ♀; same data as for holotype; voucher code SFU2NBD029; preparation codes FML-00695, LNP-00277; DNA code epes2063; GenBank code PX096946; MCZ • 1 ♂; same data as for holotype; voucher code SFU1NAA009; DNA code epes2053; GenBank code PX096945; MACN-Ar 29218 • 1 ♀; same data as for holotype; voucher code SFU1N7H026; DNA barcode SPIPA391-10; MACN-Ar 29217 • 1 ♀; same data as for holotype; voucher code SFU1NBH019; DNA barcode SPIPA390-10; MACN-Ar 29221.

Other material

PANAMA – **Chiriquí Province** • 1 ♀; same data as for holotype; voucher code SFD1DAA016; DNA code epes2184 GenBank code PX096948; MIUP • 1 ♀; same data as for holotype; voucher code SFU1N8A024; DNA code epes2203; GenBank code PX096949; MCZ • 1 ♀; same data as for holotype; voucher code SFU1NCA029; DNA code epes3208; GenBank code PX096953; MCZ • 1 ♀; same data as for holotype; voucher code SFU2NBA026; DNA code epes3209; GenBank code PX096954; MCZ • 1 ♀; same data as for holotype; voucher code SFU2NBH023; preparation code FML-01149; DNA code epes3054; GenBank code PX096950; MACN-Ar 29220 • 1 ♀; same data as for holotype; voucher code SFU2NCH031; DNA code epes3207; GenBank code PX096952; MACN-Ar 29219 • 1 ♀; same data as for holotype; voucher code SFD1DAL018; DNA code epes5062; GenBank code PX096955; MACN-Ar 29216 • 1 ♂, 3 ♀♀; same data as for holotype; CRBA • 3 ♂♂, 5 ♀♀; same locality as for holotype; 21–24 Jun. 2008; L. Piacentini and F. Labarque leg.; non-quantitative sample; MACN-Ar.

Description

Male (paratype MCZ SFU1N8L020)

Total length 2.21. Prosoma: length 1.25, width 0.98, height 0.71. Sternum: length 0.53, width 0.45. Eye diameters and interdistances: AME 0.11, PME 0.08, AME–PME 0.14. Opisthosoma: length 1.38, width 1.36, height 1.11; with posterior lateral tubercles. Leg formula: 1243. Dorsal shield of prosoma dark olive-green laterally, yellowish-white centrally forming irregular band (Fig. 16A–B). Dorsum of ocular area yellowish-white (Fig. 16A). Thoracic area of prosoma laterally higher (Fig. 16B). Sternum yellow (Fig. 16C). Dorsum of opisthosoma olive-green with five whitish-gray patches, anterior and middle ones fused, covered by sparsely thin olive-green flecks (Fig. 16A–B). Opisthosoma with two lateral posterior tubercles connected ventrally by guanine silver stripe (Fig. 16C). Epiandrium, booklung cover, tracheal spiracle, and spinneret field yellow, olive-green thick patch behind anal tubercle (Fig. 16C). Legs I–II lighter than III–IV, femora and patella yellowish-white, tibiae and metatarsi yellow but distally dark, tarsi yellow (Fig. 16A–C). Palp: paracymbium wider than long, tegulum retrolaterally massive (i.e., almost half the size of bulb), tegular spur rounded, median apophysis rounded, distally notched (see "dorsal notch" in Coddington 1986), with projection extending distally, conductor reduced (i.e., relatively smaller than embolus) partially covering embolus, embolus long, bulky and distally acute (Fig. 16D–F).

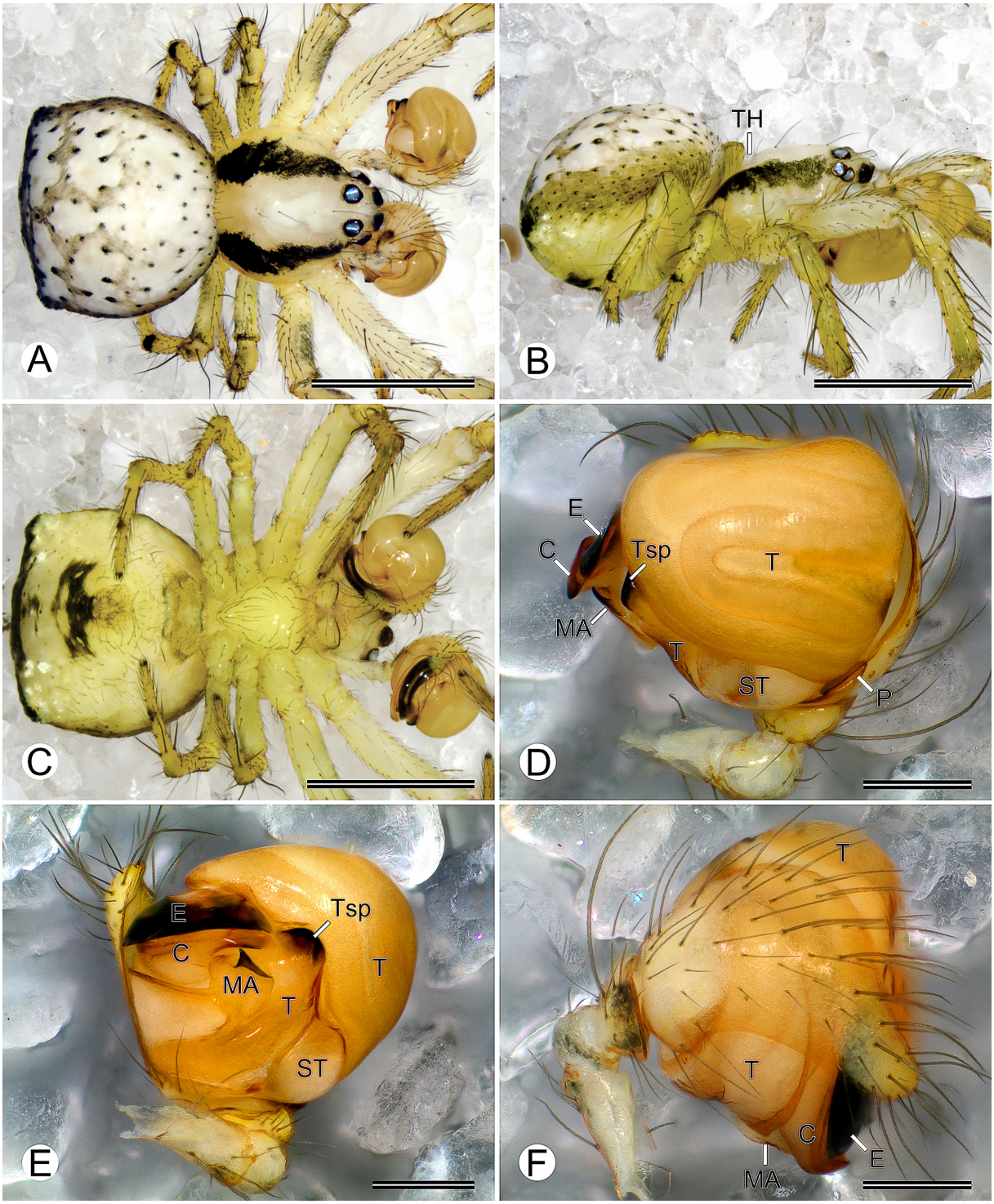

Fig. 16. *Epeirotypus kra* sp. nov., paratype, ♂ (MCZ SFU1N8L020). **A–C**. Habitus (A = dorsal view; B = lateral view; C = ventral view). **D–F**. Left palp (D = retrolateral view; E = ventral view; F = prolateral view). Abbreviations: C = conductor; E = embolus; MA = median apophysis; P = paracymbium; ST = subtegulum; T = tegulum; TH = laterally higher thoracic area; Tsp = tegular spur. Scale bars: A–C = 1 mm; D–F = 0.2 mm.

Female (paratypes MCZ SFU2NBD029, MACN-Ar 29220)
Total length 2.95. Prosoma: length 1.42, width 1.06, height 0.72. Sternum: length 0.64, width 0.51. Eye diameters and interdistances: AME 0.11, PME 0.10, AME–PME 0.12. Opisthosoma: length 1.82, width 1.80, height 1.62. Leg formula: 1243. Coloration as in male (Fig. 17A–C). Epigynal plate olive-green (Fig. 17C). Epigynal plate: domed, with transverse groove, central pit deep (Fig. 17B–C). Vulva: copulatory ducts massive, proximally with patch of gland ducts dorsally, heavily sclerotized distally inserting dorsolaterally posteriorly into spermathecae, spermathecae anteriorly sharp, sclerotized, and connate (i.e., fused one above the other), fertilization ducts sclerotized, relative small, emerging dorsally posteriorly from spermathecae, curving anteriorly to meet uterus externus (Figs 5D–E, 17D).

Records and biology

Records are limited to collections made at 1135 m a.s.l. in premontane rainforest from Reserva Forestal Fortuna (Fig. 1). Males and females have been collected mostly at night by looking up; two males and one female were collected during the day by looking down and beating, respectively.

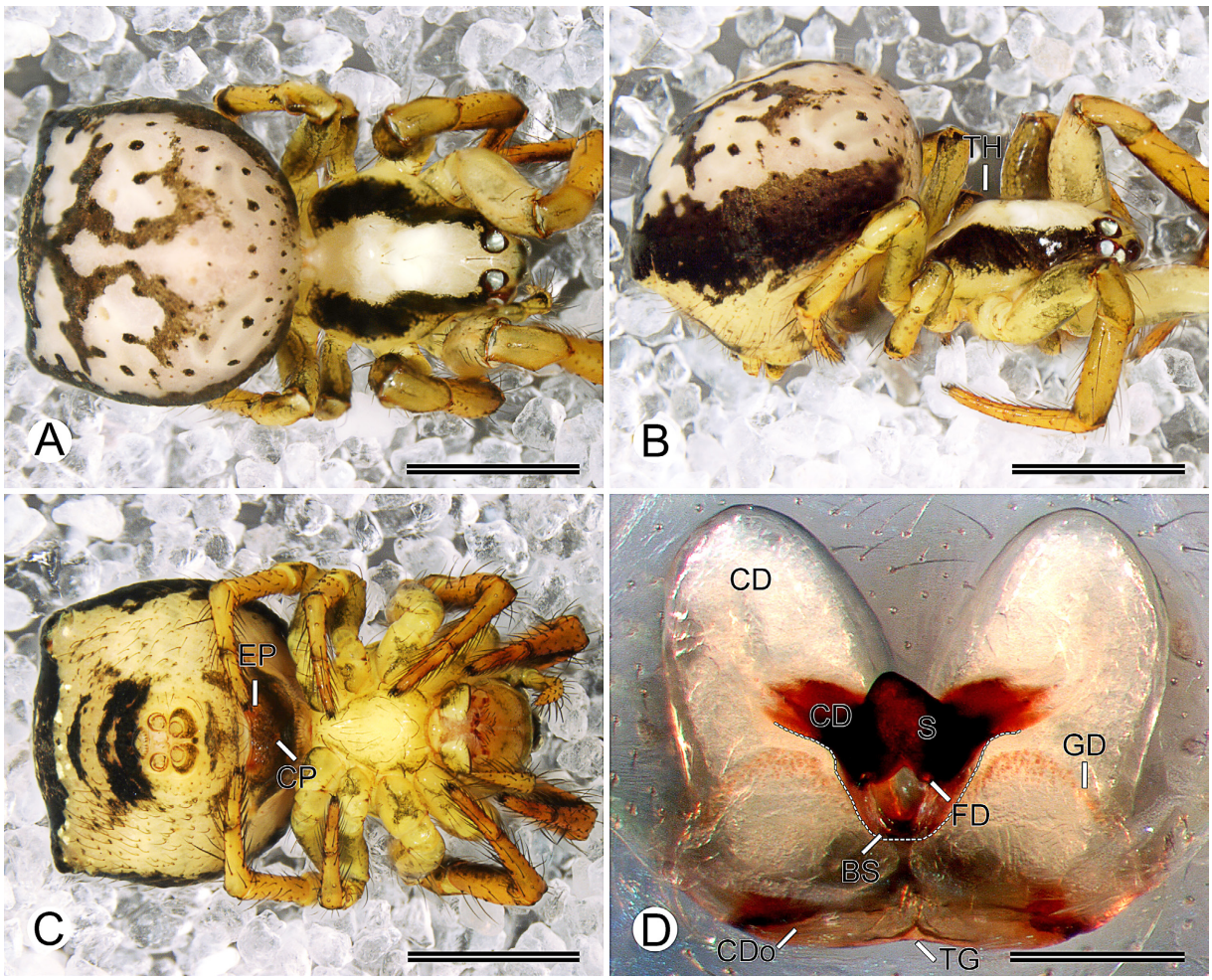

Fig. 17. *Epeirotypus kra* sp. nov., paratype, ♀ (MCZ SFU2NBD029). **A–C**. Habitus (A = dorsal view; B = lateral view; C = ventral view). **D**. Vulva, dorsal view (note the profile of the bifid septum extending posteriorly). Abbreviations: BS = bifid septum; CD = copulatory duct; CDo = copulatory duct opening; CP = central pit; EP = epigynal plate; FD = fertilization duct; GD = patch of gland ducts; S = spermatheca; TG = transverse groove; TH = laterally higher thoracic area. Scale bars: A–C = 1 mm; D = 0.2 mm.

Epeirotypus kote sp. nov.
urn:lsid:zoobank.org:act:0CBB4431-14A8-49C9-9742-70B3A4075027
Figs 1, 18–19

Diagnosis

Males and females of *Epeirotypus kote* sp. nov. resemble those of *E. kra* sp. nov. by the whitish-yellow body coloration (Figs 16A–C, 17A–C, 18A–C, 19A–C), but males of *E. kote* can be distinguished by the median apophysis distal projection relatively wide (Fig. 18E), whereas *E. kra* have the projection acuter (Fig. 16E). Females of *E. kra* can be distinguished by the vulval bifid sclerotized septum forming an inverted trapezoid (Fig. 19D), whereas in *E. kote* the bifid septum resembles a rectangle (Fig. 17D).

Etymology

The specific name is derived from ‘köte’ which means ‘fat’ in the Ngäbere language, currently spoken by the Ngäbe native people of Panama, and refers to the relatively high prosoma.

Type material

Holotype

PANAMA – **Chiriquí Province** • ♂; Parque Internacional La Amistad, Cerro Picacho, one-hectare PANCODING inventory; 8.890500° N, 82.618778° W; 2299 m a.s.l.; 12–17 Jun. 2008; M. Arnedo, L. Benavides, G. Hormiga, F. Labarque, L. Piacentini and M. Ramírez leg.; voucher code SAU1NGA024; preparation codes FML-00686, FML-00909; DNA code epes2205; GenBank code PX096958; MIUP.

Paratypes

PANAMA – **Chiriquí Province** • 1 ♀; same data as for holotype; voucher code SAD1NFP007; preparation codes FML-00696, FML-00847; DNA code epes2176; GenBank code PX096956; MACN-Ar 29069 • 1 ♂; same data as for holotype; voucher code SAU1NGH021; DNA code epes2204; GenBank code PX096957; MACN-Ar 29068 • 1 ♀; same data as for holotype; voucher code SAU1NHA026; DNA code epes2206; GenBank code PX096959; MCZ.

Description

Male (holotype MIUP SAU1NGA024)

Total length 1.97. Prosoma: length 1.16, width 0.94, height 0.71. Sternum: length 0.52, width 0.43. Eye diameters and interdistances: AME 0.09, PME 0.08, AME–PME 0.11. Opisthosoma: length 1.31, width 1.11, height 0.83; with posterior lateral tubercles. Leg formula: 1243. Dorsal shield of prosoma dark olive-green laterally, yellowish-white centrally forming smooth uniform band (Fig. 18A–B). Dorsum of ocular area yellowish-white (Fig. 18A). Thoracic area of prosoma laterally higher (Fig. 18B). Sternum yellow (Fig. 18C). Dorsum of opisthosoma olive-green with five whitish-gray patches, anterior and middle ones fused, covered by sparsely thin olive-green flecks (Fig. 18A–B). Opisthosoma with two lateral posterior tubercles connected ventrally by guanine silver stripe (Fig. 18C). Epiandrium, booklung cover, tracheal spiracle, and spinneret field yellow, epiandrum with olive-green borders, olive-green thick patch behind anal tubercle (Fig. 18C). Palp: paracymbium wider than long, tegulum retrolaterally massive, tegular spur rounded, median apophysis rounded, distally notched, with projection extending distally, conductor reduced, partially covering embolus, embolus long, bulky and distally acute (Fig. 18D–F).

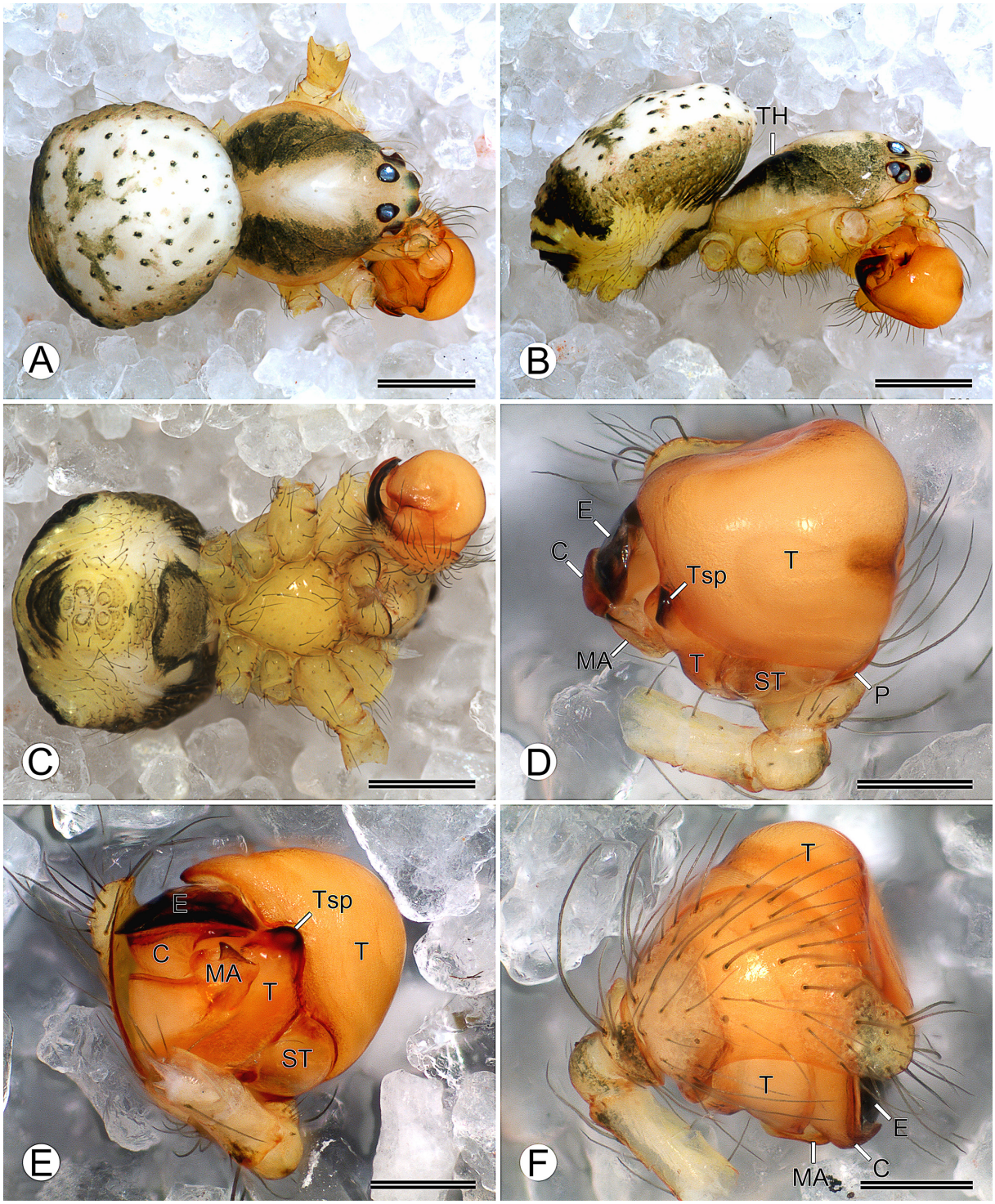

Fig. 18. *Epeirotypus kote* sp. nov., holotype, ♂ (MIUP SAU1NGA024). **A–C**. Habitus (A = dorsal view; B = lateral view; C = ventral view). **D–F**. Left palp (D = retrolateral view; E = ventral view; F = prolateral view). Abbreviations: C = conductor; E = embolus; MA = median apophysis; P = paracymbium; ST = subtegulum; T = tegulum; TH = laterally higher thoracic area; Tsp = tegular spur. Scale bars: A–C = 0.5 mm; D–F = 0.2 mm.

Female (paratype MACN-Ar 29069)
Total length 2.80. Prosoma: length 1.28, width 0.99, height 0.77. Sternum: length 0.63, width 0.50. Eye diameters and interdistances: AME 0.11, PME 0.10, AME–PME 0.13. Opisthosoma: length 1.85, width 1.91, height 0.98. Leg formula: 1243. Coloration as in male (Fig. 19A–C). Epigynal plate olive-green, domed, with transverse groove, central pit deep. Vulva: copulatory ducts massive, proximally with patch of gland ducts dorsally, heavily sclerotized distally inserting dorsolaterally posteriorly into spermathecae, spermathecae anteriorly sharp, sclerotized, and connate (i.e., fused one above the other), fertilization ducts sclerotized, relative small, emerging dorsally posteriorly from spermathecae, curving anteriorly to meet uterus externus (Fig. 19D).

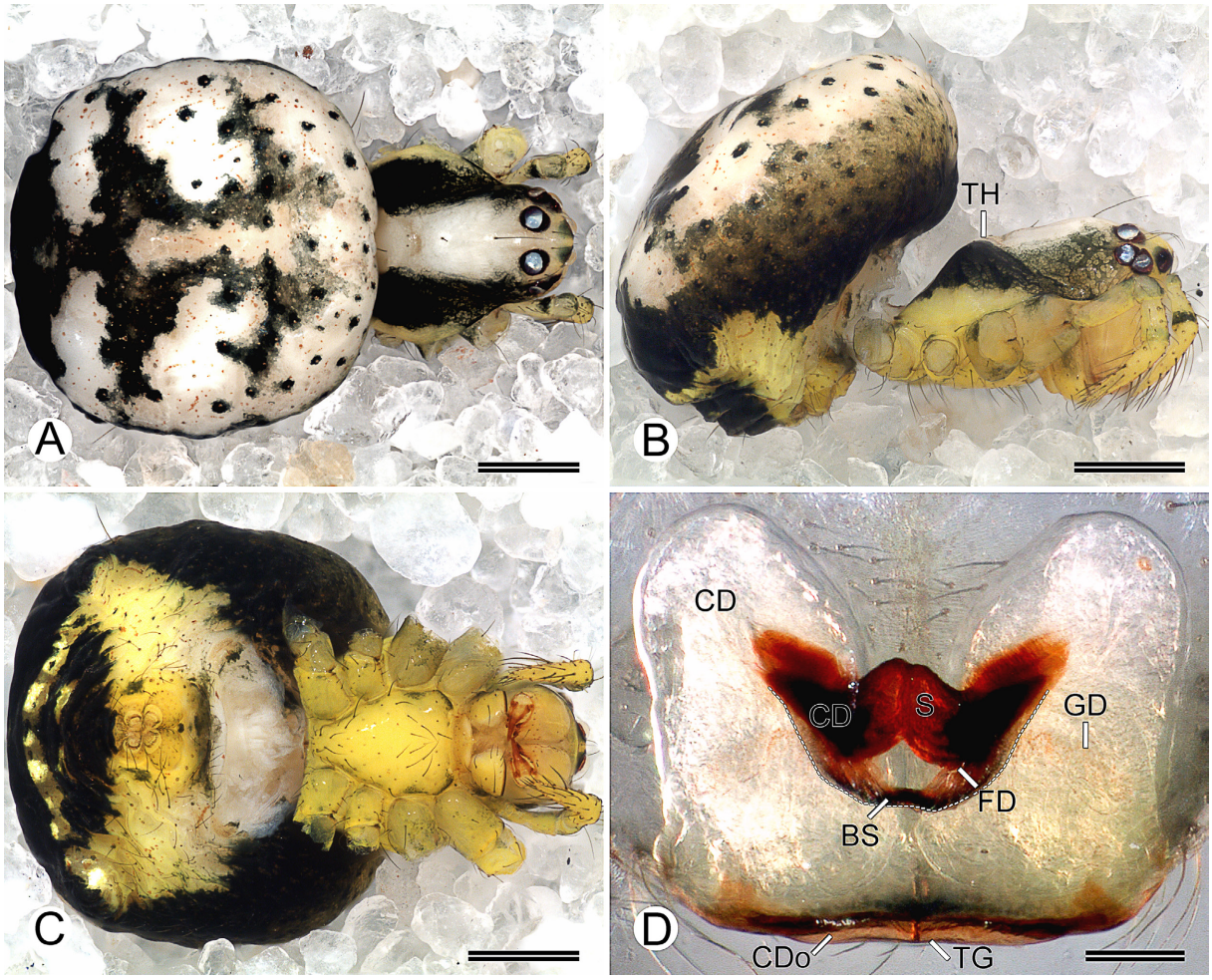

Fig. 19. *Epeirotypus kote* sp. nov., paratype, ♀ (MACN-Ar 29069). **A–C**. Habitus (A = dorsal view; B = lateral view; C = ventral view). **D**. Vulva, dorsal view (note the profile of the bifid septum extending posteriorly). Abbreviations: BS = bifid septum; CD = copulatory duct; CDo = copulatory duct opening; FD = fertilization duct; GD = patch of gland ducts; S = spermatheca; TG = transverse groove; TH = laterally higher thoracic area. Scale bars: A–C = 0.5 mm; D = 0.1 mm.

Records and biology

Records are limited to collections made at 2299 m a.s.l. in lower montane rainforest from Parque Internacional La Amistad (Fig. 1). Males and females have been collected mostly at night by looking up.

Variation

One female with evident lateral posterior tubercles.

Epeirotypus jane sp. nov.
urn:lsid:zoobank.org:act:31E9B000-A41E-4BC2-A9A2-75746FF9F8F0
Figs 1, 20

Diagnosis

Females of *Epeirotypus jane* sp. nov. resemble those of *E. kote* sp. nov. by the vulval bifid sclerotized septum forming an inverted trapezoid posteriorly (Figs 19D, 20D), but *E. jane* can be distinguished by a relatively narrow bifid septum and a darker body coloration (Fig. 20A–D), whereas *E. kote* have the bifid septum relatively wide and the body coloration lighter (i.e., whitish-yellow) (Fig. 19A–D).

Etymology

The specific name is derived from 'jane' which means 'different' in the Ngäbere language, currently spoken by the Ngäbe native people of Panama, and refers to the notable differences (i.e., number of pair bases) on the *cox 1* nucleotide sequence.

Type material

Holotype

PANAMA – **Coclé Province** • ♀; Parque Nacional General de División Omar Torrijos Herrera, El Cope, one-hectare PANCODING inventory; 8.668083° N, 80.592583° W; 760 m a.s.l.; 4–9 Jun. 2008; M. Arnedo, L. Benavides, G. Hormiga, F. Labarque and M. Ramírez leg.; voucher code STC1D5H021; MIUP.

Paratype

PANAMA – **Coclé Province** • 1 ♀; same data as for holotype; voucher code STC1D5H013; preparation codes FML-00831, FML-00910; DNA barcode SPIPA395-10; MACN-Ar.

Description

Female (paratype MACN-Ar STC1D5H013)
Total length 2.82. Prosoma: length 1.30, width 1.02, height 0.75. Sternum: length 0.59, width 0.54. Eye diameters and interdistances: AME 0.12, PME 0.10, AME–PME 0.12. Opisthosoma: length 1.94, width 1.66, height 1.71; with posterior lateral tubercles. Leg formula: 1243. Dorsal shield of prosoma dark olive-green laterally, yellowish-white centrally forming smooth uniform band (Fig. 20A–B). Dorsum of ocular area dark (Fig. 20A–B). Thoracic area of prosoma laterally higher (Fig. 20C). Sternum yellowish-orange with dark borders anteriorly (Fig. 20C). Opisthosoma color overall olive-green with five dorsal whitish-gray patches, anterior and middle ones fused, covered by sparsely thick olive-green flecks (Fig. 20A–B). Opisthosoma with two lateral posterior tubercles connected ventrally by guanine silver stripe (Fig. 20C). Epigynal plate, booklung cover, tracheal spiracle, spinneret field and behind anal tubercle olive-green, surrounded by whitish-gray area (Fig. 20C). Femora, tibiae and metatarsi brownish-orange but distally dark, patella greenish-brown, tarsi brownish-orange (Fig. 20A–C). Epigynal plate: domed, with transverse groove, central pit deep. Vulva: copulatory ducts massive, proximally with patch of gland ducts dorsally, heavily sclerotized distally inserting dorsolaterally posteriorly into spermathecae,

spermathecae anteriorly sharp, sclerotized, and connate (i.e., fused one above the other), fertilization ducts sclerotized, relative small, emerging dorsally posteriorly from spermathecae, curving anteriorly to meet uterus externus (Fig. 20D).

Male

Unknown.

Records and biology

Records are limited to collections made at 895 m a.s.l. in premontane rainforest from Parque Nacional General de División Omar Torrijos Herrera (Fig. 1). Females have been collected during the day by cryptic technique.

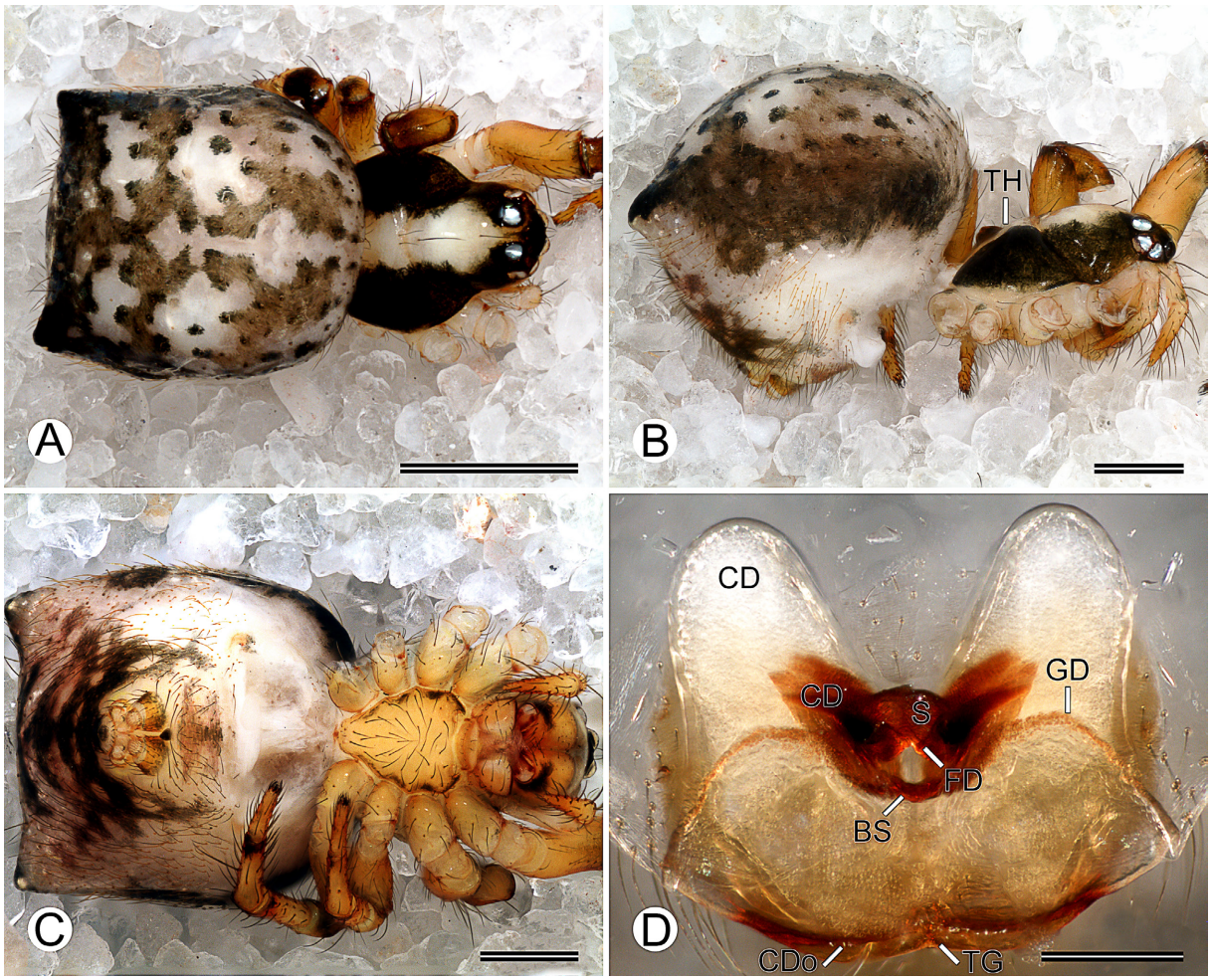

Fig. 20. *Epeirotypus jane* sp. nov., paratype, ♀ (MACN-Ar STC1D5H013). **A–C**. Habitus (A = dorsal view; B = lateral view; C = ventral view). **D**. Vulva, dorsal view. Abbreviations: BS = bifid septum; CD = copulatory duct; CDo = copulatory duct opening; FD = fertilization duct; GD = patch of gland ducts; S = spermatheca; TG = transverse groove; TH = laterally higher thoracic area. Scale bars: A = 1 mm; B–C = 0.5 mm; D = 0.2 mm.

Epeirotypus drune sp. nov.
urn:lsid:zoobank.org:act:619E7010-6456-4B4D-85B8-3797A33FD4D2
Figs 1, 21

Diagnosis

Females of *Epeirotypus drune* sp. nov. resemble those of *E. bule* sp. nov. by the body coloration overall dark gray (Figs 21A–C, 22A–C), but *E. drune* can be distinguished by the opisthosoma with three pairs of dorsal whitish-gray patches covered by sparsely thick dark gray flecks (Fig. 21A) and the vulval bifid sclerotized septum forming a wide, rounded, posterior curve (Fig. 21D), whereas *E. bule* have the opisthosoma with whitish-gray patches forming a 'happy face' in dorsal view (Fig. 22A) and have the bifid septum narrow (Fig. 22D).

Etymology

The specific name is derived from 'drune' which means 'black' in the Ngäbere language, currently spoken by the Ngäbe native people of Panama, and refers to the dark general coloration.

Type material

Holotype

PANAMA – **Chiriquí Province** • ♀; Parque Internacional La Amistad, Cerro Picacho, one-hectare PANCODING inventory; 8.890500° N, 82.618778° W; 2299 m a.s.l.; 12–17 Jun. 2008; M. Arnedo, L. Benavides, G. Hormiga, F. Labarque, L. Piacentini and M. Ramírez leg.; voucher code SAU1NCL062; DNA barcode SPIPA385-10; MIUP.

Paratypes

PANAMA – **Chiriquí Province** • 1 ♀; same data as for holotype; voucher code SAC1DHH012; preparation codes FML-00699, LNP-00545; DNA code epes7100; GenBank code PX096960; MACN-Ar 29084 • 1 ♀; same data as for holotype; voucher code SAU1NCL035; DNA code epes7240; GenBank code PX096962; MCZ • 1 ♀; same data as for holotype; voucher code SAU1NCR048; DNA code epes7237; GenBank code PX096961; CRBA.

Description

Female (paratype MACN-Ar 29084)

Total length 3.24. Prosoma: length 1.43, width 1.12, height 0.82. Sternum: length 0.70, width 0.55. Eye diameters and interdistances: AME 0.14, PME 0.14, AME–PME 0.15. Opisthosoma: length 2.28, wide 2.47, high 2.10; with posterior lateral tubercles. Leg formula: 1243. Dorsal shield of prosoma dark laterally, yellowish-white centrally (Fig. 21A). Dorsum of ocular area dark (Fig. 21A–B). Thoracic area of prosoma laterally higher (Fig. 21B). Sternum yellowish-orange with dark borders (Fig. 21C). Opisthosoma color overall dark gray with three pairs of dorsal whitish-gray patches laterally covered by sparsely thick dark gray flecks (Fig. 21A–B). Opisthosoma with two lateral posterior tubercles connected ventrally by guanine silver stripe (Fig. 21C). Epigynal plate, booklung cover, tracheal spiracle, spinneret field and behind anal tubercle dark gray, surrounded by whitish-gray area (Fig. 21C). Legs I–II darker than III–IV, femora and patella greenish-brown, tibiae and metatarsi brownish-orange but distally dark, tarsi brownish-orange (Fig. 21A–C). Epigynal plate: domed, with transverse groove, central pit deep (Fig. 21B–C). Vulva: copulatory ducts massive, proximally with patch of gland ducts dorsally, heavily sclerotized distally inserting dorsolaterally posteriorly into spermathecae, spermathecae anteriorly sharp, sclerotized, and connate (i.e., fused one above the other), fertilization ducts sclerotized, relative small, emerging dorsally posteriorly from spermathecae, curving anteriorly to meet uterus externus (Fig. 21D).

Male

Unknown.

Records and biology

Records are limited to collections made at 2299 m a.s.l. in lower montane rainforest from Parque Internacional La Amistad (Fig. 1). Females have been collected mostly at night by looking up, although a specimen was collected during the day by cryptic technique.

Variation

Some females examined have the prosoma and opisthosoma completely dark.

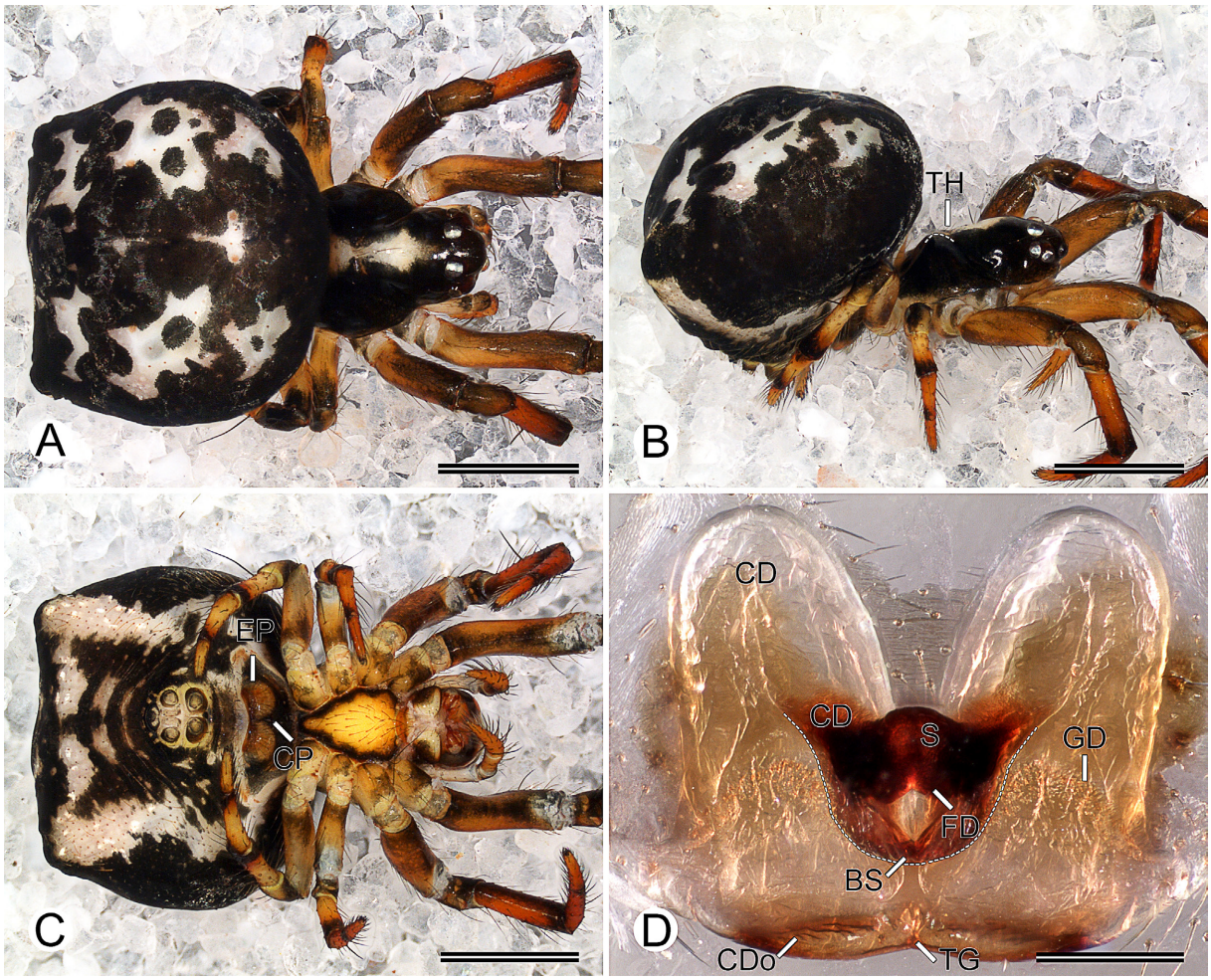

Fig. 21. *Epeirotypus drune* sp. nov., paratype, ♀ (MACN-Ar 29084). **A–C**. Habitus (A = dorsal view; B = lateral view; C = ventral view) (note the profile of the laterally higher thoracic area of prosoma). **D**. Vulva, dorsal (note the profile of the bifid septum extending posteriorly). Abbreviations: BS = bifid septum; CD = copulatory duct; CDo = copulatory duct opening; CP = central pit; EP = epigynal plate; FD = fertilization duct; GD = patch of gland ducts; S = spermatheca; TG = transverse groove; TH = laterally higher thoracic area. Scale bars: A–C = 1 mm; D = 0.2 mm.

Epeirotypus bule sp. nov.
urn:lsid:zoobank.org:act:66510266-1FD6-407A-80D8-4EA7DDF338B1
Figs 1, 22

Diagnosis

Females of *Epeirotypus bule* sp. nov. resemble those of *E. drune* sp. nov. by the body coloration overall dark gray (Figs 21A–C, 22A–C), but *E. bule* can be distinguished by the opisthosoma with whitish-gray patches forming a 'happy face' in dorsal view (Fig. 22A) and the vulval bifid sclerotized septum forming a narrow, rounded, posterior curve (Fig. 22D), whereas *E. drune* have the opisthosoma with three pairs of dorsal whitish-gray patches covered by sparsely thick dark gray flecks (Fig. 21A) and have the bifid septum wide (Fig. 21D).

Etymology

The specific name is derived from 'bule' which means 'head' in the Ngäbere language, currently spoken by the Ngäbe native people of Panama, and refers to the coloration pattern on the opisthosoma, which resembles a 'happy face' with the anterior procurved patches forming the smile and the rounded median patches suggesting eyes..

Type material

Holotype

PANAMA – **Chiriquí Province** • ♀; Parque Internacional La Amistad, Cerro Picacho, one-hectare PANCODING inventory; 8.890500° N, 82.618778° W; 2299 m a.s.l.; 12–17 Jun. 2008; M. Arnedo, L. Benavides, G. Hormiga, F. Labarque, L. Piacentini and M. Ramírez leg.; voucher code SAU2NCL028; preparation code FML-00944; DNA code epes7238; GenBank code PX096964; MIUP.

Paratypes

PANAMA – **Chiriquí Province** • 1 ♀; same data as for holotype; voucher code SAU2NCL033; preparation code FML-00968; DNA GenBank code PX096963; MIUP • 1 ♀; same data as for holotype; voucher code SAU1NCR002; DNA barcode SPIPA387-10; MACN-Ar 29326 • 1 ♀; same data as for holotype; voucher code SAC1DHH007; DNA barcode SPIPA389-10; MACN-Ar 29327 • 5 ♀♀; same data as for holotype; MCZ.

Description

Female (holotype MIUP SAU2NCL028, paratype MIUP SAU2NCL033)
Total length 2.99. Prosoma: length 1.38, width 0.99, height 0.90. Sternum: length 0.62, width 0.55. Eye diameters and interdistances: AME 0.13, PME 0.16, AME–PME 0.13. Opisthosoma: length 2.09, width 1.97, height 1.84; with posterior lateral tubercles. Leg formula: 1243. Dorsal shield of prosoma dark, fovea yellowish-white (Fig. 2A). Dorsum of ocular area dark (Fig. 22A). Thoracic area of prosoma laterally higher (Fig. 22B). Sternum dark brownish-orange (Fig. 22C). Opisthosoma color overall dark gray with three pairs of dorsal whitish-gray patches laterally, anterior and middle ones fused forming 'happy face' (Fig. 22A). Opisthosoma with two lateral posterior tubercles connected ventrally by guanine silver stripe (Fig. 22C). Epigynal plate, booklung cover, tracheal spiracle, spinneret field and behind anal tubercle dark gray, surrounded by whitish-gray area (Fig. 22C). Legs I–II darker than III–IV, femora and patella greenish-brown, tibiae and metatarsi brownish-orange but distally dark, tarsi brownish-orange (Fig. 22A–C). Epigynal plate: domed, with transverse groove, central pit deep (Fig. 22B–C). Vulva: copulatory ducts massive, proximally with patch of gland ducts dorsally, heavily sclerotized distally inserting dorsolaterally posteriorly into spermathecae, spermathecae anteriorly sharp (i.e., angular), sclerotized, and connate (i.e., fused one above the other), fertilization ducts sclerotized, relative small, emerging dorsally posteriorly from spermathecae, curving anteriorly to meet uterus externus (Fig. 22D).

Male

Unknown.

Records and biology

Records are limited to collections made at 2299 m a.s.l. in lower montane rainforest from Parque Internacional La Amistad (Fig. 1). Females have been collected mostly during the day by cryptic technique, though some specimens have been collected at night by looking up.

Variation

Some females examined have the opisthosomal whitish-gray patches separated.

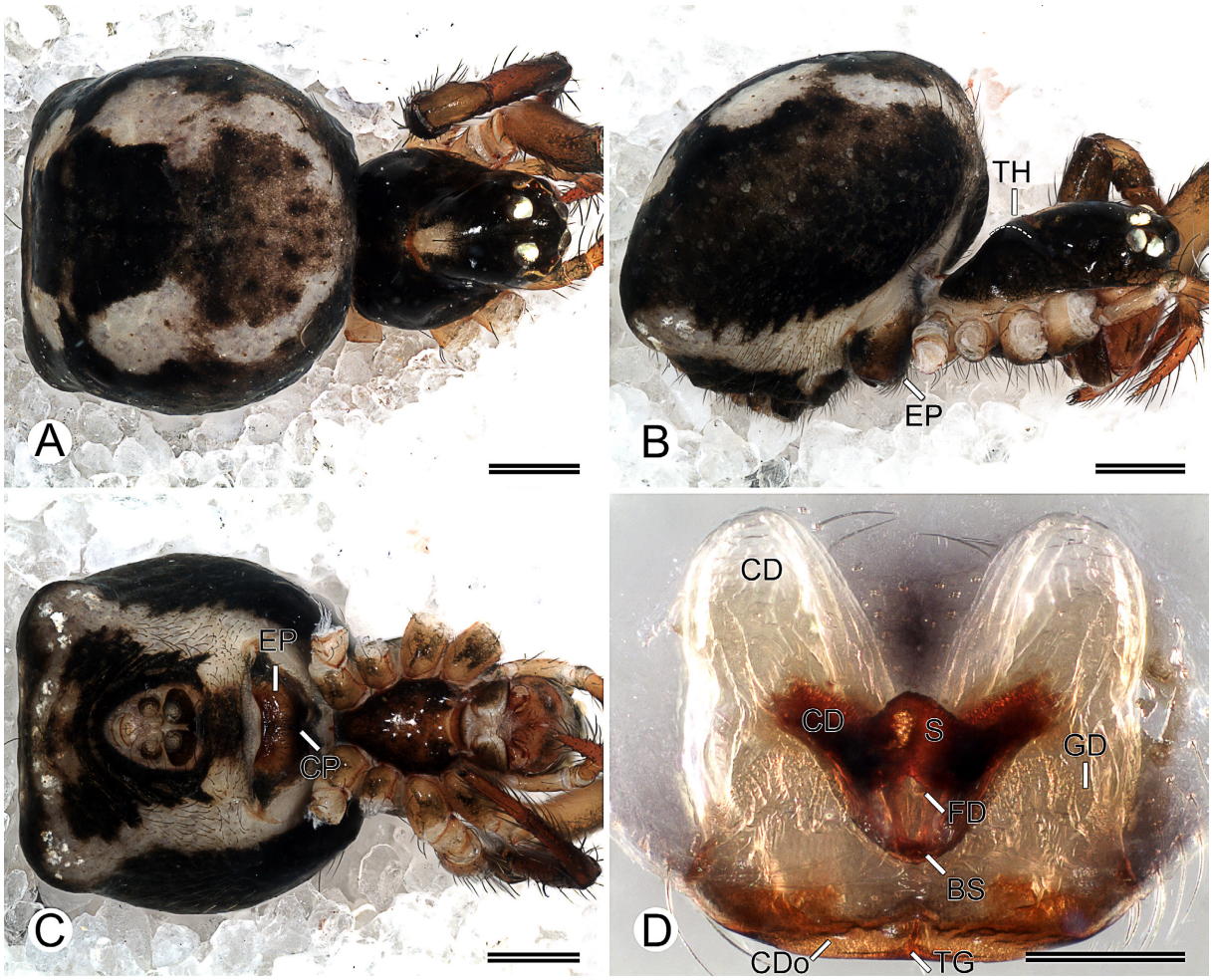

Fig. 22. *Epeirotypus bule* sp. nov. **A–C**. Holotype, ♀, habitus (MIUP SAU2NCL028) (A = dorsal view; B = lateral view; C = ventral view) (note the profile of the laterally higher thoracic area of prosoma). **D**. Paratype, ♀, vulva, dorsal view (MIUP SAU2NCL033). Abbreviations: BS = bifid septum; CD = copulatory duct; CDo = copulatory duct opening; CP = central pit; EP = epigynal plate; FD = fertilization duct; GD = patch of gland ducts; S = spermatheca; TG = transverse groove; TH = laterally higher thoracic area. Scale bars: A–C = 0.5 mm; D = 0.2 mm.

Epeirotypus tain sp. nov.
urn:lsid:zoobank.org:act:03B82D0C-2162-45CD-835C-E54EC9D83ECE
Figs 1, 23

Diagnosis

Females of *Epeirotypus tain* sp. nov. can be distinguished from those of other species of *Epeirotypus* by the opisthosoma coloration overall reddish-brown with a white transversal central stripe (Fig. 23A).

Etymology

The specific name is derived from 'tain' which means 'red' in the Ngäbere language, currently spoken by the Ngäbe native people of Panama, in reference to the overall reddish-brown coloration.

Type material

Holotype

PANAMA – **Chiriquí Province** • ♀; Reserva Forestal Fortuna, Quebrada Honda, one-hectare PANCODING inventory; 8.750083° N, 82.239083° W; 1135 m a.s.l.; 7–12 Jun. 2007; M. Arnedo, D. Dimitrov, G. Hormiga, F. Labarque and M. Ramírez leg.; voucher code SFU2NBH025; preparation codes FML-00897, LNP-00281; DNA code epes4070; GenBank code PX096965; MIUP.

Description

Female (holotype MIUP SFU2NBH025)

Total length 2.66. Prosoma: length 1.20, width 0.92, height 0.72. Sternum: length 0.54, width 0.47. Eye diameters and interdistances: AME 0.12, PME 0.12, AME–PME 0.13. Opisthosoma: length 1.81, width 2.09, height 1.74; with posterior lateral tubercles. Leg formula: 1243. Dorsal shield of prosoma dark, fovea brownish-orange (Fig. 23A–B). Dorsum of ocular area dark (Fig. 23A). Thoracic area of prosoma laterally higher (Fig. 23B). Sternum brownish-orange with reddish-brown borders (Fig. 23C). Opisthosoma color overall reddish-brown with three pairs of dorsal whitish-gray patches laterally, middle ones fused forming transversal central stripe (Fig. 23A–B), covered by sparsely thick dark flecks (Fig. 23C). Opisthosoma with two lateral posterior tubercles (Fig. 23C). Epigynal plate, tracheal spiracle and behind anal tubercle reddish-brown, covered by sparsely thin whitish-gray flecks; booklung cover whitish-gray, spinneret field orange (Fig. 23C). Legs I–II darker than III–IV, femora and patella greenish-brown, tibiae and metatarsi brownish-orange but distally dark, tarsi brownish-orange (Fig. 23A–C). Epigynal plate: domed, with transverse groove, central pit deep (Fig. 23C). Vulva: copulatory ducts massive proximally, with patch of gland ducts dorsally, and heavily sclerotized distally inserting dorsolaterally posteriorly into spermathecae, spermathecae anteriorly sharp, sclerotized, and connate (i.e., fused one above the other), fertilization ducts sclerotized, relative small, emerging dorsally posteriorly from spermathecae, curving anteriorly to meet uterus externus (Fig. 23D).

Male

Unknown.

Records and biology

Records are limited to collections made at 1135 m a.s.l. in premontane rainforest from Reserva Forestal Fortuna (Fig. 1). The only female has been collected at night by looking up.

Remarks

Females of *E. tain* sp. nov. resemble those of *E. bule* sp. nov. by the vulval bifid sclerotized septum forming a narrow, rounded, posterior curve (Figs 22D, 23D).

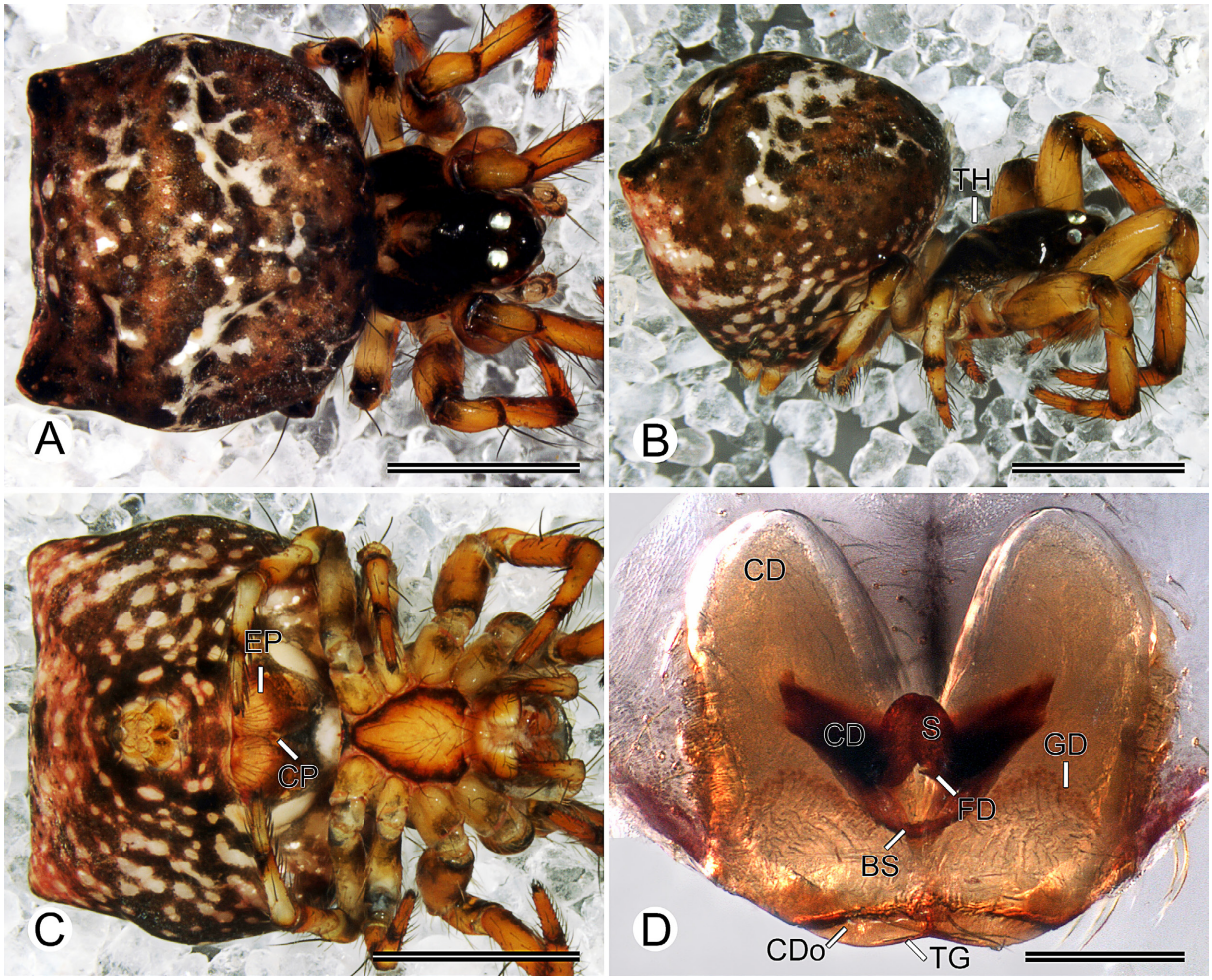

Fig. 23. *Epeirotypus tain* sp. nov., holotype, ♀ (MIUP SFU2NBH025). **A–C**. Habitus (A = dorsal view; B = lateral view; C = ventral view). **D**. Vulva, dorsal view. Abbreviations: BS = bifid septum; CD = copulatory duct; CDo = copulatory duct opening; CP = central pit; EP = epigynal plate; FD = fertilization duct; GD = patch of gland ducts; S = spermatheca; TG = transverse groove; TH = laterally higher thoracic area. Scale bars: A–C = 1 mm; D = 0.2 mm.

Naatlo Coddington, 1986

Naatlo Coddington, 1986: 44. Type species *Naatlo sutila* Coddington, 1986.

Diagnosis

Males of *Naatlo* can be distinguished from those of other theridiosomatid genera by the distally lobed embolus (Fig. 26E; see also Coddington 1986; Dupérré & Tapia 2017) (in contrast with the entire, thin laminated, or distally acute embolus in the other genera). Females of *Naatlo* can be distinguished from those of other genera by the domed (i.e., elevated ventrally) epigynal plate (absent in other genera except for *Epeirotypus*) with an epigynal flap hinged anteriorly (i.e., as an inverted 'T') (Figs 25C, 27C; see also Coddington 1986).

Description

Females of *Naatlo* have massive proximal copulatory ducts (i.e., more than three times the diameter of the duct's distal region) with a dorsal patch of gland ducts, and distal copulatory ducts heavily sclerotized (i.e., dark), inserting dorsolaterally posteriorly into the spermathecae (Figs 25D, 27D). For further genus description details, see Coddington (1986) and Labarque & Griswold (2014).

Remarks

Dupérré & Tapia (2017) suggested that a conductor relatively smaller than the embolus (see "reduced conductor" in Coddington 1986; Dupérré & Tapia 2017) and a broad paracymbium were diagnostic for *Naatlo*, but those characters are present in all the members of Epeirotypinae (see Coddington 1986).

Naatlo chi sp. nov.
urn:lsid:zoobank.org:act:1442E261-0B32-4A8B-819D-F8D0D916E174
Figs 1, 24–25

Diagnosis

Males and females of *Naatlo chi* sp. nov. resemble the males of *Naatlo mayzana* Dupérré & Tapia, 2017 by a continuous opisthosomal silver stripe, open posteriorly, that encircles most of the opisthosoma (Figs 24A–C, 25A–C; Dupérré & Tapia 2017: fig. 40), but males of *N. chi* can be distinguished by the median apophysis proximally serrated (Fig. 24E–F), whereas *N. mayzana* have the apophysis smooth (Dupérré & Tapia 2017: fig. 6). Males of *N. chi* can also be distinguished from the other species of the genus by the tegulum relatively small (i.e., less than half the size of the bulb), and a conductor with a heavily sclerotized (i.e., dark) posterior extension (Fig. 24D–F).

Etymology

The specific name is derived from 'chí' which means 'small' or 'child' in the Ngäbere language, currently spoken by the Ngäbe native people of Panama, and refers to the relatively small tegulum.

Type material

Holotype

PANAMA – **Coclé Province** • ♂; Parque Nacional General de División Omar Torrijos Herrera, El Cope, one-hectare PANCODING inventory; 8.668083° N, 80.592583° W; 760 m a.s.l.; 4–9 Jun. 2008; M. Arnedo, L. Benavides, G. Hormiga, F. Labarque and M. Ramírez leg.; voucher code STB1D9B019; MIUP.

Paratypes

PANAMA – **Chiriquí Province** • 1 ♀; Reserva Forestal Fortuna, Quebrada Honda, one-hectare PANCODING inventory; 8.750083° N, 82.239083° W; 1135 m a.s.l.; 7–12 Jun. 2007; M. Arnedo, D. Dimitrov, G. Hormiga, F. Labarque and M. Ramírez leg.; voucher code SFB1D9H035; preparation codes FML-00723, LNP-00275; DNA code naas1112; GenBank code PX096971; MACN-Ar 29008 • 1 ♂; same locality as for preceding; 21–24 Jun. 2008; L. Piacentini and F. Labarque leg.; non-quantitative sample; voucher code SFNQL8P043; preparation codes FML-00969, FML-00970; MACN-Ar. – **Coclé Province** • 1 ♂; same data as for holotype; voucher code STB1D9A009; preparation codes FML-00722, FML-00928; DNA barcode SPIPA368-10; CRBA. – **Panama Province** • 1 ♂; Parque Nacional Altos de Campana, one-hectare PANCODING inventory; 8.683444° N, 79.929833° W; 895 m a.s.l.; 14–19 Jun. 2007; M. Arnedo, D. Dimitrov, G. Hormiga, F. Labarque and M. Ramírez leg.; voucher code SCU1NDH021; preparation codes FML-00721, LNP-00282; DNA code naas1115; GenBank code PX096976; MACN-Ar 29027 • 1 ♀; same data as for preceding; voucher code SCC2NFH008; preparation code FML-00929; DNA barcode SPIPA369-10; MACN-Ar 29020 • 1 ♀; same data as for

preceding; voucher code SCD1NFD017; preparation code FML-00724; DNA code naas1185; GenBank code PX096979; CRBA.

Other material

PANAMA – **Chiriquí Province** • 6 ♀♀; Reserva Forestal Fortuna, Quebrada Honda, one-hectare PANCODING inventory; 8.750083° N, 82.239083° W; 1135 m a.s.l.; 7–12 Jun. 2007; M. Arnedo, D. Dimitrov, G. Hormiga, F. Labarque and M. Ramírez leg.; MCZ • 1 ♀; same data as for preceding; voucher code SFC1DAH012; DNA code naas1271; GenBank code PX096972; MCZ • 1 ♀; same data as for preceding; voucher code SFU1N8H023; DNA barcode SPIPA366-10; MCZ • 1 ♀; same data as for preceding; voucher code SFU1NCR045; DNA barcode SPIPA367-10; MCZ • 1 ♀; same data as for preceding; voucher code SFU1NBR036; DNA barcode SPIPA363-10; MACN-Ar 29010 • 1 ♀; same data as for preceding; voucher code SFU2NBH044; DNA code naas1268; GenBank code PX096973; MACN-Ar 29007 • 1 ♀; same data as for preceding; voucher code SFB1D8L018; DNA barcode SPIPA364-10; CRBA • 1 ♀; same data as for preceding; voucher code SFU1N7R038; DNA code naas1273; GenBank code PX096974; CRBA • 1 ♀; same data as for preceding; voucher code SFU2NCH028; DNA barcode SPIPA365-10; CRBA • 1 ♀; same data as for preceding; voucher code SFU1NCR036; DNA code naas1269; GenBank code PX096975; CRBA • 3 ♀♀; same data as for preceding; MACN-Ar 29014 • 3 ♀♀; same data as for preceding; MACN-Ar 29009 • 2 ♀♀; same data as for preceding; MACN-Ar 29011 • 4 ♀♀; same data as for preceding; CRBA • 1 ♂, 31 ♀♀; same locality as for preceding; 21–24 Jun. 2008; L. Piacentini and F. Labarque leg.; non-quantitative sample; MACN-Ar • 1 ♀; Reserva Forestal Fortuna, Sendero Zamudio; 8.732861° N, 82.284667° W; 1360 m a.s.l.; 20 Jun. 2008; L. Piacentini and F. Labarque leg.; non-quantitative sample; MACN-Ar. – **Coclé Province** • 2 ♂♂, 39 ♀♀; Parque Nacional General de División Omar Torrijos Herrera, El Cope, one-hectare PANCODING inventory; 8.668083° N, 80.592583° W, 760 m a.s.l.; 4–9 Jun. 2008; M. Arnedo, L. Benavides, G. Hormiga, F. Labarque and M. Ramírez leg.; MCZ • 1 ♂; same data as for preceding; voucher code STB1D9R019; DNA code naas1270; GenBank code PX096984; MCZ • 1 ♀; same data as for preceding; voucher code STD1N7B029; DNA code naas1186; GenBank code PX096981; MCZ • 1 ♂; same data as for preceding; voucher code STC1D5A014; DNA code naas1188; GenBank code PX096982; MACN-Ar 29046 • 1 ♀; same data as for preceding; voucher code STD1N7R022; DNA code naas1267; GenBank code PX096985; MACN-Ar 29044 • 1 ♀; same data as for preceding; voucher code STD1N7H025; DNA code naas1266; GenBank code PX096983; CRBA • 4 ♂♂, 4 ♀♀; same data as for preceding; MIUP • 1 ♂, 8 ♀♀; same data as for preceding; MACN-Ar 29040 • 7 ♀♀; same data as for preceding; MACN-Ar 29036 • 5 ♀♀; same data as for preceding; MACN-Ar 29033 • 5 ♀♀; same data as for preceding; MACN-Ar 29049 • 2 ♂♂, 4 ♀♀; same data as for preceding; MACN-Ar 29050 • 1 ♂, 4 ♀♀; same data as for preceding; MACN-Ar 29043 • 4 ♀♀; same data as for preceding; MACN-Ar 29047 • 4 ♀♀; same data as for preceding; MACN-Ar 29048 • 3 ♀♀; same data as for preceding; MACN-Ar 29034 • 1 ♂, 2 ♀♀; same data as for preceding; MACN-Ar 29045 • 2 ♀♀; same data as for preceding; MACN-Ar 29042 • 2 ♂♂, 1 ♀; same data as for preceding; MACN-Ar 29035 • 2 ♂♂, 1 ♀; same data as for preceding; MACN-Ar 29041 • 1 ♀; same data as for preceding; MACN-Ar 29039 • 1 ♀; same data as for preceding; MACN-Ar 29037 • 1 ♀; same data as for preceding; MACN-Ar 29038 • 4 ♂♂, 53 ♀♀; same data as for preceding; CRBA • 1 ♀; same data as for preceding; F. Labarque, M. Ramírez leg.; non-quantitative sample; MACN-Ar • 1 ♂, 1 ♀; Parque Nacional General de División Omar Torrijos Herrera, El Cope, Corredor Los Helechos; 8.668139° N, 80.592667° W; 790 m a.s.l.; 4 Jun. 2008; F. Labarque leg.; non-quantitative sample; MACN-Ar • 3 ♀♀, same locality as for preceding; Sendero Las Ranas; 3 Jun. 2008F. Labarque leg.; non-quantitative sample; MACN-Ar. – **Panama Province** • 6 ♂♂, 158 ♀♀; Parque Nacional Altos de Campana, one-hectare PANCODING inventory; 8.683444° N, 79.929833° W; 895 m a.s.l.; 14–19 Jun. 2007; M. Arnedo, D. Dimitrov, G. Hormiga, F. Labarque and M. Ramírez leg.; MCZ • 1 ♂; same data as for preceding; voucher code SCB1DFR042; DNA code naas1187; GenBank code PX096980; MCZ • 1 ♀; same data as for preceding; voucher code SCB1DGD011; DNA code naas1192; GenBank code PX096977; MCZ • 1 ♀; same data as for preceding; voucher code SCC1NHD013; DNA barcode SPIPA372-10; MCZ • 1 ♂; same data as

for preceding; voucher code SCU1NGH027; DNA code naas1272; GenBank code PX096978; MCZ • 1 ♀; same data as for preceding; voucher code SCC1NER014; DNA barcode SPIPA370-10; MACN-Ar 29022 • 1 ♀; same data as for preceding; voucher code SCB1DIA010; DNA barcode SPIPA371-10; CRBA • 1 ♂, 55 ♀♀; same data as for preceding; MIUP • 22 ♀♀; same data as for preceding; MACN-Ar 29029 • 17 ♀♀; same data as for preceding; MACN-Ar 29032 • 15 ♀♀; same data as for preceding; MACN-Ar 29006 • 12 ♀♀; same data as for preceding; MACN-Ar 29017 • 12 ♀♀; same data as for preceding; MACN-Ar 29023 • 10 ♀♀; same data as for preceding; MACN-Ar 29031 • 10 ♀♀; same data as for preceding; MACN-Ar 29026 • 9 ♀♀; same data as for preceding; MACN-Ar 29030 • 6 ♀♀; same data as for preceding; MACN-Ar 29001 • 5 ♀♀; same data as for preceding; MACN-Ar 29025 • 4 ♀♀; same data as for preceding; MACN-Ar 29002 • 4 ♀♀; same data as for preceding; MACN-Ar 29024 • 1 ♂, 3 ♀♀; same data as for preceding; MACN-Ar 29021 • 3 ♀♀; same data as for preceding; MACN-Ar 29015 • 3 ♀♀; same data as for preceding; MACN-Ar 29018 • 2 ♀♀; same data as for preceding; MACN-Ar 29019 • 2 ♀♀; same data as for preceding; MACN-Ar 29005 • 1 ♂, 2 ♀♀; same data as for preceding; MACN-Ar 29004 • 1 ♀; same data as for preceding; MACN-Ar 29016 • 1 ♀; same data as for preceding; MACN-Ar 29028 • 1 ♀; same data as for preceding; MACN-Ar 29003 • 4 ♂♂, 144 ♀♀; same data as for preceding; CRBA.

Description

Male (paratype MACN-Ar SFNQL8P043)

Total length 1.26. Prosoma: length 0.65, width 0.54, height 0.42. Sternum: length 0.35, width 0.31. Eye diameters and interdistances: AME 0.07, PME 0.07, AME–PME 0.07. Opisthosoma: length 0.79, width 0.68, height 0.62. Leg formula: 1243. Dorsal shield of prosoma yellowish-white laterally, olive-green centrally (Fig. 24A–B). Dorsum of the ocular area olive-green (Fig. 24A). Thoracic area of prosoma laterally higher (Fig. 24B). Sternum olive-green (Fig. 24C). Dorsum of the opisthosoma light olive-green (Fig. 24A) with wide guanine silver stripe, open posteriorly, encircling most of opisthosoma (Fig. 24B–C). Epiandrium, booklung cover, tracheal spiracle, and behind anal tubercle olive-green, surrounded by light olive-green area; spinneret field light olive-green (Fig. 24C). Legs I–II darker than III–IV, femora yellowish-white, patella, tibiae and metatarsi greenish-brown, tarsi darker greenish-brown (Fig. 24A–C). Palp: paracymbium wider than long, tegulum retrolaterally narrow, tegular spur rounded, wide, median apophysis rounded, distally notched (see "dorsal notch" in Coddington 1986), with projection extending distally, conductor reduced, partially covering embolus, with acute posterior extension, embolus distally lobed (Fig. 24D–F).

Female (paratype MACN-Ar 29020)

Total length 1.77. Prosoma: length 0.85, width 0.65, height 0.49. Sternum: length 0.41, width 0.38. Eye diameters and interdistances: AME 0.07, PME 0.10, AME–PME 0.07. Opisthosoma: length 1.25, width 1.05, height 0.97. Leg formula: 1243. Coloration darker than in male (Fig. 25A–C). Epigynal plate orange (Fig. 25C), domed, with transverse groove, epigynal flap hinged anteriorly (Fig. 25C). Vulva: copulatory ducts massive, proximally with patch of gland ducts dorsally, heavily sclerotized distally inserting dorsolaterally posteriorly into spermathecae, spermathecae ovoid, anteriorly sharp (i.e., angular), sclerotized, and connate (i.e., fused along midline), fertilization ducts sclerotized, emerging dorsally posteriorly from spermathecae, curving anteriorly to meet uterus externus (Fig. 25D).

Records and biology

Records are limited to collections made at 760 m a.s.l., 895 m a.s.l. and 1135 m a.s.l. in premontane rainforests from Parque Nacional Altos de Campana, Parque Nacional General de División Omar Torrijos Herrera and Reserva Forestal Fortuna, respectively (Fig. 1). Males and females have been collected mostly at night by looking up, although some specimens were also collected at night by looking down and others during the day by all the collection techniques.

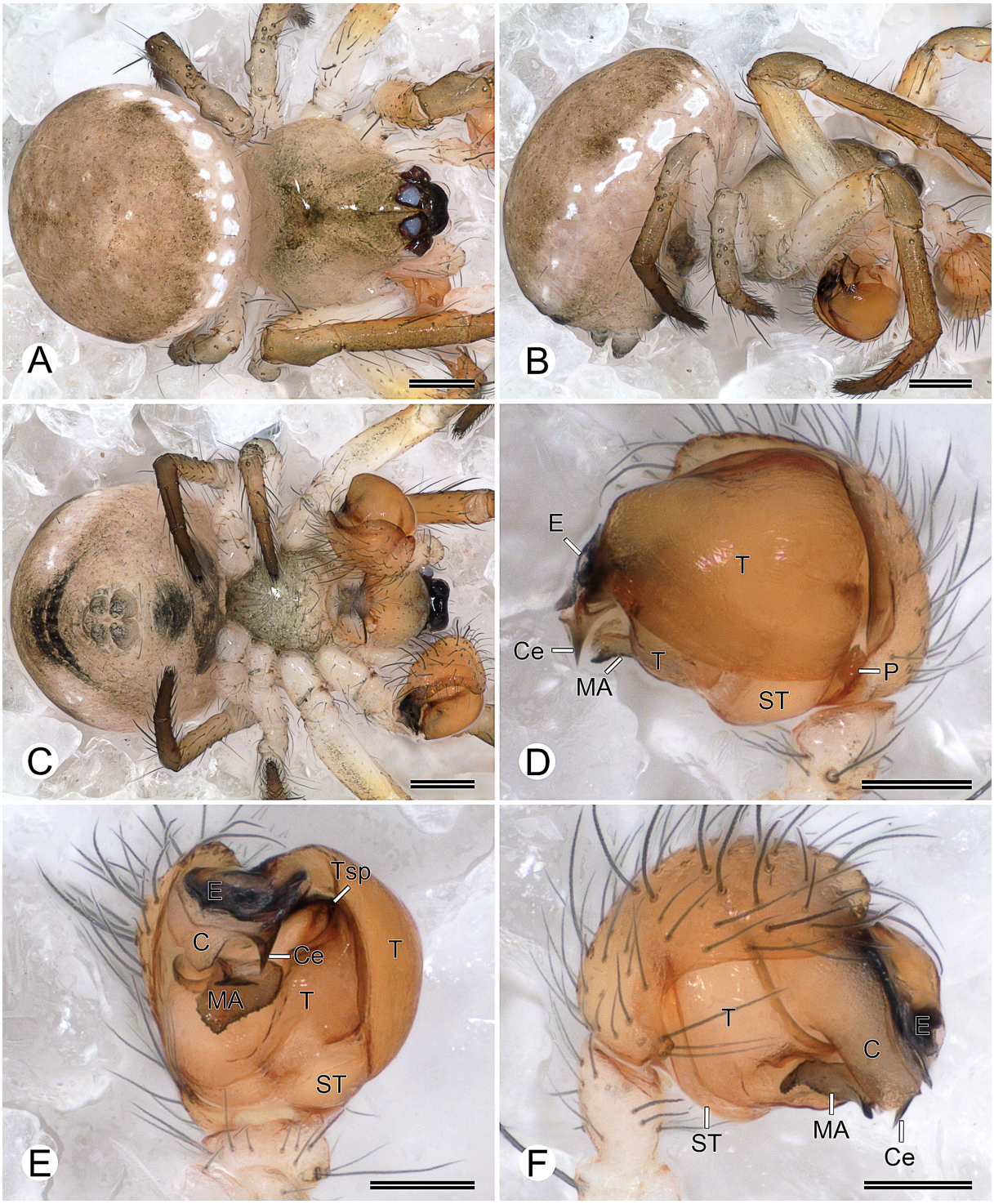

Fig. 24. *Naatlo chi* sp. nov., paratype, ♂ (MACN-Ar SFNQL8P043). **A–C**. Habitus (A = dorsal view; B = lateral view; C = ventral view). **D–F**. Left palp (D = retrolateral view; E = ventral view; F = prolateral view). Abbreviations: C = conductor; Ce = conductor posterior extension; E = embolus; MA = median apophysis; P = paracymbium; ST = subtegulum; T = tegulum; Tsp = tegular spur. Scale bars: A–C = 0.2 mm; D–F = 0.1 mm.

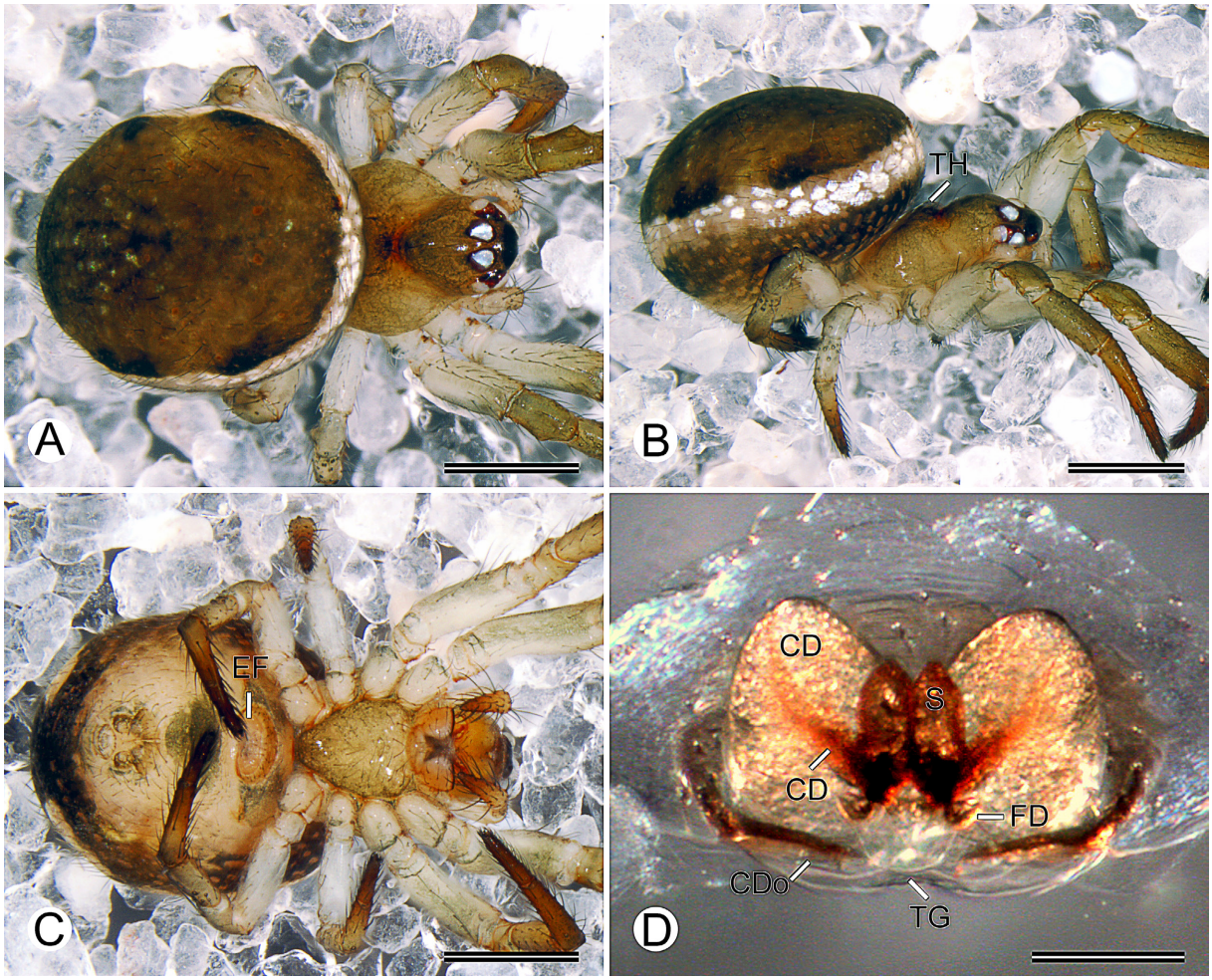

Fig. 25. *Naatlo chi* sp. nov., paratype, ♀ (MACN-Ar 29020). **A–C**. Habitus (A, dorsal, B = lateral view; C = ventral view). **D**. Vulva, dorsal view. Abbreviations: CD = copulatory duct; CDo = copulatory duct opening; EF = epigynal flap; FD = fertilization duct; S = spermatheca; TG = transverse groove; TH = laterally higher thoracic area. Scale bars: A–C = 0.5 mm; D = 0.1 mm.

Naatlo fauna (Simon, 1897)
Figs 1, 26–27

Theridiosoma fauna Simon, 1897: 483, figs 1–2, 7–8 [♀ lectotype, one ♂ and 18 ♀♀ paralectotypes from Venezuela, Carabobo, San Esteban (Muséum national d'Histoire naturelle, Paris), designated by Coddington 1989, not examined].

Naatlo fauna – Coddington 1986: 50, figs 69, 91–98 [♂, ♀] [from Colombia, Valle] [transferred from *Theridiosoma*].

Diagnosis

Females of *Naatlo fauna* resemble those of *Naatlo splendida* (Taczanowski, 1879) by the elongated opisthosoma (i.e., projecting behind the spinnerets) and by the epigynal flap narrowly hinged anteriorly and wider than the sternum (Fig. 27A–D; Coddington 1986: figs 84–86, 88, 91–93; Wienskoski 2010: figs 1a–c, 4d), but *N. fauna* can be distinguished by the three pairs of dorsal whitish-gray patches laterally

on the opisthosoma (Fig. 27A–B; Coddington 1986: figs 91–92; Wienskoski 2010: fig. 1a–b), whereas *N. splendida* have two lateral silver stripes (Coddington 1986: figs 84, 86; Wienskoski 2010: fig. 4a–b). Males of *N. fauna* can be distinguished from those of *N. splendida* by the embolus with four lobes distally (Fig. 26E; Coddington 1986: fig. 83), whereas *N. splendida* have three lobes (Coddington 1986: fig. 73).

Material examined

PANAMA – **Chiriquí Province** • 1 ♂; Reserva Forestal Fortuna, Quebrada Honda, one-hectare PANCODING inventory; 8.750083° N, 82.239083° W; 1135 m a.s.l.; 7–12 Jun. 2007; M. Arnedo, D. Dimitrov, G. Hormiga, F. Labarque and M. Ramírez leg.; voucher code SFB1DAR028; preparation codes FML-00720, LNP-00258; DNA code naafa056; GenBank code PX096967; MACN-Ar 29057 • 1 ♀; same data as for preceding; voucher code SFC1DBR019; preparation codes FML-00725, LNP-00263; DNA code naafa118; GenBank code PX096966; MACN-Ar 29056 • 1 ♀; same data as for preceding; voucher code SFB1D9R032; DNA code naafa191; GenBank code PX096968; MCZ • 1 ♂; same data as for preceding; voucher code SFB2D9R026; DNA barcode SPIPA373-10; MCZ • 1 ♀; same data as for preceding; voucher code SFD1NBR033; DNA barcode SPIPA374-10; CRBA • 1 ♀; same data as for preceding; voucher code SFU1N8A036; DNA barcode SPIPA376-10; MCZ • 1 ♀; same data as for preceding; voucher code SFU1N8R028; DNA barcode SPIPA375-10; CRBA • 1 ♂; same data as for preceding; voucher code SFU1NBR037; DNA code naafa189; GenBank code PX096969; MCZ • 1 ♂; same data as for preceding; voucher code SFU1NCD031; DNA barcode SPIPA377-10; MCZ • 1 ♀; same data as for preceding; voucher code SFU1NCL016; DNA code naaga190; GenBank code PX096970; MCZ • 2 ♂♂, 5 ♀♀; same data as for preceding; MCZ • 3 ♂♂, 3 ♀♀; same data as for preceding; MIUP • 2 ♂♂, 6 ♀♀; same data as for preceding; MACN-Ar 29054 • 1 ♂, 1 ♀; same data as for preceding; MACN-Ar 29058 • 1 ♂; same data as for preceding; MACN-Ar 29055 • 1 ♂; same data as for preceding; MACN-Ar 29053 • 5 ♂♂, 4 ♀♀; same data as for preceding; CRBA • 6 ♀♀; same locality as for preceding; 21–24 Jun. 2008; L. Piacentini and F. Labarque leg.; non-quantitative sample; MACN-Ar.

Redescription

Male (MACN-Ar 29057)

Total length 1.53. Prosoma: length 0.69, width 0.67, height 0.56. Sternum: length 0.37, width 0.35. Eye diameters and interdistances: AME 0.06, PME 0.06, AME–PME 0.08. Opisthosoma: length 0.92, width 0.83, height 0.94. Leg formula: 1243. Dorsal shield of prosoma yellowish-white laterally, olive-green centrally (Fig. 26A–B). Dorsum of ocular area olive-green (Fig. 26A). Sternum light olive-green (Fig. 26C). Dorsum of opisthosoma olive-green with three pairs of dorsal whitish-gray patches laterally (Fig. 26A). Epiandrium, booklung cover, tracheal spiracle, and behind anal tubercle olive-green, surrounded by whitish-gray area; spinneret field light olive-green (Fig. 26C). Legs I–II darker than III–IV, femora yellowish-white but distally orange, patella, tibiae, metatarsi and tarsi orange (Fig. 26A–C). Palp: paracymbium wider than long, tegulum retrolaterally narrow, tegular spur rounded, wide, median apophysis rounded, distally notched, with projection extending distally, conductor reduced, partially covering embolus, embolus distally lobed (Fig. 26D–F).

Female (MACN-Ar 29056)

Total length 1.88. Prosoma: length 0.63, width 0.53, height 0.46. Sternum: length 0.41, width 0.38. Eye diameters and interdistances: AME 0.07, PME 0.06, AME–PME 0.06. Opisthosoma: length 1.36, width 1.10, height 0.94. Leg formula: 1243. Coloration olive-greener than in male (Fig. 27A–C). Epigynal plate brownish-orange (Fig. 27C), domed, with transverse groove, epigynal flap hinged anteriorly (Fig. 27C). Vulva: copulatory ducts massive, proximally with patch of gland ducts dorsally, heavily sclerotized distally inserting dorsolaterally posteriorly into spermathecae, spermathecae ovoid, sclerotized, and connate (i.e., fused along the midline), fertilization ducts sclerotized, emerging dorsally posteriorly from spermathecae, curving anteriorly to meet uterus externus (Fig. 27D). For further species description details, see Coddington (1986).

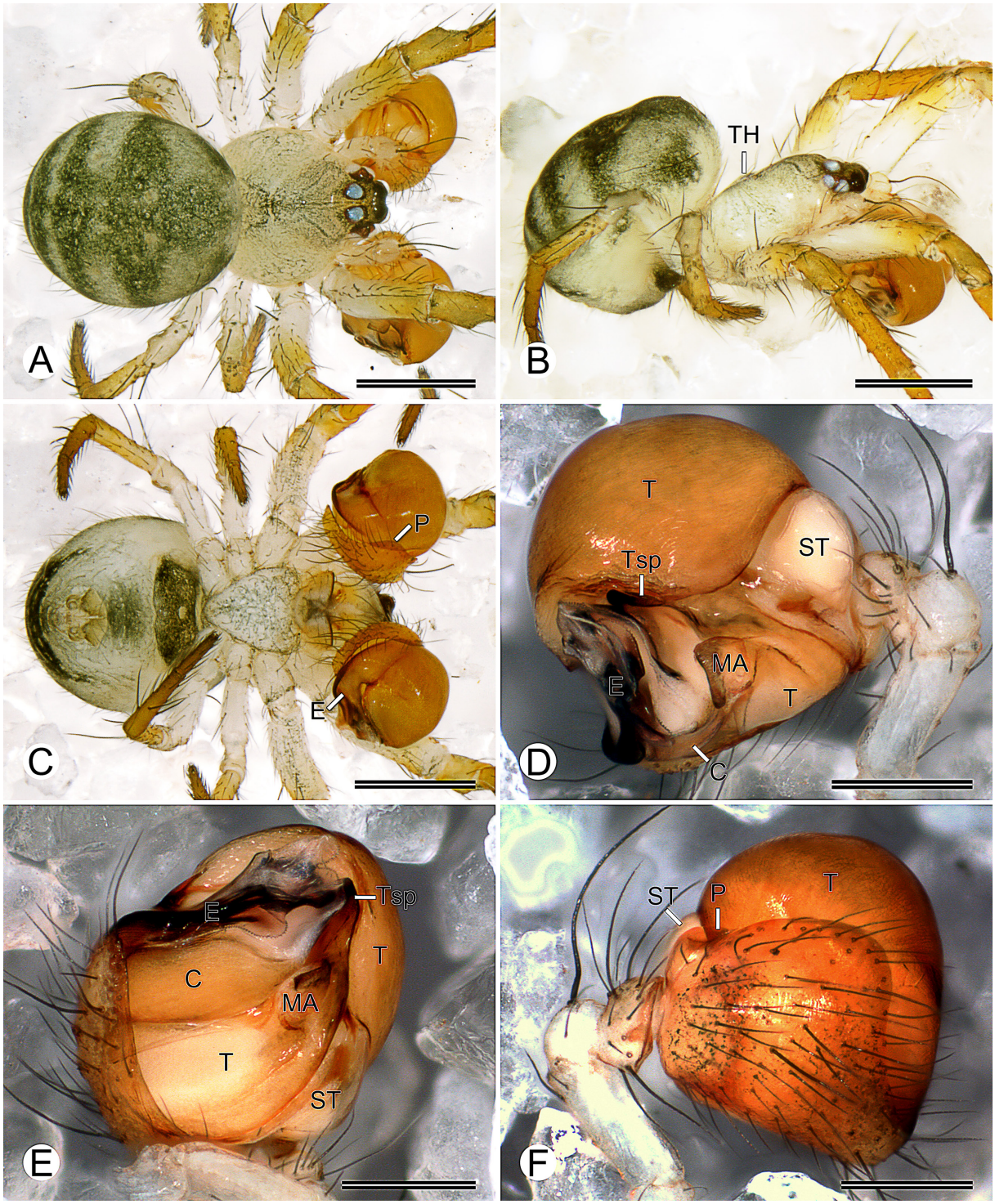

Fig. 26. *Naatlo fauna* (Simon, 1897), ♂ (MACN-Ar 29057). **A–C**. Habitus (A = dorsal view; B = lateral view; C = ventral view). **D–F**. Left palp (D = retrolateral view; E = ventral view; F = prolateral view). Abbreviations: C = conductor; E = embolus; MA = median apophysis; P = paracymbium; ST = subtegulum; T = tegulum; TH = laterally higher thoracic area; Tsp = tegular spur. Scale bars: A–C = 0.5 mm; D–F = 0.2 mm.

Records and biology

Naatlo fauna is distributed from Costa Rica to Brazil including Trinidad and Tobago (World Spider Catalog 2025). Records in this study are limited to collections made at 1135 m a.s.l. in the premontane rainforest from Reserva Forestal Fortuna (Fig. 1). Males and females have been collected mostly at night by looking up, although some specimens were also collected at night by looking down and others during the day by beating and cryptic techniques.

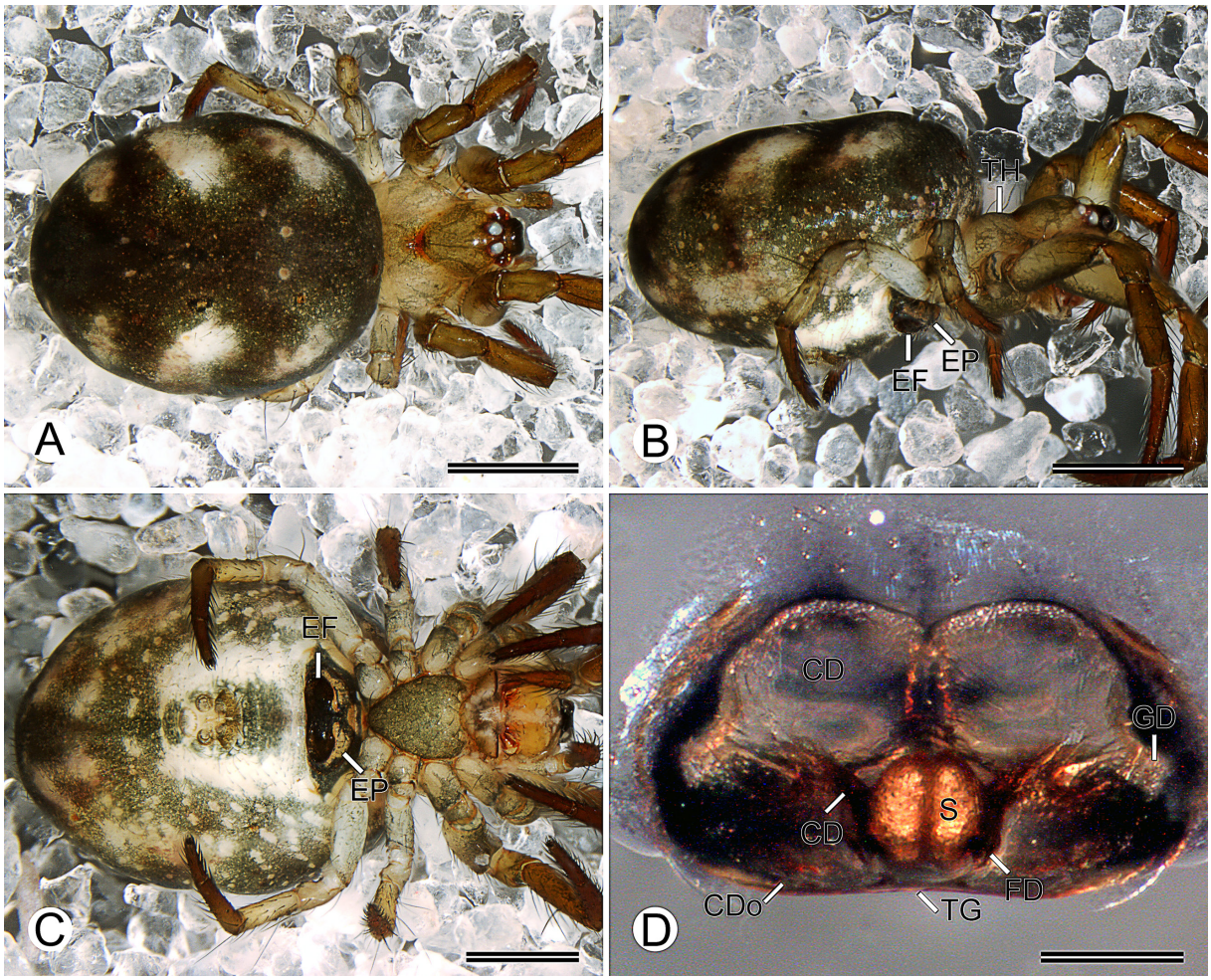

Fig. 27. *Naatlo fauna* (Simon, 1897, ♀ (MACN-Ar 29056). **A–C**. Habitus (A = dorsal; B = lateral view; C = ventral view). **D**. Vulva, dorsal view. Abbreviations: CD = copulatory duct; CDo = copulatory duct opening; EF, epigynal flap; EP = epigynal plate; FD = fertilization duct; GD = patch of gland ducts; S = spermatheca; TG = transverse groove; TH = laterally higher thoracic area. Scale bars: A–C = 0.5 mm; D = 0.2 mm.

Ogulnius O. Pickard-Cambridge, 1882

Ogulnius O. Pickard-Cambridge, 1882: 432. Type species *Ogulnius obtectus* O. Pickard-Cambridge, 1882.

Diagnosis

Males and females of *Ogulnius* can be distinguished from those of other theridiosomatid genera by the opisthosoma overhanging the prosoma (i.e., eclipsing the thoracic area) (absent in other genera), and the first tibiae with a retrolateral membranous patch (Figs 28B, 29B, 30B, 31B) (absent in other genera). Males of *Ogulnius* are also distinguished by a bifurcated mesal embolic apophysis (in contrast with non-divided or multiple times divided embolic apophysis in other genera), and its elongated prolateral branch (next to the embolus) that encircles the bulb counter-clockwise (Figs 28C–E, 30C–D; see also Coddington 1986 and Dupérré & Tapia 2017). Females of *Ogulnius* are also distinguished by having completely sclerotized copulatory ducts (in contrast with irregular and membranous or distally sclerotized copulatory ducts in other genera), with the copulatory openings exposed, protruding from beneath the transverse groove posteriorly (Figs 29D, 31D) (misinterpreted as "interrupted transverse groove" by Coddington 1986 and Dupérré & Tapia 2017; also compare "groove pockets" in Dupérré & Tapia 2017: figs 11–14, with Coddington 1986: figs 124–125) (absent in other genera).

Description

Females of *Ogulnius* have convoluted copulatory ducts that insert dorsolaterally posteriorly into spermathecae (Figs 5F–G, 29C–D, 31C–D; see also Coddington 1986 and Dupérré & Tapia 2017). For further genus description details, see Coddington (1986) and Labarque & Griswold (2014).

Remarks

Coddington (1986) suggested that a sternum truncated posteriorly was diagnostic for *Ogulnius*, but this character is also present in other theridiomatid genera (i.e., *Chthonos*, *Theridiosoma*, *Epilineutes*, *Wendilgarda*). We confirm the presence of a membranous patch on the retrolateral face of the first tibia in the two species of *Ogulnius* here examined (see also *Ogulnius obtectus* Keyserling, 1886; Coddington 1986: 57), seemingly a synapomorphy of the genus.

Ogulnius zbodro sp. nov.

urn:lsid:zoobank.org:act:8F9F5A14-A073-445F-9509-E32FC35D5C6E

Figs 1, 5F–G, 28–29

Diagnosis

Females of *Ogulnius zbodro* sp. nov. resemble those of *Ogulnius laranka* Dupérré & Tapia, 2017 and *Ogulnius puku* Dupérré & Tapia, 2017 by the exposed and separated copulatory openings (Fig. 29C–D; Dupérré & Tapia 2017: figs 11, 13), but *O. zbodro* can be distinguished by the copulatory ducts convoluting four times directly above the spermathecae (Figs 5F–G, 29D), whereas *O. laranka* and *O. puku* have the copulatory ducts convoluting separated from the spermathecae (Dupérré & Tapia 2017: figs 12, 14). Males of *O. zbodro* can be distinguished from those of *O. laranka* by the embolic apophysis prolateral branch encircling the bulb one-time counter-clockwise (Fig. 28D), whereas *O. laranka* have the prolateral branch longer, encircling the bulb about 1.75 times counter-clockwise (Dupérré & Tapia 2017: fig. 9).

Etymology

The specific name is derived from the union of two words, 'zbö' and 'dro', which mean 'God' and 'Sun' or 'bright', respectively, in the Naso language, currently spoken by the Naso Tjerdi native people of Panama, and refers to the elongated prolateral branch of the embolic apophysis that encircles the bulb one-time counter-clockwise, forming the end of a cycle, the end of day.

Type material

Holotype

PANAMA – **Panama Province** • ♂; Parque Nacional Altos de Campana, one-hectare PANCODING inventory; 8.683444° N, 79.929833° W; 895 m a.s.l.; 14–19 Jun. 2007; M. Arnedo, D. Dimitrov, G. Hormiga, F. Labarque and M. Ramírez leg.; voucher code SCD1NGR012; DNA barcode SPIPA362-10; MIUP.

Paratypes

PANAMA – **Panama Province** • 1 ♂; same data as for holotype; voucher code SCC1DER017; preparation codes FML-00714, LNP-00285; DNA code ogus1119; GenBank code PX097021; MACN-Ar 29310 • 1 ♀; same data as for holotype; voucher code SCD1DFR015; preparation codes FML-00733, FML-01148, LNP-00286; DNA code ogus1110; GenBank code PX097020; MACN-Ar 29309 • 1 ♀; same data as for holotype; voucher code SCD1DFR031; DNA barcode SPIPA120-10; CRBA • 1 ♀; same data as for holotype; voucher code SCD1DHR010; DNA barcode SPIPA361-10; MIUP • 1 ♀; same data as for holotype; voucher code SCD1DFH007; DNA code oguoc195; GenBank code PX097019; MCZ • 1 ♀; same data as for holotype; voucher code SCD1DFR014; DNA barcode SPIPA119-10; CRBA.

Other material

PANAMA – **Panama Province** • 1 ♀; same data as for holotype; voucher code SCD1DFD013; DNA barcode SPIPA360-10; MCZ • 1 ♀; same data as for holotype; voucher code SCD1NER013; DNA code oguoc193; GenBank code PX097018; MACN-Ar 29308.

Description

Male (paratype MACN-Ar 29310)

Total length 0.79. Prosoma: length 0.49, width 0.41, height 0.41; cephalic area elevated. Sternum: length 0.22, width 0.26. Eye diameters and interdistances: AME 0.06, PME 0.04, AME–PME 0.07. Opisthosoma: length 0.63, width 0.57, height 0.44; overhanging prosoma. Leg formula: 4123. Dorsal shield of prosoma orange laterally, reddish-brown centrally (Fig. 28A–B). Dorsum of the ocular area orange (Fig. 28A). Sternum reddish-brown (Fig. 28C). Opisthosoma color overall reddish-brown, dorsally lighter; smooth (i.e., no pattern) (Fig. 28A–B). Spinneret field orange (Fig. 28C). Legs orange, tibia I with retrolateral membranous patch (Fig. 28A–C). Palp: paracymbium ovoid, covering the embolic division, median apophysis anterior projection blunt, bifurcated mesal embolic apophysis, elongated retrolateral branch protruding from beneath conductor and encircling the bulb one-time counter-clockwise, embolus laminated (Fig. 28D–F).

Female (paratype MACN-Ar 29309)

Total length 0.95. Prosoma: length 0.51, width 0.42, height 0.42; cephalic area elevated. Sternum: length 0.24, width 0.28. Eye diameters and interdistances: AME 0.06, PME 0.04, AME–PME 0.06. Opisthosoma: length 0.76, width 0.67, height 0.57; overhanging prosoma. Leg formula: 4123. Coloration as in male (Fig. 29A–C). Tibia I with retrolateral membranous patch (Fig. 29B). Epigynal plate reddish-brown (Fig. 29C), with transverse groove anterior to copulatory ducts openings (Fig. 29C–D). Vulva: copulatory ducts totally sclerotized, convoluting four times and inserting dorsolaterally posteriorly into

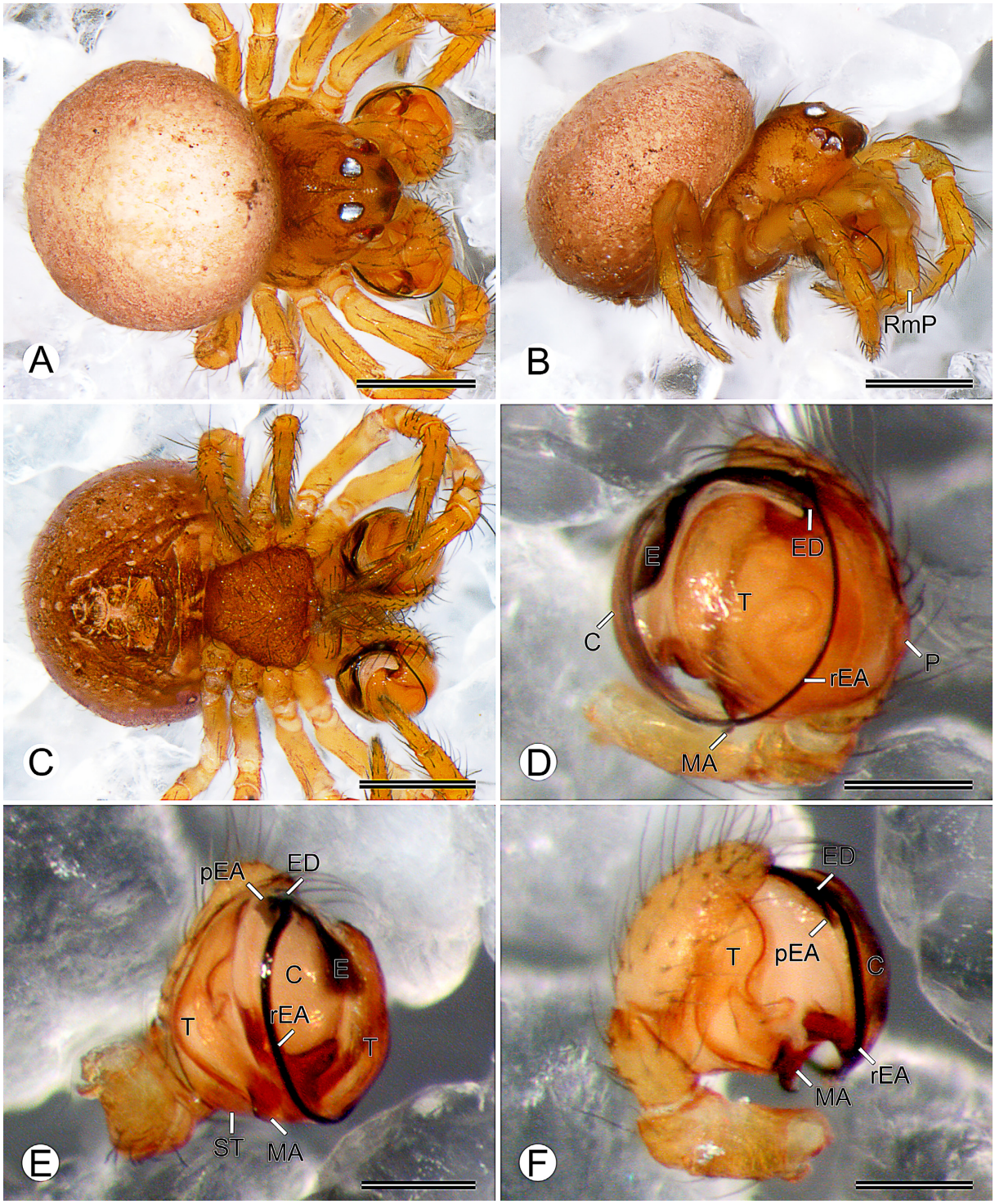

Fig. 28. *Ogulnius zbodro* sp. nov., paratype, ♂ (MACN-Ar 29310). **A–C**. Habitus (A = dorsal view; B = lateral view; C = ventral view). **D–F**. Left palp (D = retrolateral view; E = ventral view; F = prolateral view). Abbreviations: C = conductor; E = embolus; ED = embolic division; MA = median apophysis; P = paracymbium; pEA = embolic apophysis prolateral branch; rEA = embolic apophysis retrolateral branch; RmP = retrolateral membranous patch; T = tegulum; ST = subtegulum. Scale bars: A–C = 0.25 mm; D–F = 0.1 mm.

spermathecae, spermathecae anteriorly sharp (i.e., angular), sclerotized, and connate (i.e., fused along the midline), fertilization ducts sclerotized, emerging laterally posteriorly from spermathecae, curving dorsally anteriorly to meet the uterus externus (Figs 5F–G, 29D).

Records and biology

Records are limited to collections made at 895 m a.s.l. in premontane rainforest from Parque Nacional Altos de Campana (Fig. 1). Males and females have been collected mostly during the day by looking down, although a male was also collected during the day by cryptic technique and a couple at night by looking down.

Variation

Some males and females have darker coloration than the described specimens.

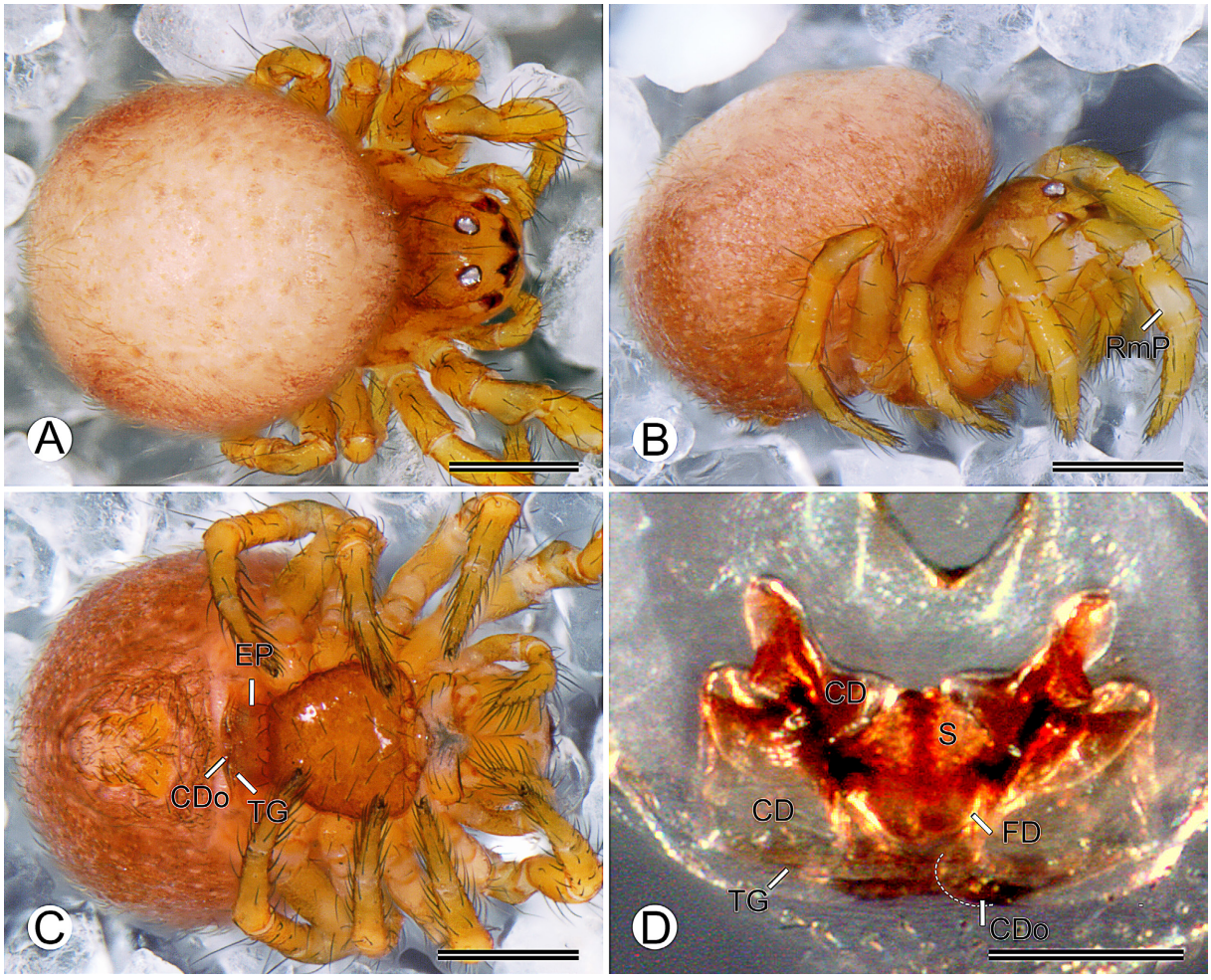

Fig. 29. *Ogulnius zbodro* sp. nov., paratype, ♀ (MACN-Ar 29309). **A–C**. Habitus (A = dorsal view; B = lateral view; C = ventral view). **D**. Vulva, dorsal view (note the profile of the copulatory openings exposed, protruding from beneath the transverse groove posteriorly). Abbreviations: CD = copulatory duct; CDo = copulatory duct opening; EP = epigynal plate; FD = fertilization duct; RmP = retrolateral membranous patch; S = spermatheca; TG = transverse groove. Scale bars: A–C = 0.25 mm; D = 0.1 mm.

Ogulnius debonaja sp. nov.
urn:lsid:zoobank.org:act:35A21BA4-9E6E-42B4-95EC-35A72FCACB74
Figs 1, 30–31

Diagnosis

Females of *Ogulnius debonaja* sp. nov. resemble those of *Ogulnius gloriae* (Petrunkevitch, 1930) by the exposed and attached copulatory openings forming a backward-pointed triangle (Fig. 31C–D; Coddington 1986: fig. 124), but *O. debonaja* can be distinguished by the copulatory ducts convoluted multiple times (Fig. 31D) and by the opisthosoma smooth (i.e., no pattern) (Fig. 31A–B), whereas *O. gloriae* have the ducts convolute three times (Coddington 1986: fig. 125) and have dorsal tubercles on the opisthosoma (Coddington 1986: figs 120–121). Males of *O. debonaja* can be distinguished from those of *O. gloriae* by the embolic apophysis prolateral branch encircling the bulb 1.25 times counter-clockwise (Fig. 30D) and a hooked anterior projection of the median apophysis (Fig. 30F), whereas *O. gloriae* have the prolateral branch smaller, encircling the bulb about 0.75 times counter-clockwise (Coddington 1986: figs 100–101), and have the projection straight (Coddington 1986: fig. 99).

Etymology

The specific name is derived from the union of two words, 'debo' and 'nã'ja', which mean 'big' and 'head', respectively, in the Naso language, currently spoken by the Naso Tjerdi native people of Panama, and refers to the elevated and bulky cephalic area of the males' prossoma.

Type material

Holotype

PANAMA – **Chiriquí Province** • ♂; Parque Internacional La Amistad, Cerro Picacho, one-hectare PANCODING inventory; 8.890500° N, 82.618778° W; 2299 m a.s.l.; 12–17 Jun. 2008; M. Arnedo, L. Benavides, G. Hormiga, F. Labarque, L. Piacentini and M. Ramírez leg.; voucher code SAC1DEH003; DNA code ogus2199; GenBank code PX097009; MIUP.

Paratypes

PANAMA – **Chiriquí Province** • 1 ♂; same data as for holotype; voucher code SAU1NDB035; preparation codes FML-00715, LNP-00543; DNA code ogus2102; GenBank code PX097017; MACN-Ar 29329 • 1 ♀; same data as for holotype; voucher code SAD1NHB024; preparation codes FML-00739, LNP-00544; DNA code ogus2101; GenBank code PX097014; MACN-Ar 29346 • 1 ♀; same data as for holotype; voucher code SAU1NCB026; DNA code oguoc196; GenBank code PX097012; MCZ • 1 ♀; same data as for holotype; voucher code SAU2NCA003; DNA barcode SPIPA358-10; MCZ • 1 ♀; same data as for holotype; voucher code SAB1DDA002; DNA barcode SPIPA356-10; MCZ • 1 ♂; same data as for holotype; voucher code SAU1NDL029; DNA barcode SPIPA355-10; MACN-Ar 29325 • 1 ♀; same data as for holotype; voucher code SAC1DDB013; DNA code oguoc103; GenBank code PX097010; MACN-Ar 29349 • 1 ♀; same data as for holotype; voucher code SAU2NCL030; DNA code oguoc198; GenBank code PX097013; MACN-Ar 29345 • 1 ♀; same data as for holotype; voucher code SAU2NCL034; DNA code oguoc194; GenBank code PX097011; CRBA • 1 ♀; same data as for holotype; voucher code SAB1DHL021; DNA code ogus2197; GenBank code PX097015; CRBA • 1 ♀; same data as for holotype; voucher code SAD1NGL022; DNA code ogus2200; GenBank code PX097016; CRBA • 1 ♂; same data as for holotype; voucher code SAU1NCL037; DNA barcode SPIPA359-10; CRBA.

Other material

PANAMA – **Chiriquí Province** • 23 ♂♂, 35 ♀♀; same data as for holotype; MCZ • 7 ♂♂, 7 ♀♀; same data as for holotype; IMFUP • 12 ♂♂, 7 ♀♀; same data as for holotype; MACN-Ar 29335 • 1 ♂, 6 ♀♀;

same data as for holotype; MACN-Ar 29332 • 6 ♀♀; same data as for holotype; MACN-Ar 29339 • 1 ♂, 4 ♀♀; same data as for holotype; MACN-Ar 29334 • 1 ♂, 3 ♀♀; same data as for holotype; MACN-Ar 29344 • 1 ♂, 3 ♀♀; same data as for holotype; MACN-Ar 29328 • 1 ♂, 3 ♀♀; same data as for holotype; MACN-Ar 29333 • 3 ♀♀; same data as for holotype; MACN-Ar 29348 • 3 ♀♀; same data as for holotype; MACN-Ar 29338 • 1 ♂, 2 ♀♀; same data as for holotype; MACN-Ar 29340 • 1 ♂, 2 ♀♀; same data as for holotype; MACN-Ar 29342 • 2 ♀♀; same data as for holotype; MACN-Ar 29341 • 1 ♀; same data as for holotype; MACN-Ar 29330 • 1 ♀; same data as for holotype; MACN-Ar 29347 • 1 ♀; same data as for holotype; MACN-Ar 29343 • 1 ♀; same data as for holotype; MACN-Ar 29331 • 1 ♀; same data as for holotype; MACN-Ar 29337 • 1 ♂; same data as for holotype; MACN-Ar 29336 • 19 ♂♂, 48 ♀♀; same data as for holotype; CRBA • 2 ♂♂, 10 ♀♀; Parque Internacional La Amistad, Sendero Retoño; 8.893833° N, 82.615083° W; 2240 m a.s.l.; 10–11 Jun. 2008; F. Labarque and M. Ramirez leg.; non-quantitative sample; MACN-Ar • 2 ♂♂; same locality as for holotype; 17–18 Jun.2008; F. Labarque and L. Piacentini leg.; MACN-Ar • 1 ♀; Reserva Forestal Fortuna, Quebrada Honda; 8.750083° N, 82.239083° W; 1135 m a.s.l. 21–24 Jun. 2008; L. Piacentini and F. Labarque leg.; non-quantitative sample; MACN-Ar. – **Coclé Province** • 1 ♀; Parque Nacional G.D. Omar Torrijos Herrera, El Cope; 8.668083° N, 80.592583° W; 760 m a.s.l.; 4–9 Jun. 2008; F. Labarque, M. Ramírez leg.; non-quantitative sample; MACN-Ar • 3 ♂♂; Parque Nacional G.D. Omar Torrijos Herrera, El Cope, Sendero Las Ranas,; 8.668138° N, 80.592667° W; 790 m a.s.l.; 3 Jun. 2008; F. Labarque leg.; non-quantitative sample; MACN-Ar.

Description

Male (paratype MACN-Ar 29329)

Total length 0.87. Prosoma: length 0.57, width 0.46, height 0.46; cephalic area elevated. Sternum: length 0.24, width 0.28. Eye diameters and interdistances: AME 0.06, PME 0.06, AME–PME 0.06. Opisthosoma: length 0.66, width 0.58, height 0.42; overhanging prosoma. Leg formula: 4123. Dorsal shield of prosoma orange (Fig. 30A–B). Dorsum of ocular area orange (Fig. 30A–B). Sternum brownish-orange (Fig. 30C). Opisthosoma color overall orangish-white, smooth (Fig. 30A–C). Epiandrium and spinneret field orange, gray patch surrounding tracheal spiracle, spinnerets and anal tubercle (Fig. 30C). Legs orange, tibia I with retrolateral membranous patch (Fig. 30A–C). Palp: paracymbium ovoid, covering embolic division, median apophysis anterior projection hooked, bifurcated mesal embolic apophysis, elongated retrolateral branch protruding from beneath conductor and encircling bulb 1.25 times counter-clockwise, embolus laminated (Fig. 30D–F).

Female (paratype MACN-Ar 29346)

Total length 1.14. Prosoma: length 0.60, width 0.44, height 0.45; cephalic area elevated. Sternum: length 0.26, width 0.29. Eye diameters and interdistances: AME 0.06, PME 0.06, AME–PME 0.07. Opisthosoma: length 0.95, width 0.92, height 0.81; overhanging prosoma. Leg formula: 4123. Coloration darker than male (Fig. 31A–C). Tibia I with retrolateral membranous patch (Fig. 31C). Epigynal plate reddish-brown (Fig. 31C), with transverse groove anterior to copulatory ducts openings (Fig. 31C–D). Vulva: copulatory ducts totally sclerotized, convoluting multiple times and inserting dorsolaterally posteriorly into spermathecae, spermathecae anteriorly sharp (i.e., angular), sclerotized, and connate (i.e., fused along midline), fertilization ducts sclerotized, emerging laterally posteriorly from spermathecae, curving dorsally anteriorly to meet uterus externus (Fig. 31D).

Records and biology

Records are limited to collections made at 895 m a.s.l. and 1135 m a.s.l. in premontane rainforest from Parque Nacional General de División Omar Torrijos Herrera and Reserva Forestal Fortuna, respectively, and at 2299 m a.s.l. in lower montane rainforest from Parque Internacional La Amistad (Fig. 1). Males and females have been collected mostly at night by looking up, although some

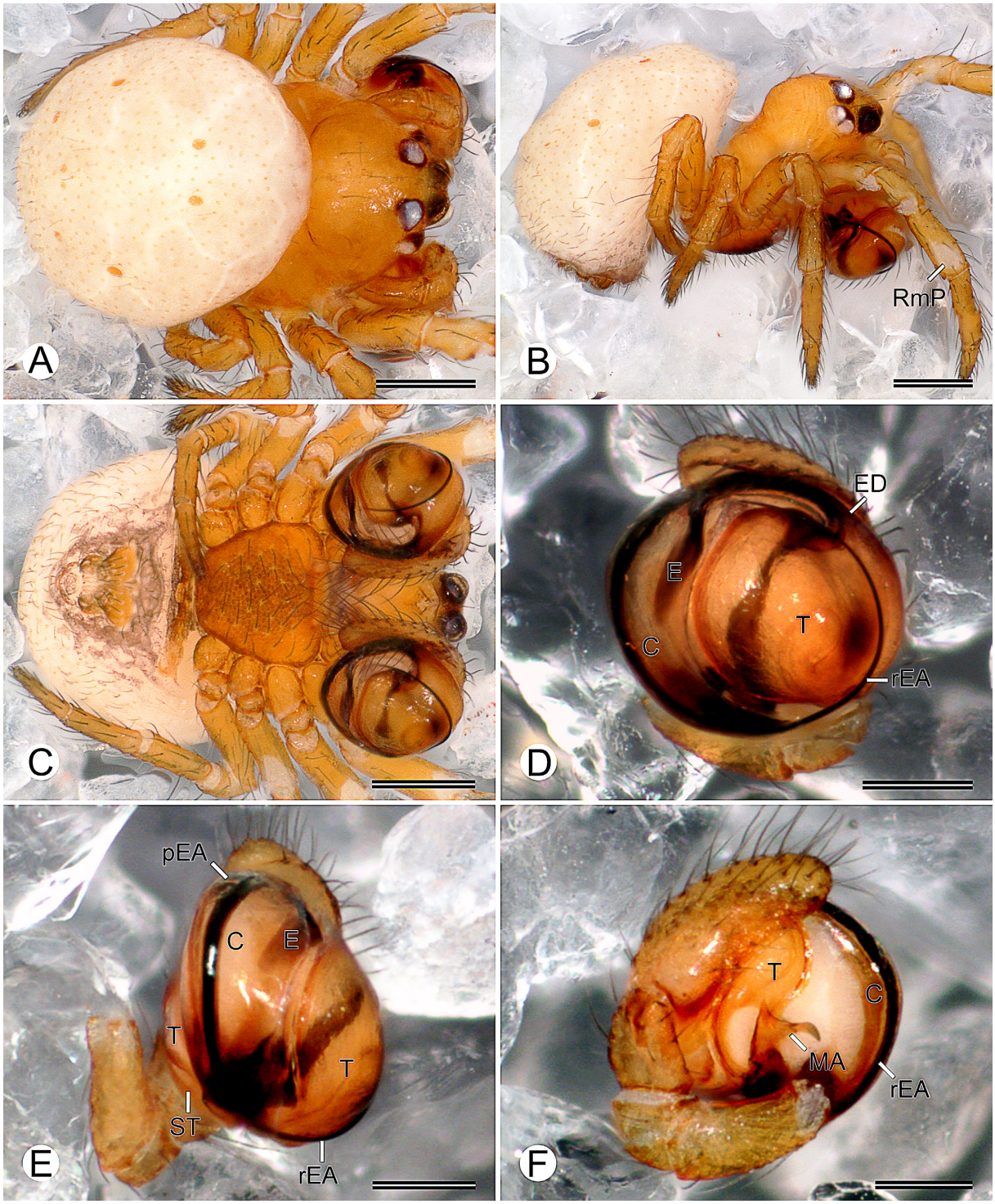

Fig. 30. *Ogulnius debonaja* sp. nov., paratype, ♂ (MACN-Ar 29329). **A–C**. Habitus (A = dorsal view; B = lateral view; C = ventral view). **D–F**. Left palp (D = retrolateral view; E = ventral view; F = prolateral view). Abbreviations: C = conductor; E = embolus; ED = embolic division; MA = median apophysis; pEA = embolic apophysis prolateral branch; rEA = embolic apophysis retrolateral branch; RmP = retrolateral membranous patch; T = tegulum; ST = subtegulum. Scale bars: A–C = 0.2 mm; D–F = 0.1 mm.

specimens were also collected at night by looking down and others during the day by cryptic, beating and looking down.

Variation

Some males and females examined have darker coloration than the described specimens.

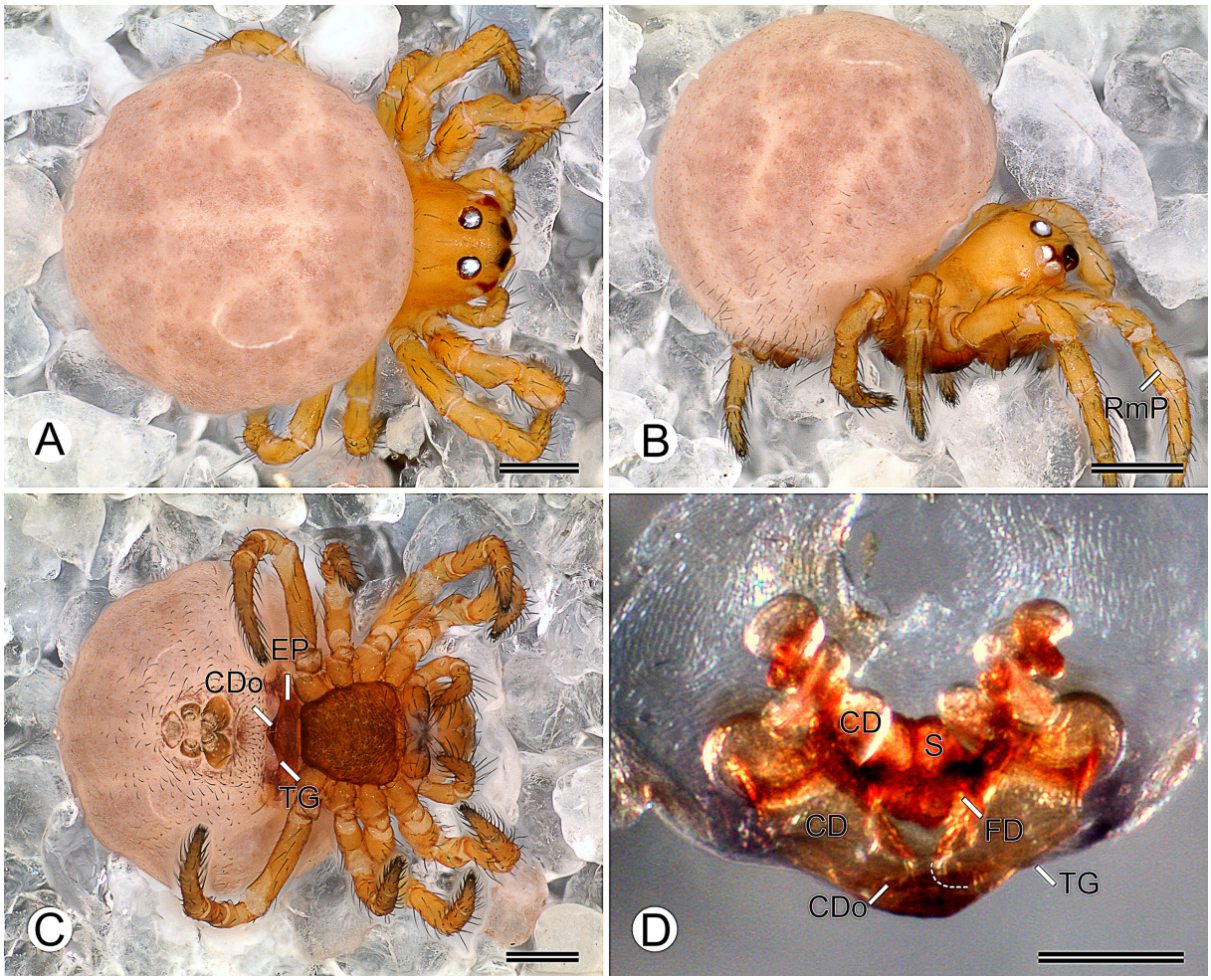

Fig. 31. *Ogulnius debonaja* sp. nov., paratype, ♀ (MACN-Ar 29346). **A–C**. Habitus (A = dorsal view; B = lateral view; C = ventral view). **D**. Vulva, dorsal view. Abbreviations: CD = copulatory duct; CDo = copulatory duct opening; EP = epigynal plate; FD = fertilization duct; RmP = retrolateral membranous patch; S = spermatheca; TG = transverse groove. Scale bars: A, C = 0.2 mm; B = 0.25 mm; D = 0.1 mm.

Theridiosoma O. Pickard-Cambridge, 1879

Theridiosoma O. Pickard-Cambridge, 1879: 193. Type species: *Theridiosoma argenteolum* O. Pickard-Cambridge, 1879 (= *Theridiosoma gemmosum* (L. Koch, 1877)).

Diagnosis

Males of *Theridiosoma* resemble those of *Andasta* Simon, 1895, *Tantra* gen. nov. and *Zoma* Saaristo, 1996 by the embolic apophysis divided multiple times (more than three times, see "fragmented" in Coddington 1986 and Labarque & Griswold 2014), forming branches prolaterally and retrolaterally to the embolus (e.g., Zhao & Li 2012: fig. 27d), but *Theridiosoma* can be distinguished by having more than one prolateral branch (see "bristle-like parts" in Coddington 1986), protruding from beneath the conductor (Fig. 32D–F; see also Coddington 1986; Rodrigues & Ott 2005; Miller *et al.* 2009; Zhao & Li 2012; Dupérré & Tapia 2017; Suzuki *et al.* 2020), whereas *Andasta* have all branches covered by the conductor (Saaristo 2010: fig. 38 6–7), *Tantra* gen. nov. have one retrolateral branch (Figs 34E, 38E, 42E) and *Zoma* have one prolateral branch (Miller *et al.* 2009: fig. 10F; Zhao & Li 2012: fig. 28d; Ballarin *et al.* 2021: fig. 5c), projecting from beneath the conductor. Females of *Theridiosoma* can be distinguished from those of other genera by the distal copulatory ducts convoluting antero-posteriorly (Figs 6A, 33D; see also Coddington 1986; Rodrigues & Ott 2005; Miller *et al.* 2009; Zhao & Li 2012; Dupérré & Tapia 2017; Suzuki *et al.* 2020).

Description

Males of *Theridiosoma* have the conductor with heavily sclerotized (i.e., dark) posterior extension (Fig. 32D–F; see also Coddington 1986; Rodrigues & Ott 2005; Miller *et al.* 2009; Zhao & Li 2012; Dupérré & Tapia 2017; Suzuki *et al.* 2020) that may have prolateral (e.g., Coddington 1986: figs 154–156) or retrolateral (e.g., Suzuki *et al.* 2020: fig. 7e–g) heavily sclerotized projections. In addition, the conductor may have a prolateral, acute and posteriorly elongated apophysis that articulates with it through a membrane (e.g., Suzuki *et al.* 2020: fig. 7e–g). The embolic apophysis prolateral branches may be filiform, flexible and elongated, with a wide (Fig. 32D–F; e.g., Zhao & Li 2012: fig. 28a–d) or an acute and heavily sclerotized tip (e.g., Suzuki *et al.* 2020: fig. 7e–g). Females of *Theridiosoma* have the epigynal plate protruding ventrally, which may be flat (i.e., straight in lateral view; Figs 6B, 33B; e.g., Suzuki *et al.* 2020: fig. 7d) or domed (i.e., curved in posterior view; e.g., Coddington 1986: figs 138, 143) and may be entire (e.g., Rodrigues & Ott 2005: fig. 6) or divided (e.g., Suzuki *et al.* 2020: fig. 5a–d), the dorsal epigynal plate exposed protruding from beneath the copulatory opening posteriorly (Fig. 33B–D; e.g., Coddington 1986: fig. 143; Dupérré & Tapia 2017: figs 28–29; Suzuki *et al.* 2020: fig. 5a, c), massive proximal copulatory ducts (i.e., more than three times the diameter of the distal region), that may be fused (e.g., Lopardo & Hormiga 2015: fig. 123a) or separated (Figs 6A, 33D), with a dorsal patch of gland ducts, and distal copulatory ducts inserting ventromedially posteriorly into the spermathecae (Fig. 6A–B; see also Coddington 1986; Rodrigues & Ott 2005; Miller *et al.* 2009; Zhao & Li 2012; Dupérré & Tapia 2017; Suzuki *et al.* 2020). For further genus description details, see Coddington (1986) and Labarque & Griswold (2014).

Remarks

Dupérré & Tapia (2017) suggested that a median apophysis distally acute with an anterior median groove was diagnostic for *Theridiosoma*, but this character is present in all the members of Theridiosomatinae (see Labarque & Griswold 2014).

Theridiosoma goodnightorum Archer, 1953
Figs 1, 6A–B, 32–33

Theridiosoma goodnightorum Archer, 1953: 11, fig. 19 [♀] [holotype ♀ from Mexico, Chiapas, Monte Libano (American Museum of Natural History, New York), not examined].

Diagnosis

Males of *Theridiosoma goodnightorum* resemble those of *Theridiosoma chiripa* Rodrigues & Ott, 2005 and *Theridiosoma sancristobalensis* Baert, 2014 by a prolateral branch of the embolic apophysis filiform, flexible, elongated and with an acute, heavily sclerotized tip protruding retrolateraly from beneath the conductor (Fig. 32D–F; see Rodrigues & Ott 2005: fig. 4, "ae"), but *T. goodnightorum* can be distinguished by having another prolateral branch of the embolic apophysis filiform, flexible, elongated and with a wide tip protruding prolaterally from beneath the heavily sclerotized posterior extension of the conductor (Fig. 32D–F), whereas in *T. chiripa*, if present, the branch is not protruding (Rodrigues & Ott 2005: fig. 4) and *T. sancristobalensis* have the protruding branch with an acute tip (misinterpreted as "embolus" in Baert 2014: figs 8–9). Females of *T. goodnightorum* resemble those of *T. chiripa* and *T. sancristobalensis* by the epigynal plate flat (Figs 6B, 33B; Rodrigues & Ott 2005: fig. 6; Baert 2014: fig. 10), but *T. goodnightorum* can be distinguished by the proximal copulatory ducts forming a squared angle (Fig. 33F), whereas *T. chiripa* and *T. sancristobalensis* have them curved (Rodrigues & Ott 2005: figs 8–9; Baert 2014: fig. 12).

Material examined

PANAMA – **Chiriquí Province** • 1 ♂; Reserva Forestal Fortuna, Quebrada Honda, one-hectare PANCODING inventory; 8.750083° N, 82.239083° W; 1135 m a.s.l.; 7–12 Jun. 2007; M. Arnedo, D. Dimitrov, G. Hormiga, F. Labarque and M. Ramírez leg.; voucher code SFD1DAR028; preparation codes FML-00719, LNP-00262; DNA code thech069; GenBank code PX096928; MACN-Ar 29231 • 1 ♀; same data as for preceding; voucher code SFD1D9L004; preparation codes FML-00726, LNP-00268; DNA code thech121; GenBank code PX096929; MACN-Ar 29235 • 1 ♀; same data as for preceding; voucher code SFD1NCD023; DNA barcode SPIPA350-10; MACN-Ar 29233 • 1 ♂; same data as for preceding; voucher code SFD1NCL025; DNA code thech182; GenBank code PX096935; MACN-Ar 29238 • 1 ♀; same data as for preceding; voucher code SFD1NAH025; DNA barcode SPIPA354-10; MCZ • 1 ♀; same data as for preceding; voucher code SFU1N8L031; DNA code thech173; GenBank code PX096938; CRBA • 1 ♀; same data as for preceding; voucher code SFC2NAR015; DNA code thech178; GenBank code PX096939; CRBA • 4 ♂♂, 10 ♀♀; same data as for preceding; MCZ • 2 ♂♂, 2 ♀♀; same data as for preceding; IMFUP • 3 ♀♀; same data as for preceding; MACN-Ar 29234 • 3 ♀♀; same data as for preceding; MACN-Ar 29232 • 2 ♀♀; same data as for preceding; MACN-Ar 29224 • 1 ♀; same data as for preceding; MACN-Ar 29237 • 1 ♀; same data as for preceding; MACN-Ar 29236 • 1 ♀; same data as for preceding; MACN-Ar 29225 • 1 ♀; same data as for preceding; MACN-Ar 29228 • 1 ♀; same data as for preceding; MACN-Ar 29227 • 1 ♀; same data as for preceding; MACN-Ar 29226 • 1 ♂; same data as for preceding; MACN-Ar 29229 • 3 ♂♂; same data as for preceding; MACN-Ar 29230 • 4 ♂♂, 6 ♀♀; same data as for preceding; CRBA • 2 ♂♂, 4 ♀♀; Parque Internacional La Amistad, Cerro Picacho, one-hectare PANCODING inventory; 8.890500° N, 82.618778° W; 2299 m a.s.l.; 12–17 Jun. 2008; M. Arnedo, L. Benavides, G. Hormiga, F. Labarque, L. Piacentini and M. Ramírez leg.; MCZ • 1 ♀; same data as for preceding; voucher code SAC1NGL018; DNA code thech180; GenBank code PX096934; MCZ • 1 ♂; same data as for preceding; voucher code SAD1NCA001; DNA barcode SPIPA352-10; MCZ • 1 ♂; same data as for preceding; voucher code SAD1NHL021; DNA code thech169; GenBank code PX096930; MCZ • 1 ♀; same data as for preceding; voucher code SAD1NCA004; DNA barcode SPIPA353-10; MCZ • 1 ♂; same data as for preceding; voucher code SAD1NCR031; DNA code thech170; GenBank code PX096931; MACN-Ar 29241 • 1 ♂; same data as for preceding; voucher code SAD1NGL024;

DNA code thech174; GenBank code PX096932; MACN-Ar 29242 • 1 ♀; same data as for preceding; voucher code SAC1DDH014; DNA code thech175; GenBank code PX096933; MACN-Ar 29243 • 1 ♀; same data as for preceding; voucher code SAC1NHL015; DNA barcode SPIPA351-10; CRBA • 1 ♂, 1 ♀; same data as for preceding; MIUP • 1 ♂; same data as for preceding; MACN-Ar 29240 • 1 ♀; same data as for preceding; MACN-Ar 29244 • 1 ♀; same data as for preceding; MACN-Ar 29239 • 5 ♂♂, 5 ♀♀; same data as for preceding; CRBA. – **Coclé Province** • 1 ♀; Parque Nacional General de División Omar Torrijos Herrera, El Cope, one-hectare PANCODING inventory; 8.668083° N, 80.592583° W; 760 m a.s.l.; 4–9 Jun. 2008; M. Arnedo, L. Benavides, G. Hormiga, F. Labarque and M. Ramírez leg.; voucher code STD1N6R021; DNA code thech171; GenBank code PX096936; MCZ • 1 ♀, same data as for preceding; voucher code STD1N6R027; preparation code FML-00991; DNA code thech172; GenBank code PX096937; CRBA • 1 ♂, 1 ♀; same locality as for preceding; 21–24 Jun. 2008; L. Piacentini and F. Labarque leg.; non-quantitative sample; MACN-Ar.

Description

Male (MACN-Ar 29231)

Total length 1.41. Prosoma: length 0.92, width 0.67, height 0.63. Sternum: length 0.36, width 0.36. Eye diameters and interdistances: AME 0.09, PME 0.08, AME–PME 0.09. Opisthosoma: length 1.03, width 0.85, height 0.73. Leg formula: 1243. Dorsal shield of prosoma dark brownish-orange laterally, yellowish-orange centrally forming an irregular band (Fig. 32A–B). Dorsum of ocular area orange (Fig. 32A–B). Sternum orange with dark borders (Fig. 32C). Opisthosoma color overall dark brownish-orange, dorsally lighter, with wide guanine silver stripe, open posteriorly, encircling half of opisthosoma (Fig. 32A–B). Epiandrium, tracheal spiracle and behind anal tubercle reddish-brown, covered by sparsely thin whitish-gray flecks; booklung cover whitish-gray, spinneret field dark brownish-orange (Fig. 32C). Femora yellowish-white but distally dark, patella, tibiae, metatarsi and tarsi orange (Fig. 32A–C). Palp: paracymbium hooked, paracymbial process (from Lopardo & Hormiga 2015, but see "cymbial lamella" in Coddington 1986 and Labarque & Griswold 2014) with a row of setae, tegulum striated (i.e., with spicules), tegular spur rounded, small, median apophysis elongated with a median groove, conductor retrolateral surface finger-printed (see "stripes" in Coddington 1986 and Labarque & Griswold 2014) covering the embolic apophysis, embolus as thin lamina, multiple divided embolic apophysis with two filiform, flexible and elongated branches protruding from beneath conductor, retrolateral distally acute and heavily sclerotized, prolateral distally wide (Fig. 32D–F; Coddington 1986: figs 130–131).

Redescription

Female (MACN-Ar 29235, CRBA STD1N6R027)

Total length 1.81. Prosoma: length 0.85, width 0.70, height 0.67. Sternum: length 0.38, width 0.38. Eye diameters and interdistances: AME 0.09, PME 0.09, AME–PME 0.08. Opisthosoma: length 1.29, width 1.20, height 1.10. Leg formula: 1243. Coloration darker than male (Fig. 33A–C). Sternum with two dark brownish-orange patches close to sternal pits (Fig. 33C). Epigynal plate brownish-orange (Fig. 33C). Epigynal plate: flat, dorsal epigynal plate exposed (Fig. 33B–C). Vulva: copulatory ducts massive proximally, and heavily sclerotized distally, proximal copulatory ducts with patch of gland ducts dorsally, distal copulatory ducts convoluting antero-posteriorly, inserting ventromedially posteriorly into spermathecae, spermathecae ovoid, sclerotized, and connate (i.e., fused along midline), fertilization ducts sclerotized, emerging laterally posteriorly from spermathecae, curving dorsally anteriorly to meet uterus externus (Figs 6A–B, 33D).

Records and biology

Theridiosoma goodnightorum has been previously recorded in Mexico and Costa Rica (World Spider Catalog 2025). Records in this study are limited to collections made at 895 m a.s.l. and 1135 m a.s.l. in premontane rainforest from Parque Nacional General de División Omar Torrijos Herrera and Reserva

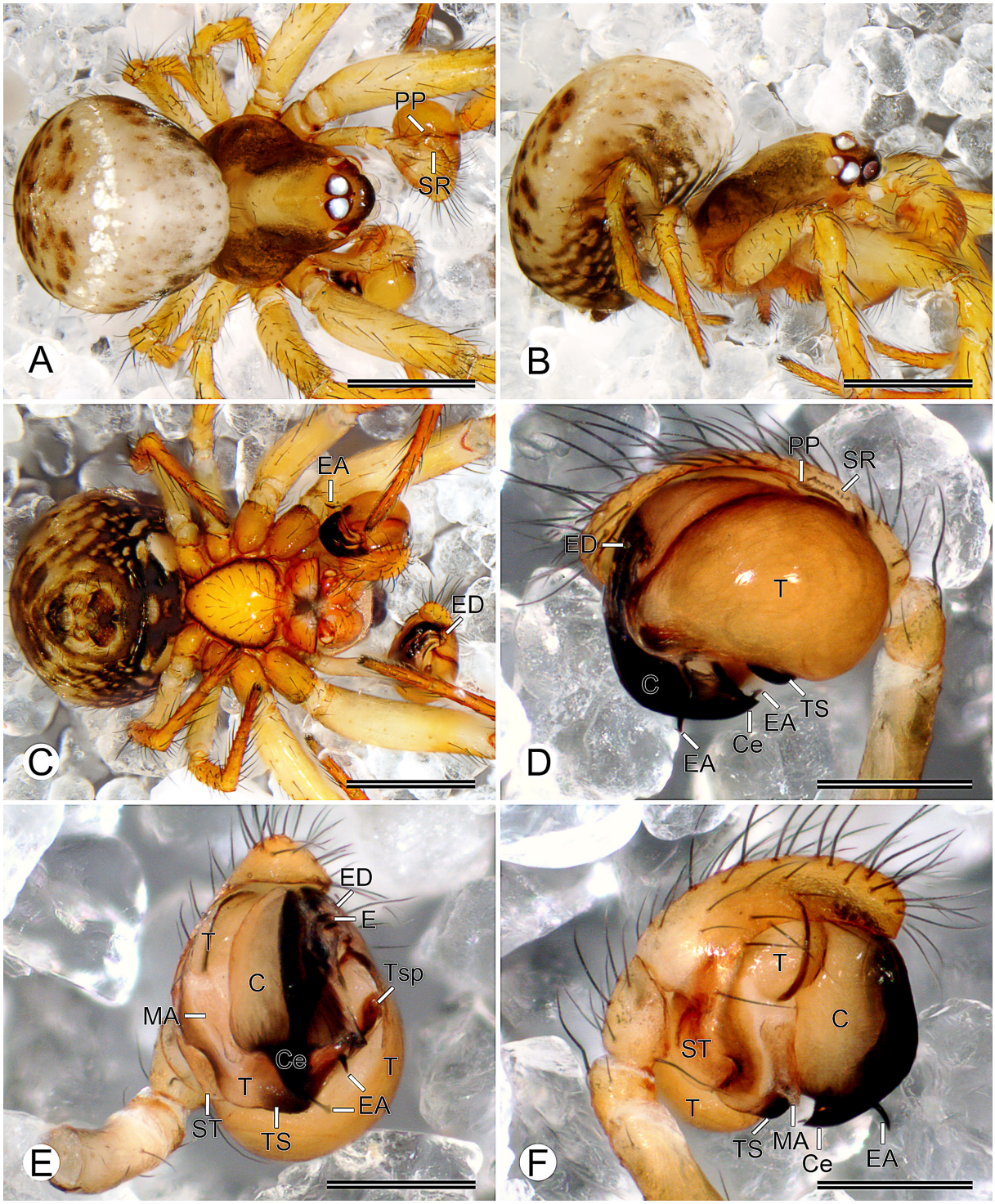

Fig. 32. *Theridiosoma goodnightorum* Archer, 1953, ♂ (MACN-Ar 29231). **A–C**. Habitus (A = dorsal view; B = lateral view; C = ventral view). **D–F**. Left palp (D = retrolateral view; E = ventral view; F = prolateral view). Abbreviations: C = conductor; Ce = conductor posterior extension; E embolus; EA = embolic apophysis; ED = embolic division; MA = median apophysis; PP = paracymbial process; SR = setae row; ST = subtegulum; T = tegulum; TS = tegular striae; Tsp = tegular spur. Scale bars: A–C = 0.5 mm; D–F = 0.2 mm.

Forestal Fortuna, respectively, and at 2299 m a.s.l. in lower montane rainforest from Parque Internacional La Amistad (Fig. 1). Males and females have been collected mostly at night by looking down, though some specimens were also collected at night by looking up and cryptic techniques, and others during the day by cryptic, and looking down.

Variation

Some males and females have a darker coloration than the described specimens.

Remarks

Whereas we have not examined the type of this species, we believe that species attribution is unproblematic. Coddington (1986: 64) examined the female type of *Theridiosoma goodnightorum* from Mexico and attributed SEM images of the male palp to this species from a specimen in Costa Rica (Coddington 1986: figs 130–131). Unfortunately, Coddington (1986) did not describe the male of *T. goodnightorum*; however, we have done so here (see Description above). Our description of the male palp of *T. goodnightorum* agrees in every way with the specimen illustrated by Coddington (1986).

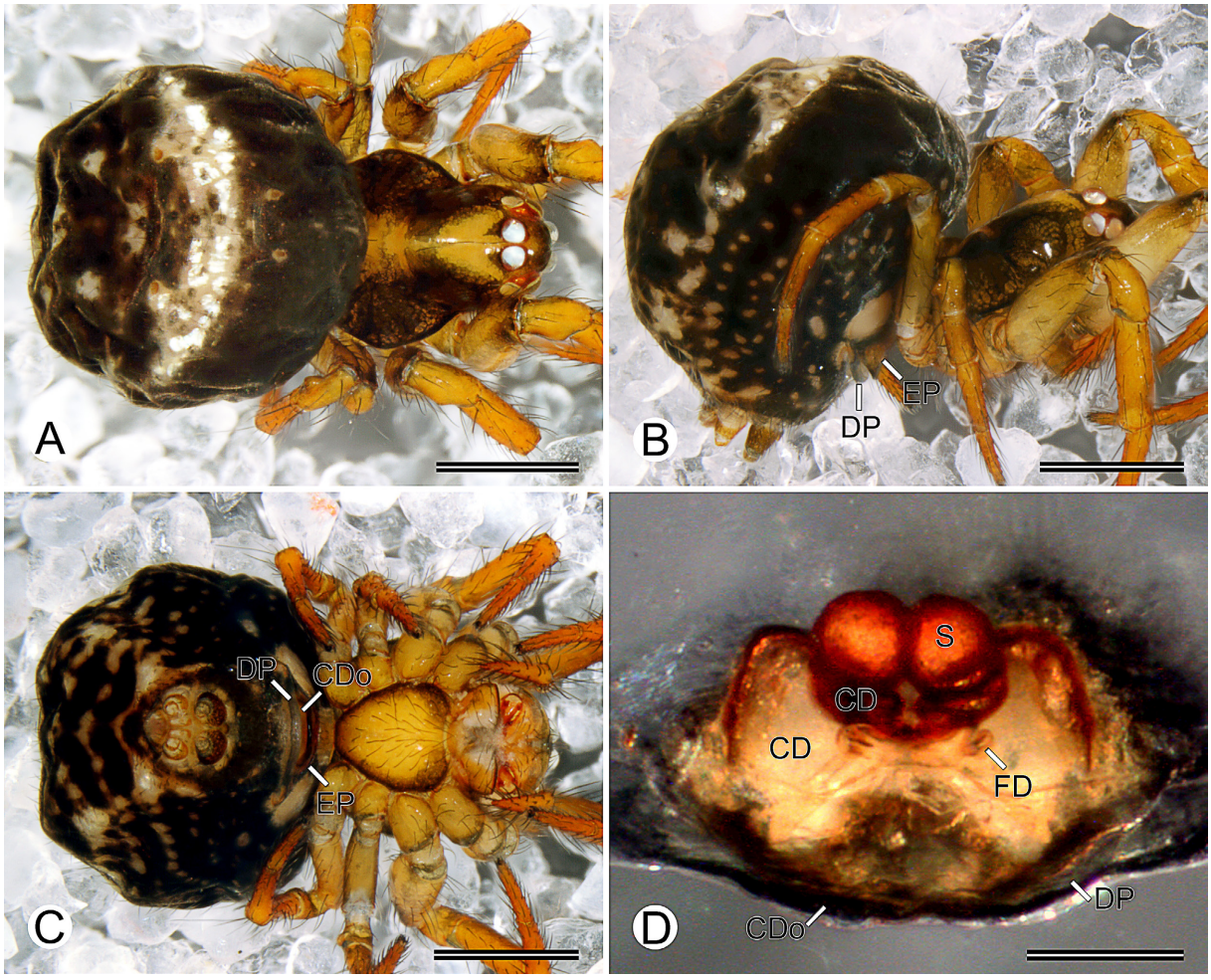

Fig. 33. *Theridiosoma goodnightorum* Archer, 1953, ♀ (MACN-Ar 29235). **A–C**. Habitus (A = dorsal view; B = lateral view; C = ventral view). **D**. Vulva, dorsal view. Abbreviations: CD = copulatory duct; CDo = copulatory duct opening; DP = epigynal dorsal plate; EP = epigynal plate; FD = fertilization duct; S = spermatheca. Scale bars: A–C = 0.5 mm; D = 0.1 mm.

Tantra gen. nov.
urn:lsid:zoobank.org:act:B6FDE0A4-873F-4730-AAE6-3F0398973A18

Type species

Tantra bugle gen. et sp. nov. by original designation.

Diagnosis

Males of *Tantra* gen. nov. resemble those of *Andasta*, *Theridiosoma* and *Zoma* by having the embolic apophysis divided multiple times (more than three times) forming branches prolaterally and retrolaterally to the embolus (e.g., Zhao & Li 2012: fig. 27d), but *Tantra* can be distinguished by having one retrolateral branch protruding from beneath the conductor (Figs 34E, 38E, 42E), whereas males of *Andasta* lack such branches (Saaristo 2010: fig. 38 6–7), and *Theridiosoma* and *Zoma* have at least one prolateral branch (Fig. 32D–F; Miller *et al.* 2009: fig. 10f; Zhao & Li 2012: fig. 28d; Ballarin *et al.* 2021: fig. 5c) protruding from beneath the conductor. Males of *Tantra* can also be distinguished from those of other genera by a tegular spur folding on itself anteriorly, forming a pocket (i.e., resembling a sclerotized wrench tool head in ventral view) (Figs 34E, 38E, 46E; Dupérré & Tapia 2017: fig. 25). Females of *Tantra* can be distinguished from those of other genera by dorsal sclerotized spurs extending from the lateral margins of the epigynal plate (Figs 6D–E, 35D–F, 39C; Dupérré & Tapia 2017: fig. 27), proximal copulatory ducts convoluting multiple times (Figs 35D–F, 37D, 48D; Dupérré & Tapia 2017: fig. 27), and distal copulatory ducts coiling dorso-ventrally and inserting ventromedially posteriorly into spermathecae (Figs 6D, 35E).

Etymology

The generic name is a noun in apposition derived from the word ‘tantra’ which means ‘net, web or weave’ (among other meanings) in Sanskrit, a historical and extinct Indo-Aryan language. Gender is masculine.

Description

Males total length between 1.03–1.43, and females 1.43–2.33. Prosoma light, dark or cephalic area dark and laterals light. Ocular area light or dark. Eyes nearly subequal, AME separated by about ½ a diameter, PME juxtaposed or separated by about ½ a diameter. Sternum smooth and flat, light, dark, or light circled by a dark line. Legs short or long, femora and patella light, olive-green or tan, tibiae, metatarsi and tarsi tan; metatarsi shorter than tibiae (except legs III); tibiae III–IV with three to four rows of trichobothria longer than tibia diameter; leg formula: 1243. Opisthosoma ovoid, light, dark or with several colors, with or without silver patches, forming transversal or longitudinal stripes or other patterns. Spinnerets light, dark or mixed. Palp with setae row on the paracymbial process (Figs 38D, 44A–D, 46A; Dupérré & Tapia 2017: fig. 24). Tegulum striated (i.e., with spicules) with tegular spur forming pocket that may be wide and rounded (Figs 38E, 40E, 44E; Dupérré & Tapia 2017: fig. 25) or elongated and acute (Figs 34E, 36E, 46E) in ventral view. Median apophysis elongated with median groove (i.e., sclerotized darker midline) (Figs 34E–F, 38E–F, 44E–F). Conductor protruded ventrally covering embolic division retrolaterally, that can be seen by transparency (Figs 34D–E, 42D–E, 44D–E), with heavily sclerotized (i.e., dark) posterior extension, that may have retrolateral heavily sclerotized projection (Figs 34E, 36E, 40E; Dupérré & Tapia 2017: fig. 25), and prolateral, acute and posteriorly elongated apophysis that articulates with conductor through membrane, which may (i.e., long; Figs 38E, 42E, 44E; Dupérré & Tapia 2017: fig. 23) or may not exceed (i.e., short; Fig. 34E) conductor extension posteriorly. Embolus as thin lamina (Figs 38E, 44E, 46E), multiple divided embolic apophysis forming branches prolaterally and retrolaterally to embolus (Figs 34C–D, 38C, 44C–D; ED), with one filiform, sclerotized (i.e., orange) and elongated retrolateral branch protruding from beneath conductor (Figs 34A, D–E, 38D–E, 40D–E, 42D–E; misinterpreted as “embolus” in Dupérré & Tapia 2017: fig. 25). Epigynal plate protruding ventrally forming dome

(i.e., curved in posterior view; Figs 35B, 39B, 45B), with small lateral pits (Fig. 6D), dorsally heavily sclerotized (i.e., reddish-brown) spurs extending from their lateral margins (Figs 6D–E, 35D–F, 39C, 48D; misinterpreted as "copulatory duct" in Dupérré & Tapia 2017: figs 27), and dorsal epigynal plate exposed, membranous, protruding from beneath copulatory opening posteriorly (Figs 6D–E, 35B–D, 39B–D, 45B–D, 48C–D; Dupérré & Tapia 2017: fig. 26). Convoluted copulatory ducts (Figs 35D–F, 37D, 48D; Dupérré & Tapia 2017: fig. 27), distal copulatory ducts coiling dorso-ventrally, inserting ventromedially posteriorly into spermathecae (Figs 6D, 35E).

Distribution

Costa Rica to Ecuador.

Remarks

Coddington (1986: 63–64) suggested that the epigynal plate of *Theridiosoma argenteolunulatum* Simon, 1897, *Theridiosoma davisi* Archer, 1953, *Theridiosoma nechodomae* Petrunkevitch, 1930, and *Theridiosoma savannum* Chamberlin & Ivie, 1944 have "lateral sclerotized spurs projecting towards the median", but he did not provide illustrations of those characters. In addition, the original male and female illustrations are not detailed enough to provide conclusive evidence for the genital characters, and thus we kept the above species as *Theridiosoma* until more detailed studies are done.

Composition

Eight new species here described, and *Tantra kullki* (Dupérré & Tapia, 2017) comb. nov., here transferred from *Theridiosoma*.

Remarks

The male and female of *Theridiosoma kullki*, and the male palp of a *Theridiosoma* sp. from Costa Rica (Coddington 1986: figs 132–133) agree in every way with the diagnostic characters here proposed for *Tantra* gen. nov.

Tantra bugle gen. et sp. nov.
urn:lsid:zoobank.org:act:0161DF51-4758-451A-9C9B-6700C84F39B6
Figs 1, 6D–E, 34–35

Diagnosis

Females of *Tantra bugle* gen. et sp. nov. resemble those of *Tantra wounaan* gen. et sp. nov. by the wide guanine silver stripe, open posteriorly, encircling most of the opisthosoma (Figs 35A–C, 37A–C), but *T. bugle* can be distinguished by the smooth (i.e., no pattern) light olive-green dorsum of the opisthosoma (Fig. 35A), whereas *T. wounaan* have the dorsum of the opisthosoma with dark olive-green irregular lines (i.e., zigzag; Fig. 37A). Males of *T. bugle* resemble those of *T. wounaan* by the tegular pocket elongated and acute, and the conductor extension with a retrolateral projection (Figs 34D–F, 36D–F), but *T. bugle* can be distinguished by the conductor apophysis short, not exceeding the conductor extension posteriorly, and the tegular pocket anterior side forming a rectangle (Fig. 34E–F), whereas *T. wounaan* have the apophysis long and the anterior side of the pocket pointed (Fig. 36E–F).

Etymology

The specific name is a noun in apposition to honor the Buglé native people of Panama, which derived from the union of two words, 'bu' and 'gle', that mean 'people, to live', or 'to be present' and 'Earth' or 'resources', respectively, in the Buglere language.

Type material

Holotype

PANAMA – **Chiriquí Province** • ♂; Reserva Forestal Fortuna, Quebrada Honda, one-hectare PANCODING inventory; 8.750083° N, 82.239083° W; 1135 m a.s.l.; 7–12 Jun. 2007; M. Arnedo, D. Dimitrov, G. Hormiga, F. Labarque and M. Ramírez leg.; voucher code SFB1D8H019; MIUP.

Paratypes

PANAMA – **Chiriquí Province** • 1 ♂; same data as for holotype; voucher code SFU2NAD032; preparation codes FML-00690, LNP-00260; DNA code thes4113; GenBank PX096919; MACN-Ar 29366 • 1 ♀; same data as for holotype; voucher code SFU2NBH034; preparation codes FML-00694, FML-00746, LNP-00276; DNA de thes4065; GenBank PX096918; MACN-Ar 29359 • 1 ♂; same data as for holotype; voucher code SFD1NAL019; DNA barcode SPIPA343-10; MCZ • 1 ♂; same data as for holotype; voucher code SFD1NCH021; DNA barcode SPIPA342-10; CRBA • 1 ♀; same data as for holotype; voucher code SFU1D9A009; preparation code FML-00982; DNA barcode SPIPA344-10; CRBA.

Other material

PANAMA – **Chiriquí Province** • 1 ♀; same data as for holotype; voucher code SFU1NCR034; DNA code thes4177; GenBank PX096920; MCZ • 1 ♀; same data as for holotype; voucher code SFU1NBA029; DNA code thes4259; GenBank PX096922; MACN-Ar 29358 • 1 ♂; same data as for holotype; voucher code SFB1DAR031; DNA code thes4181; GenBank PX096921; CRBA • 13 ♂♂, 12 ♀♀; same data as for holotype; MCZ • 4 ♂♂, 4 ♀♀; same data as for holotype; MIUP • 13 ♂♂, 12 ♀♀; same data as for holotype; MACN-Ar • 13 ♂♂, 12 ♀♀; same data as for holotype; CRBA • 2 ♂♂, 2 ♀♀; same locality as for holotype; 21–24 Jun. 2008; L. Piacentini and F. Labarque leg.; non-quantitative sample; MACN-Ar • 1 ♀; same data as for preceding; voucher code SFNQP8L012; DNA barcode SPIPA222-10; MACN-Ar.

Description

Male (paratypes MACN-Ar 29366, CRBA SFU1D9A009)

Total length 1.43. Prosoma: length 0.84, width 0.68, height 0.59. Sternum: length 0.38, width 0.38. Eye diameters and interdistances: AME 0.09, PME 0.07, AME–PME 0.09. Opisthosoma: length 0.98, width 0.78, height 0.66. Leg formula: 1243. Dorsal shield of prosoma yellowish-white laterally, greenish-yellow centrally (Fig. 34A–B). Dorsum of the ocular area greenish-yellow (Fig. 34A–B). Sternum greenish-yellow (Fig. 34C). Opisthosoma color overall yellowish-white, dorsally lighter, with dispersed silver guanine blotches anteriorly (Fig. 34A–B). Epiandrium, booklung cover, tracheal spiracle, spinneret field and behind anal tubercle olive-green (Fig. 34C). Femora and patella yellowish-white, tibiae, metatarsi and tarsi orange (Fig. 34A–C). Palp: paracymbium hooked, paracymbial process with setae row, tegulum striated with tegular spur elongated, acute, median apophysis elongated with median groove, conductor covering embolic division, conductor posterior extension with retrolateral projection, conductor apophysis relatively short, embolus laminated, multiple divided embolic apophysis, retrolateral branch filiform, sclerotized, elongated, protruding from beneath conductor (Fig. 34D–F).

Female (paratype MACN-Ar 29359)

Total length 1.95. Prosoma: length 0.97, width 0.81, height 0.71. Sternum: length 0.43, width 0.44. Eye diameters and interdistances: AME 0.09, PME 0.08, AME–PME 0.10. Opisthosoma: length 1.65, width 1.40, height 1.09. Leg formula: 1243. Coloration olive-greener than male (Fig. 35A–C). Dorsal shield of prosoma olive-green centrally (Fig. 35A–B). Dorsum of ocular area olive-green (Fig. 35A–B). Sternum olive-green (Fig. 35C). Dorsum of opisthosoma light olive-green (Fig. 35A) with wide guanine silver stripe, open posteriorly, encircling most of opisthosoma (Fig. 35B–C). Booklungs cover, tracheal

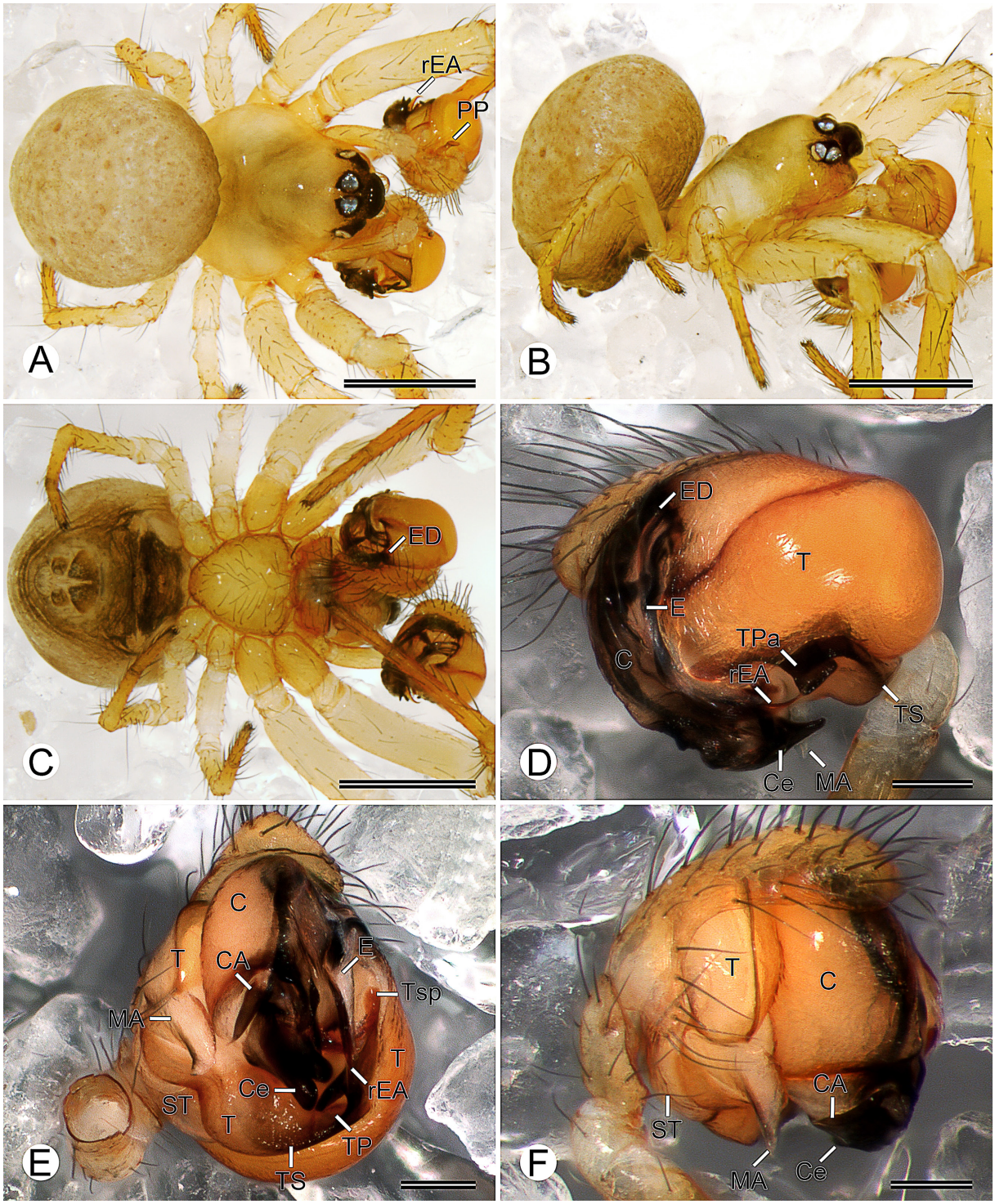

Fig. 34. *Tantra bugle* gen. et sp. nov., paratype, ♂ (MACN-Ar 29366). **A–C**. Habitus (A = dorsal view; B = lateral view; C = ventral view). **D–F**. Left palp (D = retrolateral view; E = ventral view; F = prolateral view). Abbreviations: C = conductor; CA = conductor apophysis; Ce = conductor posterior extension; E = embolus; ED = embolic division; MA = median apophysis; PP = paracymbial process; rEA = embolic apophysis retrolateral branch; ST = subtegulum; T = tegulum; TP = tegular pocket; TPa = tegular pocket anterior side; TS = tegular striae; Tsp = tegular spur. Scale bars: A–C = 0.5 mm; D–F = 0.1 mm.

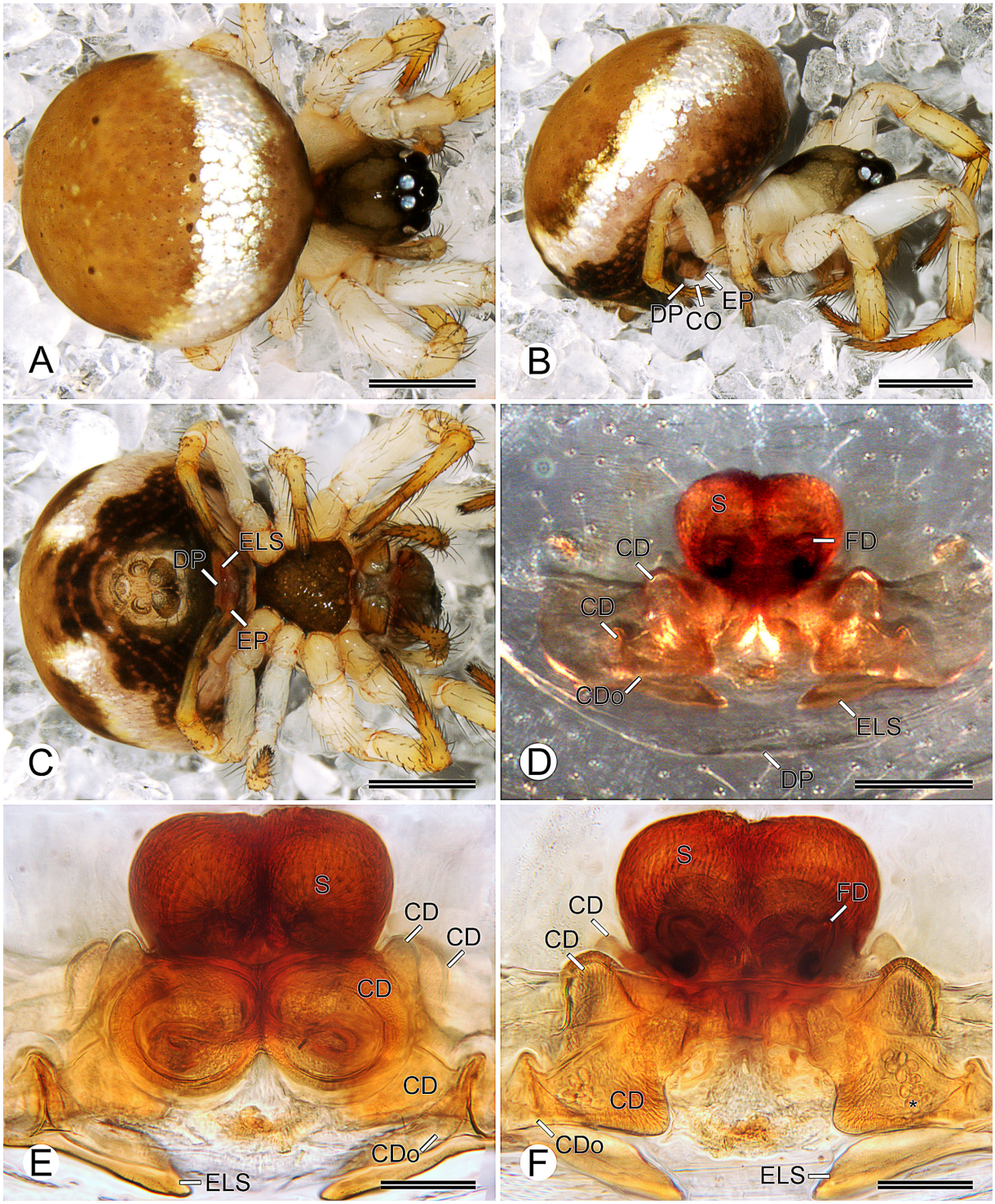

Fig. 35. *Tantra bugle* gen. et sp. nov., paratype, ♀ (MACN-Ar 29359). **A–C**. Habitus (A = dorsal view; B = lateral view; C = ventral view). **D–F**. Vulva (D–E = dorsal view; F = ventral view) (note the asterisk on an encapsulated sperm cell). Abbreviations: CD = copulatory duct; CDo = copulatory duct opening; DP = epigynal dorsal plate; ELS = epigynal lateral spur; EP = epigynal plate; FD = fertilization duct; S = spermatheca. Scale bars: A–C = 0.5 mm; D = 0.1 mm; E–F = 0.05 mm.

spiracle, and behind anal tubercle dark olive-green, spinneret field olive-green (Fig. 35C). Epigynal plate whitish-orange (Fig. 35B–C). Epigynal plate: domed, dorsal-lateral spurs extending to midline, dorsal epigynal plate exposed (Fig. 35B–C). Vulva: convoluted copulatory ducts, proximal copulatory ducts with patch of gland ducts dorsally, distal copulatory ducts coiling dorso-ventrally and inserting ventromedially posteriorly into the spermathecae, spermathecae round, sclerotized, and connate (i.e., fused along midline), fertilization ducts sclerotized, emerging laterally posteriorly from spermathecae, curving dorsally anteriorly to meet uterus externus (Fig. 35C).

Records and biology

Records are limited to collections made at 1135 m a.s.l. in premontane rainforest from Reserva Forestal Fortuna (Fig. 1). Males and females have been collected mostly during the night by looking up, and less frequently also during the day by beating, looking down and cryptic techniques.

Variation

Some females examined have a darker coloration than the described specimens, and some males have dispersed silver guanine blotches covering the dorsum of the opisthosoma.

Tantra wounaan gen. et sp. nov.
urn:lsid:zoobank.org:act:46988A87-9EF5-479A-8D85-99BE1A67ECC4
Figs 1, 36–37

Diagnosis

Females of *Tantra wounaan* gen. et sp. nov. resemble those of *Tantra bugle* gen. et sp. nov. by the wide guanine silver stripe, open posteriorly, encircling most of the opisthosoma (Figs 35A–C, 37A–C), but *T. wounaan* can be distinguished by the dark olive-green irregular lines (i.e., zigzag) on the dorsum of the opisthosoma (Fig. 37A), whereas *T. bugle* have the dorsum of the opisthosoma uniform olive-green (Fig. 35A). Males of *T. wounaan* resemble those of *T. bugle* by the tegular pocket elongated and acute, the conductor extension with a retrolateral projection (Figs 34D–F, 36D–F), but *T. wounaan* can be distinguished by the conductor apophysis long, exceeding the conductor extension posteriorly, and the tegular pocket anterior side pointed (Fig. 36E–F), whereas *T. bugle* have the apophysis short and the anterior side of the pocket forming a rectangle (Fig. 34E–F).

Etymology

The specific name is a noun in apposition to honor the Wounaan native people of Panama.

Type material

Holotype

PANAMA – **Chiriquí Province** • ♂; Parque Internacional La Amistad, Cerro Picacho, one-hectare PANCODING inventory; 8.890500° N, 82.618778° W; 2299 m a.s.l.; 12–17 Jun. 2008; M. Arnedo, L. Benavides, G. Hormiga, F. Labarque, L. Piacentini and M. Ramírez leg.; voucher code SAB2DEB029; MIUP.

Paratypes

PANAMA – **Chiriquí Province** • 1 ♂; same data as for holotype; voucher code SAD1DGH013; preparation codes FML-00710, LNP-00547; DNA code thes7099; GenBank code PX096926; MACN-Ar 29380 • 1 ♀; same data as for holotype; voucher code SAD1NFP008; preparation codes FML-00743, LNP-00546; DNA code thes7105; GenBank code PX096923; MACN-Ar 29372 • 1 ♂; same data as for holotype; voucher code SAU1NFB026; DNA barcode SPIPA330-10; MCZ • 1 ♂; same data as for

holotype; voucher code SAD1DHP001; DNA barcode SPIPA327-10; MACN-Ar 29381 • 1 ♀; same data as for holotype; voucher code SAC1DHA012; DNA barcode SPIPA328-10; CRBA • 1 ♀; same data as for holotype; voucher code SAB1DHP002; DNA barcode SPIPA329-10; CRBA.

Other material

PANAMA – **Chiriquí Province** • 1 ♂; same data as for holotype; voucher code SAD1DHL009; DNA code thes7264; GenBank code PX096924; MACN-Ar 29382 • 1 ♀; same data as for holotype; voucher code SAU1NHH023; DNA code thes7265; GenBank code PX096925; CRBA • 1 ♀; same data as for holotype; voucher code SAC1DFH010; DNA code thes7263; GenBank code PX096927; CRBA • 31 ♂♂, 73 ♀♀; same data as for holotype; MCZ • 7 ♂♂, 22 ♀♀; same data as for holotype; MIUP • 33 ♂♂, 64 ♀♀; same data as for holotype; MACN-Ar • 34 ♂♂, 60 ♀♀; same data as for holotype; CRBA • 2 ♂♂, 4 ♀♀; Parque Internacional La Amistad, Sendero Retoño; 8.893833° N, 82.615083° W; 2240 m a.s.l.; 10–11 Jun. 2008; F. Labarque and M. Ramirez leg.; non-quantitative sample; MACN-Ar • 1 ♀; Parque Internacional La Amistad, Sendero Panamá; 17–18 Jun. 2008; F. Labarque and L. Piacentini leg.; non-quantitative sample; MACN-Ar.

Description

Male (paratype MACN-Ar 29380)

Total length 1.50. Prosoma: length 0.90, width 0.70, height 0.69. Sternum: length 0.40, width 0.41. Eye diameters and interdistances: AME 0.08, PME 0.06, AME–PME 0.08. Opisthosoma: length 0.99, width 0.79, height 0.71. Leg formula: 1243. Dorsal shield of prosoma yellowish-white laterally, dark olive-green centrally (Fig. 36A–B). Dorsum of the ocular area yellowish-white (Fig. 36A–B). Sternum yellow with dark olive-green borders (Fig. 36C). Dorsum of the opisthosoma yellowish-white with light olive-green irregular lines (i.e., zigzag) (Fig. 36A–B). Epiandrium, booklung cover, tracheal spiracle, spinneret field and behind anal tubercle dark olive-green (Fig. 36C). Femora and patella yellowish-white, tibiae orange, metatarsi dark orange but distally brownish-orange, tarsi brownish-orange (Fig. 36A–C). Palp: paracymbial process with setae row, tegulum striated with tegular spur elongated, acute, median apophysis elongated with median groove, conductor covering embolic division, conductor posterior extension with retrolateral projection, conductor apophysis relatively long, embolus laminated, multiple divided embolic apophysis, retrolateral branch filiform, sclerotized, elongated, protruding from beneath conductor (Fig. 36D–F).

Female (paratype MACN-Ar 29372)

Total length 2.27. Prosoma: length 0.93, width 0.76, height 0.75. Sternum: length 0.43, width 0.42. Eye diameters and interdistances: AME 0.08, PME 0.07, AME–PME 0.11. Opisthosoma: length 1.95, width 1.68, height 1.51. Leg formula: 1243. Coloration whiter than male (Fig. 37A–C). Dorsal shield of prosoma white laterally (Fig. 37A–B). Dorsum of ocular area dark olive-green (Fig. 37A–B). Sternum white with dark olive-green borders (Fig. 37C). Dorsum of opisthosoma with wide guanine silver stripe, open posteriorly, encircling most of opisthosoma (Fig. 37B–C). Epigynal plate, booklung cover, tracheal spiracle, spinneret field, and behind anal tubercle dark olive-green (Fig. 37B–C). Femora, patella, and tibiae white, metatarsi white but distally brownish-orange, tarsi brownish-orange (Fig. 37A–C). Epigynal plate: domed, dorsal-lateral spurs extending to midline, dorsal epigynal plate exposed (Fig. 37B–C). Vulva: convoluted copulatory ducts, proximal copulatory ducts with patch of gland ducts dorsally, distal copulatory ducts coiling dorso-ventrally and inserting ventromedially posteriorly into the spermathecae (Fig. 37D).

Records and biology

Records are limited to collections made at 2299 m a.s.l. in lower montane rainforest from Parque Internacional La Amistad (Fig. 1). Males and females have been collected mostly at night by looking

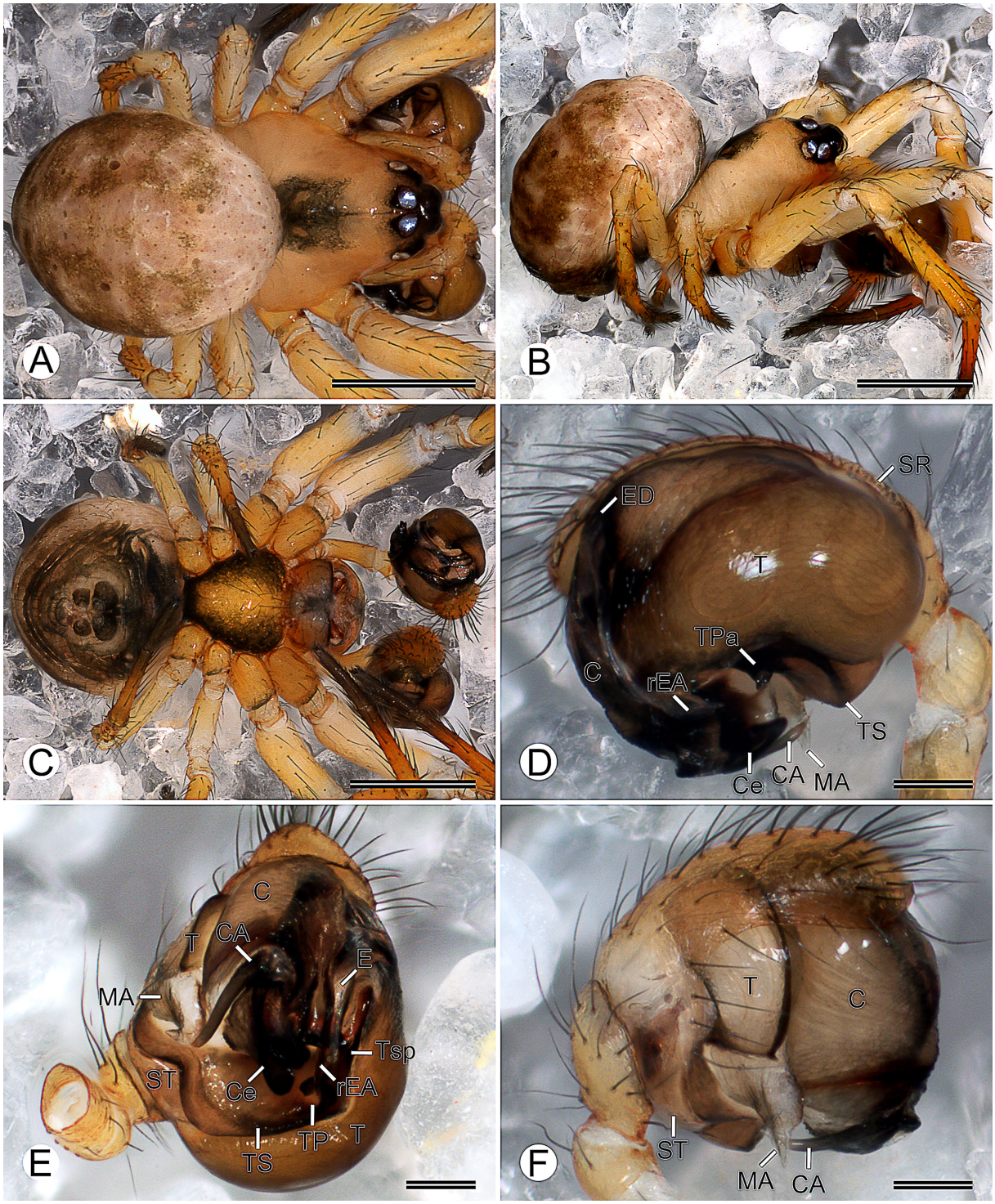

Fig. 36. *Tantra wounaan* gen. et sp. nov., paratype, ♂ (MACN-Ar 29380). **A–C**. Habitus (A = dorsal view; B = lateral view; C = ventral view). **D–F**. Left palp (D = retrolateral view; E = ventral view; F = prolateral view). Abbreviations: C = conductor; CA = conductor apophysis; Ce = conductor posterior extension; E = embolus; ED = embolic division; MA = median apophysis; rEA = embolic apophysis retrolateral branch; SR = setae row; ST = subtegulum; T = tegulum; TP = tegular pocket; Tpa = tegular pocket anterior side; TS = tegular striae; Tsp = tegular spur. Scale bars: A–C = 0.5 mm; D–F = 0.1 mm.

up and looking down, and less frequently also during the day by beating, looking down and cryptic techniques.

Variation

Some males have dispersed silver guanine blotches covering the dorsum of the opisthosoma.

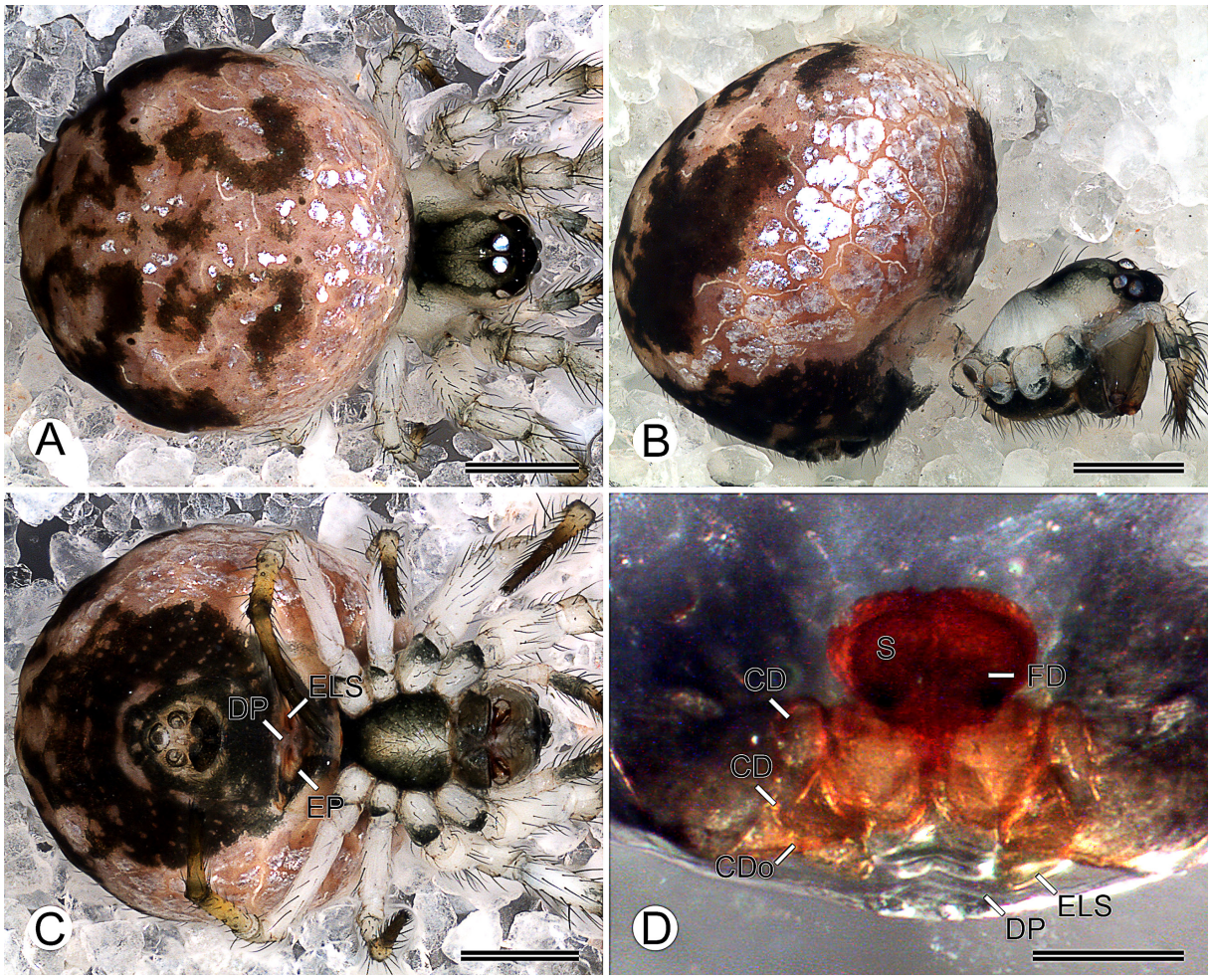

Fig. 37. *Tantra wounaan* gen. et sp. nov., paratype, ♀ (MACN-Ar 29372). **A–C**. Habitus (A = dorsal view; B = lateral view; C = ventral view). **D**. Vulva, dorsal view. Abbreviations: CD = copulatory duct; CDo = copulatory duct opening; DP = epigynal dorsal plate; ELS = epigynal lateral spur; EP = epigynal plate; FD = fertilization duct; S = spermatheca. Scale bars: A–C = 0.5 mm; D = 0.1 mm.

Tantra bribri gen. et sp. nov.
urn:lsid:zoobank.org:act:1DE5398F-CBFC-4CED-AEBD-DB95395CE9FF
Figs 1, 38–39

Diagnosis

Males and females of *Tantra bribri* gen. et sp. nov. resemble those of *Tantra ngabe* gen. et sp. nov. by the white general coloration (Figs 38A–C, 39A–C, 40A–C, 41A–C), but *T. bribri* can be distinguished by the six olive-green patches on the dorsum of the opisthosoma (Figs 38A, 39A), whereas *T. ngabe* have two olive-green patches (Figs 40A, 41A). Males of *T. bribri* also resemble those of *T. ngabe* by the tegular pocket wide and rounded (Figs 38E, 40E), but *T. bribri* can be distinguished by the pocket posterior side smooth (i.e., not projecting; Fig. 38D), whereas *T. ngabe* have it pointed (Fig. 40D).

Etymology

The specific name is a noun in apposition to honors the Bribri native people of Panama, which derived from 'bri-bri' that literally means 'hard-hard' (= strong) in the Naso language, currently spoken by the Naso Tjerdi native people of Panama, but it can also be interpreted as 'brave'.

Type material

Holotype

PANAMA – **Coclé Province** • ♂; Parque Nacional General de División Omar Torrijos Herrera, El Cope, one-hectare PANCODING inventory; 8.668083° N, 80.592583° W; 760 m a.s.l.; 4–9 Jun. 2008; M. Arnedo, L. Benavides, G. Hormiga, F. Labarque and M. Ramírez leg.; voucher code STD1D7R018; MIUP.

Paratypes

PANAMA – **Coclé Province** • 1 ♂; same data as for holotype; voucher code STC2D6R014; preparation codes FML-00962, FML-009623; DNA barcode SPIPA318-10; CRBA • 1 ♀; same data as for holotype; voucher code STD1D6H023; preparation codes FML-00745, FML-00882, FML-00964; DNA barcode SPIPA317-10; MCZ • 1 ♂; same data as for holotype; voucher code STD1D7B026; DNA code thes3250; GenBank code PX096911; MCZ • 1 ♂; same data as for holotype; voucher code STD1N7B028; DNA code thes3214; GenBank code PX096916; MACN-Ar 29351 • 1 ♀; same data as for holotype; voucher code STU1N5L020; DNA barcode SPIPA319-10; MACN-Ar 29353 • 1 ♀; same data as for holotype; voucher code STU1N7A019; DNA barcode SPIPA320-10; CRBA.

Other material

PANAMA – **Coclé Province** • 1 ♀; same data as for holotype; voucher code STU1N6H023; DNA code thes3211; GenBank code PX096908; MCZ • 1 ♀; same data as for holotype; voucher code STU1N7L028; DNA barcode SPIPA321-10; MACN-Ar 29352 • 1 ♀; same data as for holotype; voucher code STC1D8H011; DNA code thes3251; GenBank code PX096912; MACN-Ar 29350 • 1 ♀; same data as for holotype; voucher code STD1N7R021; DNA code thes3213; GenBank code PX096910; CRBA • 2 ♀♀; same data as for holotype; MCZ • 1 ♀; same data as for holotype; MIUP • 6 ♀♀; same data as for holotype; MACN-Ar • 1 ♂, 1 ♀; same data as for holotype; CRBA.

Description

Male (paratype CRBA STC2D6R014)

Total length 1.34. Prosoma: length 0.71, width 0.56, height 0.53. Sternum: length 0.33, width 0.34. Eye diameters and interdistances: AME 0.09, PME 0.06, AME–PME 0.08. Opisthosoma: length 1.01, width 0.88, height 0.76. Leg formula: 1243. Dorsal shield of prosoma white, cephalic area with olive-green speckled lines (Fig. 38A–B). Dorsum of the ocular area white (Fig. 38A–B). Sternum yellowish-

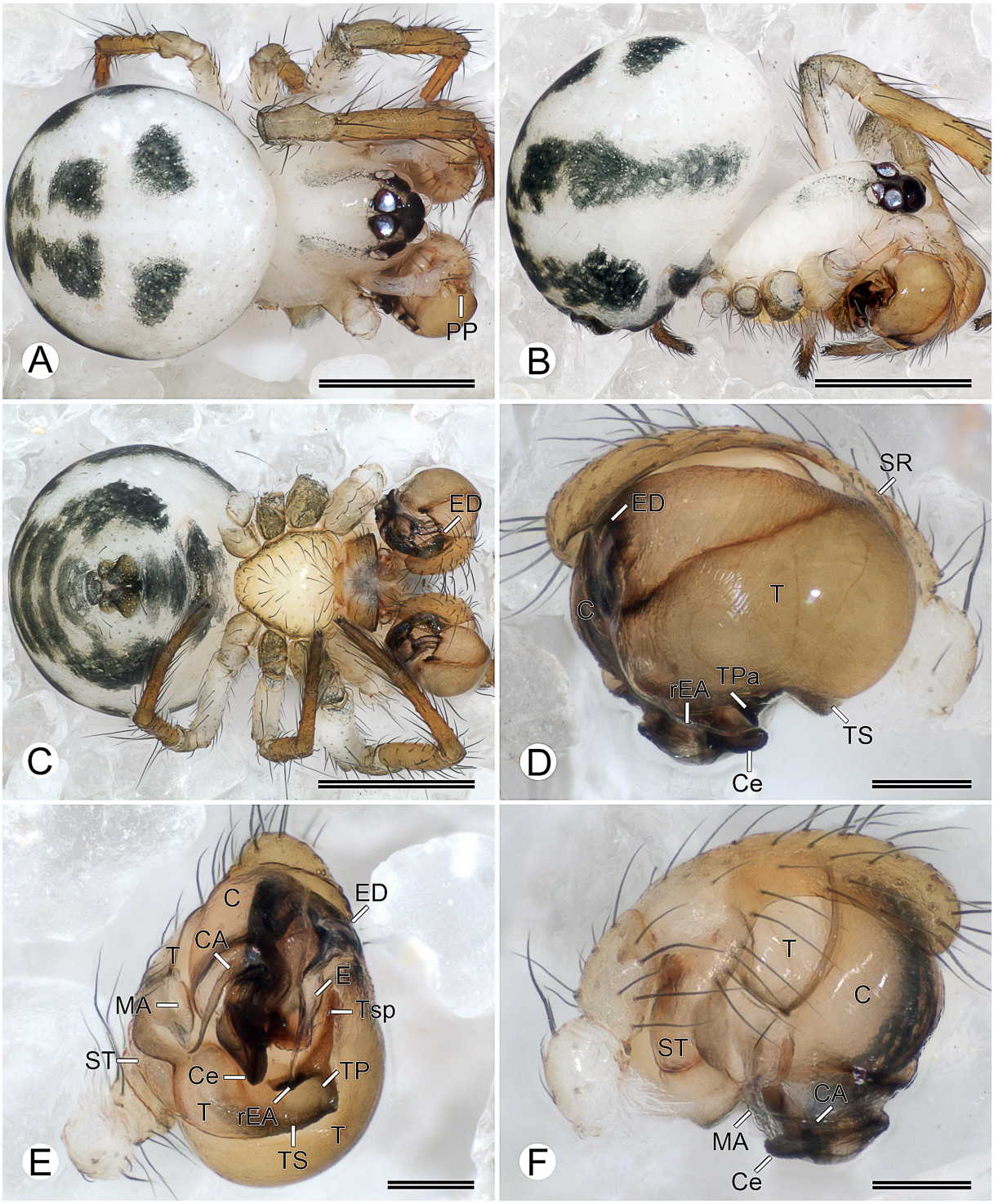

Fig. 38. *Tantra bribri* gen. et sp. nov., paratype, ♂ (CRBA STC2D6R014). **A–C**. Habitus (A = dorsal view; B = lateral view; C = ventral view). **D–F**. Left palp (D = retrolateral view; E = ventral view; F = prolateral view). Abbreviations: C = conductor; CA = conductor apophysis; Ce = conductor posterior extension; E = embolus; ED = embolic division; MA = median apophysis; PP = paracymbial process; rEA = embolic apophysis retrolateral branch; SR = setae row; ST = subtegulum; T = tegulum; TP = tegular pocket; TPa = tegular pocket anterior side; TS = tegular striae; Tsp = tegular spur. Scale bars: A–C = 0.5 mm; D–F = 0.1 mm.

white with olive-green borders (Fig. 38C). Dorsum of the opisthosoma white with six dark olive-green patches posteriorly and dispersed silver guanine blotches anteriorly (Fig. 38A–B). Opisthosoma with two lateral transversal dark olive-green bands (Fig. 38B). Epiandrium, booklung cover, tracheal spiracle, and behind anal tubercle dark olive-green, spinneret field olive-green (Fig. 38C). Femora white but distally olive-green, patella greenish-brown, tibiae, metatarsi and tarsi orange (Fig. 38A–C). Palp: paracymbium hooked, paracymbial process with setae row, tegulum striated with tegular spur wide, rounded, median apophysis elongated with median groove, conductor covering embolic division, conductor posterior extension with small retrolateral projection, conductor apophysis relatively long, embolus laminated, multiple divided embolic apophysis, retrolateral branch filiform, sclerotized, elongated, protruding from beneath conductor (Fig. 38D–F).

Female (paratype MCZ STD1D6H023)
Total length 1.43. Prosoma: length 0.69, width 0.56, height 0.51. Sternum: length 0.33, width 0.34. Eye diameters and interdistances: AME 0.07, PME 0.07, AME–PME 0.07. Opisthosoma: length 1.01, width 0.92, height 0.72. Leg formula: 1243. Coloration as in male (Fig. 39A–C). Epigynal plate whitish-

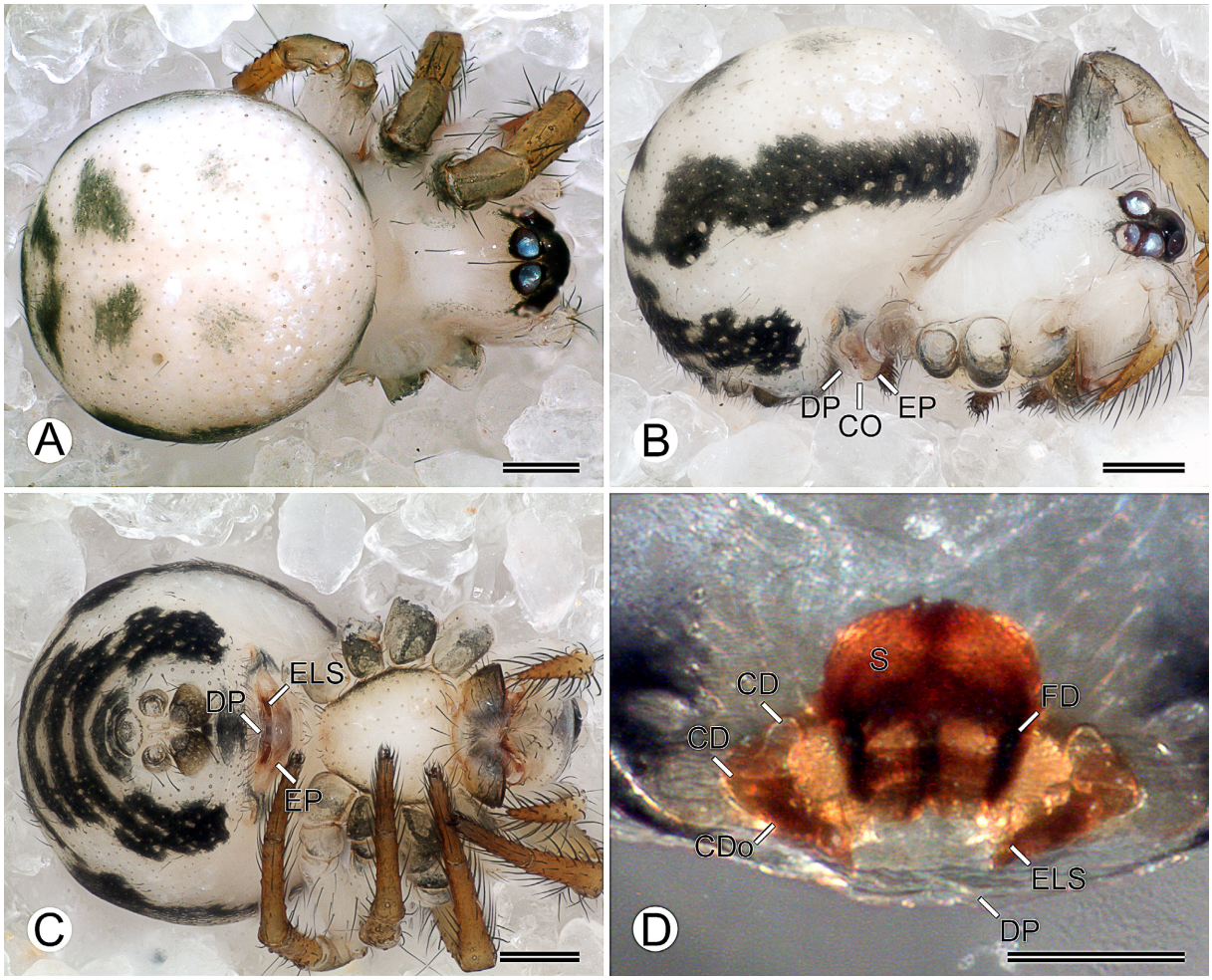

Fig. 39. *Tantra bribri* gen. et sp. nov., paratype, ♀ (MCZ STD1D6H023). **A–C**. Habitus (A = dorsal view; B = lateral view; C = ventral view). **D**. Vulva, dorsal view. Abbreviations: CD = copulatory duct; CDo = copulatory duct opening; DP = epigynal dorsal plate; ELS = epigynal lateral spur; EP = epigynal plate; FD = fertilization duct; S = spermatheca. Scale bars: A–C = 0.2 mm; D = 0.1 mm.

orange (Fig. 39B–C). Epigynal plate: domed, dorsal-lateral spurs extending to midline, dorsal epigynal plate exposed (Fig. 39B–C). Vulva: convoluted copulatory ducts, proximal copulatory ducts with patch of gland ducts dorsally, distal copulatory ducts coiling dorso-ventrally and inserting ventromedially posteriorly into spermathecae, spermathecae round, sclerotized, and connate (i.e., fused along midline), fertilization ducts sclerotized, emerging laterally posteriorly from spermathecae, curving dorsally anteriorly to meet uterus externus (Fig. 39D).

Records and biology

Records are limited to collections made at 895 m a.s.l. in premontane rainforest from Parque Nacional General de División Omar Torrijos Herrera (Fig. 1). Males and females have been collected mostly during the night by looking down and looking up, although males and females were also collected during the day by cryptic technique.

Variation

Some males and females examined have lighter coloration than the described specimens.

Tantra ngabe gen. et sp. nov.
urn:lsid:zoobank.org:act:365DF39F-7853-4DFD-902A-4DC8E972D4BD
Figs 1, 40–41

Diagnosis

Males and females of *Tantra ngabe* gen. et sp. nov. resemble those of *Tantra bribri* gen. et sp. nov. by the white general coloration (Figs 38A–C, 39A–C, 40A–C, 41A–C), but *T. ngabe* can be distinguished by the two olive-green patches on the dorsum of the opisthosoma (Figs 40A, 41A), whereas *T. bribri* have six olive-green patches (Figs 38A, 39A). Males of *T. ngabe* also resemble those of *T. bribri* by the tegular pocket wide and rounded (Figs 38D–F, 40D–F), but *T. ngabe* can be distinguished by the pocket posteriorly side pointed (Fig. 40D), whereas *T. bribri* have it smooth (i.e., not projecting) (Fig. 38D).

Etymology

The specific name is a noun in apposition to honor the Ngäbe native people of Panama, which derived from the union of two words, ‘ngä’ and ‘be’, that mean ‘person, people’ and ‘born and see, feel or exist’, respectively, in the Ngäbere language.

Type material

Holotype

PANAMA – **Chiriquí Province** • ♂; Reserva Forestal Fortuna, Quebrada Honda, one-hectare PANCODING inventory; 8.750083° N, 82.239083° W; 1135 m a.s.l.; 7–12 Jun. 2007; M. Arnedo, D. Dimitrov, G. Hormiga, F. Labarque and M. Ramírez leg.; voucher code SFB1DBA017; DNA barcode SPIPA347-10; MIUP.

Paratypes

PANAMA – **Chiriquí Province** • 1 ♂; same data as for holotype; voucher code SFD1DAR027; preparation codes FML-00708, LNP-00259; DNA code thes3114; GenBank code PX096914; MACN-Ar 29079 • 1 ♀; same data as for holotype; voucher code SFU2NAD033; preparation codes FML-00744, LNP-00256; DNA code thes3067; GenBank code PX096913; MACN-Ar 29077 • 1 ♂; same data as for holotype; voucher code SFC1DBD015; DNA barcode SPIPA346-10; MACN-Ar 29076 • 1 ♀; same data as for holotype; voucher code SFC1DCR013; DNA barcode SPIPA348-10; MIUP • 1 ♀; same data as for holotype; voucher code SFD1DAA017; DNA barcode SPIPA349-10; CRBA.

Other material

PANAMA – **Chiriquí Province** • 1 ♂; same data as for holotype; voucher code SFC1DBH007; DNA code thes3212; GenBank code PX096909; MCZ • 1 ♀; same data as for holotype; voucher code SFU1NCR044; DNA code thes3210; GenBank code PX096915; MCZ • 1 ♀; same data as for holotype; voucher code SFD1NAD013; DNA code thes3249; GenBank code PX096917; MACN-Ar 29082 • 1 ♀; same data as for holotype; voucher code SFD1NCA011; DNA barcode SPIPA345-10; CRBA • 1 ♂, 5 ♀♀; same data as for holotype; MCZ • 1 ♀; same data as for holotype; MIUP • 2 ♀♀; same data as for holotype; MACN-Ar 29083 • 1 ♀; same data as for holotype; MACN-Ar 29080 • 1 ♀; same data as for holotype; MACN-Ar 29078 • 1 ♀; same data as for holotype; MACN-Ar 29081 • 1 ♂, 5 ♀♀; same data as for holotype; CRBA • 1 ♂, 2 ♀♀; same locality as for holotype; 21–22 Jun. 2008; L. Piacentini and F. Labarque leg.; non-quantitative sample; MACN-Ar.

Description

Male (paratype MACN-Ar 29079)

Total length 1.34. Prosoma: length 0.78, width 0.59, height 0.60. Sternum: length 0.33, width 0.34. Eye diameters and interdistances: AME 0.09, PME 0.08, AME–PME 0.08. Opisthosoma: length 0.96, width 0.83, height 0.70. Leg formula: 1243. Dorsal shield of prosoma white, cephalic area with soft olive-green speckled lines (Fig. 40A–B). Dorsum of the ocular area white (Fig. 40A–B). Sternum yellowish-white with olive-green borders (Fig. 40C). Dorsum of opisthosoma white with two dark olive-green patches posteriorly (Fig. 40A–B). Opisthosoma with two lateral transversal dark olive-green bands (Fig. 40B). Epiandrium, booklung cover, tracheal spiracle, and behind anal tubercle dark olive-green, spinneret field olive-green (Fig. 40C). Femora white but distally olive-green, patella greenish-brown, tibiae, metatarsi and tarsi orange (Fig. 40A–C). Palp: paracymbium hooked, paracymbial process with setae row, tegulum striated with tegular spur wide, rounded, median apophysis elongated with median groove, conductor covering embolic division, conductor posterior extension with small retrolateral projection, conductor apophysis relatively long, embolus laminated, multiple divided embolic apophysis, retrolateral branch filiform, sclerotized, elongated, protruding from beneath conductor (Fig. 40D–F).

Female (paratype MACN-Ar 29077)

Total length 1.86. Prosoma: length 0.77, width 0.65, height 0.60. Sternum: length 0.36, width 0.36. Eye diameters and interdistances: AME 0.08, PME 0.07, AME–PME 0.08. Opisthosoma: length 1.41, width 1.40, height 1.29. Leg formula: 1243. Coloration as in male but opisthosoma with dispersed silver guanine blotches anteriorly (Fig. 41A–C). Epigynal plate whitish-orange (Fig. 41B–C), domed, with dorsal-lateral spurs extending to the midline, dorsal epigynal plate exposed (Fig. 41B–C). Vulva: convoluted copulatory ducts, proximal copulatory ducts with patch of gland ducts dorsally, distal copulatory ducts coiling dorso-ventrally and inserting ventromedially posteriorly into spermathecae, spermathecae round, sclerotized, and connate (i.e., fused along midline), fertilization ducts sclerotized, emerging laterally posteriorly from spermathecae, curving dorsally anteriorly to meet uterus externus (Fig. 41D).

Records and biology

Records are limited to collections made at 1135 m a.s.l. in premontane rainforest from Reserva Forestal Fortuna (Fig. 1). Males and females have been collected during the day by looking down and cryptic technique, and during the night by looking up and looking down.

Variation

Some males examined have the dorsum of the opisthosoma with dispersed silver guanine blotches anteriorly.

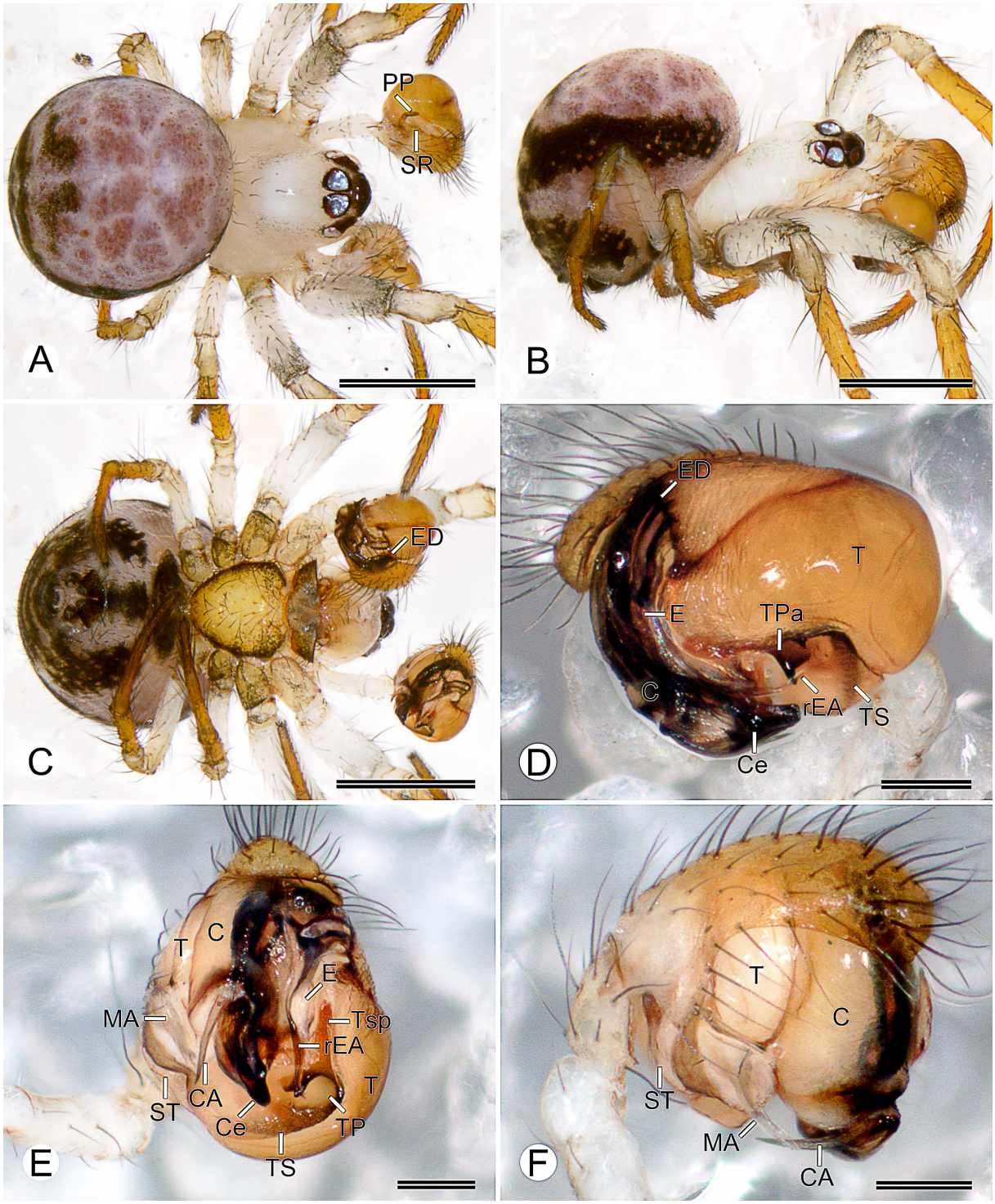

Fig. 40. *Tantra ngabe* gen. et sp. nov., paratype, ♂ (MACN-Ar 29079). **A–C**. Habitus (A = dorsal view; B = lateral view; C = ventral view). **D–F**. Left palp (D = retrolateral view; E = ventral view; F = prolateral view). Abbreviations: C = conductor; CA = conductor apophysis; Ce = conductor posterior extension; E = embolus; ED = embolic division; MA = median apophysis; PP = paracymbial process; rEA = embolic apophysis retrolateral branch; SR = setae row; ST = subtegulum; T = tegulum; TP = tegular pocket; Tpa = tegular pocket anterior side; TS = tegular striae; Tsp = tegular spur. Scale bars: A–C = 0.5 mm; D–F = 0.1 mm.

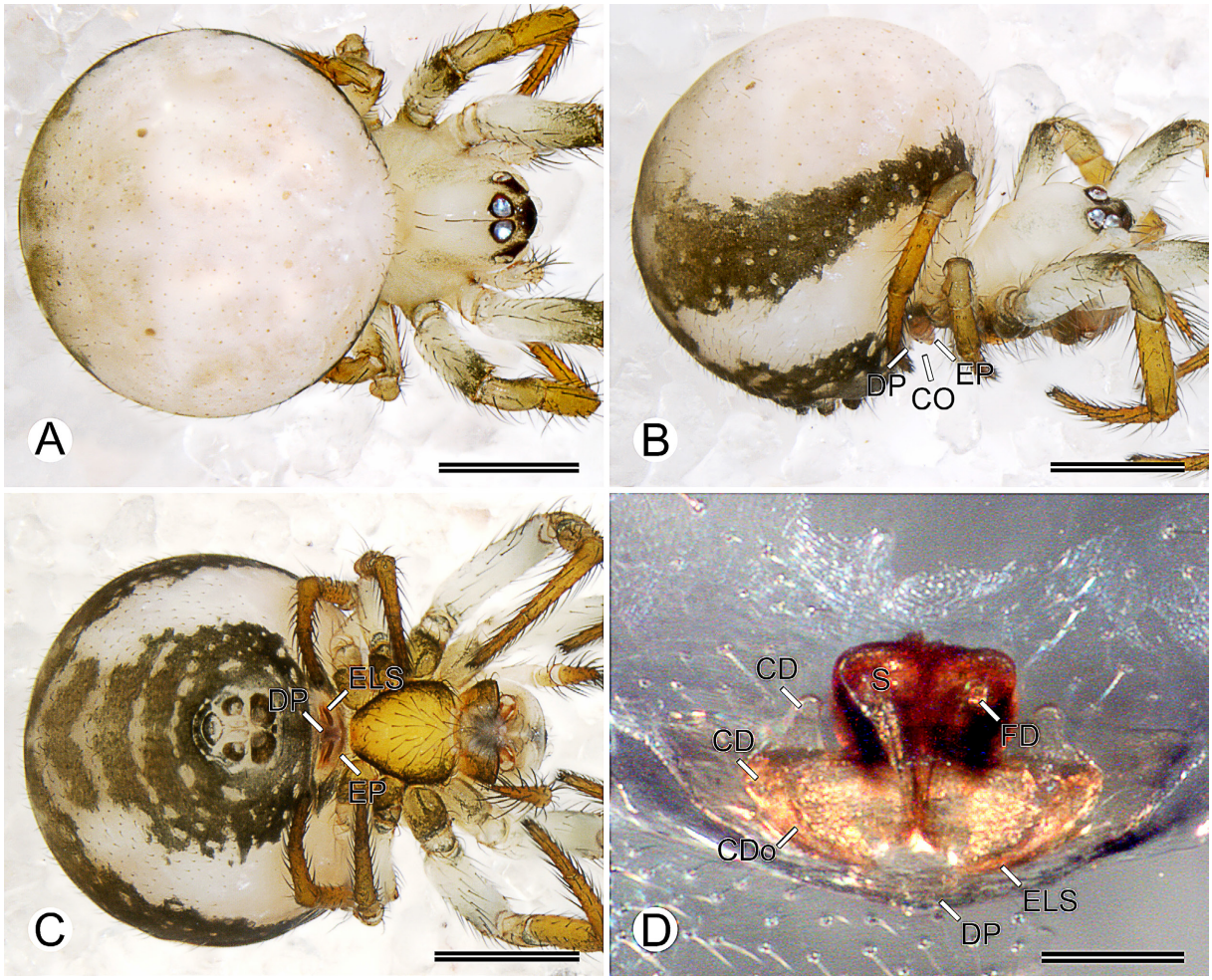

Fig. 41. *Tantra ngabe* gen. et sp. nov., paratype, ♀ (MACN-Ar 29077). **A–C**. Habitus (A = dorsal view; B = lateral view; C = ventral view). **D**. Vulva, dorsal view. Abbreviations: CD = copulatory duct; CDo = copulatory duct opening; DP = epigynal dorsal plate; ELS = epigynal lateral spur; EP = epigynal plate; FD = fertilization duct; S = spermatheca. Scale bars: A–C = 0.5 mm; D = 0.1 mm.

Tantra embera gen. et sp. nov.
urn:lsid:zoobank.org:act:E46AF587-D9A6-46A3-B581-7F29B912EE55
Figs 1, 42–43

Diagnosis

Males and females of *Tantra embera* gen. et sp. nov. resemble those of *Tantra naso* gen. et sp. nov. and *Tantra kuna* gen. et sp. nov. by the wide guanine silver stripe centrally (i.e., above the second pair of opisthosomal apodemes), open posteriorly (Figs 42A–B, 43A–B, 44A–B, 45A–B, 46A–B, 47A–B), but *T. embera* and *T. naso* can be distinguished by the dispersed silver guanine blotches anteriorly (Figs 42A–B, 43A–B, 44A–B, 45A–B), whereas *T. kuna* have two thick silver guanine patches anteriorly, connected to the silver stripe (Figs 46A–B, 47A–B). Females of *T. embera* can be distinguished by the sternum yellowish-white with olive-green borders and olive-green thick patches anteriorly (Fig. 43C), whereas *T. naso* have the borders thick (i.e., almost covering all the sternum) and dark olive-green (Fig. 45C). Males of *T. embera* also resemble those of *T. naso* and *T. kuna* by the conductor extension lacking a

retrolateral projection, and the conductor apophysis long, exceeding the conductor extension posteriorly (Figs 42D–F, 44D–F, 46D–F), but *T. embera* and *T. naso* can be distinguished by the tegular pocket wide and rounded (Figs 42E, 44E), whereas *T. kuna* have it squared (Fig. 46E). Males of *T. embera* can be distinguished by the conductor apophysis distally acute, sharpening gradually (Fig. 42E–F), whereas *T. naso* have the apophysis sharpening abruptly (Fig. 44D, F).

Etymology

The specific name is a noun in apposition to honor the Emberá native people of Panama, which derived from the union of two words, 'embe' and 'ra', that mean 'man' and 'up', respectively, in the Emberá language.

Type material

Holotype

PANAMA – **Panama Province** • ♂; Parque Nacional Altos de Campana, one-hectare PANCODING inventory; 8.683444° N, 79.929833° W; 895 m a.s.l.; 14–19 Jun. 2007; M. Arnedo, D. Dimitrov, G. Hormiga, F. Labarque and M. Ramírez leg.; voucher code SCC1DHL012; MIUP.

Paratypes

PANAMA – **Coclé Province** • 1 ♂; Parque Nacional General de División Omar Torrijos Herrera, El Cope, one-hectare PANCODING inventory; 8.668083° N, 80.592583° W; 760 m a.s.l.; 4–9 Jun. 2008; M. Arnedo, L. Benavides, G. Hormiga, F. Labarque and M. Ramírez leg.; voucher code STB1D5L027; DNA barcode SPIPA333-10; MACN-Ar 29207 • 1 ♂; same data as for preceding; voucher code STD1D6B017; DNA barcode SPIPA332-10; CRBA • 1 ♀; same data as for preceding; voucher code STU1N4R024; DNA barcode SPIPA334-10; MCZ • 1 ♀; same data as for preceding; voucher code STU2N8R022; DNA code thes6236; GenBank code PX096901; CRBA • 1 ♂; same data as for preceding; voucher code STD1N4R020; DNA code thes6235; GenBank code PX096898; CRBA • 1 ♀; same data as for preceding; voucher code STD1N6R022; DNA code thes6234; GenBank code PX096897; CRBA • 1 ♂; same data as for preceding; voucher code STD1N7L011; DNA code thes6227; GenBank code PX096900; CRBA • 1 ♂; same data as for preceding; voucher code STD1N7R030; DNA code thes6232; GenBank code PX096902; CRBA. – **Panama Province** • 1 ♂; same data as for holotype; voucher code SCU2NDA017; preparation codes FML-00712, LNP-00290; DNA code thes6106; GenBank code PX096893; MACN-Ar 29200 • 1 ♀; same data as for holotype; voucher code SCU2NHH021; preparation codes FML-00727, LNP-00288; DNA code thes6107; GenBank code PX096899; MACN-Ar 29203 • 1 ♂; same data as for holotype; voucher code SCC2NGR018; DNA code thes6233; GenBank code PX096896; CRBA • 1 ♀; same data as for holotype; voucher code SCD2NFA020; DNA barcode SPIPA335-10; MACN-Ar 29201 • 1 ♀; same data as for holotype; voucher code SCD1DEL018; DNA barcode SPIPA336-10; CRBA.

Other material

PANAMA – **Coclé Province** • 2 ♂♂, 4 ♀♀; Parque Nacional General de División Omar Torrijos Herrera, El Cope, one-hectare PANCODING inventory; 8.668083° N, 80.592583° W; 760 m a.s.l.; 4–9 Jun. 2008; M. Arnedo, L. Benavides, G. Hormiga, F. Labarque and M. Ramírez leg.; MCZ • 1 ♂, 1 ♀; same data as for preceding; MIUP • 5 ♂♂, 7 ♀♀; same data as for preceding; MACN-Ar • 3 ♂♂, 6 ♀♀; same data as for preceding; CRBA. – **Panama Province** • 1 ♀; same data as for holotype; voucher code SCD1DFL016; DNA code thes6230; GenBank code PX096894; MCZ • 1 ♀; same data as for holotype; voucher code SCC1NHA009; DNA code thes6231; GenBank code PX096895; CRBA • 6 ♂♂, 3 ♀♀; same data as for holotype; MCZ • 1 ♂, 2 ♀♀; same data as for holotype; MIUP • 2 ♂♂, 2 ♀♀; same data as for holotype; MACN-Ar • 4 ♂♂, 4 ♀♀; same data as for holotype; CRBA.

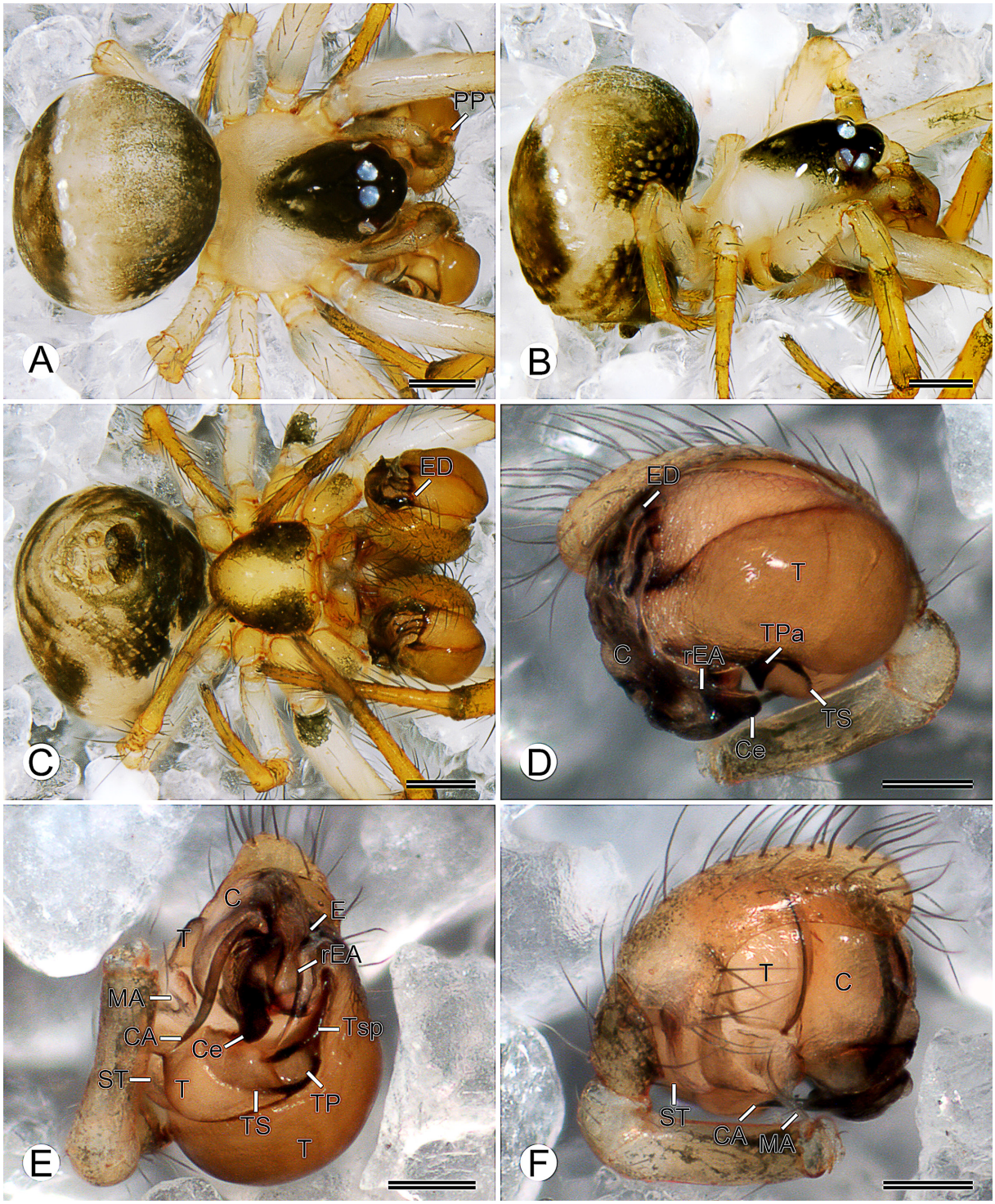

Fig. 42. *Tantra embera* gen. et sp. nov., paratype, ♂ (MACN-Ar 29200). **A–C**. Habitus (A = dorsal view; B = lateral view; C = ventral view). **D–F**. Left palp (D = retrolateral view; E = ventral view; F = prolateral view). Abbreviations: C = conductor; CA = conductor apophysis; Ce = conductor posterior extension; E = embolus; ED = embolic division; MA = median apophysis; PP = paracymbial process; rEA = embolic apophysis retrolateral branch; ST = subtegulum; T = tegulum; TP = tegular pocket; TPa = tegular pocket anterior side; TS = tegular striae; Tsp = tegular spur. Scale bars: A–C = 0.2 mm; D–F = 0.1 mm.

Description

Male (paratype MACN-Ar 29200)

Total length 1.18. Prosoma: length 0.67, width 0.54, height 0.56. Sternum: length 0.31, width 0.33. Eye diameters and interdistances: AME 0.08, PME 0.06, AME–PME 0.08. Opisthosoma: length 0.80, width 0.72, height 0.55. Leg formula: 1243. Dorsal shield of prosoma yellowish-white laterally, dark olive-green centrally (Fig. 42A–B). Dorsum of ocular area dark olive-green (Fig. 42A–B). Sternum yellowish-white with dark olive-green borders and olive-green thick patches anteriorly (Fig. 42C). Opisthosoma olive-green posteriorly, lighter anteriorly, with wide guanine silver stripe centrally, open posteriorly (Fig. 42A–B). Epiandrium, booklung cover, tracheal spiracle, anterior lateral spinnerets field and behind anal tubercle dark olive-green; other spinnerets orange (Fig. 42C). Legs I–II darker than III–IV, femora yellowish-white but I–II with proximal dark olive-green patch ventrally, patella yellow, tibiae and metatarsi orange but proximally and distally darker, and tarsi orange (Fig. 42A–C). Palp: paracymbium hooked, paracymbial process with setae row, tegulum striated with tegular spur wide, rounded, median apophysis elongated with a median groove, conductor covering embolic division, conductor posterior extension lacking retrolateral projection, conductor apophysis relatively long, embolus laminated,

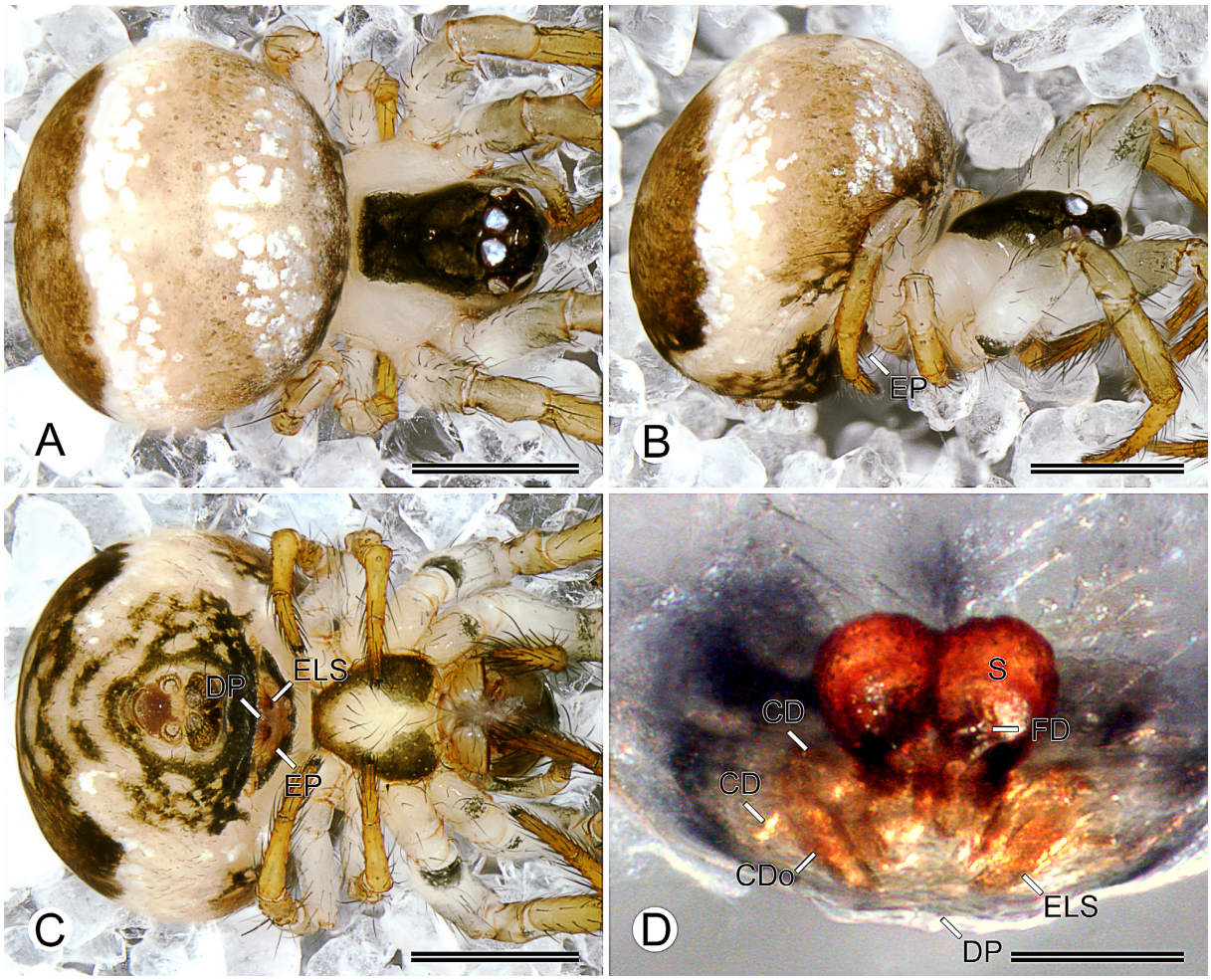

Fig. 43. *Tantra embera* gen. et sp. nov., paratype, ♀ (MACN-Ar 29203). **A–C**. Habitus (A = dorsal view; B = lateral view; C = ventral view). **D**. Vulva, dorsal view. Abbreviations: CD = copulatory duct; CDo = copulatory duct opening; DP = epigynal dorsal plate; ELS = epigynal lateral spur; EP = epigynal plate; FD = fertilization duct; S = spermatheca. Scale bars: A–C = 0.5 mm; D = 0.2 mm.

multiple divided embolic apophysis, retrolateral branch filiform, sclerotized, elongated, protruding from beneath conductor (Fig. 42D–F).

Female (paratype MACN-Ar 29203)
Total length 1.59. Prosoma: length 0.80, width 0.65, height 0.52. Sternum: length 0.37, width 0.37. Eye diameters and interdistances: AME 0.08, PME 0.08, AME–PME 0.10. Opisthosoma: length 1.26, width 1.17, height 0.97. Leg formula: 1243. Coloration as in male but dorsum of opisthosoma with dispersed silver guanine blotches anteriorly (Fig. 43A–C). Epigynal plate whitish-orange (Fig. 43B–C). Epigynal plate: domed, dorsal-lateral spurs extending to midline, dorsal epigynal plate exposed (Fig. 43B–C). Vulva: convoluted copulatory ducts, proximal copulatory ducts with patch of gland ducts dorsally, distal copulatory ducts coiling dorso-ventrally and inserting ventromedially posteriorly into spermathecae, spermathecae round, sclerotized, and connate (i.e., fused along the midline), fertilization ducts sclerotized, emerging laterally posteriorly from spermathecae, curving dorsally anteriorly to meet uterus externus (Fig. 43C).

Records and biology

Records are limited to collections made at 760 m a.s.l. and 895 m a.s.l. in premontane rainforest from Parque Nacional Altos de Campana and Parque Nacional General de División Omar Torrijos Herrera, respectively (Fig. 1). Males and females have been collected during the day and night mostly by looking down, and less frequently also by beating, looking up and cryptic techniques.

Variation

Some females examined have darker coloration than the described specimens, and some males have the dorsum of the opisthosoma with dispersed silver guanine blotches anteriorly.

Tantra naso gen. et sp. nov.

urn:lsid:zoobank.org:act:FC52FC41-90D2-4ED9-B3DB-CB6814C4366C

Figs 1, 44–45

Diagnosis

Males and females of *Tantra naso* gen. et sp. nov. resemble those of *Tantra embera* gen. et sp. nov. and *Tantra kuna* gen. et sp. nov. by the wide guanine silver stripe centrally (i.e., above the second pair of opisthosomal apodemes), open posteriorly (Figs 42A–B, 43A–B, 44A–B, 45A–B, 46A–B, 47A–B), but *T. naso* and *T. embera* can be distinguished by dispersed silver guanine blotches anteriorly (Figs 42A–B, 43A–B, 44A–B, 45A–B), whereas *T. kuna* have two thick silver guanine patches anteriorly, connected to the silver stripe (Figs 46A–B, 47A–B). Females of *T. naso* can be distinguished by the sternum with thick, olive-green borders? (i.e., almost covering all the sternum) (Fig. 45C), whereas *T. embera* have the sternum yellowish-white with olive-green thick patches anteriorly (Fig. 43C). Males of *T. naso* also resemble those of *T. embera* and *T. kuna* by the conductor extension lacking a retrolateral projection, and the conductor apophysis long, exceeding the conductor extension posteriorly (Figs 42D–F, 44D–F, 46D–F), but *T. naso* and *T. embera* can be distinguished by the tegular pocket wide and rounded (Figs 42E, 44E), whereas *T. kuna* have it squared (Fig. 46E). Males of *T. naso* can be distinguished by the conductor apophysis distally acute, sharpening abruptly (Fig. 44D, F), whereas *T. embera* have the apophysis sharpening gradually (Fig. 42E–F).

Etymology

The specific name is a noun in apposition to honor the Naso native people of Panama, which derived from the union of two words, ‘na’ and ‘so’, that mean ‘life or water’ and ‘to be or to believe’, respectively, in the Naso Tjerdi language.

Type material

Holotype

PANAMA – **Chiriquí Province** • ♂; Parque Internacional La Amistad, Cerro Picacho, one-hectare PANCODING inventory; 8.890500° N, 82.618778° W; 2299 m a.s.l.; 12–17 Jun. 2008; M. Arnedo, L. Benavides, G. Hormiga, F. Labarque, L. Piacentini and M. Ramírez leg.; voucher code SAU1NDH032; DNA code thes6179; GenBank code PX096888; MIUP.

Paratypes

PANAMA – **Chiriquí Province** • 1 ♂; same data as for holotype; voucher code SAD1NGP019; preparation codes FML-00941, FML-00942; DNA barcode SPIPA322-10; MACN-Ar 29246 • 1 ♀; same data as for holotype; voucher code SAB1DER005; preparation code FML-00939; DNA barcode SPIPA326-10; MACN-Ar 29247 • 1 ♀; same data as for holotype; voucher code SAD1NGB029; preparation code FML-00728; DNA code thes6225; GenBank code PX096889; MACN-Ar 29248 • 1 ♂; same data as for holotype; voucher code SAD1DHP002; preparation code FML-00729; DNA code thes6226; GenBank code PX096892; CRBA • 1 ♀; same data as for holotype; voucher code SAC1DGB022; DNA barcode SPIPA325-10; MCZ • 1 ♀; same data as for holotype; voucher code SAU2NFA018; DNA barcode SPIPA323-10; MCZ.

Other material

PANAMA – **Chiriquí Province** • 1 ♀; same data as for holotype; voucher code SAD1NCR003; DNA barcode SPIPA324-10; MACN-Ar 29307 • 1 ♀; same data as for holotype; voucher code SAU1NDB029; DNA code thes6229; GenBank code PX096891; CRBA • 1 ♀; same data as for holotype; voucher code SAB1DDL017; DNA code thes6228; GenBank code PX096890; CRBA • 1 ♂, 10 ♀♀; same data as for holotype; MCZ • 1 ♂, 2 ♀♀; same data as for holotype; MIUP • 3 ♂♂, 13 ♀♀; same data as for holotype; MACN-Ar • 1 ♂, 10 ♀♀; same data as for holotype; CRBA.

Description

Male (paratypes MACN-Ar 29246, CRBA SAD1DHP002)

Total length 1.22. Prosoma: length 0.71, width 0.61, height 0.56. Sternum: length 0.35, width 0.35. Eye diameters and interdistances: AME 0.09, PME 0.07, AME–PME 0.10. Opisthosoma: length 0.83, width 0.72, height 0.56. Leg formula: 1243. Dorsal shield of prosoma yellowish-white laterally, dark olive-green centrally (Fig. 44A–B). Dorsum of ocular area dark olive-green (Fig. 44A–B). Sternum yellowish-white with dark olive-green borders and olive-green thick patches anteriorly (Fig. 44C). Opisthosoma olive-green posteriorly, lighter anteriorly, with wide guanine silver stripe centrally, open posteriorly, and dispersed silver guanine blotches anteriorly (Fig. 44A–B). Epiandrium, booklung cover, tracheal spiracle, anterior lateral spinnerets field and behind anal tubercle dark olive-green; other spinnerets orange (Fig. 44C). Legs I–II darker than III–IV, femora yellowish-white but I–II distally darker and II with proximal dark olive-green patch ventrally, patella yellow, tibiae and metatarsi orange but proximally and distally darker, and tarsi orange (Fig. 44A–C). Palp: paracymbium hooked, paracymbial process with setae row, tegulum striated with tegular spur wide, rounded, median apophysis elongated with median groove, conductor covering embolic division, conductor posterior extension lacking retrolateral projection, conductor apophysis relatively long, embolus laminated, multiple divided embolic apophysis, retrolateral branch filiform, sclerotized, elongated, protruding from beneath the conductor (Fig. 44D–F).

Female (paratype MACN-Ar 29247)

Total length 1.79. Prosoma: length 0.73, width 0.66, height 0.60. Sternum: length 0.37, width 0.38. Eye diameters and interdistances: AME 0.08, PME 0.07, AME–PME 0.10. Opisthosoma: length 1.47, width 1.42, height 1.15. Leg formula: 1243. Coloration darker than males (Fig. 45A–C). Epigynal plate olive-green (Fig. 45B–C). Epigynal plate: domed, dorsal-lateral spurs extending to midline, dorsal epigynal

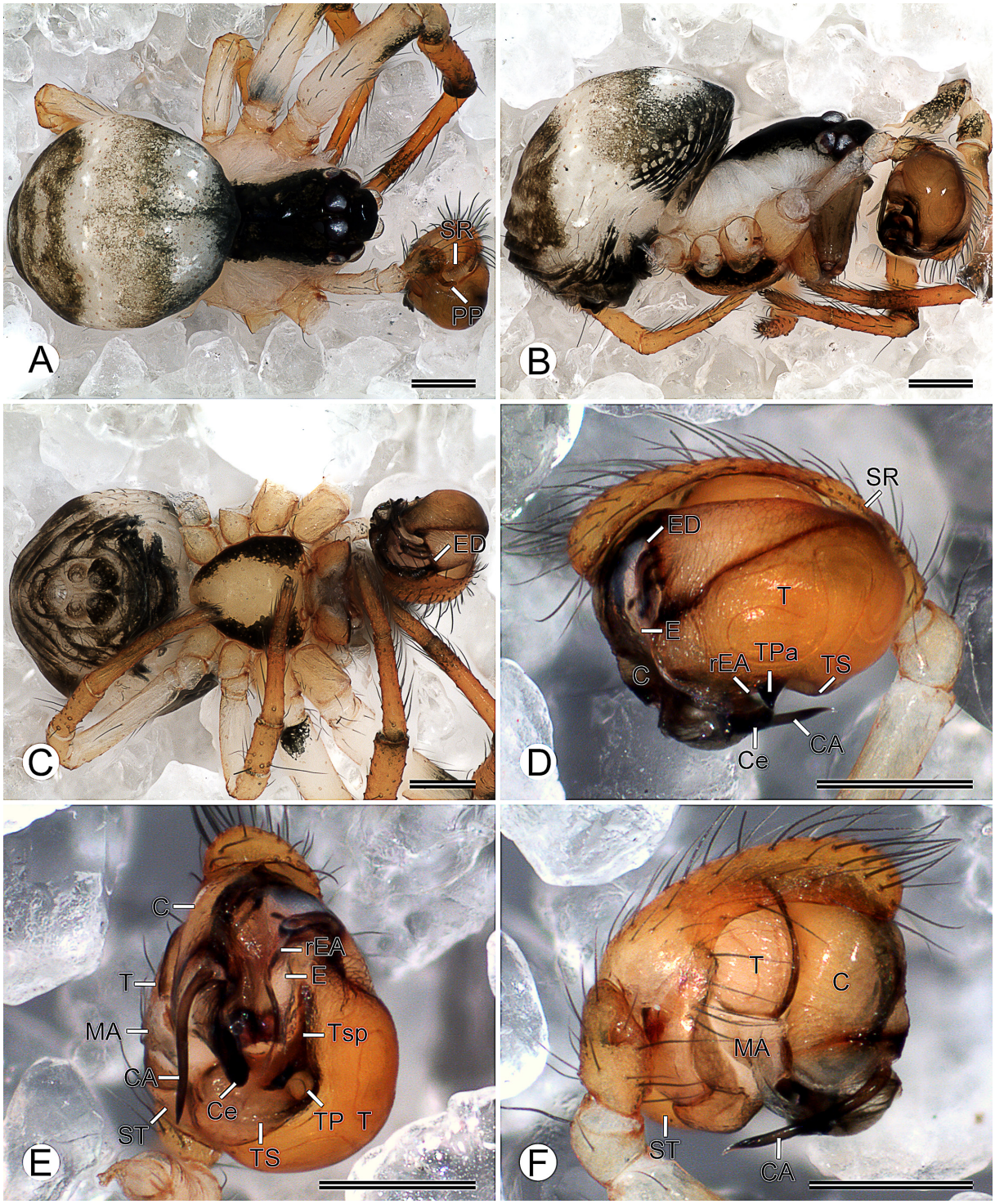

Fig. 44. *Tantra naso* gen. et sp. nov., paratypes, ♂♂. **A–C**. Habitus (MACN-Ar 29246) (A = dorsal view; B = lateral view; C = ventral view). **D–F**. Left palp (CRBA SAD1DHP002) (D = retrolateral view; E = ventral view; F = prolateral view). Abbreviations: C = conductor; CA = conductor apophysis; Ce = conductor posterior extension; E = embolus; ED = embolic division; MA = median apophysis; PP = paracymbial process; rEA = embolic apophysis retrolateral branch; SR = setae row; ST = subtegulum; T = tegulum; TP = tegular pocket; TPa = tegular pocket anterior side; TS = tegular striae; Tsp = tegular spur. Scale bars: 0.2 mm.

plate exposed (Fig. 45B–C). Vulva: convoluted copulatory ducts, proximal copulatory ducts with patch of gland ducts dorsally, distal copulatory ducts coiling dorso-ventrally and inserting ventromedially posteriorly into spermathecae, spermathecae round, sclerotized, and connate (i.e., fused along midline), fertilization ducts sclerotized, emerging laterally posteriorly from spermathecae, curving dorsally anteriorly to meet the uterus externus (Fig. 45D).

Records and biology

Records are limited to collections made at 2299 m a.s.l. in lower montane rainforest from Parque Internacional La Amistad (Fig. 1). Males and females have been collected mostly during the night by looking down and looking up, and less frequently also by beating and cryptic techniques.

Variation

Some females examined have a lighter coloration than the described specimens.

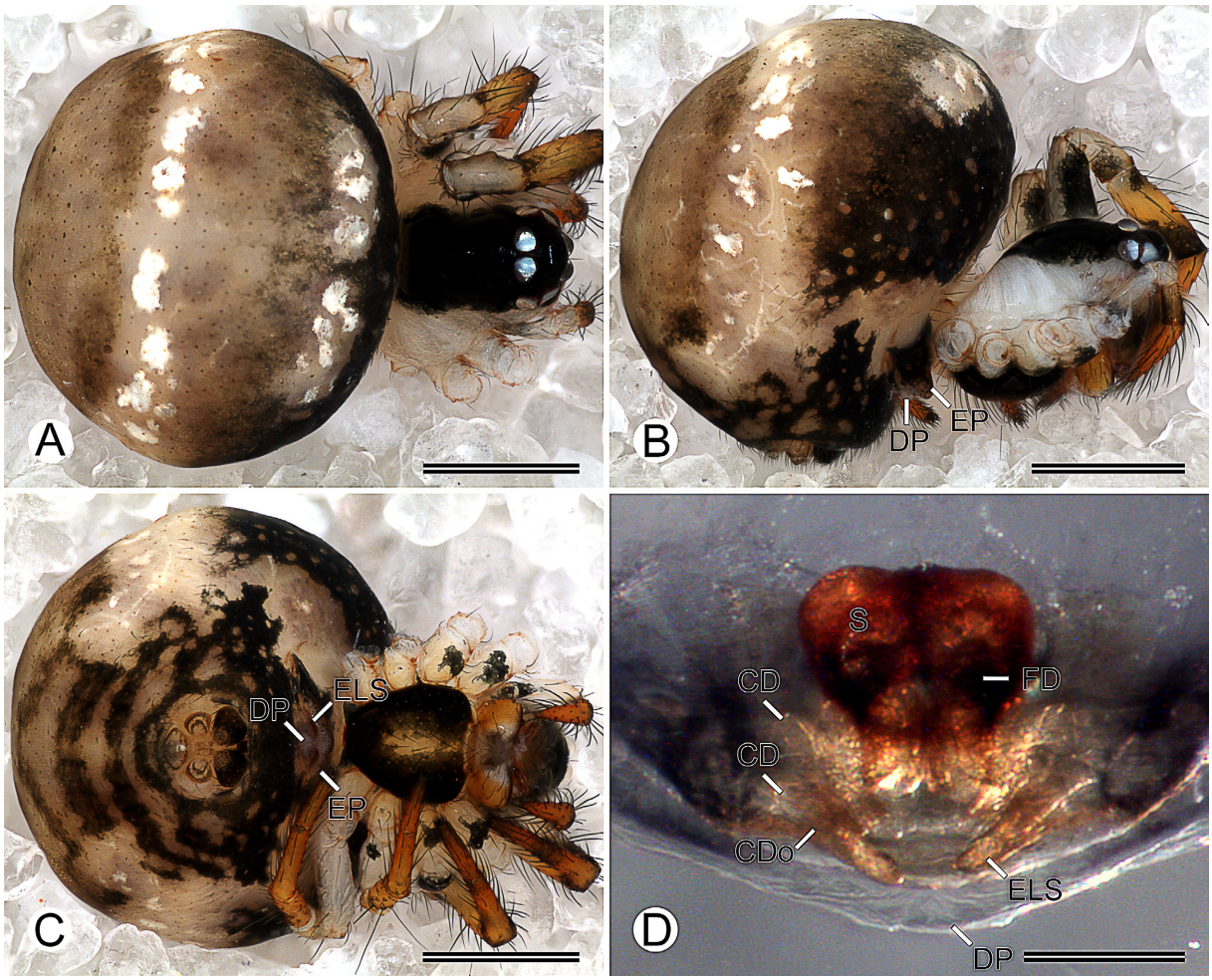

Fig. 45. *Tantra naso* gen. et sp. nov., paratype, ♀ (MACN-AR 29247). **A–C**. Habitus (A = dorsal view; B = lateral view; C = ventral view). **D**. Vulva, dorsal view. Abbreviations: CD = copulatory duct; CDo = copulatory duct opening; DP = epigynal dorsal plate; ELS = epigynal lateral spur; EP = epigynal plate; FD = fertilization duct; S = spermatheca. Scale bars: A–C = 0.5 mm; D = 0.1 mm.

Tantra kuna gen. et sp. nov.
urn:lsid:zoobank.org:act:B978B050-5D60-4564-B6E0-56F84C03AAF8
Figs 1, 46–47

Diagnosis

Males and females of *Tantra kuna* gen. et sp. nov. resemble those of *Tantra embera* gen. et sp. nov. and *Tantra naso* gen. et sp. nov. by the wide guanine silver stripe centrally (i.e., above the second pair of opisthosomal apodemes), open posteriorly (Figs 42A–B, 43A–B, 44A–B, 45A–B, 46A–B, 47A–B), but *T. kuna* can be distinguished by the two thick silver guanine patches anteriorly, connected to the silver stripe (Figs 46A–B, 47A–B), whereas *T. embera* and *T. naso* have dispersed silver guanine blotches anteriorly, not forming discrete patches (Figs 42A–B, 43A–B, 44A–B, 45A–B). Males of *T. kuna* also resemble those of *T. embera* and *T. naso* and by the tegular pocket wide and rounded, the conductor extension lacking a retrolateral projection, and the conductor apophysis long, exceeding the conductor extension posteriorly (Figs 42D–F, 44D–F, 46D–F), but *T. kuna* can be distinguished by the tegular pocket squared (Fig. 46E), whereas *T. embera* and *T. naso* have it wide and rounded (Figs 42E, 44E).

Etymology

The specific name is a noun in apposition to honor the Kuna native people of Panama, which derived from 'dule' or 'tule' that means 'person' in the Kuna language.

Type material

Holotype

PANAMA – **Chiriquí Province** • ♂; Reserva Forestal Fortuna, Quebrada Honda, one-hectare PANCODING inventory; 8.750083° N, 82.239083° W; 1135 m a.s.l.; 7–12 Jun. 2007; M. Arnedo, D. Dimitrov, G. Hormiga, F. Labarque and M. Ramírez leg.; voucher code SFD1NAH037; DNA barcode SPIPA121-10; MIUP.

Paratypes

PANAMA – **Chiriquí Province** • 1 ♂; same data as for holotype; voucher code SFC2DCD016; preparation codes FML-00711, LNP-00257; DNA code thes5122; GenBank code PX096904; MACN-Ar 29075 • 1 ♀; same data as for holotype; voucher code SFC1DBD011; preparation codes FML-00742, LNP-00265; DNA code thes5066; GenBank code PX096903; MACN-Ar 29073 • 1 ♀; same data as for holotype; voucher code SFD1NBH019; preparation code FML-00894; DNA barcode SPIPA339-10; MIUP • 1 ♀; same data as for holotype; voucher code SFD1NBH034; preparation code FML-00965; DNA barcode SPIPA122-10; MACN-Ar 29074.

Other material

PANAMA – **Chiriquí Province** • 1 ♂; same data as for holotype; voucher code SFD1D8H025; DNA barcode SPIPA337-10; MCZ • 1 ♀; same data as for holotype; voucher code SFD1DAL020; DNA code thes5262; GenBank code PX096907; MCZ • 1 ♀; same data as for holotype; voucher code SFD1NAH022; DNA barcode SPIPA338-10; MACN-Ar 29072 • 1 ♂; same data as for holotype; voucher code SFU2NAA014; DNA code thes5261; GenBank code PX096906; CRBA • 1 ♀; same data as for holotype; voucher code SFU2NAH042; DNA code thes5260; GenBank code PX096905; CRBA.

Description

Male (paratype MACN-Ar 29075)

Total length 1.03. Prosoma: length 0.65, width 0.48, height 0.50. Sternum: length 0.32, width 0.35. Eye diameters and interdistances: AME 0.09, PME 0.07, AME–PME 0.07. Opisthosoma: length 0.71, width 0.59, height 0.48. Leg formula: 1243. Dorsal shield of prosoma white, cephalic area with olive-

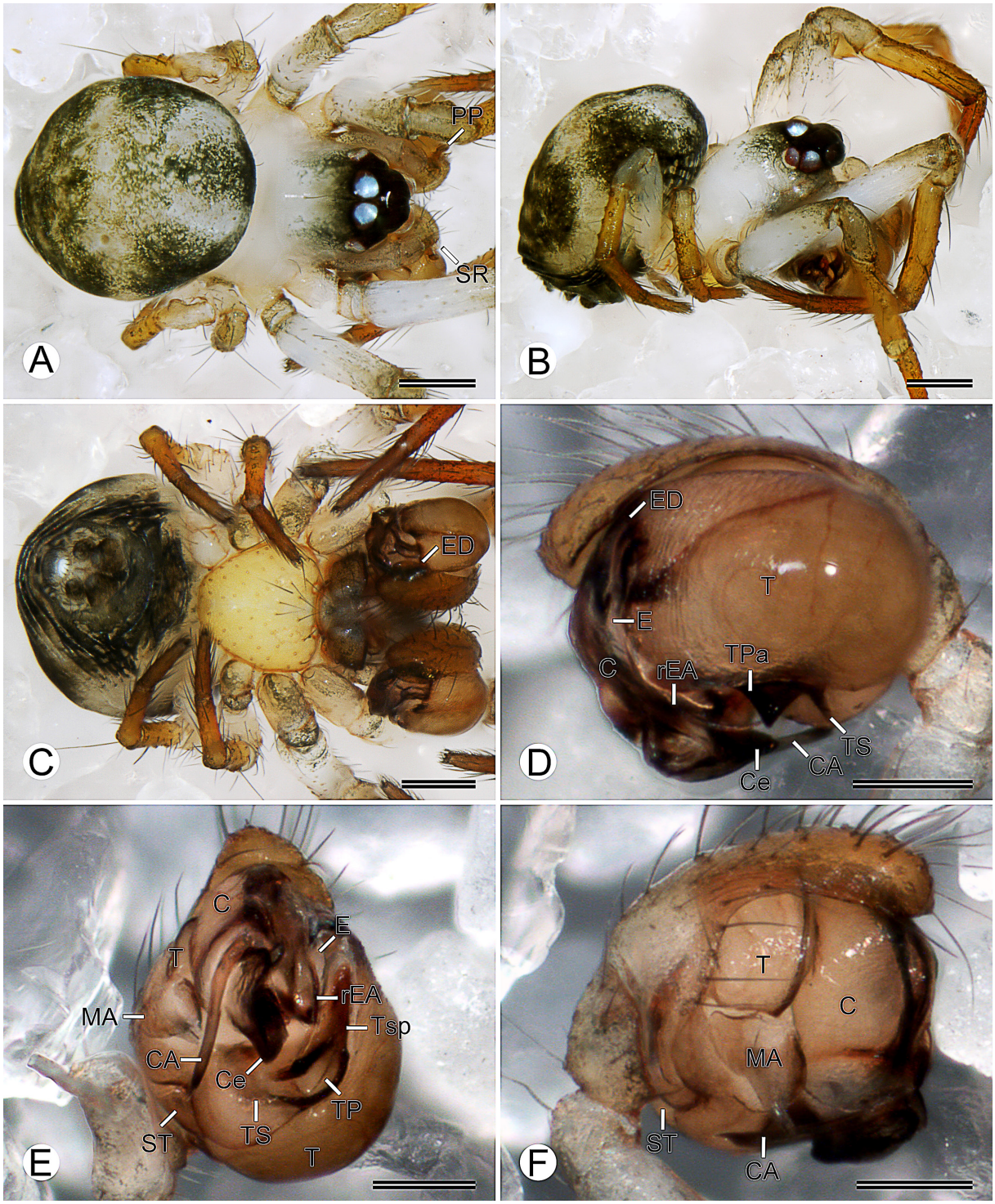

Fig. 46. *Tantra kuna* gen. et sp. nov., paratype, ♂ (MACN-Ar 29075). **A–C**. Habitus (A = dorsal view; B = lateral view; C = ventral view). **D–F**. Left palp (D = retrolateral view; E = ventral view; F = prolateral view). Abbreviations: C = conductor; CA = conductor apophysis; Ce = conductor posterior extension; E = embolus; ED = embolic division; MA = median apophysis; PP = paracymbial process; rEA = embolic apophysis retrolateral branch; SR = setae row; ST = subtegulum; T = tegulum; TP = tegular pocket; TPa = tegular pocket anterior side; TS = tegular striae; Tsp = tegular spur. Scale bars: A–C = 0.2 mm; D–F = 0.1 mm.

green speckled lines (Fig. 46A–B). Dorsum of ocular area dark olive-green (Fig. 46A–B). Sternum yellow (Fig. 46C). Opisthosoma color overall dark olive-green, with wide guanine silver stripe centrally, open posteriorly, connected to two thick silver guanine patches anteriorly (Fig. 46A–B). Epiandrium, booklung cover, tracheal spiracle, spinneret field and behind anal tubercle dark olive-green (Fig. 46C). Femora white but olive-green distally, patella olive-green, tibiae, metatarsi and tarsi orange (Fig. 46A–C). Palp: paracymbium hooked, paracymbial process with setae row, tegulum striated with tegular spur elongated, acute, median apophysis elongated with median groove, conductor covering embolic division, conductor posterior extension lacking retrolateral projection, conductor apophysis relatively long, embolus laminated, multiple divided embolic apophysis, retrolateral branch filiform, sclerotized, elongated, protruding from beneath conductor (Fig. 46D–F).

Female (paratypes MACN-Ar 29074, MACN-Ar 29073, MIUP SFD1NBH019)
Total length 1.62. Prosoma: length 0.71, width 0.59, height 0.55. Sternum: length 0.33, width 0.35. Eye diameters and interdistances: AME 0.09, PME 0.07, AME–PME 0.08. Opisthosoma: length 1.23, width 1.14, height 0.92. Leg formula: 1243. Coloration as in male but cephalic area of the prosoma olive-green

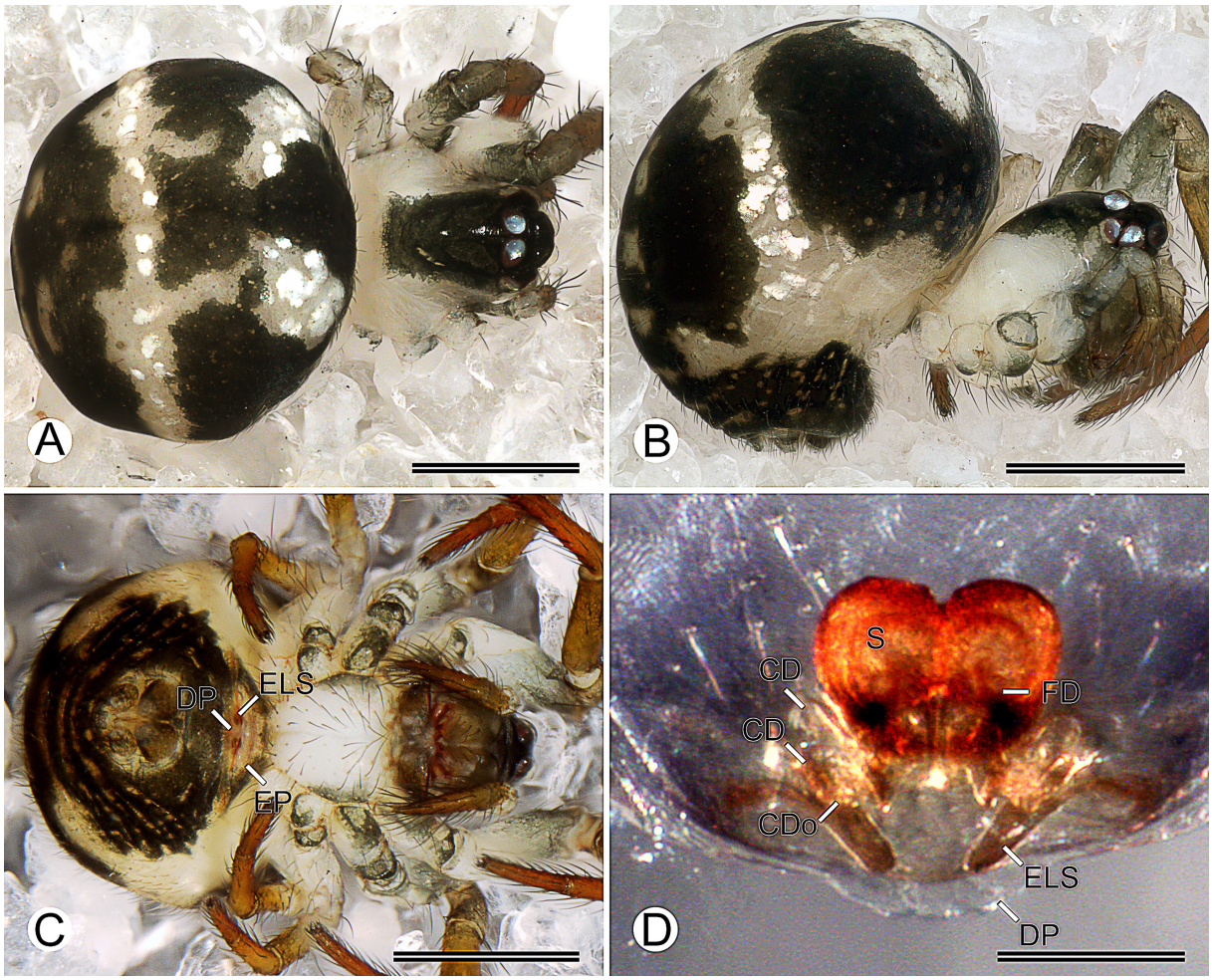

Fig. 47. *Tantra kuna* gen. et sp. nov., paratypes, ♀♀ (A–B: MACN-Ar 29074; C: MACN-Ar 29073; D: MIUP: SFD1NBH019). **A–C**. Habitus (A = dorsal view; B = lateral view; C = ventral view). **D**. Vulva, dorsal view. Abbreviations: CD = copulatory duct; CDo = copulatory duct opening; DP = epigynal dorsal plate; ELS = epigynal lateral spur; EP = epigynal plate; FD = fertilization duct; S = spermatheca. Scale bars: A–C = 0.5 mm; D = 0.1 mm.

and sternum white with olive-green borders (Fig. 47A–C). Epigynal plate whitish-orange (Fig. 47C). Epigynal plate: domed, dorsal-lateral spurs extending to midline, dorsal epigynal plate exposed (Fig. 47C). Vulva: convoluted copulatory ducts, proximal copulatory ducts with patch of gland ducts dorsally, distal copulatory ducts coiling dorso-ventrally and inserting ventromedially posteriorly into spermathecae, spermathecae round, sclerotized, and connate (i.e., fused along the midline), fertilization ducts sclerotized, emerging laterally posteriorly from spermathecae, curving dorsally anteriorly to meet uterus externus (Fig. 47D).

Records and biology

Records are limited to collections made at 1135 m a.s.l. in premontane rainforest from Reserva Forestal Fortuna (Fig. 1). Males and females have been collected during the day and night mostly by looking down, and less frequently also by looking up and cryptic techniques.

Variation

Some females examined have darker coloration than the described specimens.

Tantra sichid gen. et sp. nov.
urn:lsid:zoobank.org:act:943B599C-7045-4D4C-B61F-F94A2184221F
Figs 1, 48

Diagnosis

Females of *Tantra sichid* gen. et sp. nov. can be distinguished from those of other species of *Tantra* by the opisthosoma coloration overall dark olive-green, posteriorly lighter, with two round silver guanine patches ventrally (Fig. 48A–C).

Etymology

The specific name is derived from ‘sichid’ which means ‘black’ in the Kuna language, currently spoken by the Kuna native people of Panama, and refers to the overall dark coloration of this species.

Type material

Holotype

PANAMA – **Chiriquí Province** • ♀; Parque Internacional La Amistad, Sendero Retoño; 8.893833° N, 82.615083° W; 2240 m a.s.l.; 10–11 Jun. 2008; F. Labarque and M. Ramirez leg.; non-quantitative sample; voucher code SANQB8L020; preparation code FML-00960, FML-00961; MIUP.

Description

Female (holotype MIUP SANQB8L020)

Total length 2.33. Prosoma: length 0.98, width 0.69, height 0.71. Sternum: length 0.37, width 0.41. Eye diameters and interdistances: AME 0.07, PME 0.07, AME–PME 0.08. Opisthosoma: length 1.62, width 1.58, height 1.44. Leg formula: 1243. Dorsal shield of prosoma yellowish-white laterally, dark centrally, covering almost all of thoracic area (Fig. 48A–B). Dorsum of ocular area dark (Fig. 48A–B). Sternum olive-green with dark borders (Fig. 48C). Opisthosoma dark gray anteriorly, lighter posteriorly, with two round silver guanine patches ventrally (Fig. 48A–C). Epigynal plate, booklung cover, tracheal spiracle, and behind anal tubercle dark gray; spinneret field olive-green (Fig. 48B–C). Femora olive-green but distally darker, patella yellowish-orange, tibiae, metatarsi and tarsi orange (Fig. 48A–C). Epigynal plate: domed, dorsal-lateral spurs extending to midline, dorsal epigynal plate exposed (Fig. 48B–C). Vulva: convoluted copulatory ducts, proximal copulatory ducts with patch of gland ducts dorsally, distal copulatory ducts coiling dorso-ventrally and inserting ventromedially posteriorly into

spermathecae, spermathecae round, sclerotized, and connate (i.e., fused along the midline), fertilization ducts sclerotized, emerging laterally posteriorly from spermathecae, curving dorsally anteriorly to meet the uterus externus (Fig. 48D).

Male

Unknown.

Records and biology

Records are limited to collections made at 2240 m a.s.l. in the lower montane rainforest of Parque Internacional La Amistad (Fig. 1).

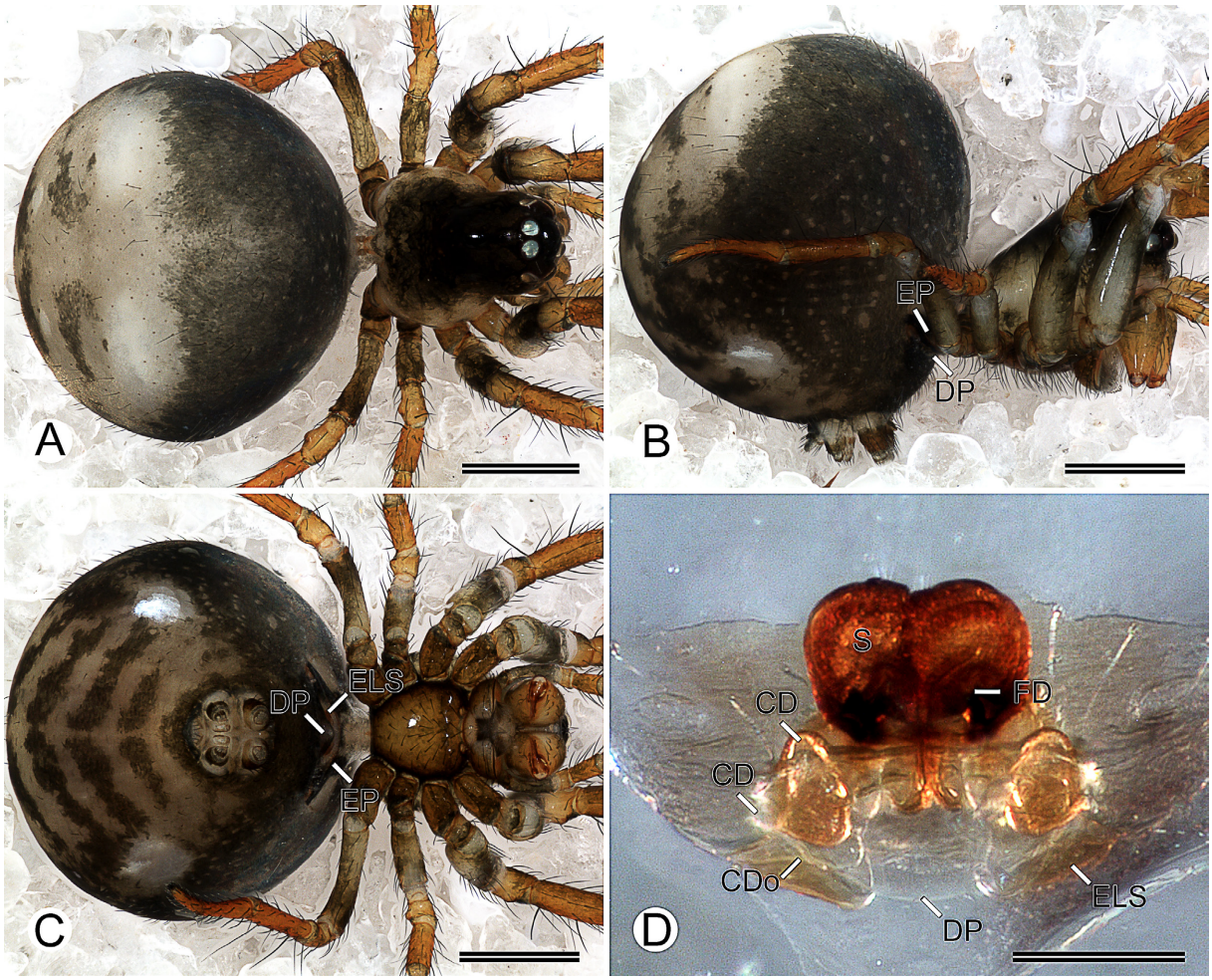

Fig. 48. *Tantra sichid* gen. et sp. nov., holotype, ♀ (MIUP SANQB8L020). **A–C**. Habitus (A = dorsal view; B = lateral view; C = ventral view). **D**. Vulva, dorsal view. Abbreviations: CD = copulatory duct; CDo = copulatory duct opening; DP = epigynal dorsal plate; ELS = epigynal lateral spur; EP = epigynal plate; FD = fertilization duct; S = spermatheca. Scale bars: A–C = 0.5 mm; D = 0.1 mm.

Baalzebub Coddington, 1986

Baalzebub Coddington, 1986: 71. Type species *Baalzebub baubo* Coddington, 1986:72.

Diagnosis

Males of *Baalzebub* can be distinguished from those of other theridiosomatid genera by the massive retrolateral tegulum (i.e., almost half the size of the bulb) extending posteriorly (Figs 49E, 51E, 53E, 55E, 58E; see also Coddington 1986) (in contrast with extending retrolateraly in Epeirotypinae, and no massive tegulum in most genera), and a deep trough (i.e., cleft) in the median apophysis (absent in other genera), forming a posterior serrated border and an anterior acute border (Figs 49E, 51E, 53E, 55E, 58E; see also Coddington 1986). Females of *Baalzebub* can be distinguished from those of other genera by the backward-pointed triangular epigynal plate (i.e., not a scape) with a deep central pit (Figs 50D, 52D, 54D, 56D, 57D; see also Coddington 1986) (absent in other genera), and the distally connated spermathecae (Figs 50D, 52D, 54D, 56D, 57D; see also Coddington 1986) (in contrast with separated or fully connated spermathecae in other genera).

Description

Males and females of *Baalzebub* may have the first tibiae curved (i.e., sinuated) and prolateral rows of strong macrosetae on the first metatarsi (Figs 50B, 52B, 55C). Females of *Baalzebub* have irregular membranous copulatory ducts that insert ventromedially posteriorly into the spermathecae (Figs 50D, 52D, 54D, 56D, 57D). For genus description and further details, see Coddington (1986) and Labarque & Griswold (2014).

Baalzebub innatuledi sp. nov.

urn:lsid:zoobank.org:act:F96D4B68-591E-4C1E-B4F1-D9131A74804C

Figs 1, 49–50

Diagnosis

Males and females of *Baalzebub innatuledi* sp. nov. also resemble those of *Baalzebub sukia* sp. nov. by the overall dark coloration (Figs 49A–C, 50A–C, 51A–C, 52A–C), but *B. innatuledi* can be distinguished by three pairs of round guanine silver patches centrally on the dorsum of the opisthosoma (Figs 49A–C, 50A–C), whereas *B. sukia* have one pair (i.e., above the second pair of opisthosomal apodemes) (Figs 51A–C, 52A–C). Females of *B. innatuledi* resemble those of *B. sukia* by the subtriangular spermathecae (i.e., forming a square angle laterally), connated distally, forming a straight line anteriorly (Figs 50D, 52D), but *B. innatuledi* can be distinguished by the backward-pointed triangular epigynal plate posteriorly wide (Fig. 50C–D), whereas *B. sukia* have it acuter (Fig. 52C–D).

Etymology

The specific name is derived from ‘innatuledi’ which indicates the person specialized in the study of plants and rocks in the Kuna language, currently spoken by the Kuna native people of Panama.

Type material

Holotype

PANAMA – **Chiriquí Province** • ♂; Parque Internacional La Amistad, Cerro Picacho, one-hectare PANCODING inventory; 8.890500° N, 82.618778° W; 2299 m a.s.l.; 12–17 Jun. 2008; M. Arnedo, L. Benavides, G. Hormiga, F. Labarque, L. Piacentini and M. Ramírez leg.; voucher code SAD1NGB023; DNA code baaba258; GenBank code PX096881; MIUP.

Paratypes

PANAMA – **Chiriquí Province** • 1 ♂; same data as for holotype; voucher code SAD1NGA015; preparation codes FML-00718, LNP-00541; DNA code baaba104; GenBank code PX096878; MACN-Ar 28998 • 1 ♀; same data as for holotype; voucher code SAC1NDA004; preparation code FML-00738; DNA code baaba257; GenBank code PX096880; MACN-Ar 28997 • 1 ♀; same data as for holotype; voucher code SAD1NFL017; preparation code FML-00898; MCZ.

Other material

PANAMA – **Chiriquí Province** • 1 ♂; same data as for holotype; voucher code SAD1NHL025; DNA code baaba256; GenBank code PX096879; MCZ • 1 ♀; same data as for holotype; voucher code SAC1DER002; DNA barcode SPIPA422-10; MIUP • 1 ♀; same data as for holotype; voucher code SAC2NDB010; DNA barcode SPIPA423-10; CRBA • 1 ♂; same data as for holotype CRBA.

Description

Male (paratype MACN-Ar 28998)

Total length 1.25. Prosoma: length 0.68, width 0.61, height 0.55. Sternum: length 0.33, width 0.35. Eye diameters and interdistances: AME 0.09, PME 0.07, AME–PME 0.07. Opisthosoma: length 0.90, width 0.81, height 0.67. Leg formula: 1243. Dorsal shield of prosoma dark (Fig. 49A–B). Dorsum of the ocular area dark (Fig. 49A–B). Sternum dark olive-green (Fig. 49C). Opisthosoma color overall dark gray, with three dorsal pairs of round guanine silver patches laterally, first pair above the second pair of opisthosomal apodemes, second pair smaller (Fig. 49A–B). Epiandrium, booklung cover, tracheal spiracle, and behind the anal tubercle dark gray; anterior lateral spinnerets field olive-green, other spinnerets orange (Fig. 49C). Femora and patella greenish-yellow with olive-green speckles, tibiae orange but distally olive-green, metatarsi and tarsi orange (Fig. 49A–C). Palp: paracymbium hooked, paracymbial process with setae row, median apophysis with a deep trough, conductor covering the embolic division, embolus laminated, multiple divided embolic apophysis (Fig. 49D–F).

Female (paratype MACN-Ar 28997)

Total length 1.33. Prosoma: length 0.60, width 0.53, height 0.49. Sternum: length 0.31, width 0.32. Eye diameters and interdistances: AME 0.08, PME 0.07, AME–PME 0.08. Opisthosoma: length 0.89, width 0.80, height 0.77. Leg formula: 1243. Coloration as in male, but sternum with dark borders (Fig. 50A–C). Epigynal plate whitish-orange (Fig. 50B–C), triangular, backward-pointed, central pit deep (Fig. 50C–D). Vulva: copulatory ducts irregular and membranous, inserting ventromedially posteriorly into spermathecae, subtriangular spermathecae, sclerotized, and connated distally, forming straight line anteriorly, fertilization ducts sclerotized, emerging laterally posteriorly from spermathecae, curving dorsally anteriorly to meet uterus externus (Fig. 50D).

Records and biology

Records are limited to collections made at 2299 m a.s.l. in lower montane rainforest from Parque Internacional La Amistad (Fig. 1). Males and females have been collected mostly during the night by looking down, and less frequently females were also collected at daytime by cryptic technique.

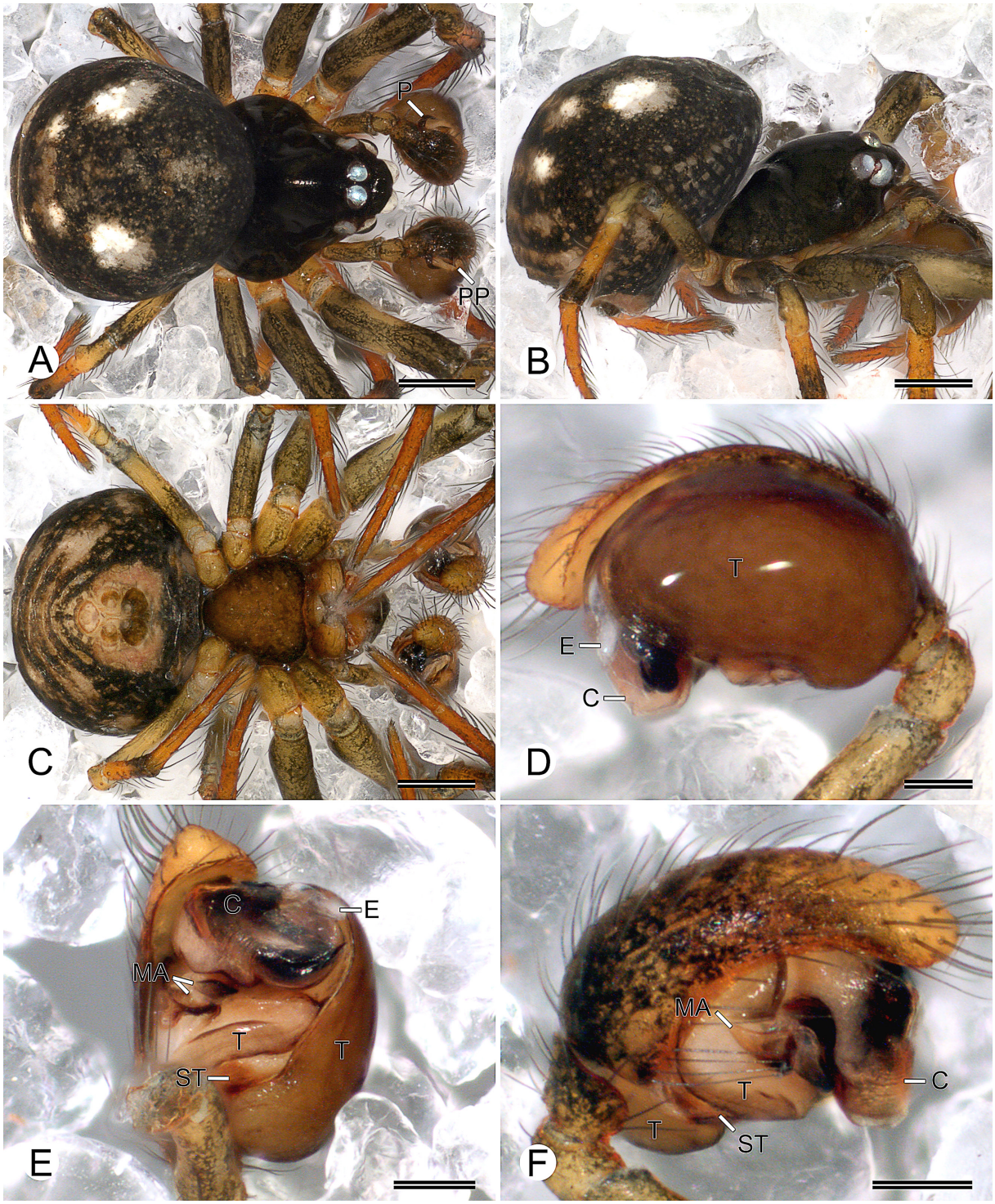

Fig. 49. *Baalzebub innatuledi* sp. nov., paratype, ♂ (MACN-Ar 28998). **A–C**. Habitus (A = dorsal view; B = lateral view; C = ventral view). **D–F**. Left palp (D = retrolateral view; E = ventral view; F = prolateral view). Abbreviations: C = conductor; E = embolus; MA = median apophysis; P = paracymbium; PP = paracymbial process; ST = subtegulum; T = tegulum. Scale bars: A–C = 0.25 mm; D–F = 0.1 mm.

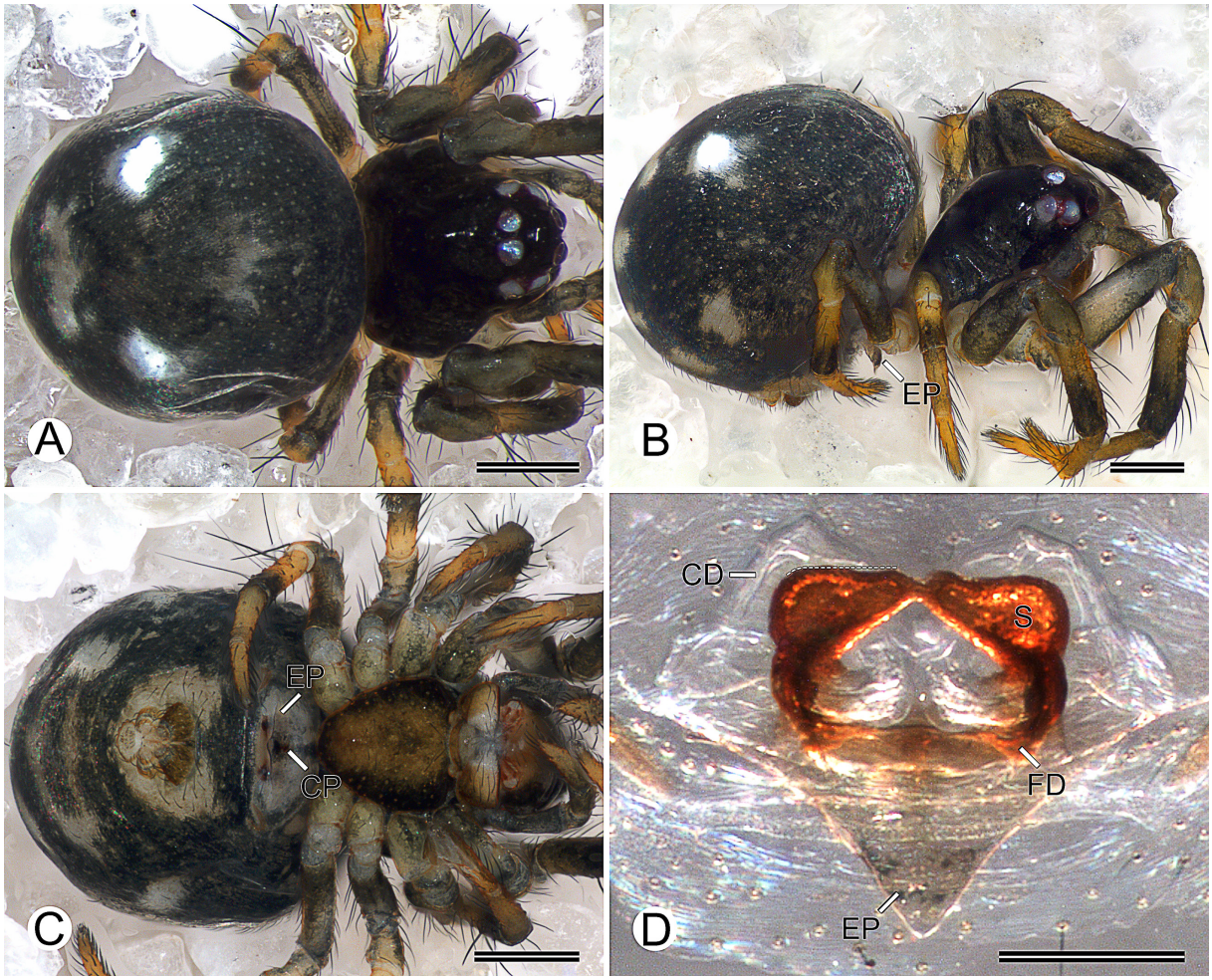

Fig. 50. *Baalzebub innatuledi* sp. nov., paratype, ♀ (MACN-Ar 28997). **A–C**. Habitus (A = dorsal view; B = lateral view; C = ventral view). **D**. Vulva, dorsal (note the profile of the straight subtriangular spermathecae). Abbreviations: CD = copulatory duct; CP = central pit; EP = epigynal plate; FD = fertilization duct; S = spermatheca. Scale bars: A, C = 0.25 mm; B = 0.2 mm; D = 0.1 mm.

Baalzebub sukia sp. nov.
urn:lsid:zoobank.org:act:A30E74E7-A9B7-4F33-B7B2-30AD228CCBE6
Figs 1, 51–52

Diagnosis

Males and females of *Baalzebub sukia* sp. nov. also resemble those of *Baalzebub innatuledi* sp. nov. by the overall dark coloration (Figs 49A–C, 50A–C, 51A–C, 52A–C), but *B. sukia* can be distinguished by one pair of round guanine silver patches centrally on the dorsum of the opisthosoma (i.e., above the second pair of opisthosomal apodemes) (Figs 51A–B, 52A–B), whereas *B. innatuledi* have three pairs (Figs 49A–B, 50A–B). Females of *B. sukia* resemble those of *B. innatuledi* by the subtriangular spermathecae (i.e., forming a square angle laterally), connated distally, forming a straight line anteriorly (Figs 50D, 52D), but *B. sukia* can be distinguished by the backward-pointed triangular epigynal plate posteriorly acute (Fig. 52C–D), whereas *B. innatuledi* have it wider (Fig. 50C–D).

Etymology

The specific name is derived from the word ‘sukia’ which means ‘shaman’ in the Naso, Ngäbe and Buglé languages.

Type material

Holotype

PANAMA – **Chiriquí Province** • ♂; Parque Internacional La Amistad, Cerro Picacho, one-hectare PANCODING inventory; 8.890500° N, 82.618778° W; 2299 m a.s.l.; 12–17 Jun. 2008; M. Arnedo, L. Benavides, G. Hormiga, F. Labarque, L. Piacentini and M. Ramírez leg.; voucher code SAD1NHL020; DNA barcode SPIPA421-10; MIUP.

Paratypes

PANAMA – **Chiriquí Province** • 1 ♂; same data as for holotype; voucher code SAU1NCH032; preparation codes FML-00839, FML-00899; DNA barcode SPIPA425-10; MACN-Ar 29071 • 1 ♀; same data as for holotype; voucher code SAC1DGH006; preparation code FML-00900; MACN-Ar 29070 • 1 ♀; same data as for holotype; voucher code SAC1DFB011; preparation code FML-00736; DNA code baaba254; GenBank code PX096882; MCZ • 1 ♂; same data as for holotype; voucher code SAU1NGH020; DNA barcode SPIPA424-10; MCZ.

Other material

PANAMA – **Chiriquí Province** • 1 ♀; same data as for holotype; MCZ • 2 ♀♀; same data as for holotype; CRBA.

Description

Male (paratypes MACN-Ar 29071, MCZ SAC1DFB011)

Total length 1.53. Prosoma: length 0.86, width 0.72, height 0.72. Sternum: length 0.40, width 0.43. Eye diameters and interdistances: AME 0.07, PME 0.07, AME–PME 0.08. Opisthosoma: length 1.20, width 0.99, height 0.89. Leg formula: 1243. Dorsal shield of prosoma dark (Fig. 51A–B). Dorsum of the ocular area dark (Fig. 51A–B). Sternum dark olive-green (Fig. 51C). Opisthosoma color overall dark gray with three dorsal whitish-gray patches centrally, and second patch with one pair of round guanine silver patches laterally (Fig. 51A–B). Epiandrium, booklung cover, tracheal spiracle, spinneret field and behind anal tubercle dark gray (Fig. 51C). Femora greenish-yellow but distally olive-green, patella olive-green, tibiae, metatarsi and tarsi brownish-orange (Fig. 51A–C). Palp: paracymbium hooked, paracymbial process with setae row, median apophysis with deep trough, conductor covering embolic division, embolus laminated, multiple divided embolic apophysis (Fig. 51D–F).

Female (paratype MACN-Ar 29070)

Total length 1.98. Prosoma: length 0.77, width 0.64, height 0.54. Sternum: length 0.35, width 0.37. Eye diameters and interdistances: AME 0.07, PME 0.07, AME–PME 0.06. Opisthosoma: length 1.49, width 1.29, height 1.39. Leg formula: 1243. Coloration as in male (Fig. 52A–C). Epigynal plate: triangular, backward-pointed, central pit deep (Fig. 52C–D). Vulva: copulatory ducts irregular and membranous, inserting ventromedially posteriorly into spermathecae, subtriangular spermathecae, sclerotized, and connated distally, forming straight line anteriorly, fertilization ducts sclerotized, emerging laterally posteriorly from spermathecae, curving dorsally anteriorly to meet uterus externus (Fig. 52D).

Records and biology

Records are limited to collections made at 2299 m a.s.l. in lower montane rainforest from Parque Internacional La Amistad (Fig. 1). Females have been collected mostly during the day by looking down and cryptic techniques; males have been collected during the night by looking down and looking up.

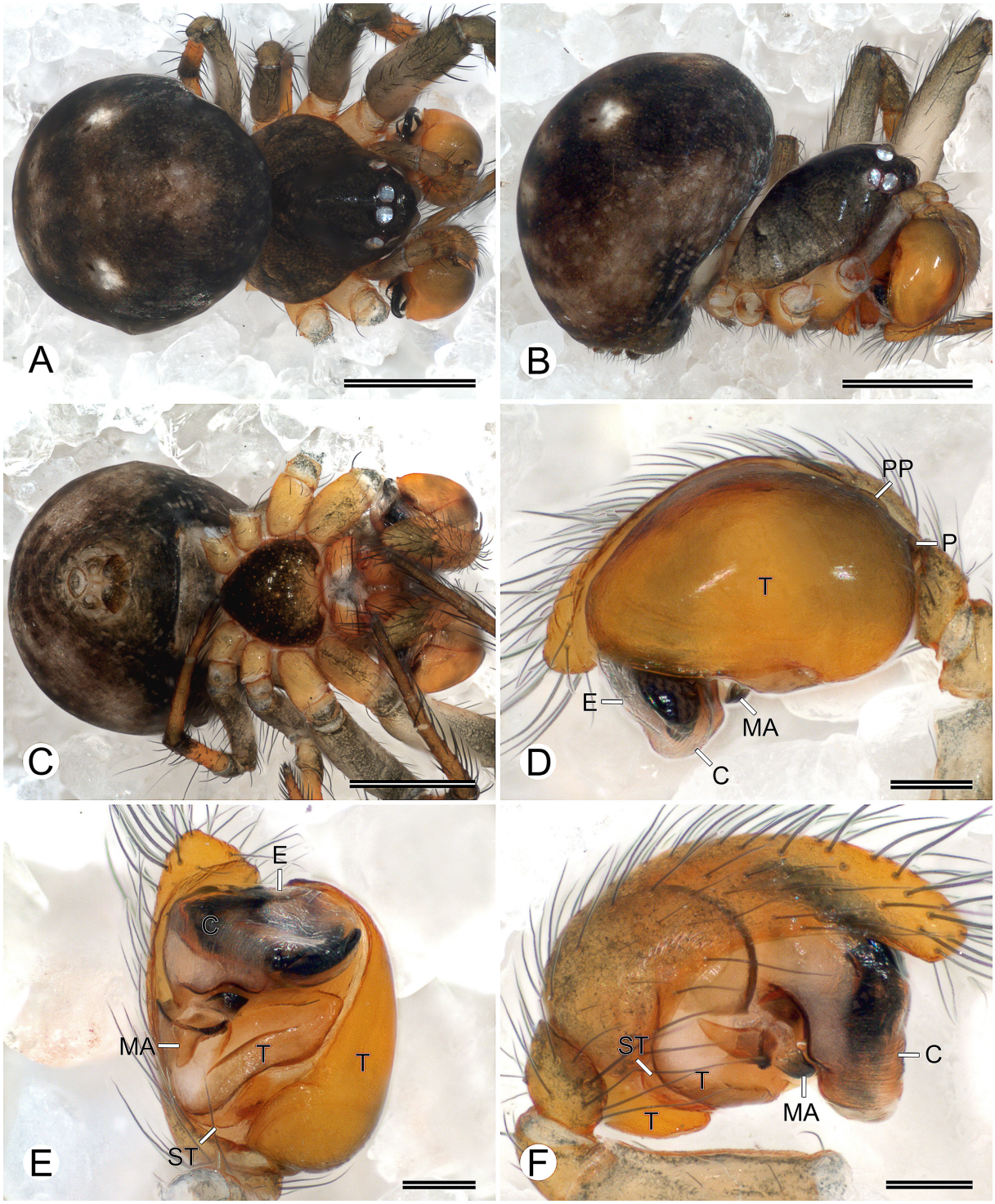

Fig. 51. *Baalzebub sukia* sp. nov., paratype, ♂ (MACN-Ar 29071). **A–C**. Habitus (A = dorsal view; B = lateral view; C = ventral view). **D–F**. Left palp (D = retrolateral view; E = ventral view; F = prolateral view). Abbreviations: C = conductor; E = embolus; MA = median apophysis; P = paracymbium; PP = paracymbial process; ST = subtegulum; T = tegulum. Scale bars: A–C = 0.5 mm; D–F = 0.1 mm.

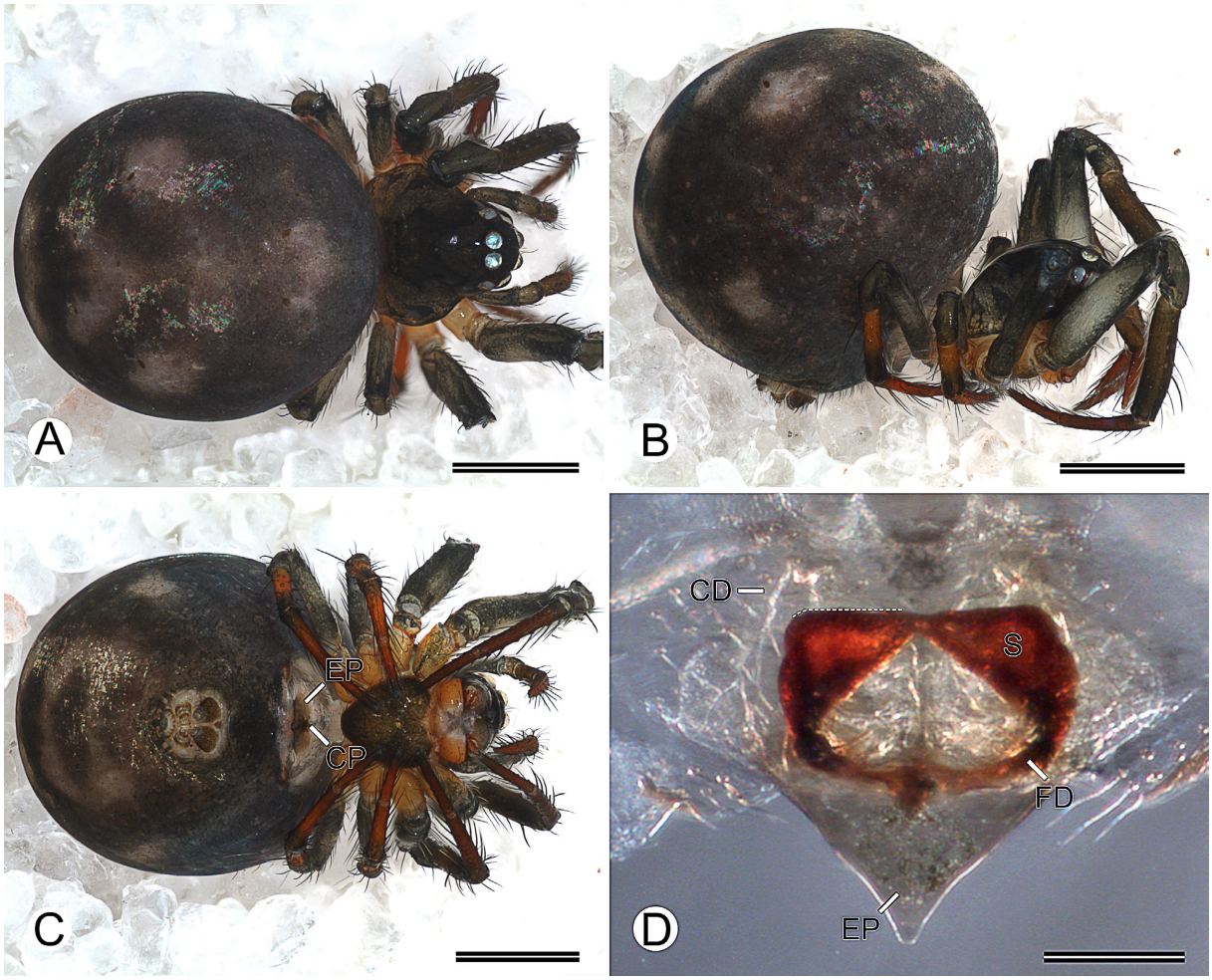

Fig. 52. *Baalzebub sukia* sp. nov., paratypes, ♀♀ (A–C: MACN-Ar 29070; D: MCZ SAC1DFB011). **A–C**. Habitus (A = dorsal view; B = lateral view; C = ventral view). **D**. Vulva, dorsal (note the profile of the straight subtriangular spermathecae). Abbreviations: CD = copulatory duct; CP = central pit; EP = epigynal plate; FD = fertilization duct; S = spermatheca. Scale bars: A–C = 0.5 mm; D = 0.1 mm.

Baalzebub jaibana sp. nov.
urn:lsid:zoobank.org:act:6ED8C145-687E-4976-9BD7-F21397F63188
Figs 1, 53–54

Diagnosis

Males and females of *Baalzebub jaibana* sp. nov. resemble the males of *Baalzebub antomia* sp. nov. by the overall light coloration (Figs 53A–C, 54A–C, 55A–C), but *B. jaibana* can be distinguished by one dorsal pair of round guanine silver patches centrally on the opisthosoma (Figs 53A–B, 54A–B), whereas *B. antomia* have it smooth (i.e., no pattern) (Fig. 55A–B). Males of *B. jaibana* can be distinguished by the retrolateral massive tegulum smooth (i.e., no spicules) and the base of the posterior serrated border of the median apophysis longer than wide (Fig. 53D–E), whereas *B. antomia* have several rows of spicules on the tegulum (i.e., see arrows in figure) and a wider than long posterior border of the median apophysis (Fig. 55D–E). Despite the overall coloration, females of *B. jaibana* resemble those of *Baalzebub absoguedi* sp. nov. by the suboval spermathecae (i.e., rounded laterally), connated distally,

forming a curved line anteriorly, and by the backward-pointed triangular epigynal plate anteriorly wide (i.e., wider than the sclerotized vulva) (Figs 54D, 56D). Females of *B. jaibana* can be distinguished by backward-pointed plate not projecting posteriorly (i.e., not exceeding the triangular shape) (Fig. 54D), whereas *B. absoguedi* have it projected (i.e., exceeding the triangular shape) (Fig. 56D).

Etymology

The specific name is derived from 'jaibana' which means 'shaman', the one that contacts the spirits in the Emberá language, currently spoken by the Emberá native people of Panama.

Type material

Holotype

PANAMA – **Panama Province** • ♂; Parque Nacional Altos de Campana, one-hectare PANCODING inventory; 8.683444° N, 79.929833° W; 895 m a.s.l.; 14–19 Jun. 2007; M. Arnedo, D. Dimitrov, G. Hormiga, F. Labarque and M. Ramírez leg.; voucher code SCD2NGL023; DNA barcode SPIPA417-10; MIUP.

Paratypes

PANAMA – **Panama Province** • 1 ♂; same data as for holotype; voucher code SCU1NEH011; preparation codes FML-00716, LNP-00287; DNA code baas1108; GenBank code PX096987; MACN-Ar 29059 • 1 ♀; same data as for holotype; voucher code SCD2NGL022; preparation code FML-00737; DNA code baaba253; GenBank code PX096986; MCZ • 1 ♀; same data as for holotype; voucher code SCU1NHR026; preparation code LNP-00284; DNA code baas1116; GenBank code PX096988; MACN-Ar 29061.

Other material

PANAMA – **Panama Province** • 1 ♀; same data as for holotype; voucher code SCU1DHL016; DNA barcode SPIPA419-10; MCZ • 1 ♀; same data as for holotype; voucher code SCD1DFR022; DNA barcode SPIPA420-10; MACN-Ar 29060 • 1 ♀; same data as for holotype; voucher code SCD1DHR006; DNA barcode SPIPA416-10; CRBA • 1 ♀; same data as for holotype; voucher code SCD1DFR025; DNA barcode SPIPA418-10; CRBA.

Description

Male (paratype MACN-Ar 29059)

Total length 1.26. Prosoma: length 0.62, width 0.50, height 0.48. Sternum: length 0.28, width 0.29. Eye diameters and interdistances: AME 0.06, PME 0.05, AME–PME 0.07. Opisthosoma: length 0.84, width 0.81, height 0.74. Leg formula: 1243. Dorsal shield of prosoma white, thoracic area with olive-green speckled lines (Fig. 53A–B). Dorsum of ocular area olive-green (Fig. 53A–B). Sternum light yellow, olive-green speckled anteriorly (Fig. 53C). Dorsum of opisthosoma olive-green, with one dorsal whitish-gray patch centrally (i.e., above first pair of opisthosomal apodemes), and one dorsal pair of round guanine silver patches centrally (i.e., above third pair of opisthosomal apodemes) (Fig. 53A–B). Epiandrium and booklung cover olive-green, tracheal spiracle, spinneret field, and behind anal tubercle light olive-green (Fig. 53C). Legs I–II darker than III–IV, femora white but distally olive-green, patella olive-green, tibiae, metatarsi and tarsi yellow (Fig. 53A–C). Palp: paracymbium hooked, paracymbial process with setae row, median apophysis with deep trough, conductor covering the embolic division, embolus laminated, multiple divided embolic apophysis (Fig. 53D–F).

Female (paratypes MCZ SCD2NGL022, MACN-Ar 29061)

Total length 1.12. Prosoma: length 0.53, width 0.50, height 0.42. Sternum: length 0.28, width 0.30. Eye diameters and interdistances: AME 0.07, PME 0.05, AME–PME 0.05. Opisthosoma: length 0.90, width 0.78, height 0.68. Leg formula: 1243. Coloration as in male, but opisthosoma olive-green ventrally

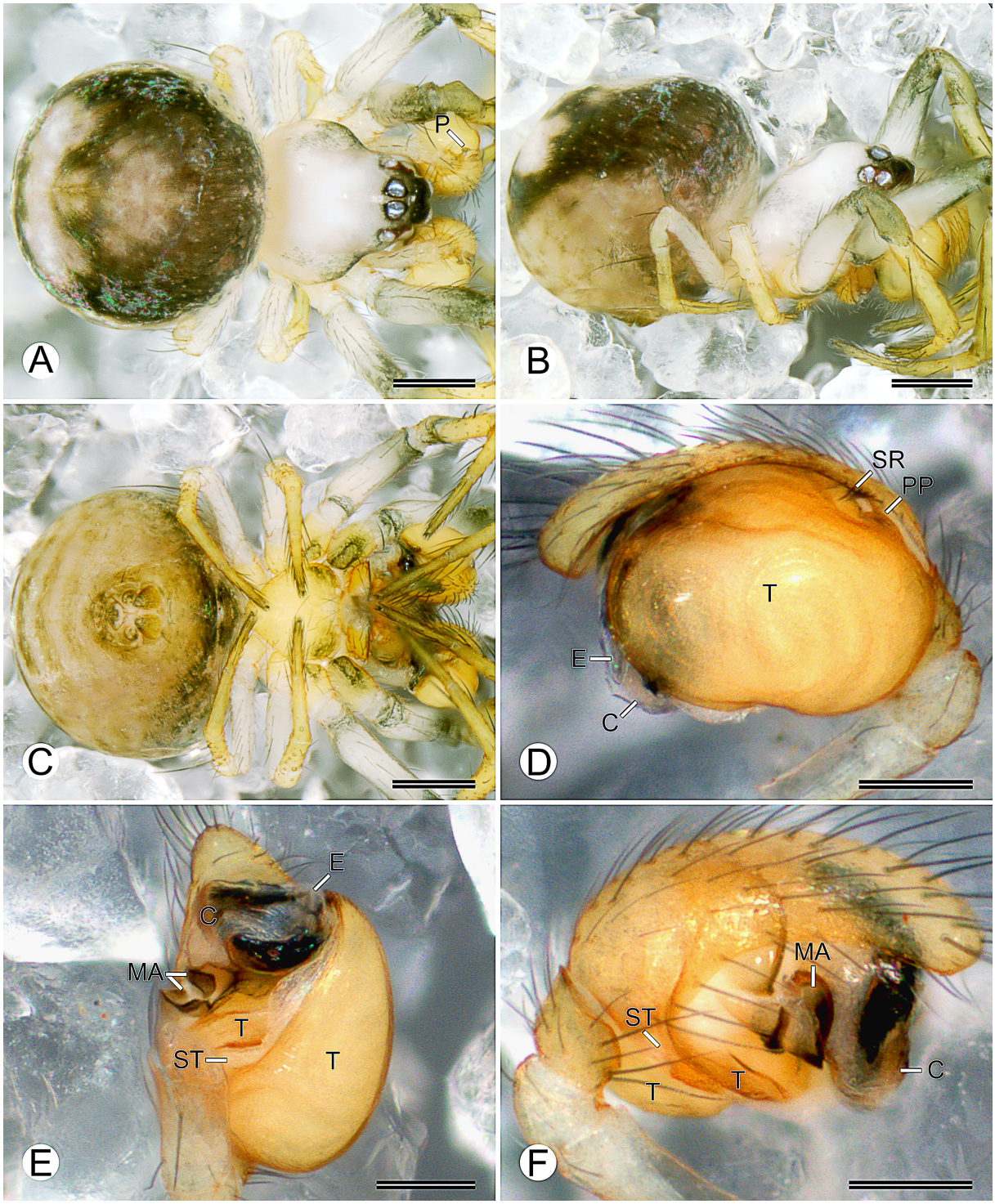

Fig. 53. *Baalzebub jaibana* sp. nov., paratype, ♂ (MACN-Ar 29059). **A–C**. Habitus (A = dorsal view; B = lateral view; C = ventral view). **D–F**. Left palp (D = retrolateral view; E = ventral view; F = prolateral view). Abbreviations: C = conductor; E = embolus; MA = median apophysis; P = paracymbium; PP = paracymbial process; SR = setae row; ST = subtegulum; T = tegulum. Scale bars: A–C = 0.25 mm; D–F = 0.1 mm.

(Fig. 54A–C). Epigynal plate whitish-orange (Fig. 54C), triangular, wide proximally, backward-pointed, central pit deep (Fig. 54C–D). Vulva: copulatory ducts irregular and membranous, inserting ventromedially posteriorly into spermathecae, suboval spermathecae, sclerotized, and connated distally, forming a curved line anteriorly, fertilization ducts sclerotized, emerging laterally posteriorly from spermathecae, curving dorsally anteriorly to meet the uterus externus (Fig. 54D).

Records and biology

Records are limited to collections made at 760 m a.s.l. in premontane rainforest at Parque Nacional Altos de Campana (Fig. 1). Males and females have been collected during the day and night by looking down and cryptic techniques.

Variation

Some females have the thoracic area of the prosoma fully covered by an olive-green speckled pattern.

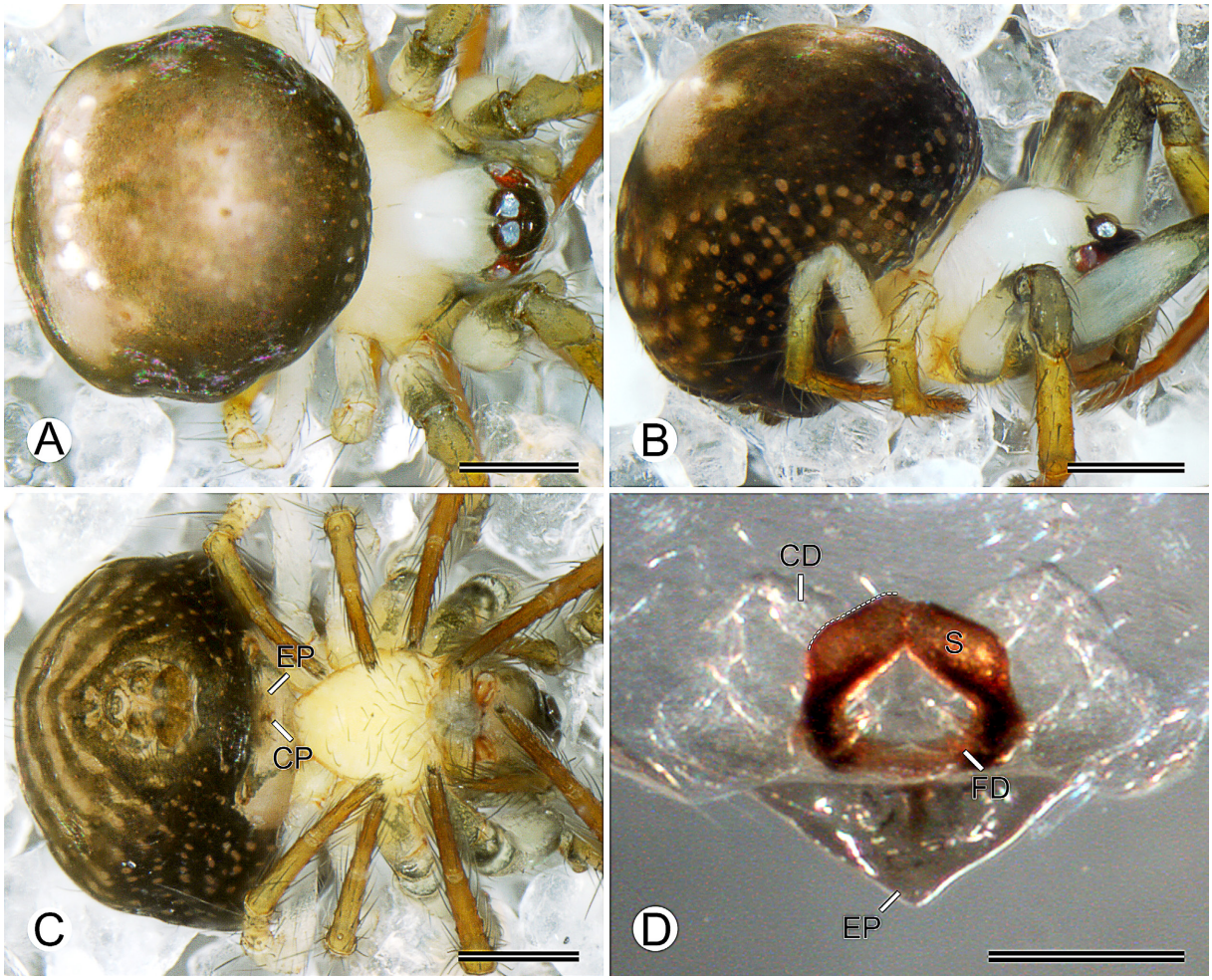

Fig. 54. *Baalzebub jaibana* sp. nov., paratypes, ♀♀ (A–C: MCZ SCD2NGL022; D: MACN-Ar 29061). **A–C**. Habitus (A = dorsal view; B = lateral view; C = ventral view). **D**. Vulva, dorsal (note the profile of the straight subtriangular spermathecae). Abbreviations: CD = copulatory duct; CP = central pit; EP = epigynal plate; FD = fertilization duct; S = spermatheca. Scale bars: A–C = 0.25 mm; D = 0.1 mm.

Baalzebub antomia sp. nov.
urn:lsid:zoobank.org:act:79F3BC9B-B2DF-4DDE-854E-68F88DDD11EB
Figs 1, 55

Diagnosis

Males of *Baalzebub antomia* sp. nov. resemble those of *Baalzebub jaibana* sp. nov. by the overall light coloration (Figs 53A–C, 54A–C, 55A–C), but *B. antomia* can be distinguished by the opisthosoma smooth (i.e., no pattern) (Fig. 55A–B), whereas *B. jaibana* have one dorsal pair of round guanine silver patches centrally on it (Fig. 53A–B). Males of *B. antomia* can be distinguished by the retrolateral massive tegulum with several rows of spicules (i.e., see arrows in figure) and the base of the posterior serrated border of the median apophysis wider than long (Fig. 55D–E), whereas *B. jaibana* have the tegulum smooth (i.e., no spicules) and a longer than wide posterior border of the median apophysis (Fig. 53D–E).

Etymology

The specific name is a noun in apposition to honor Antomia, a mythological being of the folklore of the Emberá native people of Panama, which lives underwater and is responsible for causing people to shudder. Antomia is also known as 'Madre del agua' (Mother of the water).

Type material

Holotype

PANAMA – **Coclé Province** • ♂; Parque Nacional G.D. Omar Torrijos Herrera, El Cope, Sendero Las Ranas; 8.668139° N, 80.592667° W; 790 m a.s.l.; 3 Jun. 2008; F. Labarque leg.; non-quantitative sample; voucher code STNQ38L013; preparation codes FML-00974, FML-00975; MIUP.

Description

Male (holotype MIUP STNQ38L013)

Total length 1.06. Prosoma: length 0.55, width 0.50, height 0.50. Sternum: length 0.27, width 0.30. Eye diameters and interdistances: AME 0.07, PME 0.06, AME–PME 0.06. Opisthosoma: length 0.79, width 0.63, height 0.61. Leg formula: 1243. Dorsal shield of prosoma white (Fig. 55A–B). Dorsum of the ocular area white (Fig. 55A–B). Sternum light olive-green (Fig. 55C). Opisthosoma color overall light olive-green, smooth (i.e., no pattern) (Fig. 55A–C). Epiandrium, booklung cover, tracheal spiracle, spinneret field, and behind the anal tubercle light olive-green (Fig. 55C). Femora and patella white, tibiae greenish-yellow, metatarsi and tarsi brownish-orange; metatarsus I with strong prolateral macrosetae (Fig. 55A–C). Palp: paracymbium hooked, paracymbial process with setae row, median apophysis with a deep trough, conductor covering the embolic division, embolus laminated, multiple divided embolic apophysis (Fig. 55D–F).

Female

Unknown.

Records and biology

Record is limited to collections made at 895 m a.s.l. in the premontane rainforest at Parque Nacional General de División Omar Torrijos Herrera (Fig. 1).

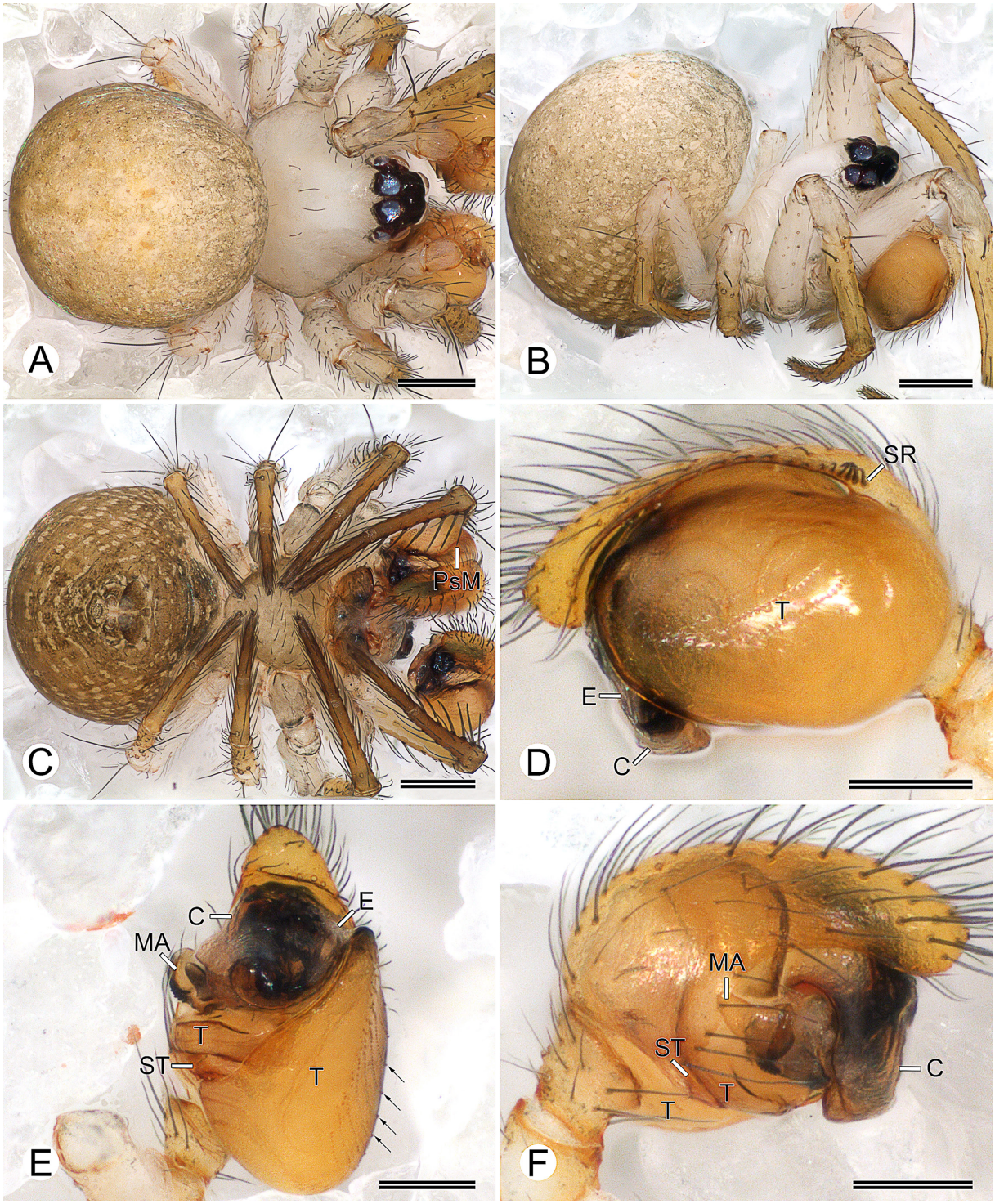

Fig. 55. *Baalzebub antomia* sp. nov., holotype, ♂ (MIUP STNQ38L013). **A–C**. Habitus (A = dorsal view; B = lateral view; C = ventral view). **D–F**. Left palp (D = retrolateral view; E = ventral view; F = prolateral view) (note black arrows to the spicules rows). Abbreviations: C = conductor; E = embolus; MA = median apophysis; PsM = prolateral strong macrosetae; SR = setae row; ST = subtegulum; T = tegulum. Scale bars: A–B = 0.2 mm; C–D = 0.1 mm.

Baalzebub absoguedi sp. nov.
urn:lsid:zoobank.org:act:2BE5DE98-634F-4869-849B-CA3EC4CE1BAD
Figs 1, 56

Diagnosis

Females of *Baalzebub absoguedi* sp. nov. resemble those of *Baalzebub jaibana* sp. nov. by the suboval spermathecae (i.e., rounded laterally), connated distally, forming a curved line anteriorly, and by the backward-pointed triangular epigynal plate anteriorly wide (i.e., wider than the sclerotized vulva) (Figs 54D, 56D). Females of *B. absoguedi* can be distinguished by the backward-pointed plate projecting posteriorly (i.e., exceeding the triangular shape) (Fig. 56D) and the overall dark coloration (Fig. 56A–C), whereas *B. jaibana*. have the plate not projecting posteriorly (i.e., not exceeding the triangular shape) (Fig. 54D) and an overall light coloration (Fig. 54A–C).

Etymology

The specific name is derived from 'absoguedi' which indicates the person specialized in the chants that chases away the bad spirits in the Kuna language, currently spoken by the Kuna native people of Panama.

Type material

Holotype

PANAMA – **Coclé Province** • ♀; Parque Nacional G.D. Omar Torrijos Herrera, El Cope, Sendero Las Ranas; 8.668139° N, 80.592667° W; 790 m a.s.l.; 3 Jun. 2008; F. Labarque leg.; non-quantitative sample; voucher code STNQ38L016; preparation codes FML-00972, FML-00973; MIUP.

Description

Female (holotype MIUP STNQ38L016)

Total length 1.40. Prosoma: length 0.70, width 0.60, height 0.56. Sternum: length 0.35, width 0.34. Eye diameters and interdistances: AME 0.08, PME 0.07, AME–PME 0.07. Opisthosoma: length 1.09, width 0.9, height 0.85. Leg formula: 1243. Dorsal shield of prosoma dark (Fig. 56A). Dorsum of ocular area dark (Fig. 56A). Sternum yellowish-orange with dark olive-green borders (Fig. 56C). Opisthosoma color overall dark gray, anteriorly lighter, with three dorsal pairs of round guanine silver patches laterally, first pair above second pair of opisthosomal apodemes, second pair smaller (Fig. 56A–B). Booklungs cover white, tracheal spiracle, and behind anal tubercle dark gray, spinneret field orange with one pair of round guanine silver patches laterally (Fig. 56C). Femora yellowish-white but distally olive-green, patella olive-green, tibiae, metatarsi and tarsi orange (Fig. 56A–C). Epigynal plate brownish-orange (Fig. 56C), triangular, wide proximally, backward-pointed, central pit deep (Fig. 56C–D). Vulva: copulatory ducts irregular and membranous, inserting ventromedially posteriorly into spermathecae, suboval spermathecae, sclerotized, and connated distally, forming curved line anteriorly, fertilization ducts sclerotized, emerging laterally posteriorly from spermathecae, curving dorsally anteriorly to meet uterus externus (Fig. 56D).

Male

Unknown.

Records and biology

The single record is limited to a collection made at 895 m a.s.l. in premontane rainforest from Parque Nacional General de División Omar Torrijos Herrera (Fig. 1).

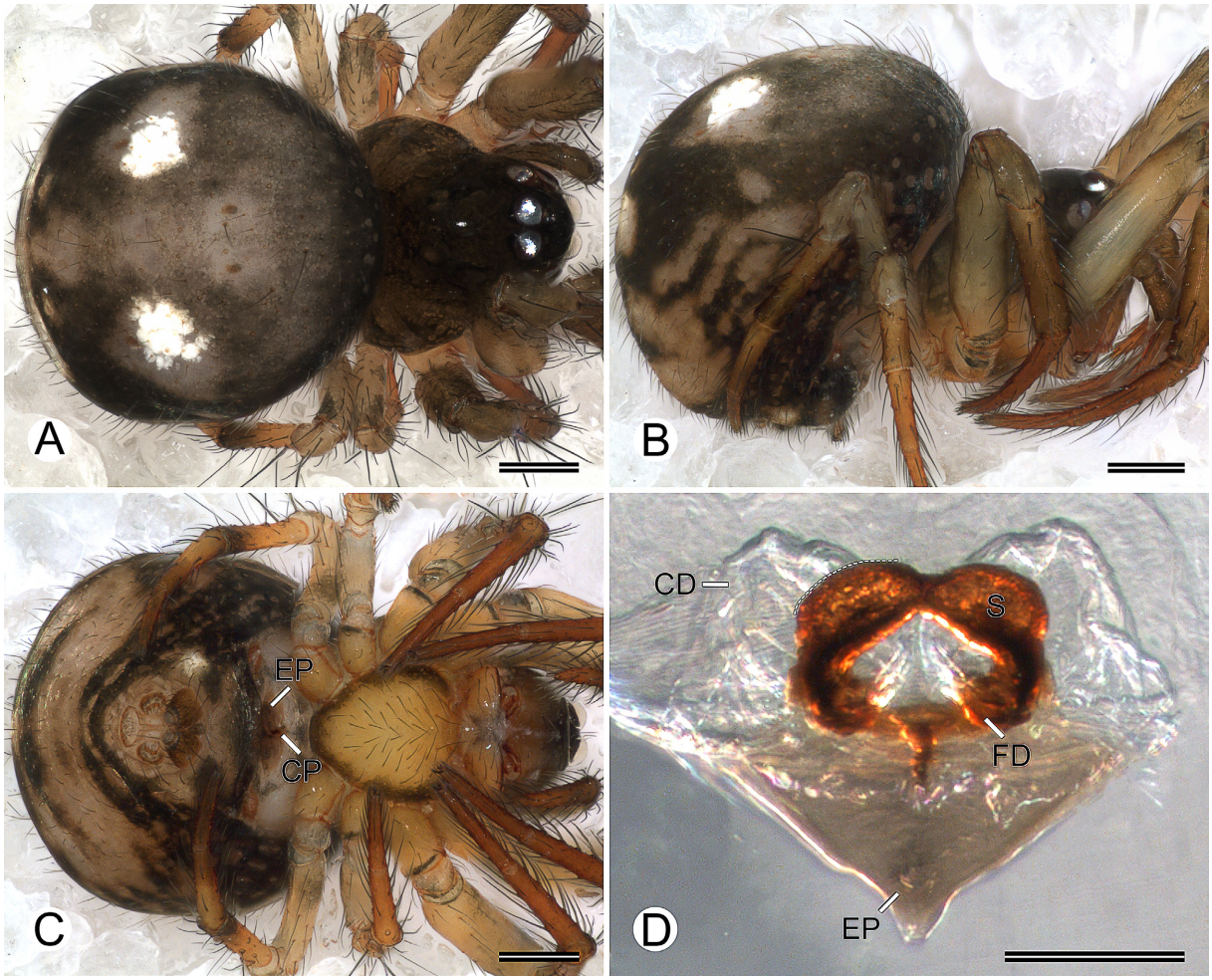

Fig. 56. *Baalzebub absoguedi* sp. nov., holotype, ♀ (MIUP STNQ38L016). **A–C**. Habitus (A = dorsal view; B = lateral view; C = ventral view). **D**. Vulva, dorsal (note the profile of the curved suboval spermathecae). Abbreviations: CD = copulatory duct; CP = central pit; EP = epigynal plate; FD = fertilization duct; S = spermatheca. Scale bars: A–C = 0.2 mm; D = 0.1 mm.

Baalzebub nele sp. nov.
urn:lsid:zoobank.org:act:3C1E0BD7-8300-4C0E-BA78-2B0CC4C40626
Figs 1, 57

Diagnosis

Females of *Baalzebub nele* sp. nov. resemble those of *Baalzebub baubo* Coddington, 1986 by the suboval spermathecae (i.e., rounded laterally), distally connated, forming a curved line anteriorly, and by the backward-pointed triangular epigynal plate anteriorly narrow (i.e., as wide as the sclerotized vulva) (Fig. 57D; Coddington 1986: fig. 184). Females of *B. nele* can be distinguished from those of *B. baubo* by the opisthosoma dark laterally and the spinneret field with one pair of round guanine silver patches laterally (Fig. 57B–C), whereas *B. baubo* have light patches laterally on the opisthosoma and no silver patches next to the spinnerets (Coddington 1986: fig. 180).

Etymology

The specific name is derived from 'nele' which indicates the person that has visions, dreams and revelations to diagnose diseases in the Kuna language, currently spoken by the Kuna native people of Panama.

Type material

Holotype

PANAMA – **Chiriquí Province** • ♀; Reserva Forestal Fortuna, Quebrada Honda, one-hectare PANCODING inventory; 8.750083° N, 82.239083° W; 1135 m a.s.l.; 7–12 Jun. 2007; M. Arnedo, D. Dimitrov, G. Hormiga, F. Labarque and M. Ramírez leg.; voucher code SFD1D8R013; preparation codes FML-00735, LNP-00261; DNA code baaba060; GenBank code PX096875; MIUP.

Paratypes

PANAMA – **Panama Province** • 1 ♀; Parque Nacional Altos de Campana, one-hectare PANCODING inventory; 8.683444° N, 79.929833° W; 895 m a.s.l.; 14–19 Jun. 2007; M. Arnedo, D. Dimitrov, G. Hormiga, F. Labarque and M. Ramírez leg.; voucher code SCD1DEL017; DNA code baaba255; GenBank code PX096877; MACN-Ar 29062 • 1 ♀; same data as for preceding; voucher code SCD1DFR013; DNA code baaba252; GenBank code PX096876; MACN-Ar 29063.

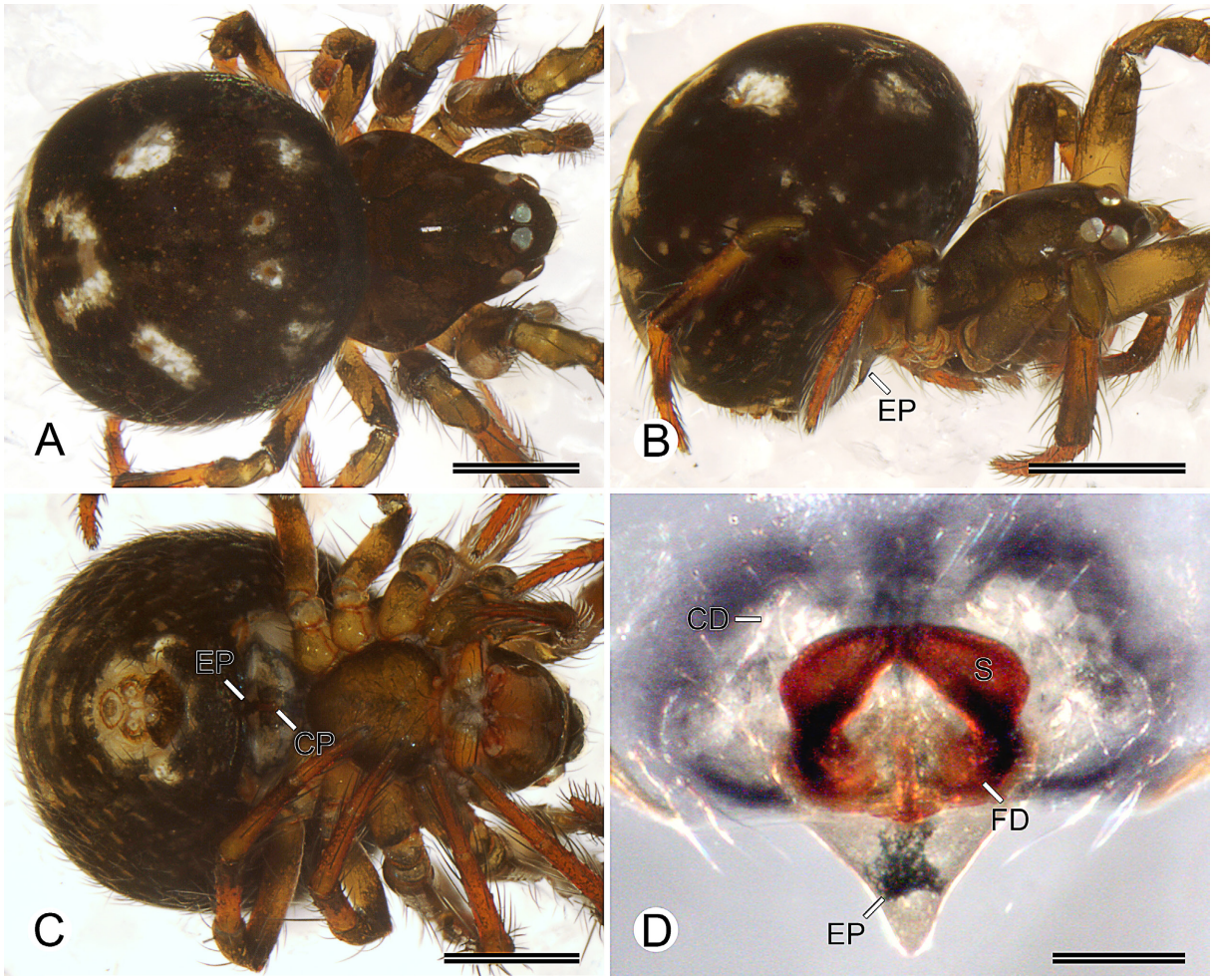

Fig. 57. *Baalzebub nele* sp. nov., holotype, ♀ (MIUP SFD1D8R013). **A–C**. Habitus (A = dorsal view; B = lateral view; C = ventral view). **D**. Vulva, dorsal view. Abbreviations: CD = copulatory duct; EP = epigynal plate; FD = fertilization duct; S = spermatheca. Scale bars: A–C = 0.5 mm; D = 0.025 mm.

Description

Female (holotype MIUP SFD1D8R013)

Total length 2.16. Prosoma: length 0.89, width 0.87, height 0.61. Sternum: length 0.47, width 0.50. Eye diameters and interdistances: AME 0.12, PME 0.09, AME–PME 0.08. Opisthosoma: length 1.32, width 1.39, height 1.04. Leg formula: 1243. Dorsal shield of prosoma dark (Fig. 57A–B). Dorsum of ocular area dark (Fig. 57A–B). Sternum dark olive-green with dark borders (Fig. 57C). Opisthosoma color overall dark gray, with four dorsal pairs of round guanine silver patches laterally, first and second pairs above first pair of opisthosomal apodemes, fourth pair touching anteriorly (Fig. 57A–B). Epigynal plate and booklung cover whitish-orange, tracheal spiracle, and behind anal tubercle dark gray; anterior lateral spinnerets field olive-green, other spinnerets orange (Fig. 57C). Femora and patella greenish-yellow with olive-green speckles distally, tibiae orange but distally olive-green, metatarsi and tarsi orange (Fig. 57A–C). Epigynal plate: triangular, narrow proximally, backward-pointed, central pit deep (Fig. 57C–D). Vulva: copulatory ducts irregular and membranous, inserting ventromedially posteriorly into spermathecae, suboval spermathecae, sclerotized, and connated distally, forming curved line anteriorly, fertilization ducts sclerotized, emerging laterally posteriorly from spermathecae, curving dorsally anteriorly to meet uterus externus (Fig. 57D).

Male

Unknown.

Records and biology

Records are limited to collections made at 760 m a.s.l. and 1135 m a.s.l. in premontane rainforest at Parque Nacional Altos de Campana and Reserva Forestal Fortuna, respectively (Fig. 1). Males and females have been collected during the day by looking down and cryptic techniques.

Variation

Some females have darker coloration than the described specimen.

Baalzebub albonotatus (Petrunkevitch, 1930)

Figs 1, 58

Theridiosoma albonotatum Petrunkevitch, 1930: 305, figs 177–179 [♀] [holotype ♀ from Puerto Rico, Rio Grande, El Yunque National Forest (Peabody Museum of Natural History, New Haven), not examined].

Baalzebub albonotatus – Coddington 1986: 74, figs 163–164, 167 [♂, ♀] [transferred from *Theridiosoma*].

Diagnosis

Males and females of *B. albonotatus* can be distinguished from the other congeneric species by the longitudinal guanine blotches silver band centrally on the dorsum of the opisthosoma (Fig. 58A–C; Petrunkevitch 1930: fig. 178) (absent in other cogeneric species).

Material examined

PANAMA– **Chiriquí Province** • 1 ♂; Reserva Forestal Fortuna, Sendero Zamudio; 8.732861° N, 82.284667° W; 1360 m a.s.l.; 20 Jun. 2008; L. Piacentini and F. Labarque leg.; non-quantitative sample; voucher code SFNQK8L001; preparation codes FML-00835, FML-00836; DNA barcode SPIPA232-10; MACN-Ar.

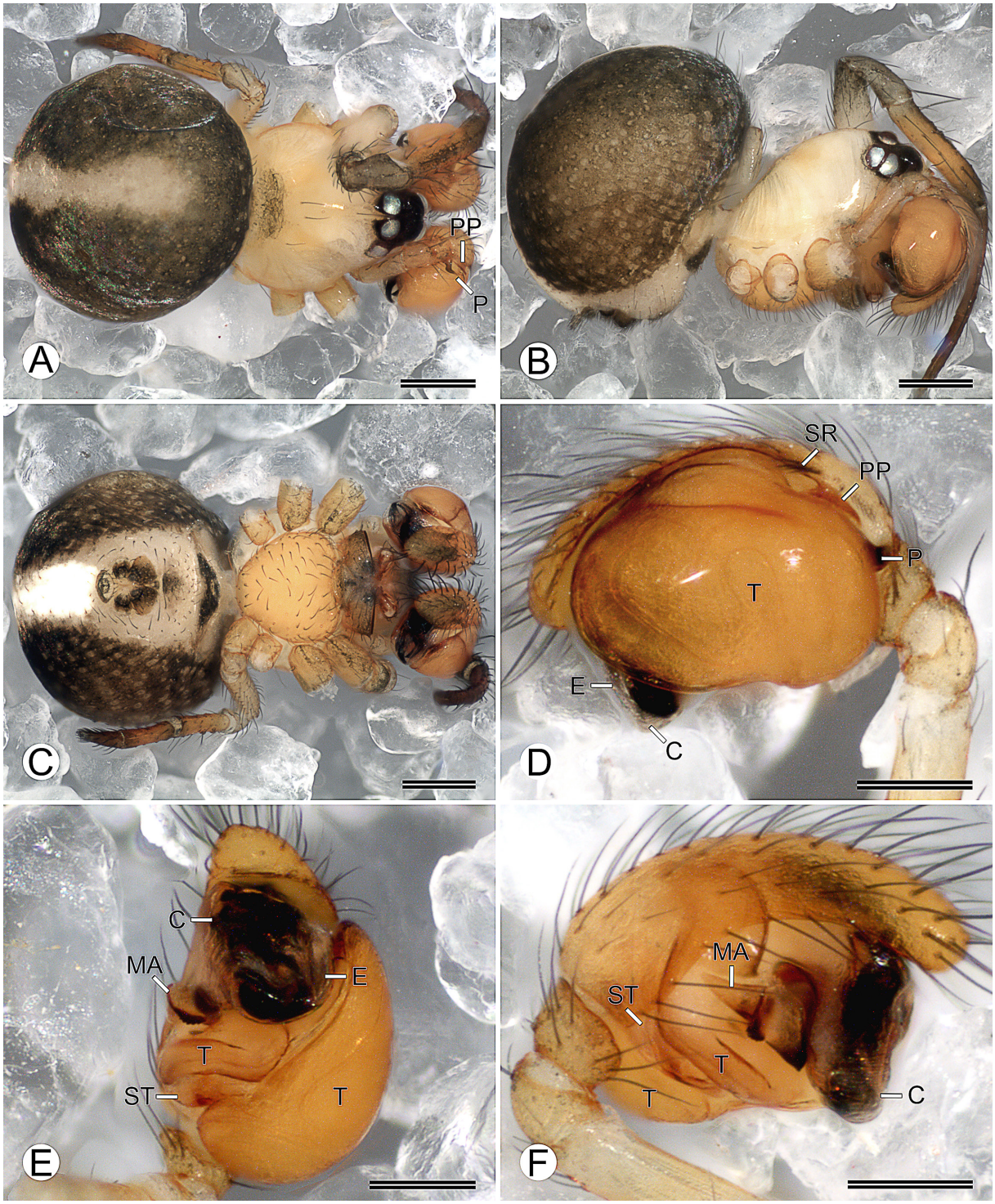

Fig. 58. *Baalzebub albonotatus* (Petrunkevitch, 1930), ♂ (MACN-Ar SFNQK8L001). **A–C**. Habitus (A = dorsal view; B = lateral view; C = ventral view). **D–F**. Left palp (D = retrolateral view; E = ventral view; F = prolateral view). Abbreviations: C = conductor; E = embolus; MA = median apophysis; P = paracymbium; PP = paracymbial process; SR = setae row; ST = subtegulum; T = tegulum. Scale bars: A–C 0.2 mm; D–F 0.1 mm.

Description

Male (MACN-Ar SFNQK8L001)

Total length 1.11. Prosoma: length 0.51, width 0.45, height 0.48. Sternum: length 0.27, width 0.31. Eye diameters and interdistances: AME 0.06, PME 0.05, AME–PME 0.05. Opisthosoma: length 0.64, width 0.69, height 0.77. Leg formula: 1243. Dorsal shield of prosoma yellow, thoracic area olive-green centrally (Fig. 58A–B). Dorsum of ocular area dark (Fig. 58A–B). Sternum yellowish-orange (Fig. 58C). Opisthosoma color overall olive-green, with dorsal longitudinal guanine blotches silver band centrally (Fig. 58A–C). Epiandrium, tracheal spiracle, and spinneret field dark olive-green, and booklung cover whitish-gray (Fig. 58C). Femora yellowish-white but distally olive-green, patella olive-green, tibiae and metatarsi orange, and tarsi brownish-orange (Fig. 58A–C). Palp: paracymbium hooked, paracymbial process with setae row, median apophysis with deep trough, conductor covering embolic division, embolus laminated, multiple divided embolic apophysis (Fig. 58D–F; Coddington 1986: figs 163–164).

Female

For female species description, see Petrunkevitch (1930).

Records and biology

Baalzebub albonotatus has been found in Puerto Rico (World Spider Catalog 2025) and Panama. Records in this study are limited to collections made at 1135 m a.s.l. in premontane rainforest from Reserva Forestal Fortuna (Fig. 1).

Remarks

Whereas we have not examined the type of this species, we believe that species attribution is unproblematic. Coddington (1986: 72–74) examined male and female specimens of *Baalzebub albonotatus* from Puerto Rico (misspelled as "*B. albinotatus*"), provided SEM images of the male palp of this species (Coddington 1986: figs 163–164), and distinguished it from *Baalzebub baubo* by "a median dorsal white stripe on the abdomen" (Coddington 1986: 74). Unfortunately, Coddington (1986) did not describe the male of *B. albonotatus*; however, we have done so here (see Description above). Our diagnosis aligns perfectly with the female description of *B. albonotatus* by Petrunkevitch (1930: 305) and the comparative diagnosis with *B. baubo* by Coddington (1986: 74). Additionally, our description of the male palp of *B. albonotatus* agrees in every way with the specimen illustrated by Coddington (1986).

Epilineutes Coddington, 1986

Epilineutes Coddington, 1986: 74. Type species *Adrasta globosa* O. Pickard-Cambridge, 1896; by original designation.

Diagnosis

Males of *Epilineutes* can be distinguished from those of other theridiosomatid genera by the thin, elongated, distally acute, median apophysis retrolateral projection extending anteriorly (Fig. 59E; see also Coddington 1986) (absent in other genera). Females of *Epilineutes* can be distinguished from those of other genera by the notched epigynal posterior margin (Coddington 1986: fig. 173) (absent in other genera).

Description

Males of *Epilineutes* have tripartite embolic apophysis, retrolaterally finger-printed conductor, and sub-rectangular median apophysis with denticles (Fig. 59D–F; Coddington 1986: figs 189–190). Females of *Epilineutes* have a dorsal scape protruding from beneath the notched epigynal plate transverse

groove (Fig. 60D; Coddington 1986: fig. 173), and irregular membranous copulatory ducts inserting ventromedially posteriorly into spermathecae (Fig. 60D). For genus description details, see Coddington (1986) and Labarque & Griswold (2014).

Epilineutes globosus (O. Pickard-Cambridge, 1896)
Figs 1, 6C, F, 59–60

Adrasta globosa O. Pickard-Cambridge, 1896: 192, pl. 24 figs 5, 5a–f [♂], figs 6, 6a–b [♀] [a series of 3 ♂♂ and 5 ♀♀ syntypes from Mexico, Tabasco, Teapa (The Natural History Museum, London), not examined].

Theridiosoma globosum – F.O. Pickard-Cambridge 1902: 414 [transfer from *Adrasta*].
Epilineutes globosus – Coddington 1986: 79, figs 169–178, 188–195 [♂, ♀] [transferred from *Theridiosoma*].

Diagnosis

Males and females of *E. globosus* can be distinguished from those of other theridiosomatid species following the genus diagnosis (see above). For species diagnosis details, see Coddington (1986).

Material examined

PANAMA – **Chiriquí Province** • 1 ♂; Reserva Forestal Fortuna, Quebrada Honda, one-hectare PANCODING inventory; 8.750083° N, 82.239083° W; 1135 m a.s.l.; 7–12 Jun. 2007; M. Arnedo, D. Dimitrov, G. Hormiga, F. Labarque and M. Ramírez leg.; voucher code SFU1N8A034; preparation codes FML-00689, LNP-00272; DNA code epigl064; GenBank code PX096886; MACN-Ar 29093 • 1 ♀; same data as for preceding; voucher code SFD1D8D007; preparation codes FML-00741, FML-01144, LNP-00278; DNA code epigl055; GenBank code PX096883; MACN-Ar 29090 • 1 ♂; same data as for preceding; voucher code SFU1NAH031; DNA barcode SPIPA379-10; MACN-Ar 29092 • 1 ♀; same data as for preceding; voucher code SFU1NAR037; DNA barcode SPIPA378-10; MACN-Ar 29088 • 1 ♂; same data as for preceding; voucher code SFU1NBA005; DNA barcode SPIPA380-10; MACN-Ar 29094 • 1 ♂; same data as for preceding; voucher code SFU1NBD031; DNA barcode SPIPA382-10; MACN-Ar 29085 • 1 ♀; same data as for preceding; voucher code SFD1DAL017; DNA code epigl165; GenBank code PX096887; MACN-Ar 29087 • 1 ♀; same data as for preceding; voucher code SFB1D9H034; DNA code epigl202; GenBank code PX096885; MACN-Ar 29091 • 1 ♂; same data as for preceding; voucher code SFB1DAL022; DNA code epigl201; GenBank code PX096884; MCZ • 1 ♀; same data as for preceding; voucher code SFD1NBA013; DNA barcode SPIPA381-10; CRBA • 14 ♂♂, 12 ♀♀; same data as for preceding; MCZ • 2 ♂♂, 2 ♀♀; same data as for preceding; MIUP • 1 ♂, 1 ♀; same data as for preceding; MACN-Ar • 4 ♂♂, 1 ♀; same data as for preceding; CRBA • 2 ♂♂, 1 ♀; same locality as for preceding; 21–24 Jun. 2008; L. Piacentini and F. Labarque leg.; non-quantitative sample; MACN-Ar.

Redescription

Male (MACN-Ar 29093)
Total length 1.09. Prosoma: length 0.54, width 0.55, height 0.56. Sternum: length 0.31, width 0.34. Eye diameters and interdistances: AME 0.07, PME 0.08, AME–PME 0.07. Opisthosoma: length 0.68, width 0.72, height 0.80. Leg formula: 1243. Dorsal shield of prosoma dark olive-green laterally, olive-green centrally (Fig. 59A–B). Dorsum of ocular area dark olive-green (Fig. 59A–B). Sternum dark olive-green (Fig. 59C). Dorsum of opisthosoma whitish-olive-green (Fig. 59A). Epiandrium, booklung cover, tracheal spiracle, spinneret field and behind anal tubercle olive-green (Fig. 59C). Legs I–II darker than III–IV, femora and patella light olive-green, tibiae and metatarsi, tarsi brownish-orange (Fig. 59A–C).

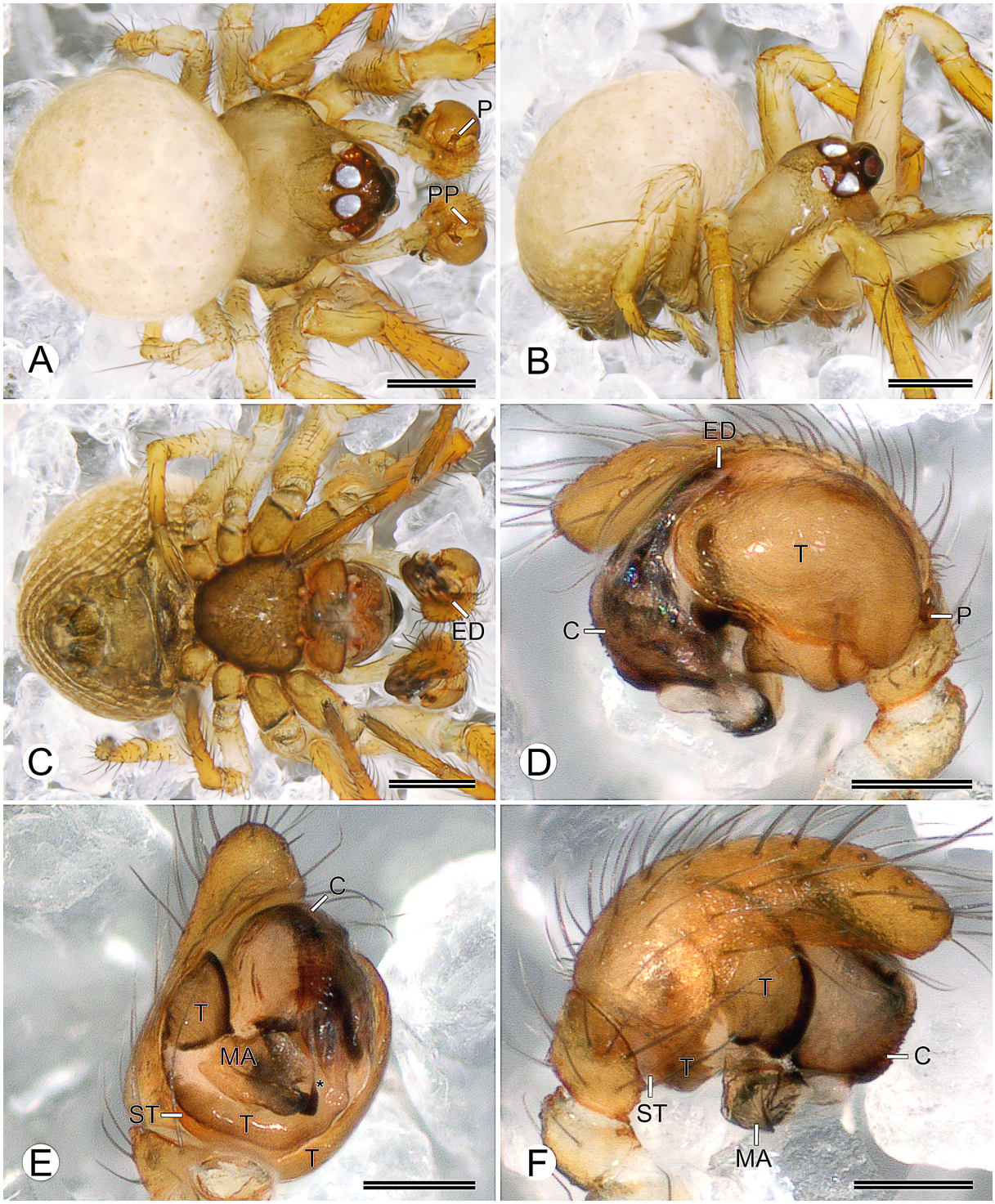

Fig. 59. *Epilineutes globosus* (O. Pickard-Cambridge, 1896), ♂ (MACN-Ar 29093). **A–C**. Habitus (A = dorsal view; B = lateral view; C = ventral view). **D–F**. Left palp (D = retrolateral view; E = ventral view; F = prolateral view), asterisk shows the retrolateral projection of the MA extending anteriorly. Abbreviations: C = conductor; ED = embolic division; MA = median apophysis; P = paracymbium; PP = paracymbial process; ST = subtegulum; T = tegulum. Scale bars: A–C = 0.25 mm; D–F = 0.1 mm.

Palp: paracymbium hooked, paracymbial process with setae row, median apophysis sub-rectangular with median groove and retrolateral projection extending anteriorly, conductor retrolateral surface finger-printed covering embolic apophysis, embolus as thin lamina, tripartite embolic apophysis (Fig. 59D–F; Coddington 1986: figs 176–178, 188–191).

Female (MACN-Ar 29090)
Total length 1.65. Prosoma: length 0.64, width 0.63, height 0.61. Sternum: length 0.36, width 0.38. Eye diameters and interdistances: AME 0.08, PME 0.08, AME–PME 0.07. Opisthosoma: length 1.24, width 1.18, height 1.26. Leg formula: 1243. Coloration as in male but dorsum of opisthosoma covered sparsely by guanine silver patches (Fig. 60A–C). Epigynal plate olive-green (Fig. 60C), flat, with transverse groove notched, dorsal scape present (Fig. 60C–D; Coddington 1986: fig. 173). Vulva: copulatory ducts irregular and membranous, inserting ventromedially posteriorly into spermathecae, spermathecae anteriorly sharp (i.e., angular), sclerotized, and connated distally, forming triangle, fertilization ducts sclerotized, emerging laterally posteriorly from spermathecae, curving dorsally anteriorly to meet uterus externus (Fig. 60D; Coddington 1986: fig. 174). For further species description details, see Coddington (1986).

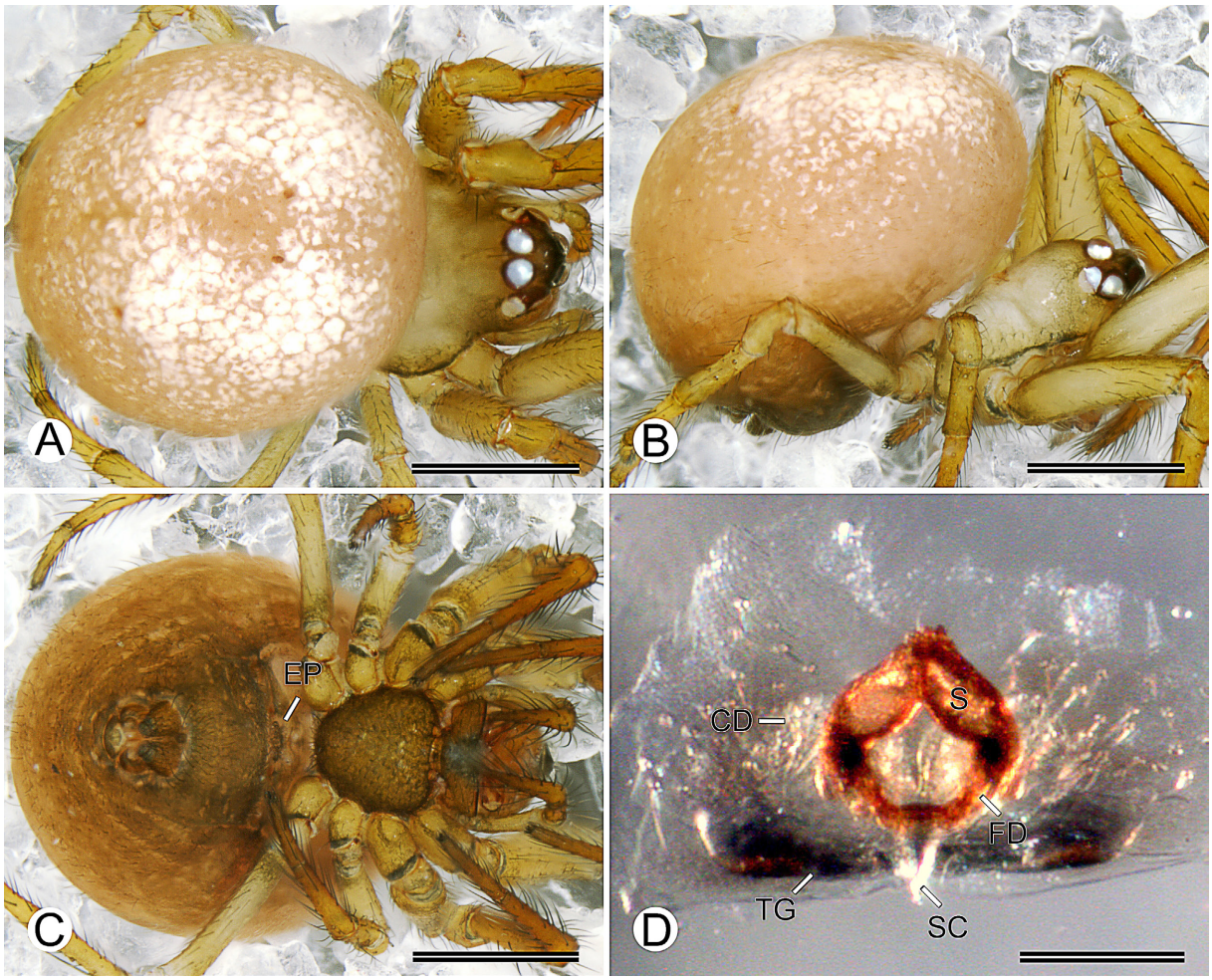

Fig. 60. *Epilineutes globosus* (O. Pickard-Cambridge, 1896), ♀ (MACN-Ar 29090). **A–C**. Habitus (A = dorsal view; B = lateral view; C = ventral view). **D**. Vulva, dorsal view. Abbreviations: CD = copulatory duct; EP = epigynal plate; FD = fertilization duct; S = spermatheca; SC = dorsal scape; TG = transverse groove). Scale bars: A–C = 0.5 mm; D = 0.1 mm.

Records and biology

Epilineutes globosus is distributed from Mexico to Brazil (World Spider Catalog 2025). Records in this study are limited to collections made at 1135 m a.s.l. in premontane rainforest from Reserva Forestal Fortuna (Fig. 1). Males and females have been collected mostly at night by looking up, although some specimens were also collected at night by looking down and others during the day by looking down and cryptic techniques.

Wendilgarda Keyserling, 1886

Wendilgarda Keyserling, 1886: 129. Type species *Wendilgarda mexicana* Keyserling, 1886.

Diagnosis

Males and females of *Wendilgarda* can be distinguished from those of other genera by the uniform orangish-yellow coloration on the prosoma and opisthosoma (Figs 61A–C, 62A–C; see also Coddington 1986) (absent in most genera, except in some species of *Ogulnius*) and by their unique web architecture with a dendritic pattern of not-sticky horizontal lines, which hold sticky vertical lines that attach to the water surface of a moving stream (Coddington & Valerio 1980; Coddington 1986; Cotoras *et al.* 2021). Males of *Wendilgarda* can also be distinguished from those of other genera by the mesal embolic apophysis branch elongated, protruding from beneath the conductor and lying along the prolateral side of the conductor itself (Fig. 61E, see also Coddington 1986) (in contrast with embolic apophysis branches not lying on the conductor in other genera). Females of *Wendilgarda* can also be distinguished from those of other genera by the fluted (i.e., crumpled in cross-section), double-pointed eggsacs (Coddington 1986: figs 200–201) (in contrast with squared or rounded eggsacs in other genera).

Description

Males of *Wendilgarda* have tripartite embolic apophysis, retrolaterally finger-printed conductor, and sub-rectangular median apophysis with denticles (Fig. 61D–F; Coddington 1986: figs 196–197). Females of *Wendilgarda* have dorsal scape protruding from beneath epigynal plate posterior margin (Fig. 62C–D; Coddington 1986: figs 206, 213, 219), irregular membranous proximal copulatory ducts, convoluted and heavily sclerotized distal copulatory ducts, inserting ventromedially posteriorly into spermathecae (Fig. 62D). For genus description details, see Coddington (1986) and Labarque & Griswold (2014).

Remarks

Females of the type species *Wendilgarda mexicana* Keyserling, 1886 present separated spermathecae (Coddington 1986: fig. 207).

Wendilgarda clara Keyserling, 1886
Figs 1, 7, 61–62

Wendilgarda clara Keyserling, 1886: 132, pl. 15 figs 210, 210a–d [♀] [holotype ♀ from Brazil, Amazonas Prov. (Department of Entomology, Oxford University Museum of Natural History, Oxford), not examined].

Wendilgarda theridionina Simon, 1895: 919, fig. 986 [♂] [a series of 21 syntype ♂♂ and 18 ♀♀ from Venezuela, Carabobo Prov., San Esteban (Muséum National d'Histoire Naturelle, Paris), not examined] [synonymized by Coddington 1986].

Wendilgarda panamica Archer, 1953: 15, fig. 23 [holotype ♀ from Panama, Panama, Barro Colorado Island, Lake Gatun (American Museum of Natural History, New York), not examined] [synonymized by Coddington 1986].

Wendilgarda hassleri Archer, 1953: 16, figs 24, 28 [holotype ♂ from Guyana, upper Shudikar River (American Museum of Natural History, New York), not examined] [synonymized by Coddington 1986].

Diagnosis

Males of *Wendilgarda clara* can be distinguished from those of *Wendilgarda galapagensis* Archer, 1953, *Wendilgarda mexicana* Keyserling, 1886, and *Wendilgarda mustelina* Simon, 1898 by the mesal branch elongated lying along the prolateral side of the conductor (Fig. 61D–F; Coddington 1986: figs 196–198, 217), whereas *W. galapagensis*, *W. mexicana*, and *W. mustelina* lack such branches (Coddington 1986: figs 199, 210; Lopez & Emerit 1986: fig. 13; Viquez 2020: fig. 7a). Females of *W. clara* can be distinguished from those of *W. galapagensis*, *W. mexicana*, and *W. mustelina* by the thin epigynal dorsal scape (Figs 7A–C, 62C–D; Coddington 1986: figs 206–207), whereas *W. galapagensis*, *W. mexicana*, and *W. mustelina* have the dorsal scape wider (Coddington 1986: figs 213–215; Lopez & Emerit 1986: fig. 12; Víquez 2020: fig. 7b).

Material examined

PANAMA – **Chiriquí Province** • 1 ♂; Reserva Forestal Fortuna, Quebrada Honda, one-hectare PANCODING inventory; 8.750083° N, 82.239083° W; 1135 m a.s.l.; 7–12 Jun. 2007; M. Arnedo, D. Dimitrov, G. Hormiga, F. Labarque and M. Ramírez leg.; voucher code SFD2NBL020; preparation codes FML-00717, LNP-00274; DNA code wens1057; GenBank code PX0970; MACN-Ar 29222 • 1 ♀; same data as for preceding; voucher code SFD1NBL018; preparation codes FML-00734, FML-01145, LNP-00264; DNA code wens1068; GenBank code PX097005; MACN-Ar 29223 • 1 ♂; same data as for preceding; voucher code SFD1NBL030; DNA code wenclf11; GenBank code PX097007; MCZ • 1 ♂; same data as for preceding; voucher code SFU1N7H040; DNA code wencle11; GenBank code PX097006; MIUP • 1 ♂; same data as for preceding; voucher code SFD1NBL036; DNA code wenclg11; GenBank code PX097008; CRBA • 1 ♂; same locality as for preceding; 1135 m a.s.l.; 21–24 Jun. 2008; L. Piacentini and F. Labarque leg.; non-quantitative sample; MACN-Ar.

Redescription

Male (MACN-Ar 29222)

Total length 1.61. Prosoma: length 0.80, width 0.82, height 0.73. Sternum: length 0.43, width 0.45. Eye diameters and interdistances: AME 0.09, PME 0.07, AME–PME 0.09. Opisthosoma: length 1.01, width 0.97, height 1.04. Leg formula: 1243. Dorsal shield of prosoma orangish-yellow (Fig. 61A–B). Dorsum of ocular area orangish-yellow (Fig. 61A–B). Sternum orangish-yellow (Fig. 61C). Opisthosoma color overall orangish-yellow (Fig. 61A). Epiandrium, booklung cover, tracheal spiracle, spinneret field and behind anal tubercle orangish-yellow (Fig. 61C). Femora and patella orangish-yellow, tibiae, metatarsi, and tarsi orange (Fig. 61A–C). Palp: paracymbium hooked, paracymbial process with setae row, median apophysis sub-rectangular with median groove, conductor retrolateral surface finger-printed covering embolic apophysis, embolus as thin lamina, tripartite embolic apophysis, mesal branch elongated lying along prolateral side of conductor (Fig. 61D–F; Coddington 1986: figs 196–198, 217).

Female (MACN-Ar 29223)

Total length 1.60. Prosoma: length 0.78, width 0.82, height 0.78. Sternum: length 0.41, width 0.47. Eye diameters and interdistances: AME 0.09, PME 0.07, AME–PME 0.09. Opisthosoma: length 1.11, width 1.09, height 1.11. Leg formula: 1243. Coloration as in male (Fig. 62A–C). Epigynal plate orangish-yellow (Fig. 62C), flat, with dorsal scape (Fig. 62C–D; Coddington 1986: figs 213–215). Vulva: proximal

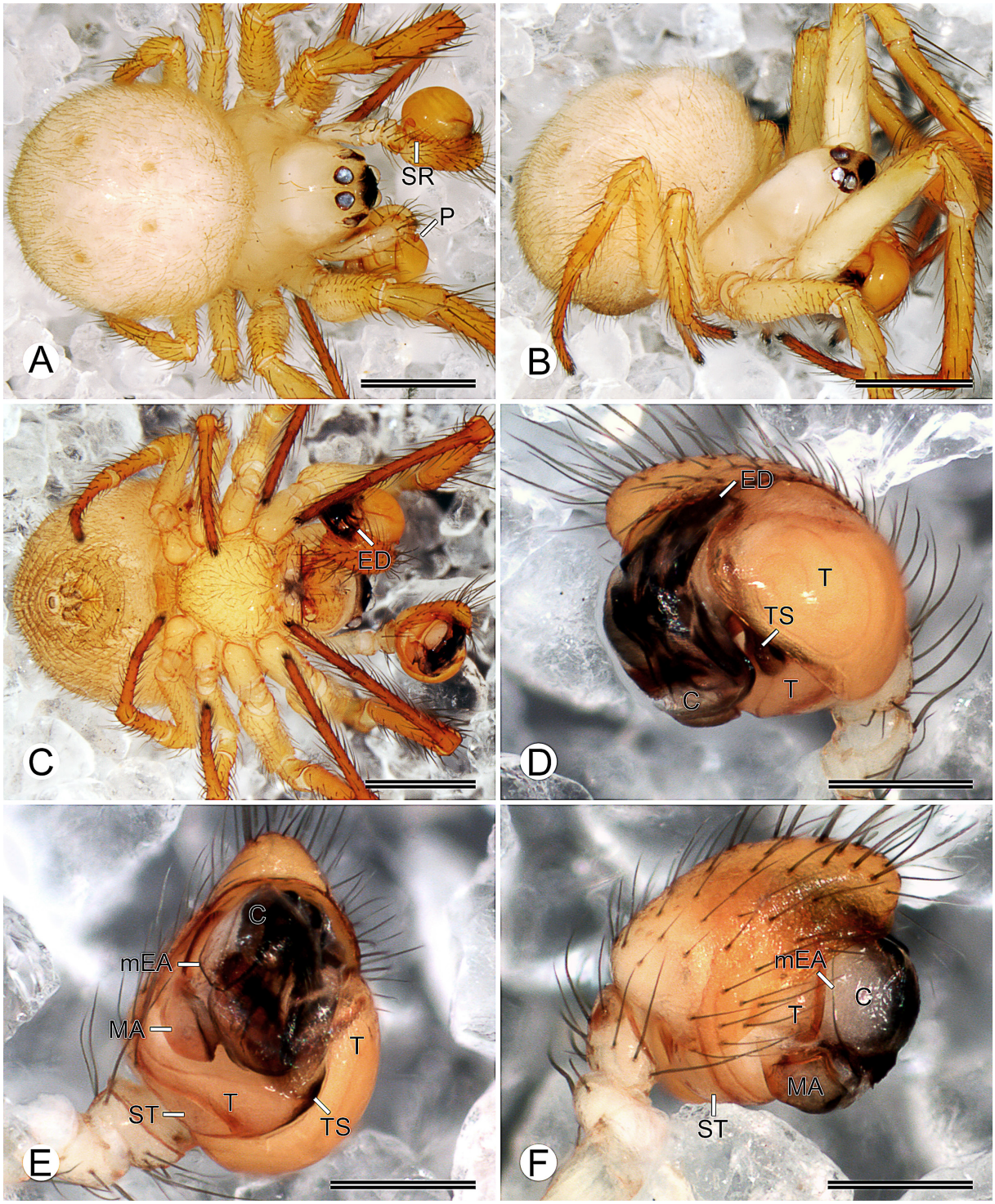

Fig. 61. *Wendilgarda clara* Keyserling, 1886, ♂ (MACN-Ar 29222). **A–C**. Habitus (A = dorsal view; B = lateral view; C = ventral view). **D–F**. Left palp (D = retrolateral view; E = ventral view; F = prolateral view). Abbreviations: C = conductor; ED = embolic division; MA = median apophysis; mEA = embolic apophysis mesal branch; P = paracymbium; SR = setae row; ST = subtegulum; T = tegulum; TS = tegular striae. Scale bars: A–C = 0.5 mm; D–F = 0.2 mm.

copulatory ducts irregular and membranous, distal copulatory ducts convoluted, inserting ventromedially posteriorly into spermathecae, spermathecae oval, sclerotized, and connated (i.e., fused along midline), fertilization ducts sclerotized, emerging laterally posteriorly from spermathecae, curving dorsally anteriorly to meet uterus externus (Fig. 62D; Coddington 1986: fig. 215). For further species description details, see Coddington (1986).

Records and biology

Wendilgarda clara is distributed from Guatemala to Brazil, including the West Indies (World Spider Catalog 2025). Records in this study are limited to collections made at 1135 m a.s.l. in premontane rainforest from Reserva Forestal Fortuna (Fig. 1). Males and females have been collected mostly at night by looking down.

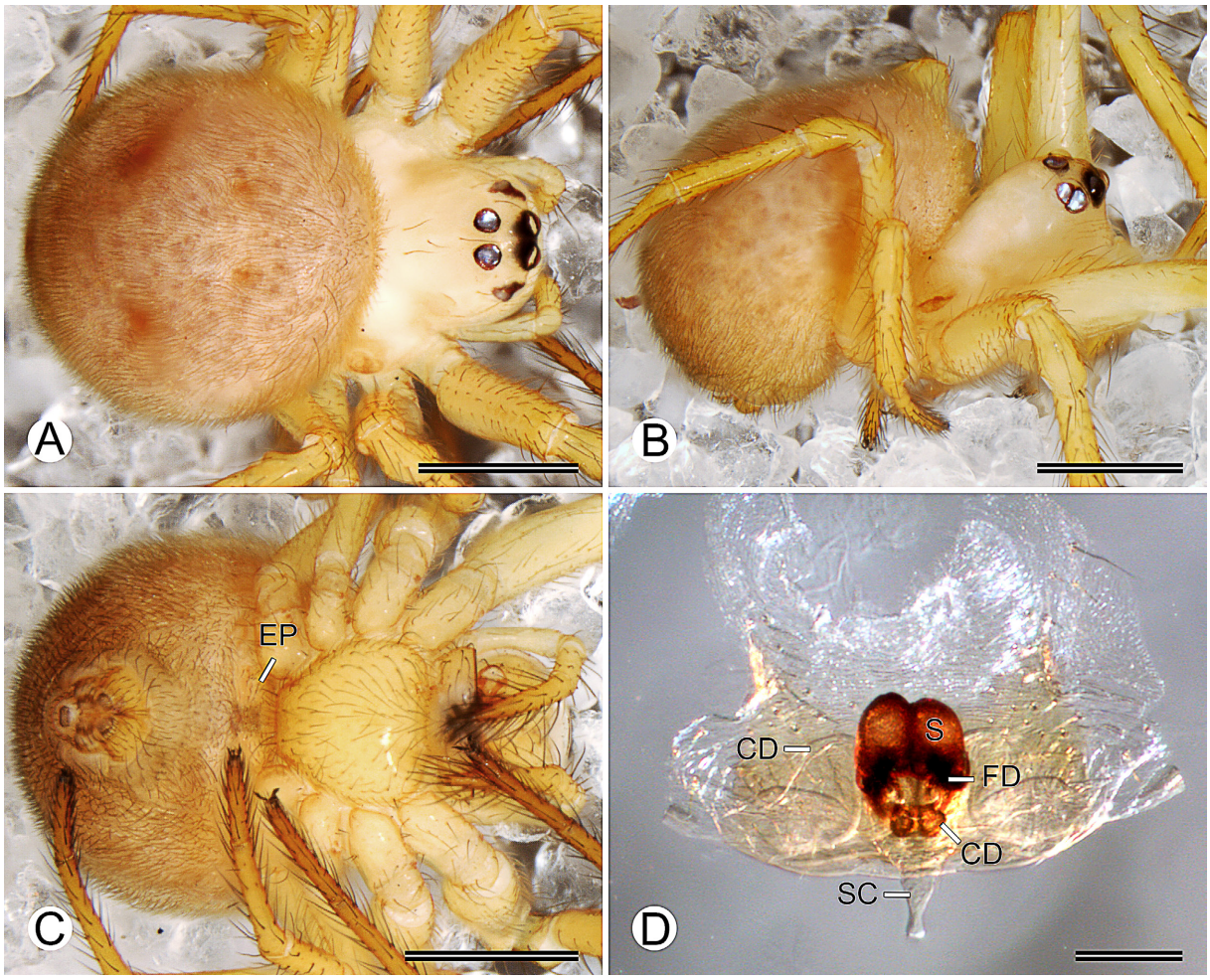

Fig. 62. *Wendilgarda clara* Keyserling, 1886, ♀ (MACN-Ar 29223). **A–C**. Habitus (A = dorsal view; B = lateral view; C = ventral view). **D**. Vulva, dorsal view. Abbreviations: CD = copulatory duct; EP = epigynal plate; FD = fertilization duct; S = spermatheca; SC = dorsal scape. Scale bars: A–C = 0.5 mm; D = 0.1 mm.

Discussion

Taxonomy and species diversity

Species delimitation in Theridiosomatidae is challenging due to the morphological uniformity of the genital structures, a primary diagnostic character in spider taxonomy (Coddington 1986; Labarque & Griswold 2014; Bond *et al*. 2022). Our results indicate that fast morphospecies identification aligned with integrative species recognition in 63% of the cases, while GMYC analysis produced a higher number of putative species (43 clusters). However, upon detailed morphological examination, only 24 of these 40 Panamanian GMYC clusters (60%) could be morphologically diagnosed and formally recognized as species. The remaining 16 groups (40%) lacked diagnostic morphological characters, leading to the decision to merge them into five nominal species based on genital morphology, coloration, and body shape.

This result highlights a central issue in species delimitation using DNA barcoding – single-marker molecular analyses often overestimate species richness due to population-level genetic structuring (Cao *et al*. 2016; Rivera-Quiroz & Álvarez-Padilla 2023). Although DNA barcoding has been successfully applied in spiders (e.g., Castalanelli *et al*. 2014; Oh *et al*. 2022), its use as a standalone species identification tool is controversial (Sharkey *et al*. 2021; Bond *et al*. 2022). Our findings align with studies showing that COI-based species delimitation methods, such as GMYC, tend to fragment populations into multiple genetic clusters that do not always correspond to biologically meaningful species (Pons *et al*. 2006; Wang *et al*. 2008; Cao *et al*. 2016). For this reason, we followed a conservative approach, recognizing only those GMYC clusters that were morphologically diagnosable.

This decision aligns with broader debates in taxonomy about the trade-offs between speed and taxonomic rigor (Godfray 2002, 2007; Godfray *et al*. 2008). The need for faster species documentation has led to proposals for minimalistic, barcode-only taxonomic approaches (Sharkey *et al*. 2021), which prioritize speed at the expense of morphological diagnoses, taxonomic usability, and long-term scientific reliability (Rivera-Quiroz & Álvarez-Padilla 2023). However, integrative approaches – which combine morphology and molecular data – provide greater taxonomic stability and usability (Cao *et al*. 2016; Bond *et al*. 2022). Our study demonstrates that barcoding can aid species discovery but should not replace morphological examination, as morphology remains the most accessible and universally applicable tool for species identification (Rivera-Quiroz & Álvarez-Padilla 2023).

Despite the challenges of morphological identification, our findings support the efficacy of gross morphology as a first-pass sorting tool in Theridiosomatidae. The low degree of morphological misidentification (37%) suggests that morphology-based sorting is efficient for rapid biodiversity assessments, even in challenging taxa (Miller *et al*. 2014; Álvarez-Padilla *et al*. 2020). Additionally, most molecular clusters were geographically restricted, indicating a strong correlation between species distribution and genetic differentiation. Future research integrating broader geographic sampling, nuclear markers, and ecological data will further clarify species boundaries in this group.

Biodiversity assessment

Biodiversity assessments in hyperdiverse tropical ecosystems face significant challenges, particularly in specimen identification and species delimitation (Taylor 1983; de Carvalho *et al.* 2005, 2007). The taxonomic impediment slows the process of species discovery, making it difficult to document biodiversity efficiently (Fontaine *et al*. 2012). Our study compared different species identification methods – morphospecies sorting, GMYC clusters, and integrative species delimitation – to evaluate how different approaches impact biodiversity estimates.

Our results show that alpha diversity estimates were generally consistent across identification methods, with RFF being the richest locality, followed by PILA, COPE, and PNAC. However, beta diversity estimates varied considerably depending on the approach used. While fast morphospecies and integrative methods indicated species sharing across localities, the GMYC approach identified only two shared species between COPE and PNAC, suggesting a much higher species turnover. This discrepancy likely results from the tendency of molecular methods to detect fine-scale population structure rather than species-level differences, potentially inflating species turnover estimates (Cao *et al*. 2016; Rivera-Quiroz & Álvarez-Padilla 2023). Our findings also provide insights into elevational species richness patterns, particularly in relation to Rapoport's rule (Stevens 1989). This rule predicts a decline in species richness with increasing altitude, as species at higher elevations tend to have broader ecological tolerances and larger geographic ranges. However, our results, like those of many previous arthropod studies (Balslev 1988; Olson 1994; Van der Werff & Consiglio 2004), contradict this notion. We found that species richness peaked at the mid-elevations (RFF, 1135 m a.s.l.), rather than decreasing continuously with altitude. This is consistent with previous research indicating that endemism and species richness in tropical arthropods frequently peak at mid- to high elevations, rather than showing the latitudinal or altitudinal decline predicted by Rapoport's rule (Olson 1994; Deltshev 2000). The high proportion of single-locality endemic species at mid- and high elevations sites (PILA and RFF, 72.7% and 64.7% endemism, respectively), further supports the idea that restricted dispersal and specialized ecological requirements may be more influential than broad-scale climatic gradients in structuring spider diversity.

Additionally, unexpected species turnover patterns were detected. RFF shares more species with COPE and PNAC (180–253 km away) than with PILA (only 45 km away). This suggests that geographic proximity alone does not predict species similarity, and that historical biogeographic events, habitat discontinuities, and dispersal barriers may play a significant role in shaping species distributions (Colwell & Coddington 1994; Coddington *et al*. 2009).

Despite these complexities, our sampling completeness analysis suggests that our inventory is nearly complete, with species accumulation curves reaching an asymptote and abundance/incidence-based estimators predicting that only 1–2 species were missed. The low percentage of rare species (4% singletons, 7% doubletons) further supports this conclusion. While additional sampling may still reveal cryptic diversity, these results confirm that the integrative taxonomic framework used here is effective in capturing Theridiosomatidae diversity across Panamanian cloud forests.

Ecological patterns

Environmental factors play a crucial role in shaping the diversity of Theridiosomatidae, particularly through prey availability and web architecture. Theridiosomatids typically construct orb-webs in low vegetation or near the forest floor, primarily preying on nematocerans and other dipterans (Coddington 1986). Previous studies have found a higher dipteran species richness at mid-to-higher elevations (~2000 m a.s.l.) compared to lower elevations (~300 m a.s.l.) in tropical regions (Whittaker 1952; Guevara & Aviles 2009). This pattern is consistent with our findings, as species richness of Theridiosomatidae peaked at mid- to higher elevations, coinciding with a high dipteran diversity. Such a relationship suggests that prey availability may be a key factor driving diversity of Theridiosomatidae across different elevations.

In addition to species richness patterns, Theridiosomatidae exhibit diverse web architectures that reflect adaptations to different ecological niches. The dominant species in our surveyed localities belong to the genera *Naatlo*, *Epilineutes*, and *Tantra* gen. nov., all of which construct complete or anastomosed orb webs with a tension line that distorts the web into a conical shape (Coddington 1986). This structure allows spiders to catapult their prey into the web upon release of tension, an effective strategy for

capturing flying insects (Coddington 1986). Other genera display distinct web modifications and behavioral adaptations. For example, species of *Ogulnius* construct irregular webs near the leaf litter, species of *Wendilgarda* spin highly modified webs with vertical sticky lines in contact with water surfaces, and species of *Chthonos* likely do not spin webs at all (Coddington 1989; Cotoras *et al.* 2021). The presence of these specialized web types suggests that Theridiosomatidae have diversified their foraging strategies in response to different environmental conditions and prey availability.

While our standardized sampling methods were effective in capturing species-rich genera with conspicuous web structures, we recognize that certain genera may be underrepresented due to a collection bias. Species with cryptic behaviors (e.g., web-less *Chthonos*) or microhabitat specialization (e.g., *Wendilgarda* near water) may require targeted sampling efforts to fully assess their diversity. Future research incorporating behavioral observations and habitat-specific sampling will provide further insights into the ecological roles and web diversity of Theridiosomatidae.

Concluding remarks

The urgency of biodiversity documentation has never been greater, given the ongoing global biodiversity crisis (Myers *et al*. 2000; Godfray 2002, 2007; Rivera-Quiroz & Álvarez-Padilla 2023). Our study demonstrates how integrative taxonomic approaches can accelerate species discovery while maintaining scientific rigor and taxonomic usability. By combining standardized sampling methods, morphological assessments, and DNA barcoding, we unveiled 29 species of ray spiders, including 27 novel to science. These findings contribute not only to taxonomy but also to a wider ecological and biogeographic research, reinforcing the importance of detailed species documentation for conservation and biodiversity assessments (Coddington *et al*. 2009; Bond *et al*. 2022).

As highlighted in recent discussions on taxonomic workflows, the minimization of morphological data in favor of barcode-based species recognition speeds up descriptions but risks reducing the usability and robustness of taxonomic literature (Sharkey *et al*. 2021; Rivera-Quiroz & Álvarez-Padilla 2023). While metabarcoding and metagenomic approaches provide powerful tools for large-scale biodiversity monitoring (Janzen *et al*. 2009; Meier *et al*. 2021), our results show that morphology remains essential for making accurate taxonomic decisions and formally describing species. This study reinforces that integrative approaches, which incorporate multiple lines of evidence, remain the most effective strategy for robust species delimitation (Cao *et al*. 2016; Bond *et al*. 2022).

Beyond taxonomic methodology, our results also highlight critical biodiversity patterns in Neotropical cloud forests. The high levels of species endemism observed at mid- to high elevations emphasize the importance of these habitats for conservation efforts (Olson 1994; Deltshev 2000; Van der Werff & Consiglio 2004). Moreover, our findings regarding species turnover and unexpected geographic patterns suggest that future biogeographic research should consider historical dispersal limitations and microhabitat specialization as key drivers of spider diversity.

Moving forward, we advocate collaborative, open-access taxonomic efforts that integrate morphological, molecular, and ecological data (Miller *et al*. 2014; Álvarez-Padilla *et al*. 2020). The taxonomic impediment will not be solved solely by accelerating descriptions, but by making taxonomic data more accessible, reproducible, and useful for scientific and conservation applications (Bond *et al*. 2022; Rivera-Quiroz & Álvarez-Padilla 2023). By combining traditional taxonomic expertise with modern molecular tools, we can ensure that species descriptions are not only rapid but also robust and scientifically valuable.

Acknowledgments

We extend our gratitude to our dear friends and colleagues Ligia Benavides Silva and Dimitar Dimitrov, whose participation during the inventories was indispensable. We are extremely grateful to our cherished friends Mónica Mejia and Temistocles "Temi" Tejedor, whose warm hospitality, unwavering friendship, and invaluable support were essential to the success of this project. We are also deeply appreciative of the invaluable support and cooperation extended by the authorities and dedicated staff at the Smithsonian Tropical Research Institution (STRI, Panama), as well as the diligent park rangers, who not only facilitated our logistical needs but also assisted with the collecting permits and provided crucial field assistance within the Panamanian National Parks. We owe special thanks to Carlos Espinoza and Alberto González for their logistical support in the Fortuna Forest Reserve (RFF), and to Amarilis Mendoza, director of the National Environmental Authority ANAM of La Chorrera (Panama), for her instrumental role in making fieldwork possible at the Altos de Campana National Park (PNAC). We are also indebted to the anonymous reviewers whose insightful comments and suggestions greatly enriched the manuscript. Furthermore, FML wishes to thank Nuria Macías-Hernández, Leticia Bidegaray-Batista, Carles Ribera, Gema Blasco-Melia (CRBA), Fabián Tricárico (MACN-Ar), and Scott Serrata (CAS) for their invaluable assistance and training in molecular laboratory techniques and SEM imaging. FML thank the Biodiversity Institute of Ontario (BIO) and the Canadian Center for DNA Barcoding (CCDB) for supported a stay and for sequencing samples for this study, and Paul Hebert, Alex Borisenko, Natalia Ivanova, Alex Smith, Rick Turner, Gergin Blagoev and Nadya Nikolova for help during the stay. FML also express his gratitude to a postdoctoral fellowship from the Schlinger Chair of Arachnology at the California Academy of Sciences, two postdoctoral grants from the Fundação de Amparo à Pesquisa do Estado de São Paulo (FAPESP 2014/23369-2 and 2018/20625-9), and a doctoral scholarship from Consejo Nacional de Investigaciones Científicas y Técnicas (CONICET) for their support. JP and MA wish to thank the Fundación BBVA for their support through the 3rd Call for Research Grants in Conservation Biology. MR was supported by a FONCYT grant PICT-2019-2745. GH acknowledges support from US National Science foundation DEB grants 1457300, 1754289 and 2154246.

References

Agnarsson I., Coddington J.A., & Kuntner M. 2013. Systematics: progress in the study of spider diversity and evolution. *In*: Penney D. (ed.) *Spider Research in the 21st Century: Trends and Perspectives*: 58–111. Siri Scientific Press, Rochdale, UK.

Altschul S., Madden T., Schäffer A., Zhang J., Zhang Z., Miller W. & Lipman D. 1997. Gapped BLAST and PSI-BLAST: a new generation of protein database search programs. *Nucleic Acids Research* 25 (17): 3389–3402. https://doi.org/10.1093/nar/25.17.3389

Álvarez-Padilla F., Galán-Sánchez M.A. & Salgueiro-Sepúlveda F.J. 2020. A protocol for online documentation of spider biodiversity inventories applied to a Mexican tropical wet forest (Araneae, Araneomorphae). *Zootaxa* 4722 (3): 241–269. https://doi.org/10.11646/zootaxa.4722.3.3

Archer A.F. 1953. Studies in the orbweaving spiders (Argiopidae). 3. *American Museum Novitates* 1622: 1–27.

Astrin J.J., Huber B.A., Misof B. & Klütsch C.F.C. 2006. Molecular taxonomy in pholcid spiders (Pholcidae, Araneae): evaluation of species identification methods using CO1 and 16S rRNA. *Zoologica Scripta* 35 (5): 441–457. https://doi.org/10.1111/j.1463-6409.2006.00239.x

Baert L. 2014. New spider species (Araneae) from the Galápagos Islands (Ecuador). *Bulletin de la Société royale belge d'Entomologie/Bulletin van de Koninklijke Belgische Vereniging voor Entomologie* 149: 263–271.

Ballarin F., Yamasaki T. & Su Y.C. 2021. A survey on poorly known rainforest litter-dwelling spiders of Orchid Island (Lanyu, Taiwan) with the description of a new species (Araneae: Linyphiidae, Tetrablemmidae, and Theridiosomatidae). *Zootaxa* 4927 (2): 197–208. https://doi.org/10.11646/zootaxa.4927.2.2

Balslev H. 1988. Distribution patterns of Ecuadorean plant species. *Taxon* 37: 567–577. https://doi.org/10.2307/1221100

Bond J.E., Godwin R.L., Colby J.D., Newton L.G., Zahnle X.J., Agnarsson I., Hamilton C.A. & Kuntner M. 2022. Improving taxonomic practices and enhancing its extensibility—An example from araneology. *Diversity* 14 (1): 5. https://doi.org/10.3390/d14010005

Britton T., Anderson C.L., Jacquet D., Lundqvist S. & Bremer K. 2007. Estimating divergence times in large phylogenetic trees. *Systematic Biology* 56: 741–752. https://doi.org/10.1080/10635150701613783

Burnham K.P. & Overton W.S. 1978. Estimation of the size of a closed population when capture probabilities vary among animals. *Biometrika* 65: 623–633. https://doi.org/10.2307/2335915

Burnham K.P. & Overton W.S. 1979. Robust estimation of population size when capture probabilities vary among animals. *Ecology* 60: 927–936. https://doi.org/10.2307/1936861

Cao X., Liu J., Chen J., Zheng G., Kuntner M. & Agnarsson I. 2016. Rapid dissemination of taxonomic discoveries based on DNA barcoding and morphology. *Scientific Reports* 6: 37066. https://doi.org/10.1038/srep37066

de Carvalho M.R., Bockmann F.A., Amorim D.S., de Vivo M., de Toledo-Piza M., Menezes N.A., de Figueiredo J.L., Castro R.M.C., Gill A.C., Mceachran J.D., Compagno L.J.V., Schelly R.C., Britz R., Lundberg J.G., Vari R.P. & Nelson G. 2005. Revisiting the taxonomic impediment. *Science* 307: 353–4. https://doi.org/10.1126/science.307.5708.353b

de Carvalho M.R., Bockmann F.A., Amorim D.S., Brandão C.R.F., de Vivo M., de Figueiredo J.L., Bristki H.A., de Pinna M.C.C., Menezes N.A., Maques F.P.L., Papavero N., Cancello E.M., Crisci J.V., Mceachran J.D., Schelly R.C., Lundberg J.G., Gill A.C., Britz R., Wheeler Q.D., Stiassny M.L., Parenti L.R., Page L.M., Wheeler W.C., Faivovich J., Vari R.P., Grande L., Humphries C.J., DeSalle R., Ebach M.C. & Nelson G.J. 2007. Taxonomic impediment or impediment to taxonomy? A commentary on systematics and the cybertaxonomic-automation paradigm. *Evolutionary Biology* 34: 140–143. https://doi.org/10.1007/s11692-007-9011-6

Castalanelli M.A., Teale R., Rix M.G., Kennington W.J. & Harvey M.S. 2014. Barcoding of mygalomorph spiders (Araneae: Mygalomorphae) in the Pilbara bioregion of Western Australia reveals a highly diverse biota. *Invertebrate Systematics* 28 (4): 375–385. https://doi.org/10.1071/IS13058

Chamberlin R.V. & Ivie W. 1944. Spiders of the Georgia region of North America. *Bulletin of the University of Utah* 35 (9): 1–267. https://doi.org/10.1093/aesa/38.2.167

Chao A. 1984. Non-parametric estimation of the number of classes in a population. *Scandanavian Journal of Statistics* 11: 265–270.

Chao A. 1987. Estimating the population size for capture-recapture data with unequal catchability. *Biometrics* 43: 783–791. https://doi.org/10.2307/2531532

Chao A., Chazdon R.L., Colwell R.K. & Shen T. 2005. Capítulo 7. Un nuevo método estadístico para la evaluación de la similitud en la composición de especies con datos de incidencia y abundancia. *In*: Halffter G., Soberón J., Koleff P. & Melic A. (eds) *Sobre Diversidad Biológica: El significado de las diversidades alfa, beta y gamma*. m3m: Monografías Tercer Milenio, 4, Sociedad Entomológica Aragonesa, Zaragoza, Spain.

Chazdon R.L., Colwell R.K., Denslow J.S. & Guariguata M.R. 1998. Statistical methods for estimating species richness of woody regeneration in primary and secondary rain forests of NE Costa Rica. *In*: Dallmeier F. & Comiskey J.A. (eds) *Forest Biodiversity Research, Monitoring and Modeling: Conceptual Background and Old World Case Studies*: 285–309. Parthenon Publishing, Paris.

Clement M., Posada D. & Crandall K.A. 2000. TCS: a computer program to estimate gene genealogies. *Molecular Ecology* 9: 1657–1659. https://doi.org/10.1046/j.1365-294x.2000.01020.x

Clerck C. 1757. *Aranei Svecici. Svenska spindlar, uti sina hufvud-slågter indelte samt under några och sextio särskildte arter beskrefne och med illuminerade figurer uplyste*. Laurentius Salvius, Stockholmiae [= Stockholm]. https://doi.org/10.5962/bhl.title.119890

Coddington J.A. 1986. The genera of the spider family Theridiosomatidae. *Smithsonian Contribution to Zoology* 422: 1–96. https://doi.org/10.5479/si.00810282.422

Coddington J.A. & Valerio C.G. 1980. Observations on the web and behavior of *Wendilgarda* spiders (Araneae: Theridiosomatidae). *Psyche* 87 (1–2): 93–105. https://doi.org/10.1155/1980/69153

Coddington J.A., Griswold C.E., Dávila D.S., Peñaranda E. & Larcher S.F. 1991. Designing and testing sampling protocols to estimate biodiversity in tropical ecosystems. *In*: Dudley E.C. (ed.) *The Unity of Evolutionary Biology: Proceedings of the Fourth International Congress of Systematics and Evolutionary Biology*: 44–60. Discorides Press, Portland, Oregon, USA.

Coddington J.A., Young L.H. & Coyle F.A. 1996. Estimating spider species richness in a southern Appalachian cove hardwood forest. *The Journal of Arachnology* 24: 111–128.

Coddington J.A., Agnarsson I., Miller J.A., Kunter M. & Hormiga G. 2009. Undersampling bias: the null hypothesis for singleton species in tropical arthropod surveys. *Journal of Animal Ecology* 78 (3): 573–584. https://doi.org/10.1111/j.1365-2656.2009.01525.x

Coddington J.A., Agnarsson I., Cheng R.C., Čandek K., Driskell A., Frick H., Gregorič M., Kostanjšek R., Kropf C., Kweskin M., Lokovšek T., Pipan M., Vidergar N. & Kuntner M. 2016. DNA barcode data accurately assign higher spider taxa. *PeerJ* 4: e2201. https://doi.org/10.7717/peerj.2201

Colwell R.K. 2004. EstimateS: statistical estimation of species richness and shared species from samples (software and user's guide). Ver. 9.1. Available from https://www.robertkcolwell.org/pages/1407 [accessed 19 Mar. 2023].

Colwell R.K. & Coddington J.A. 1994. Estimating terrestrial biodiversity through extrapolation. *Philosophical Transactions of the Royal Society of London B – Biological Sciences* 345: 101–118. https://doi.org/10.1098/rstb.1994.0091

Colwell R.K., Mao C.X. & Chang J. 2005. Capítulo 6. Interpolando, extrapolando y comparando las curvas de acumulación de especies basadas en su incidencia. *In*: Halffter G., Soberón J., Koleff P. & Melic A. (eds) *Sobre Diversidad Biológica: El significado de las diversidades alfa, beta y gamma*. m3m: Monografías Tercer Milenio, 4, Sociedad Entomológica Aragonesa, Zaragoza, España.

Cotoras D.D., Suenaga M. & Mikheyev A.S. 2021. Intraspecific niche partition without speciation: individual level web polymorphism within a single island spider population. *Proceedings of the Royal Society B – Biological Sciences* 288: 20203138.20203138. http://doi.org/10.1098/rspb.2020.3138

Dayrat B. 2005. Towards integrative taxonomy. *Biological Journal of the Linnean Society* 85: 407–15. https://doi.org/10.1111/j.1095-8312.2005.00503.x

Deltshev C. 2000. The endemic spiders (Araneae) of the Balkan Peninsula. *Ekológia (Bratislava)* 19 (3): 59–65.

Dupérré N. & Tapia E. 2017. On some minuscule spiders (Araneae: Theridiosomatidae, Symphytognathidae) from the Chocó region of Ecuador with the description of ten new species. *Zootaxa* 4341 (3): 375–399. https://doi.org/10.11646/zootaxa.4341.3.3

Ezard T., Fujisawa T. & Barraclough T. 2009. 'Splits: SPecies' limits by threshold statistics. R Package Ver. 1.0. Available from http://r-forge.r-project.org/projects/splits [accessed 19 Mar. 2023].

Folmer O., Black M., Hoeh W., Lutz R. & Vrijenhoek R. 1994. DNA primers for amplification of mitochondrial cytochrome c oxidase subunit I from diverse metazoan invertebrates. *Molecular Marine Biology Biotechnology* 3 (5): 294–299.

Fontaine B., Perrard A. & Bouchet P. 2012. 21 years of shelf life between discovery and description of new species. *Current Biology* 22 (22): R943–R944. https://doi.org/10.1016/j.cub.2012.10.029

Fujisawa T. & Barraclough T.G. 2013. Delimiting species using single-locus data and the generalized mixed Yule coalescent approach: a revised method and evaluation on simulated data sets. *Systematic Biology* 62 (5): 707–724. https://doi.org/10.1093/sysbio/syt033

Godfray H.C.J. 2002. Challenges for taxonomy. *Nature* 417 (6884): 17–19. https://doi.org/10.1038/417017a

Godfray H.C.J. 2007. Linnaeus in the information age. *Nature* 446 (7133): 259–260. https://doi.org/10.1038/446259a

Godfray H.C.J., Mayo S.J. & Scoble M.J. 2008. Pragmatism and rigour can coexist in taxonomy. *Evolutionary Biology* 35: 309–311. https://doi.org/10.1007/s11692-008-9041-8

Guevara J. & Avilés L. 2009. Elevational changes in the composition of insects and other terrestrial arthropods at tropical latitudes: a comparison of multiple sampling methods and social spider diets. *Insect Conservation and Diversity* 2: 142–152. https://doi.org/10.1111/j.1752-4598.2008.00043.x

Hall T.A. 1999. BioEdit: a user-friendly biological sequence alignment editor and analysis program for Windows 95/98/NT. *Nucleic Acids Symposium Serie* 41: 95–98.

Hebert P.D.N., Cywinska A., Ball S.L. & deWaard J.R. 2003a. Biological identification through DNA barcodes. *Proceedings of the Royal Society of London B – Biological Sciences* 270: 313–321. https://doi.org/10.1098/rspb.2002.2218

Hebert P.D.N., Ratnasingham S. & deWaard J.R. 2003b. Barcoding animal life: cytochrome c oxidase subunit 1 divergences among closely related species. *Proceedings of the Royal Society of London B – Biological Sciences* 270 (Supplement 1): S96–9. https://doi.org/10.1098/rsbl.2003.0025

Hebert P.D.N., Penton E.H., Burns J.M., Janzen D.H. & Hallwachs W. 2004. Ten species in one: DNA barcoding reveals cryptic species in the neotropical skipper butterfly *Astraptes fulgerator*. *PNAS* 101 (41): 14812–14817. https://doi.org/10.1073/pnas.0406166101

Hickman V.V. 1931. A new family of spiders. *Proceedings of the Zoological Society of London (B)* 101 (4): 1321–1328. https://doi.org/10.1111/j.1096-3642.1931.tb01063.x

Ivanova N.V. & Grainger C.M. 2007. CCDB Protocols, COI Amplification. Available from https://ccdb.ca/site/wp-content/uploads/2016/09/CCDB_Amplification.pdf [accessed 19 Mar. 2023].

Ivanova N.V., deWaard J. & Hebert P.D.N. 2006. An inexpensive, automation-friendly protocol for recovering high-quality DNA. *Molecular Ecology Notes* 6: 998–1002. https://doi.org/10.1111/j.1471-8286.2006.01428.x

Janzen D.H., Hallwachs W., Blandin P., Burns J.M., Cadiou J.M., Chacon I., Dapkey T., Deans A.R., Epstein M.E., Espinoza B., Franclemont J.G., Haber W.A., Hajibabaei M., Hall J.P.W., Hebert P.D.N.,

Gauld I.D., Harvey D.J., Hausmann A., Kitching I.J., Lafontaine D., Landry J., Lemaire C., Miller J.Y., Miller J.S., Miller L., Miller S.E., Montero J., Munroe E., Green S.R., Ratnasingham S., Rawlins J.E., Robbins R.K., Rodriguez J.J., Rougerie R., Sharkey M.J., Smith M.A., Solis M.A., Sullivan J.B., Thiaucourt P., Wahl D.B., Weller S.J., Whitfield J.B., Willmott K.R., Wood D.M., Woodley N.E. & Wilson J.J. 2009. Integration of DNA barcoding into an ongoing inventory of complex tropical biodiversity. *Molecular Ecology Resources* 9: 1–26. https://doi.org/10.1111/j.1755-0998.2009.02628.x

Keyserling E. 1886. *Die Spinnen Amerikas. Theridiidae*. Verlag von Bauer & Raspe (E. Küster), Nürnberg. https://doi.org/10.5962/bhl.title.64832

Khmelik V.V., Kozub D. & Glazunov A. 2006. Helicon Focus. Ver. 3.10.3. and 4.01. Available from https://www.heliconsoft.com/heliconsoft-products/helicon-focus/ [accessed 19 Mar. 2023].

Koch L. 1877. Verzeichniss der bei Nürnberg bis jetzt beobachteten Arachniden (mit Ausschluss der Ixodiden und Acariden) und Beschreibungen von neuen, hier vorkommenden Arten. *Abhandlungen der Naturhistorischen Gesellschaft zu Nürnberg* 6: 113–198.

Kulkarni S., Wood H., Lloyd M. & Hormiga G. 2020. Spider-specific probe set for ultraconserved elements offers new perspectives on the evolutionary history of spiders (Arachnida, Araneae). *Molecular Ecology Resources* 20 (1): 185–203. https://doi.org/10.1111/1755-0998.13099

Kulkarni S., Wood H.M. & Hormiga G. 2023. Phylogenomics illuminates the evolution of orb webs, respiratory systems and the biogeographic history of the world's smallest orb-weaving spiders (Araneae, Araneoidea, Symphytognathoids). *Molecular Phylogenetics and Evolution* 186: e107855. https://doi.org/10.1016/j.ympev.2023.107855

Labarque F.M. & Griswold C.E. 2014. New ray spiders from Southeast Asia: The new Philippine genus *Tagalogonia* gen. nov. and continental genus *Coddingtonia* Miller, Griswold & Yin, 2009 (Araneae: Theridiosomatidae), with comments on their intergeneric relationships. *In*: William C. & Gosliner T. (eds) *The Coral Triangle: The 2011 Hearts Philippine Biodiversity Expedition*: 407–426. California Academy of Sciences, San Francisco, California.

Lamarck J.B.P.A. 1801. *Système des animaux sans vertèbres*. Paris, l'auteur. https://doi.org/10.5962/bhl.title.14255

Librado P. & Rozas J. 2009. DnaSP v5: A software for comprehensive analysis of DNA polymorphism data. *Bioinformatics* 25: 1451–1452. https://doi.org/10.1093/bioinformatics/btp187

Lopardo L. & Hormiga G. 2015. Out of the twilight zone: phylogeny and evolutionary morphology of the orb-weaving spider family Mysmenidae, with a focus on spinneret spigot morphology in symphytognathoids (Araneae, Araneoidea). *Zoological Journal of the Linnean Society* 173: 527–786. https://doi.org/10.1111/zoj.12199

Lopardo L. & Uhl G. 2014. Testing mitochondrial marker efficacy for DNA barcoding in spiders: a test case using the dwarf spider genus *Oedothorax* (Araneae : Linyphiidae : Erigoninae). *Invertebrate Systematics* 28: 501–521. https://doi.org/10.1071/IS14017

Lopardo L., Giribet G. & Hormiga G. 2010. Morphology to the rescue: molecular data and the signal of morphological characters in combined phylogenetic analyses—a case study on mysmenid spiders (Araneae, Mysmenidae), with comments on the evolution of web architecture. *Cladistics* 27: 278–330. https://doi.org/10.1111/j.1096-0031.2010.00332.x

Lopez A. & Emerit M. 1986. *Wendilgarda mustelina arnouxi* n. ssp et la glande labio-sternale des Theridiosomatidae (Araneae). *Mémoires de Biospéologie* 12: 67–76.

Meier R., Blaimer B.B., Buenaventura E., Hartop E., Srivathsan A. & Yeo D. 2021. A re-analysis of the data in Sharkey *et al*.'s (2021) minimalist revision reveals that BINs do not deserve names, but BOLD Systems needs a stronger commitment to open science. *Cladistics* 38 (2): 264–275. https://doi.org/10.1111/cla.12489

Messing J. 1983. [2] New M13 vectors for cloning. *Methods in Enzymology* 101: 20–78. https://doi.org/10.1016/0076-6879(83)01005-8

Miller J.A., Griswold C.E. & Yin C.M. 2009. The symphytognathoid spiders of the Gaoligongshan, Yunnan, China (Araneae, Araneoidea): Systematics and diversity of micro-orbweavers. *ZooKeys* 11: 9–195. https://doi.org/10.3897/zookeys.11.160

Miller J.A., Miller J.H., Pham D.S. & Beentjes K.K. 2014. Cyberdiversity: improving the informatic value of diverse tropical arthropod inventories. *PLoS One* 9 (12): e115750. https://doi.org/10.1371/journal.pone.0115750

Miller M.A., Pfeiffer W. & Schwartz T. 2010. Creating the CIPRES Science Gateway for inference of large phylogenetic trees. *In*: IEEE *Proceedings of the Gateway Computing Environments Workshop (GCE)*: 1–8. New Orleans, LA. https://doi.org/10.1109/GCE.2010.5676129

Monaghan M.T., Wild R., Elliot M., Fujisawa T., Balke M., Inward D.J.G., Lees D.C., Ranaivosolo R., Eggleton P., Barraclough T.G. & Vogler A.P. 2009. Accelerated species inventory on Madagascar using coalescent-based models of species delineation. *Systematic Biology* 58 (3): 298–311. https://doi.org/10.1093/sysbio/syp027

Myers N., Mittermeier R.A., Mittermeier C.G., da Fonseca G.A.B. & Kent J. 2000. Biodiversity hotspots for conservation priorities. *Nature* 403: 853–858. https://doi.org/10.1038/35002501

Nogueira A., Pinto-da-Rocha R. & Brescovit A. 2006. Comunidade de aranhas orbitelas (Arachnida, Araneae) na região da Reserva Florestal do Morro Grande, Cotia, São Paulo, Brasil. *Biota Neotropica* 6: 1–24.

Oh J.H., Kim S. & Lee S. 2022. DNA barcodes reveal population-dependent cryptic diversity and various cases of sympatry of Korean leptonetid spiders (Araneae: Leptonetidae). *Scientific Reports* 12 (1): 1–16. https://doi.org/10.1038/s41598-022-18666-y

Oliver I. & Beattie A.J. 1996. Invertebrate morphospecies as surrogates for species: A case study. *Conservation Biology* 10 (1): 99–109. https://doi.org/10.1046/j.1523-1739.1996.10010099.x

Olson D.M. 1994. The distribution of leaf litter invertebrates along a Neotropical altitudinal gradient. *Journal of Tropical Ecology* 10 (2): 129–150. https://doi.org/10.1017/S0266467400007793

Padial J., Castroviejo-Fisher S., Kohler J., Vila C., Chaparro J. & De la Riva I. 2009. Deciphering the products of evolution at the species level: the need for an integrative taxonomy. *Zoologica Scripta* 38: 431–447. https://doi.org/10.1111/j.1463-6409.2008.00381.x

Paradis E., Claude J. & Strimmer K. 2004. APE: analyses of phylogenetics and evolution in R language. *Bioinformatics* 20: 289–290. https://doi.org/10.1093/bioinformatics/btg412

Petrunkevitch, A. 1928. Systema Aranearum. *Transactions of the Connecticut Academy of Arts and Sciences* 29: 1–270.

Petrunkevitch A. 1930. The spiders of Porto Rico. Part two. *Transactions of the Connecticut Academy of Arts and Sciences* 30: 159–356.

Pickard-Cambridge F.O.1902. Arachnida - Araneida and Opiliones. *Biologia Centrali-Americana, Zoology, London* 2: 313–424.

Pickard-Cambridge O. 1879. On some new and rare British spiders, with characters of a new genus. *Annals and Magazine of Natural History* (5) 4 (21): 190–215. https://doi.org/10.1080/00222937908679818

Pickard-Cambridge O. 1882. On new genera and species of Araneidea. *Proceedings of the Zoological Society of London* 50 (3): 423–442. https://doi.org/10.1111/j.1096-3642.1882.tb02749.x

Pickard-Cambridge O. 1894. Arachnida. Araneida. *Biologia Centrali-Americana, Zoology, London* 1: 121–144.

Pickard-Cambridge O. 1896. Arachnida. Araneida. *Biologia Centrali-Americana, Zoology, London* 1: 161–224.

Planas E., Fernández-Montraveta C. & Ribera C. 2013. Molecular systematics of the wolf spider genus *Lycosa* (Araneae: Lycosidae) in the Western Mediterranean Basin. *Molecular Phylogenetics and Evolution* 67 (2): 414–428. https://doi.org/10.1016/j.ympev.2013.02.006

Pons J., Barraclough T.G., Gomez-Zurita J., Cardoso A., Duran D.P., Hazell S., Kamoun S., Sumlin W.D. & Vogler A.P. 2006. Sequence-based species delimitation for the DNA taxonomy of undescribed insects. *Systematic Biology* 55: 595–609. https://doi.org/10.1080/10635150600852011

Posada D. 2004. *Collapse: Describing Haplotypes from Sequence Alignments. Ver. 1.2*. University of Vigo, Vigo, Spain. Available from https://www.softpedia.com/get/Science-CAD/Collapse.shtml [accessed 19 Mar. 2023].

Powell J.R., Monaghan M.T., Öpik M. & Rillig M.C. 2011. Evolutionary criteria outperform operational approaches in producing ecologically relevant fungal species inventories. *Molecular Ecology* 20 (3): 655–666. https://doi.org/10.1111/j.1365-294X.2010.04964.x

Rambaut A. 2006–2014. *Tree Figure Drawing Tool. Ver. 1.4*. Institute of Evolutionary Biology, University of Edinburgh. Available from http://tree.bio.ed.ac.uk/ [accessed 19 Mar. 2023].

Ratnasingham S. & Hebert P.D.N. 2007. BOLD: The Barcode of Life Data System (www.barcodinglife.org). *Molecular Ecology Notes* 7: 355–364. https://doi.org/10.1111/j.1471-8286.2007.01678.x

Ricetti J. & Bonaldo A. 2008. Diversidade e estimativas de riqueza de aranhas em quatro fitofisionomias na Serra do Cachimbo, Pará, Brasil. *Iheringia, Série Zoologia* 98: 88–99. https://doi.org/10.1590/S0073-47212008000100013

Rivera-Quiroz F.A. & Álvarez-Padilla F. 2023. Integration or minimalism: twenty-one new species of ghost spiders (Anyphaenidae: Anyphaena) from Mexico. *European Journal of Taxonomy* 865: 1–94. https://doi.org/10.5852/ejt.2023.865.2097

Rodrigues E.N.L. & Ott R. 2005. Nova espécie de *Theridiosoma* (Araneae, Theridiosomatidae) do sul do Brasil. *Iheringia, Série Zoologia, Porto Alegre* 95 (1): 79–81. https://doi.org/10.1590/S0073-47212005000100011

Saaristo M.I. 1996. Theridiosomatid spiders of the granitic islands of Seychelles (Araneae, Theridiosomatidae). *Phelsuma* 4: 48–52.

Saaristo M.I. 2010. Araneae. *In*: Gerlach J. & Marusik Y.M. (eds) *Arachnida and Myriapoda of the Seychelles Islands*: 8–306. Siri Scientific Press, Manchester.

Sanger F., Nicklen S. & Coulson A.R. 1977. DNA sequencing with chain-terminating inhibitors. *PNAS* 74 (12): 5463–5467. https://doi.org/10.1073/pnas.74.12.5463

Scharff N., Coddington J.A., Griswold C.E., Hormiga G. & De Place Bjorn P. 2003. When to quit? Estimating spider species richness in a northern European deciduous forest. *Journal of Arachnology* 31: 246–273. https://doi.org/10.1636/0161-8202(2003)031[0246:WTQESS]2.0.CO;2

Sharkey M.J., Janzen D.H., Hallwachs W., Chapman E.G., Smith M.A., Dapkey T., Brown A., Ratnasingham S., Naik S., Manjunath R., Perez K., Milton M., Hebert P., Shaw S.R., Kittel R.N., Solis M.A., Metz M.A., Goldstein P.Z., Brown J.W., Quicke D.L.J., Achterberg C.V., Brown B.V. & Burns J.M. 2021. Minimalist revision and description of 403 new species in 11 subfamilies of Costa Rican braconid parasitoid wasps, including host records for 219 species. *ZooKeys* 1013: 1–665. https://doi.org/10.3897/zookeys.1013.55600

Simon E. 1881. *Les arachnides de France. Tome cinquième, première partie.* Roret, Paris.

Simon E. 1895. *Histoire naturelle des araignées. Deuxième édition, tome premier.* Roret, Paris, 761–1084. https://doi.org/10.5962/bhl.title.51973

Simon E. 1897. Études arachnologiques. 27e Mémoire. XLII. Descriptions d'espèces nouvelles de l'ordre des Araneae. *Annales de la Société entomologique de France* 65: 465–510.

Simon E. 1898. On the spiders of the island of St Vincent. Part III. *Proceedings of the Zoological Society of London* 65 (4): 860–890. https://doi.org/10.1111/j.1096-3642.1898.tb01390.x

Sørensen L.L., Coddington J.A. & Scharff N. 2002. Inventorying and estimating subcanopy spider diversity using semiquantitative sampling methods in an Afromontane forest. *Environmental Entomology* 31: 319–330. https://doi.org/10.1603/0046-225X-31.2.319

Stamatakis A. 2006. RAxML-VI-HPC: Maximum likelihood-based phylogenetic analyses with thousands of taxa and mixed models. *Bioinformatics* 22 (21): 2688–2690. https://doi.org/10.1093/bioinformatics/btl446

Stamatakis A. 2014. RAxML Version 8: A tool for phylogenetic analysis and post-analysis of large phylogenies. *Bioinformatics* 30 (9): 1312–1313. https://doi.org/10.1093/bioinformatics/btu033

Stamatakis A., Hoover P. & Rougemont J. 2008. A rapid bootstrap algorithm for the RAxML web-servers. *Systematic Biology* 57 (5): 758–771. https://doi.org/10.1080/10635150802429642

Stevens G.C. 1989. The latitudinal gradient in geographical range: how so many species coexist in the tropics. *American Naturalist* 133: 240–256. https://doi.org/10.1086/284913

Suzuki Y., Serita R. & Hiramatsu T. 2020. Japanese spiders of the genus *Theridiosoma* (Araneae: Theridiosomatidae) with the description of four new species. *Acta Arachnologica* 69 (2): 133–150. https://doi.org/10.2476/asjaa.69.133

Suzuki Y., Hiramatsu T. & Tatsuta H. 2022. Two new species and a new genus of ray spiders (Araneae, Theridiosomatidae) from the Ryukyu Islands, southwest Japan, with notes on their natural history. *ZooKeys* 1109: 76–101. https://doi.org/10.3897/zookeys.1109.83807

Talavera G., Dincă V. & Vila R. 2013. Factors affecting species delimitations with the GMYC model: insights from a butterfly survey. *Methods in Ecology and Evolution* 4 (12): 1101–1110. https://doi.org/10.1111/2041-210X.12107

Taylor R.W. 1983. Descriptive taxonomy: past, present, and future. *In*: Highley E. & Taylor R.W. (eds) *Australian Systematic Entomology: A Bicentenary Perspective*: 93–134. CSIRO, Melbourne.

Van der Werff H. & Consiglio T. 2004. Distribution and conservation significance of endemic species of flowering plants in Peru. *Biodiversity and Conservation* 13: 1699–1713. https://doi.org/10.1023/B:BIOC.0000029334.69717.f0

Víquez C. 2020. Aracnofauna (Arachnida) de la Isla del Coco, Costa Rica, con la descripción de tres nuevas especies. *Revista de Biología Tropical* 68 (1): S115–S143. https://doi.org/10.15517/rbt.v68iS1.41174

Wang Q., Li S., Wang R. & Paquin P. 2008. Phylogeographic analysis of Pimoidae (Arachnida: Araneae) inferred from mitochondrial cytochrome c oxidase subunit I and nuclear 28S rRNA gene regions. *Journal of Zoological Systematics and Evolutionary Research* 46 (2): 96–104. https://doi.org/10.1111/j.1439-0469.2007.00441.x

Wheeler Q.D. 2004. Taxonomic triage and the poverty of phylogeny. *Philosophical Transactions of the Royal Society B – Biological Sciences* 359: 571–583. https://doi.org/10.1098/rstb.2003.1452

Wheeler Q.D. 2008. *The New Taxonomy*. CRC Press, Boca Raton, Florida.

Wheeler Q.D. 2023. *Species, Science and Society: The Role of Systematic Biology*. Taylor & Francis.

Whittaker R.H. 1952. A study of summer foliage insect communities in the Great Smoky Mountains. *Ecological Monographs* 22: 1–44. https://doi.org/10.2307/1948527

Wienskoski E. 2010. The genus *Naatlo* (Araneae: Theridiosomatidae): distribution and taxonomic history. *Revista Brasileira de Biociências* 8 (2): 131–138.

Will K.W., Mishler B.D. & Wheeler Q.D. 2005. The perils of DNA barcoding and the need for integrative taxonomy. *Systematic Biology* 54 (5): 844–851. https://doi.org/10.1080/10635150500354878

World Spider Catalog 2025. *World spider catalog. Ver. 26*. Natural History Museum Bern. Available from http://wsc.nmbe.ch [accessed on 23 Mar. 2025].

Zhang J.S., Yu H. & Lin Y.C. 2023. *Simonia* gen. nov., a new spider genus (Araneae, Theridiosomatidae) from Southeast Asia. *ZooKeys* 1185: 277–294. https://doi.org/10.3897/zookeys.1185.104120

Zhao Q.Y. & Li S.Q. 2012. Eleven new species of theridiosomatid spiders from southern China (Araneae, Theridiosomatidae). *ZooKeys* 255: 1–48. https://doi.org/10.3897/zookeys.255.3272

Printed versions of all papers are deposited in the libraries of four of the institutes that are members of the *EJT* consortium: Muséum national d'Histoire naturelle, Paris, France; Meise Botanic Garden, Belgium; Royal Museum for Central Africa, Tervuren, Belgium; Royal Belgian Institute of Natural Sciences, Brussels, Belgium. The other members of the consortium are: Natural History Museum of Denmark, Copenhagen, Denmark; Naturalis Biodiversity Center, Leiden, the Netherlands; Museo Nacional de Ciencias Naturales-CSIC, Madrid, Spain; Leibniz Institute for the Analysis of Biodiversity Change, Bonn – Hamburg, Germany; National Museum of the Czech Republic, Prague, Czech Republic; The Steinhardt Museum of Natural History, Tel Aviv, Israël.

Supplementary files

Supp. file 1. Complete data matrix containing all specimens and COI sequences, including the outgroups. https://doi.org/10.5852/ejt.2025.1010.3021.13541

Supp. file 2. Haplotype data matrix including only DNA sequences from the defined haplotypes. https://doi.org/10.5852/ejt.2025.1010.3021.13543

Supp. file 3. Partition scheme used in RAxML analyses. https://doi.org/10.5852/ejt.2025.1010.3021.13545

Supp. file 4. Phylogenetic tree obtained from the RAxML analysis. https://doi.org/10.5852/ejt.2025.1010.3021.13547